Biogas clean-up using a novel hollow fibre membrane bioreactor for end-use applications

Jewel Das

Supervisor: Prof. Piet N. L. Lens

A thesis submitted to the National University of Ireland Galway (NUI Galway) as fulfilment of the requirements for the degree of Doctor of Philosophy (PhD)

School of Natural Sciences, NUI Galway

April 2022

Declaration

I, Jewel Das, declare that this thesis or any part thereof has not been, or is not currently being, submitted for any degree at the National University of Ireland, or any other University. I further declare that the work embodied is my own.

Jewel Das

Summary

The aim of this research was to develop a novel hollow fibre membrane bioreactor (HFMB) that can be used for H_2S laden waste gas treatment and biogas desulfurization. In addition, the aim was to utilize the HFMB for simultaneous removal of H_2S and NH_3 from raw biogas. Prior to study the HFMB, recent advancement of biological biogas purification technologies was reviewed including the challenges and future scope of these technologies.

In the first phase of this PhD research, the feasibility of the polyethersulfone based HFMB configuration was established for biological removal of gas-phase H_2S (up to ~ 650 ppm_v) employing three lab-scale HFMBs. In the second phase, resilience of the HFMB was tested under different operating conditions including H_2S concentrations (up to ~ 3600 ppm_v), empty bed residence time (EBRT, up to 62 s), famine period, shock loads, pH and different biomass types. The HFMB achieved ~ 100% removal efficiency (RE) with an elimination capacity (EC) of 30-34 g m^{-3} h^{-1} at ~ 20°C under steady-state operation. The critical loading rate of H_2S was ~ 135 g m^{-3} h^{-1} under transient-state operation.

In the third phase, the HFMB was tested for simultaneous removal of H_2S (up to ~ 1850 ppm_v) and NH_3 (up to ~ 1030 ppm_v) from raw biogas at different EBRT. The HFMB achieved ~ 100% RE for both H_2S (up to ~ 1850 and 1200 ppm_v at an EBRT187 and 46 s, respectively) and NH_3 (up to ~ 460 and 750 ppm_v at an EBRT 187 and 46 s, respectively). At an EBRT of 46 s, the RE of both H_2S and NH_3 varied in the range of 85-97 and 73-95%, respectively, when the inlet biogas laden with ~ 1200-1700 ppm_v of H_2S and 750-1050 ppm_v of NH_3. The critical loading rates of H_2S and NH_3 were ~ 150 and 40 g m^{-3} h^{-1}, respectively. This study confirms that the HFMB can be useful for H_2S and NH_3 laden waste gas treatment and biogas purification.

Acknowledgement

I would like to express my sincere gratitude to Science Foundation Ireland (SFI) and National University of Ireland Galway (NUI Galway) for awarding a scholarship through the SFI Research Professorship Programme entitled *Energy Technologies for Biofuels, Bioenergy and a Sustainable Irish Bioeconomy* (IETSBIO^3) to pursue this PhD course. I acknowledge my employer, Bangladesh Council of Scientific and Industrial Research (BCSIR) for approving deputation to enrol in PhD course in Ireland.

It is my privilege to work under supervision of Professor Piet N. L. Lens. I have been inspired by Prof. Piet because of his continuous motivation, commitment and guidance during entire period of the PhD. Thank you, Sir for your great support. I am also thankful to Dr. Eldon R. Rene (Senior Lecturer, IHE Delft Institute for water education, the Netherlands) for his recommendation regarding the PhD application. I acknowledge my Graduate Research Committee (GRC) members Prof. Henry Curran, Prof. Xinmin Zhan and Prof. Vincent O'Flaherty for their feedback during the GRC meetings.

I feel proud to be a group member of IETSBIO^3, an international team of researchers led by Prof. Piet Lens, where I had the opportunity to learn and share our views, not only about research but also about the cultures, customs, foods and many more. I am thankful to all of my previous and present colleagues in the group including all the PhDs, Postdocs, Research Assistants and visiting researchers for their excellent support, sharing knowledge and love during the entire journey.

I salute to all COVID-19 frontline fighters and response teams including Health Service Executive (HSE), Ireland for their initiatives to keep us safe during the pandemic.

I am also grateful to my family members, friends and seniors for their love and support during the entire PhD journey. I believe, whatever I have learned or gained during this PhD are the blessings of holy Trio (Sree Ramakrishna, Maa Sarada and Swami Vivekananda). Joy Thakur, Maa, Swamiji!

Contents

List of figures

List of tables

List of publications and chapter contributions

The work contained in this thesis consists of the following publications in international peer-reviewed journals:

Publications	Author contributions
Chapter 2: Das, J., Ravishankar, H., Lens, P.N.L., 2022. Biological biogas purification: recent developments, challenges and future prospects. Journal of Environmental Management. 304, 114198. https://doi.org/10.1016/j.jenvman.2021.114198	**Das, J.**: Conceptualization, Methodology, Visualization, Writing - original draft, Writing - review & editing. **Ravishankar, H.**: Writing - review & editing. **Lens, P.N.L.**: Conceptualization, Supervision, Funding acquisition, Writing - review & editing.
Chapter 3: Das, J., Ravishankar, H., Lens, P.N.L., 2022. Biological removal of gas-phase H_2S in hollow fibre membrane bioreactors. Journal of Chemical Technology & Biotechnology. Early View. https://doi.org/10.1002/jctb.6999	**Das, J.**: Conceptualization, Methodology, Formal analysis, Investigation, Data curation, Visualization, Writing - original draft, Writing - review & editing. **Ravishankar, H.**: Resources, Methodology, Writing - review & editing. **Lens, P.N.L.**: Supervision, Funding acquisition, Resources, Writing - review & editing.

The submitted manuscripts for publication in international peer-reviewed journals:

Submitted manuscripts	Author contributions
Chapter 4: Das, J., Lens, P.N.L., 2022. Resilience of hollow fibre membrane bioreactors for treating H_2S under steady state and transient conditions	**Das, J.**: Conceptualization, Methodology, Formal analysis, Investigation, Data curation, Visualization, Writing - original draft, Writing - review & editing. **Lens, P.N.L.**: Supervision, Funding acquisition, Resources, Writing - review & editing.
Chapter 5: Das, J., Nolan, S., Lens, P.N.L., 2022. Simultaneous removal of H_2S and NH_3 from raw biogas in hollow fibre membrane bioreactors.	**Das, J.**: Conceptualization, Methodology, Formal analysis, Investigation, Data curation, Visualization, Writing - original draft, Writing - review & editing. **Nolan, S.**: Resources, Writing - review & editing. **Lens, P.N.L.**: Supervision, Funding acquisition, Resources, Writing - review & editing.

Funding

This PhD thesis was supported by Science Foundation Ireland (SFI) through the SFI Research Professorship Programme entitled *Innovative Energy Technologies for Biofuels, Bioenergy and a Sustainable Irish Bioeconomy* (IETSBIO^3; grant number 15/RP/2763) and the SFI Research Infrastructure research grant *Platform for Biofuel Analysis* (Grant Number 16/RI/3401).

Nomenclature

AB - airlift bioreactor

AD - anaerobic digestion

BF - biofilter

BS - bioscrubber

BTF - biotrickling filter

CHP - combined heat and power

COD - chemical oxygen demand

CSTB - continuously stirred tank bioreactor

DO - dissolved oxygen

EBRT - empty bed residence time

EC - elimination capacity

GB - gas-lift bioreactor

GRT - gas retention time

HFM - hollow fibre membrane

HFMB - hollow fibre membrane bioreactor

HFMC - hollow fibre membrane contactors

H-PES - hydrophilic polyethersulfone

HRT - hydraulic retention time

ILR - inlet loading rate

J - flux

K_G - overall mass-transfer coefficient

NSM - nutrient salt medium

OLR - organic loading rate

OT - operating time

RE - removal efficiency

TP - target pollutants

UASB - upflow anaerobic sludge blanket

Chapter 1

General introduction

1.1. Background

Biogas, a clean and accessible source of energy, is produced through a complex range of biochemical processes such as hydrolysis, acidogenesis, acetogenesis and methanogenesis, during the anaerobic digestion (AD) of organic wastes wherein microorganisms and enzymes degrade organic matter and produce biogas (Angelidaki et al., 2018; Sahota et al., 2018). The utilization of biogas is increasing gradually, as it is a renewable energy source and can be applied on a wide scale of organic biomass types. Apart from the methane (CH_4) content, all other constituents such as carbon dioxide (CO_2), hydrogen sulfide (H_2S), ammonia (NH_3), siloxanes and volatile organic compounds (VOCs) are unwanted pollutants in raw biogas (Khan et al., 2021; Rodero et al., 2018) that need to be removed.

H_2S can be removed by physico-chemical and biological methods. Within the physico-chemical approach, hollow fibre membrane contactors (HFMCs) are used for several applications including H_2S removal from gas mixtures (Bazhenov et al., 2018). The pollutant removal performance of a HFMC varies depending on the membrane type, e.g. polyethersulfone, polyvinylidene fluoride or polydimethylsiloxane (Bazhenov et al., 2018; Hedayat et al., 2011); contactor design, e.g. counter flow or parallel flow (Bazhenov et al., 2018); absorption chemicals, e.g. a methyldiethanolamine solution (Mirfendereski et al., 2019) and operating conditions, e.g. high operational pressure (Marzouk et al., 2010). H_2S absorption in a porous membrane contactor decreases with increasing CO_2 concentration, resulting in a higher consumption of absorption chemicals to keep H_2S into the liquid phase (Tilahun et al., 2018).

The hollow fibre membrane bioreactor (HFMB) concept was first introduced in 1970s to immobilize enzymes and cells on the solid support material, i.e. the hollow fibre membranes (Łabęcki et al., 1996). The dead-end hollow fibre modules (i.e. gas is fed from one side of the hollow fibres while the other side of the fibres is sealed) were mainly used for wastewater treatment, where the HFMBs were operated at high pressure to fulfil

the high aeration requirements of the immobilized microorganisms (Pankhania et al., 1994). The HFMBs were subjected to excess biomass growth on the membrane and required regular (daily) backwash using compressed air followed by a water flush (Pankhania et al., 1994). The HFMB configuration with hydrophobic hollow fibre membrane modules was subsequently applied for other applications such as VOCs treatment (Ergas et al., 1999) and hydrogenotrophic denitrification of contaminated groundwater (Ergas and Reuss, 2001). Till to date, no work has thus far reported on the application of HFMB for biological raw biogas purification.

1.2. Problem statement

The presence of H_2S in biogas is an important issue because H_2S is a harmful environmental pollutant that causes severe corrosion on biogas fired appliances and metallic accessories (e.g. compressors, engines, gas storage tanks, pipes, pumps and valves) prior to energy production (Noorain et al., 2019). Apart from on-farm biogas plants, H_2S emissions can be associated with other sources such as geothermal power plants (Renato et al., 2017), volcanic and geothermal areas (D'Alessandro et al., 2009), and industries and services including gas and oil refineries, pulp and paper mills, and sewage treatment plants (Bates et al., 2013). NH_3 also induces corrosion in engines and pipelines during combustion (Khan et al., 2021). Hence, the biogas impurities such as H_2S and NH_3 must be treated for end-use application, i.e. biogas utilization processes such as natural gas grid injection or electricity generation (Angelidaki et al., 2018; Atelge et al., 2021).

The physico-chemical and biological methods are two generic categories used for biogas purification (Fernández et al., 2013). The physico-chemical methods such as absorption (e.g. water or amine scrubbing), adsorption (e.g. pressure swing) and membrane separation (e.g. mixed matrix membrane) are commonly used for removing biogas impurities (Atelge et al., 2021; Sahota et al., 2018). However, the physico-chemical methods have several limitations such as (i) energy-intensive in terms of operational pressure, temperature, regeneration of the adsorbents or chemicals used (Sahota et al., 2018), (ii) require pre-treatments for some methods including pressure swing adsorption and membrane separation (Sahota et al., 2018), and (iii) intensive use

of chemicals (Borgne and Baquerizo, 2019) which can be toxic to humans and the environment (Angelidaki et al., 2018).

In contrast, biological methods are effective for the treatment of a wide range of impurities, including the H_2S, NH_3 and VOCs, present in biogas and polluted air (Khanongnuch et al., 2022). Functional microorganisms, bioreactor configurations (e.g. biotrickling filter or bioscrubber) and their operating conditions are the key aspects for efficient biological waste gas treatment (Khanongnuch et al., 2022). Innovations such as integration of autotrophic denitrification with the biogas desulfurization process (Lin et al., 2018) or development of haloalkaliphilic bio-desulfurizing system (Mu et al., 2021) are being carried out to optimize the biological H_2S treatment process with better design and operating conditions.

Biological desulfurization is the most suitable approach for treating H_2S from biogas (Zeng et al., 2018). Three types of bioreactors, i.e. the biofilter, biotrickling filter and bioscrubber, are mainly reported for desulfurization of biogas and industrial gas streams (Lin et al., 2018). There are both advantages and drawbacks of these different bioreactor configurations used for waste gas treatment (Borgne and Baquerizo, 2019; Khanongnuch et al., 2022). For example, biofilters provide efficient removal of low H_2S concentrations with low investment and operational costs (compared to biotrickling filters or bioscrubbers), but have issues like packing material compaction, filter bed replacement and difficulties regarding pH control (Borgne and Baquerizo, 2019). Selection of a suitable bioreactor configuration is essential for waste gas treatment but depends on the pollutant types, their characteristics, concentrations, geographic location and cost (Khanongnuch et al., 2022). To achieve optimum pollutant removal performance, further research is required for better understanding of the microbial dynamics in the bioreactors as well as improving the design characteristics of the bioreactors to overcome the existing limitations and develop novel bioreactor configurations, keeping in mind the operating conditions such as fluctuations of pH, temperature, pollutant concentrations and flow rates (Khanongnuch et al., 2022).

1.3. Research objectives

The main objective of this thesis was to configure and utilize a novel hollow fibre membrane bioreactor (HFMB) that can be applied for H_2S laden waste gas treatment

under different operating conditions. In addition, the aim was to test the feasibility of the HFMB configuration for mixed pollutants, mainly H_2S and NH_3, removal from raw biogas.

The specific objectives were the following:

i. To review the biological techniques that are applied for the removal or conversion of biogas impurities (mainly H_2S, CO_2, NH_3, siloxanes and VOCs), identify the challenges related to biological removal of single or mixed pollutants in terms of different bioreactor configurations and operational limitations of each technique, and develop a conceptual framework Driver-Pressure-Stress-Impact-Response (DPSIR) and Strengths-Weaknesses-Opportunities-Threats (SWOT) analysis.
ii. To fabricate a novel HFMB and test its feasibility for biological removal of gas-phase H_2S.
iii. To investigate the long-term H_2S removal performance and resilience of the HFMB employing different operating conditions (e.g. inlet H_2S concentrations, empty bed residence times, shock loads and starvation period) and shell side operational parameters (e.g. effect of pH, membrane attached biofilm and suspended biomass).
iv. To treat H_2S and NH_3, simultaneously, from raw biogas using the HFMB under different operating conditions, i.e. loading rate and empty bed residence time.

1.4. Outline of the thesis

Figure 1.1 shows an overview of the chapters of this PhD thesis. There are six chapters in the thesis. Chapter 1 presents a general overview of this thesis including the background, problem statement, research objectives and thesis outline.

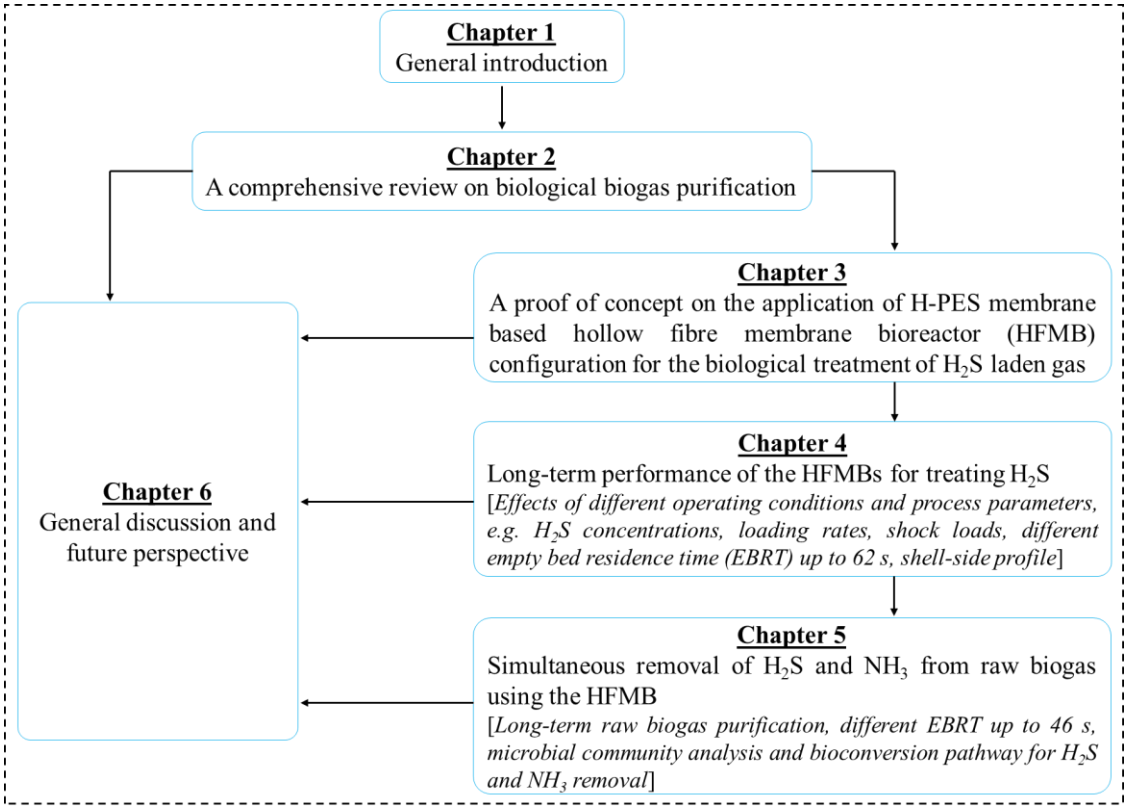

Figure 1.1: Overview of the outline of this PhD thesis.

Considering the advantages of biological biogas purification processes, Chapter 2 reviews the biological techniques applied for the removal or conversion of biogas impurities to provide new insights and perspectives on biological techniques for raw biogas purification. The working principles, advantages, limitations and challenges of biological approaches for both upstream and downstream treatment of biogas (including H_2 assisted biogas upgrading) have been described in the review chapter. Apart from conventional end-of-pipe treatment, the cleaner production approach, such as key process parameters that enhance process stability in anaerobic digesters and minimize biogas impurities, is also considered in the review chapter. Finally, a conceptual framework of DPSIR and SWOT analysis has been carried out to analyse the present situation and future scope of biological biogas clean-up technologies.

Chapter 3 reports the feasibility of a novel HFMB configuration for biological desulfurization of a biogas mimic using three lab-scale HFMBs. The performance of the HFMB has been assessed in terms of H_2S flux, gas-liquid mass transfer, removal efficiency, elimination capacity and characterization of the microbial population of the attached and suspended biomass in the HFMB.

Chapter 4 investigates the long-term H_2S removal performance of the HFMB where the resilience of the HFMB has been tested employing different operating conditions including the inlet H_2S concentration (up to ~ 3600 ppm_v), empty bed residence time (187, 92 and 62 s), shock load (up to 208 g m^{-3} h^{-1}) and starvation period. The liquid profile has also been investigated to identify the ideal mode of operation of the reactor mixed liquor on the shell side of the HFMB. Finally, a biokinetic study has been performed for projecting the H_2S removal performance of the HFMB.

Chapter 5 investigates the long-term raw biogas purification performance of the HFMB at an empty bed residence time of 187, 92 and 46 s. The flux and gas-liquid mass transfer profile of the biogas constituents through the hollow fibres have been assessed. A microbial community analysis has also been carried out to reveal the possible bioconversion pathway and microorganisms involved in the simultaneous removal of H_2S and NH_3 from biogas.

Chapter 6 provides a general discussion based on the findings as well as knowledge gained from this thesis. The practical implications of this research, future perspectives and recommendations are also included in this final chapter.

1.5. References

Angelidaki, I., Treu, L., Tsapekos, P., Luo, G., Campanaro, S., Wenzel, H., Kougias, P.G., 2018. Biogas upgrading and utilization: Current status and perspectives. Biotechnology Advances. 36, 452-466.

Atelge, M.R., Senol, H., Djaafri, M., Hansu, T.A., Krisa, D., Atabani, A., Kıvrak, H.D., 2021. A critical overview of the state-of-the-art methods for biogas purification and utilization processes. Sustainability. 13, 11515.

Bates, M.N., Garrett, N., Crane, J., Balmes, J.R., 2013. Associations of ambient hydrogen sulfide exposure with self-reported asthma and asthma symptoms. Environmental Research. 122, 81-87.

Bazhenov, S.D., Bildyukevich, A.V., Volkov, A.V., 2018. Gas-liquid hollow fiber membrane contactors for different applications. Fibers. 6, 76.

Borgne, S.L., Baquerizo, G., 2019. Microbial ecology of biofiltration units used for the desulfurization of biogas. ChemEngineering. 3, 72.

D'Alessandro, W., Brusca, L., Kyriakopoulos, K., Michas, G., Papadakis, G., 2009. Hydrogen sulphide as a natural air contaminant in volcanic/geothermal areas: the case of Sousaki, Corinthia (Greece). Environmental Geology. 57, 1723-1728.

Ergas, S.J., Reuss, A.F., 2001. Hydrogenotrophic denitrification of drinking water using a hollow fibre membrane bioreactor. Journal of Water Supply: Research and Technology -AQUA. 50, 161-171.

Ergas, S.J., Shumway, L., Fitch, M.W., Neemann, J.J., 1999. Membrane process for biological treatment of contaminated gas streams. Biotechnology and Bioengineering. 63, 431-441.

Fernández, M., Ramírez, M., Pérez, R.M., Gómez, J.M., Cantero, D., 2013. Hydrogen sulphide removal from biogas by an anoxic biotrickling filter packed with Pall rings. Chemical Engineering Journal. 225, 456-463.

Hedayat, M., Soltanieh, M., Mousavi, S.A., 2011. Simultaneous separation of H_2S and CO_2 from natural gas by hollow fiber membrane contactor using mixture of alkanolamines. Journal of Membrane Science. 377, 191-197.

Khan, M.U., Lee, J.T.E., Bashir, M.A., Dissanayake, P.D., Ok, Y.S., Tong, Y.W., Shariati, M.A., Wu, S., Ahring, B. K., 2021. Current status of biogas upgrading for direct biomethane use: A review. Renewable and Sustainable Energy Reviews. 149, 111343.

Khanongnuch, R., Abubackar, H.N., Keskin, T., Gungormusler, M., Duman, G., Aggarwal, A., Behera, S.K., Li, L., Bayar, B., Rene, E.R., 2022. Bioprocesses for resource recovery from waste gases: Current trends and industrial applications. Renewable and Sustainable Energy Reviews. 156, 111926.

Łabęcki, M., Bowen, B.D., Piret, J.M., 1996. Two-dimensional analysis of protein transport in the extracapillary space of hollow-fibre bioreactors. Chemical Engineering Science. 51, 4197-4213.

Lin, S., Mackey, H.R., Hao, T., Guo, G., van Loosdrecht, M.C.M., Chen, G., 2018. Biological sulfur oxidation in wastewater treatment: A review of emerging opportunities. Water Research. 143, 399-415.

Marzouk, S.A., Al-Marzouqi, M.H., Abdullatif, N., Ismail, Z.M., 2010. Removal of percentile level of H_2S from pressurized H_2S-CH_4 gas mixture using hollow fiber membrane contactors and absorption solvents. Journal of Membrane Science. 360, 436-441.

Mirfendereski, S.M., Niazi, Z., Mohammadi, T., 2019. Selective removal of H_2S from gas streams with high CO_2 concentration using hollow-fiber membrane contractors. Chemical Engineering & Technology. 42, 196-208.

Mu, T., Yang, M., Xing, J., 2021. Performance and characteristic of a haloalkaliphilic bio-desulfurizing system using *Thioalkalivibrio verustus* D301 for efficient removal of H_2S. Biochemical Engineering Journal. 165, 107812.

Noorain, R., Kindaichi, T., Ozaki, N., Aoi, Y., Ohashi, A., 2019. Biogas purification performance of new water scrubber packed with sponge carriers. Journal of Cleaner Production. 214, 103-111.

Pankhania, M., Stephenson, T., Semmens, M.J., 1994. Hollow fibre bioreactor for wastewater treatment using bubbleless membrane aeration. Water Research. 28, 2233-2236.

Renato, S., Domenico, G., Claudia, T., Carlo, T., Giuseppe, D.N., Maria, P., 2017. Modelling of hydrogen sulfide dispersion from the geothermal power plants of Tuscany (Italy). Science of the Total Environment. 583, 408-420.

Rodero, M.R., Ángeles, R., Marín, D., Díaz, I., Colzi, A., Posadas, E., Lebrero, R., Muñoz, R., 2018. Biogas Purification and Upgrading Technologies, in: Tabatabaei, M., Ghanavati, H. (Eds.), Biogas, Biofuel and Biorefinery Technologies 6. Springer, Cham, pp. 239-276.

Sahota, S., Shah, G., Ghosh, P., Kapoor, R., Sengupta, S., Singh, P, Vijay, V., Sahay, A., Vijay, V.K., Thakur, I.S., 2018. Review of trends in biogas upgradation technologies and future perspectives. Bioresource Technology Reports. 1, 79-88.

Tilahun, E., Sahinkaya, E., Çalli, B., 2018. A hybrid membrane gas absorption and bio-oxidation process for the removal of hydrogen sulfide from biogas. International Biodeterioration & Biodegradation. 127, 69-76.

Zeng, Y., Xiao, L., Zhang, X., Zhou, J., Ji, G., Schroeder, S., Liu, G., Yan, Z., 2018. Biogas desulfurization under anoxic conditions using synthetic wastewater and biogas slurry. International Biodeterioration & Biodegradation. 133, 247-255.

Chapter 2

Biological biogas purification: recent developments, challenges and future prospects

A modified version of this chapter has been published as:

Das, J., Ravishankar, H., Lens, P.N.L., 2022. Biological biogas purification: recent developments, challenges and future prospects. *Journal of Environmental Management*. 304, 114198. https://doi.org/10.1016/j.jenvman.2021.114198

Abstract

Raw biogas generated in the anaerobic digestion (AD) process contains several undesired constituents such as H_2S, CO_2, NH_3, siloxanes and VOCs. These gases affect the direct application of biogas, and are a prime concern in biogas utilization processes. Conventional physico-chemical biogas purification methods are energy-intensive and expensive. To promote sustainable development and environmental friendly technologies, biological biogas purification technologies can be applied. This review describes biological technologies for both upstream and downstream processing in terms of pollutant removal mechanisms and efficiency, bioreactor configurations and different operating conditions. Limitations of the biological approaches and their future scope are also highlighted. A conceptual framework Driver-Pressure-Stress-Impact-Response (DPSIR) and Strengths-Weaknesses-Opportunities-Threats (SWOT) analysis have been applied to analyse the present situation and future scope of biological biogas clean-up technologies.

2.1. Introduction

Anaerobic digestion (AD) generates raw biogas from waste organic materials through complex biochemical processes. The application of the AD process and utilization of biogas is increasing rapidly as a renewable energy source (Angelidaki et al., 2018; Sahota et al., 2018; Xu et al., 2018). Wastes such as livestock manure, agricultural residues, municipal organic solids, sewage sludge and food residues are cheap and abundant sources of organic matter for biogas production via AD (Khalil et al., 2019). Recent trend in biogas production emphasizes on 'biological innovations to improve biogas production' through adopting various upstream, mainstream and downstream strategies (Tabatabaei et al., 2020a; Tabatabaei et al., 2020b).

Biogas produced through the AD process has both economical (e.g. heat, electricity and fuel generation; application of digestate from the AD process as fertilizer) and environmental (e.g. organic waste management, nutrient recovery, reduction of water and air pollution, odour mitigation) benefits (Angelidaki et al., 2018; Sahota et al., 2018). Global biogas supply is expected to increase from 1.5 EJ (in 2015) to 14.4 EJ by 2050 (IRENA, 2020). Bioenergy, i.e. biogas as well as solid and liquid biofuels, represent ~ 70% share of the global renewable energy supply and ~ 10% share of the total primary

energy supply (IRENA, 2020). According to International Renewable Energy Agency (IRENA) energy transformation scenario, the current share of the global renewable energy in electricity generation is ~ 25% which differs by region (Figure 2.1). The share is expected to increase up to ~ 85% by 2050.

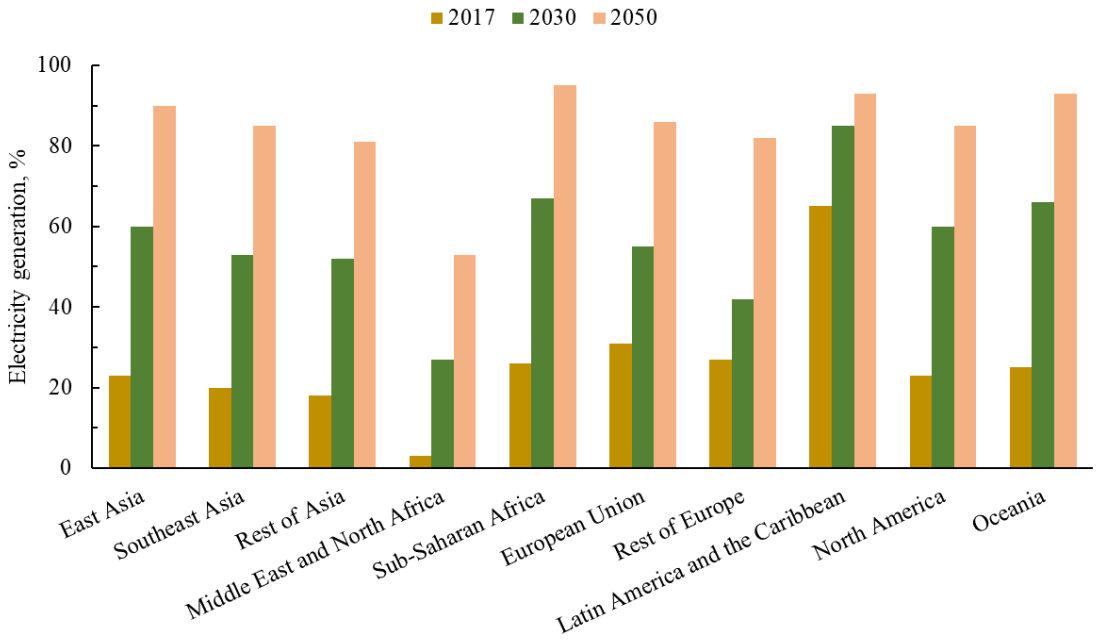

Figure 2.1: Global renewable energy share projection in electricity generation (Reference: IRENA, 2020).

The composition of raw biogas (Table 2.1) depends on the nature of the substrate, operating conditions (e.g. pH, temperature or retention time) and configuration of the anaerobic digester (Franco-Morgado et al., 2018; Khan et al., 2021; Li et al., 2019). Methane (CH_4) and carbon dioxide (CO_2) are the main constituents of biogas generated during the AD process. Apart from the CH_4 content, the presence of other gases in raw biogas (Table 2.1) is a prime concern in direct biogas utilization (Mulu et al., 2021). For example, AD of cattle manure can yield high NH_3 concentrations (~ 2000 ppm_v) in the raw biogas (Guo et al., 2009).

Conventional biogas upgrading techniques generally focus on CO_2 removal due to its relatively high concentration in raw biogas. However, raw biogas containing H_2S (even in trace amounts) must also be treated before its end-use application, as H_2S is toxic and corrosive (Noorain et al., 2019; Pokorna and Zabranska, 2015; Rodero et al., 2018). NH_3, siloxanes and volatile organic compounds (VOCs) are other unwanted pollutants in raw

biogas, usually present in much lower concentrations than H_2S. For example, NH_3 induces corrosion in engines and pipelines during combustion (Khan et al., 2021; Rodero et al., 2018), siloxanes (e.g. octamethylcyclotetrasiloxane) in silicium deposits during combustion, which form microcrystalline quartz deposits on engine surfaces resulting in abrasion, overheating, and malfunctioning of engines and valves (García et al., 2021; Yang and Corsolini, 2019), whereas combustion of VOCs such as benzene and other aromatic compounds give an unpleasant smell to biogas, and are potentially toxic to human health (Carriero et al., 2018). Hence, comprehensive biogas purification is required prior to its application, i.e. to generate electricity or to upgrade to biomethane quality as green alternative fuel to natural gas (Mulu et al., 2021; Rodero et al., 2018; Yang and Corsolini, 2019).

Table 2.1: Composition of raw biogas generated in anaerobic digesters and biomethane.

Biogas constituents*	Unit	Composition of	
		Raw biogas	Biomethane**
CH_4	%	45-75	> 95
CO_2	%	25-65	< 2
H_2	%	0	< 6
H_2S	ppm_v	50-20000	< 5
NH_3	ppm_v	< 10000	3-20
H_2O	%	5-10	NR
N_2	%	< 3	NR
O_2	%	< 1	0.2-0.5
Hydrocarbons	mg m^{-3}	< 200	NR
Siloxanes	mg m^{-3}	< 40	< 6
Mercaptans	mg m^{-3}	trace level	< 5-10
Aromatic compounds	mg m^{-3}	trace level	< 1

Note: * - The information provided here was taken from the following references: Franco-Morgado et al., 2018; Khan et al., 2021; Mulu et al., 2021; Rodero et al., 2018; Sahota et al., 2018; Yang and Corsolini, 2019; ** - Biomethane composition has been summarised according to European regulations for natural gas grid injection where the composition can be flexible in terms of parameters (e.g. CO_2 or NH_3 content) depending on the implementing country; NR - not reported

Conventional physico-chemical methods for biogas upgrading achieve a methane recovery of > 96%, but are highly energy-intensive and have large environmental impacts (Angelidaki et al., 2019; Kapoor et al., 2019; Rodero et al., 2018). Among all biogas purification techniques, water scrubbing (which shares 41% of the global upgrading market) is the leading global biogas upgrading process, followed by chemical scrubbing (22%), pressure swing adsorption (21%), and membrane separation (10%) (Maurya et al.,

2019). However, those physico-chemical methods have several limitations: (i) requirement of large amounts of water even when considering water regeneration and high electricity cost (e.g. 0.34 kWh m^{-3} raw biogas) for applying high pressure in pressurized water scrubbing (Noorain et al., 2019; Kadam and Panwar, 2017), (ii) high energy consumption and amine degradation in the amine scrubbing process (Abdeen et al., 2016; Hosseinipour and Mehrpooya, 2019), and (iii) need for H_2S removal prior to membrane separation of CO_2 from CH_4. Energy consumption of the membrane separation process depends on the applied pressure, the membrane area and the biomethane characteristics, i.e. CH_4 purity (Baena-Moreno et al., 2019a).

Application of biological methods began nearly 70 years ago for treatment of odours, i.e. hydrogen sulfide, ammonia, mercaptans and hydrocarbons (Barbusinski et al., 2017). Biological methods have drawn more attention in the 21st century, especially in the field of waste-gas treatment and biogas upgrading due to its benefit compared to conventional physico-chemical methods. The main advantages of biological methods are: (i) sustainable and simple operation, (ii) low cost, and (iii) environment friendly (Angelidaki et al., 2019; Barbusinski et al., 2017; Rybarczyk et al., 2019; Wang et al., 2019a). To promote sustainable development and environmental friendly technologies, biological methods for biogas clean-up are being developed for specific applications that include (i) electricity generation, (ii) biomethane production (alternative to natural gas), and (iii) waste-gas valorisation.

Recent literature on biogas treatment reviews conventional physico-chemical biogas upgrading technologies with main focus in CO_2 removal from biogas (Angelidaki et al., 2019; Angelidaki et al., 2018; Baena-Moreno et al., 2019a; Baena-Moreno et al., 2019b; Kadam and Panwar, 2017; Mulu et al., 2021; Prussi et al., 2019). The limitations of the conventional biogas upgrading technologies are also discussed in a recent review (Khan et al., 2021). However, only few review articles have discussed on biological biogas purification, mainly CO_2 (Angelidaki et al., 2019; Angelidaki et al., 2018) and H_2S (Khan et al., 2021; Struk et al., 2020) removal from biogas. Considering the advantages of biological purification processes for biogas treatment, this review aims to provide a comprehensive overview of the biological techniques applied for the removal or conversion of biogas impurities such as H_2S, CO_2, NH_3, siloxanes and VOCs. Recent advancement in biological biogas purification technologies in terms of pollutant removal

mechanisms, bioreactor configurations and removal efficiencies under different operating conditions has been discussed in brief. In addition, this review discusses the challenges related to biological removal of single or mixed pollutants from biogas, operational limitations of bioreactors, and presents integrated approaches for biogas upgrading.

2.2. Biological processes for biogas clean-up

Biological biogas purification techniques have been mainly developed to achieve H_2S and CO_2 removal, and ongoing research focuses on the optimization of biological purification processes and development of new technologies (Kapoor et al., 2019; Maurya et al., 2019; San-Valero et al., 2019; Zhuo et al., 2019). This section overviews recent progress in biological removal of biogas impurities in terms of bioreactor configurations, pollutant removal mechanisms and removal efficiencies under different operating conditions.

2.2.1. H_2S removal

Biological H_2S removal mechanism

Microorganisms play a key role in H_2S bioconversion processes, and their activity can significantly improve the H_2S removal efficiency (RE). During the bioconversion, H_2S is used by microbes as energy source (Vikrant et al., 2018). Table 2.2 summarizes the general stoichiometric equations of the H_2S bioconversion by phototrophic and chemotrophic microorganisms. Both phototrophs and chemotrophs convert H_2S into sulfate (SO_4^{2-}) as the end product via elemental sulfur (S^0) as an intermediate. During the bioconversion, H_2S acts as electron donor, while O_2 or NO_3^- act as electron acceptor allowing the microorganisms to grow. Sulfur oxidizing bacteria generally use inorganic carbon as carbon source (e.g. CO_2) for their growth (Kennes et al., 2009; Syed et al., 2006). The pH tolerance and optimum pH of the H_2S bioconversion varies over a wide range, depending on the microbial species present in the system (Abatzoglou and Boivin, 2009; Pokorna and Zabranska, 2015). For example, *Acidithiobacillus thiooxidans* can survive at low pH (< 1.0), whereas *Thiobacillus thioparus* has an optimum growth in the pH range 6-8. In contrast, *Thioalkalivibrio* sp. can efficiently treat sulfide at pH 10 (Arellano-García et al., 2018).

Table 2.2: Reaction mechanisms of phototrophic and chemotrophic H_2S bioconversion.

Bacteria	Reaction mechanism and stoichiometric equation for biomass growth	Reference
Phototrophs e.g. *Cholorobium limicola*	$2H_2S + CO_2 + light \rightarrow 2S^0 + CH_2O + H_2O$ $H_2S + 2CO_2 + 2H_2O + light \rightarrow SO_4^{2-} + 2CH_2O + 2H^+$	Sun et al., 2019b; Syed et al., 2006
Chemotrophs e.g. *Thiobacillus thioparus; Halothiobacillus neapolitanus*	Under aerobic condition $2HS^- + O_2 \rightarrow 2S^0 + 2OH^-$ $2S^0 + 3O_2 + 2OH^- \rightarrow 2SO_4^{2-} + 2H^+$ $H_2S + 2O_2 \rightarrow SO_4^{2-} + 2H^+$ *Stoichiometric equation* $0.444H_2S + 0.4HS^- + 1.2555O_2 + 0.0865H_2O + 0.346CO_2 + 0.0865HCO_3^- + 0.0865NH_4^+ \rightarrow 0.844SO_4^{2-} + 1.288H^+ + 0.0865C_5H_7NO_2$	Syed et al., 2006; Sun et al., 2019b Kennes et al., 2009
e.g. *Thiobacillus denitrificans; Thiobacillus versutus; Thiomicrospira denitrificans*	Under anoxic condition $5S^{2-} + 8NO_3^- + 8H^+ \rightarrow 5SO_4^{2-} + 4N_2 + 4H_2O$ $5S^{2-} + 2NO_3^- + 12H^+ \rightarrow 5S^0 + N_2 + 6H_2O$ $4HS^- + NO_3^- + 6H^+ \rightarrow 4S^0 + NH_4^+ + 3H_2O$ *Stoichiometric equation* $HS^- + 1.23NO_3^- + 0.573H^+ + 0.438HCO_3^- + 0.027CO_2 + 0.093NH_4^+ \rightarrow 0.093C_5H_7O_2N + 0.866H_2O + 0.614N_2 + SO_4^{2-}$ $S^0 + 0.876NO_3^- + 0.343H_2O + 0.379HCO_3^- + 0.023CO_2 + 0.080NH_4^+ \rightarrow 0.080C_5H_7O_2N + 0.824H^+ + 0.44N_2 + SO_4^{2-}$ $S^{2-} + 0.67NO_2^- + 2.67H^+ \rightarrow S^0 + 0.33N_2 + 1.33H_2O$ $S^{2-} + 2.67NO_2^- + 2.67H^+ \rightarrow SO_4^{2-} + 1.33N_2 + 1.33H_2O$ $S^0 + 3NO_3^- + H_2O \rightarrow SO_4^{2-} + 3NO_2^- + 2H^+$ $S^0 + 2NO_2^- \rightarrow SO_4^{2-} + N_2$	Sun et al., 2019b Capua et al., 2019 Pokorna and Zabranska, 2015
e.g. *Acidithiobacillus ferrooxidans*	Fe (II) to Fe (III) oxidation $2FeSO_4 + H_2SO_4 + 0.5O_2 \rightarrow Fe_2(SO_4)_3 + H_2O$ $H_2S + Fe_2(SO_4)_3 \rightarrow H_2SO_4 + FeSO_4 + S^0$	Abatzoglou and Boivin, 2009

Biological desulfurization

Microaerobic treatment

Microaerobic treatment (Figure 2.2) represents dosing of small amounts of oxygen (O_2) or air in the headspace of an anaerobic digester for biogas desulfurization (Wasajja et al., 2020). Under limited O_2 conditions, microaerophilic sulfur oxidizing autotrophic bacteria (e.g. *Acidithiobacillus* sp., *Arcobacter* sp., *Sulfurimonas* sp., *Sulfuricuvum* sp., *Thiobacillus* sp., *Thiomonas* sp. and *Thiofaba* sp.) convert H_2S into different end products such as elemental sulfur (S^0), thiosulfate ($S_2O_3^{2-}$) and sulfate (SO_4^{2-}), depending on the supplied O_2/H_2S ratio (Rodero et al., 2018; Toledo-Cervantes et al., 2017). Apart from H_2S removal from the headspace, this process can also treat dissolved sulfide in the digester mixed liquor (Okoro and Sun, 2019). Microaeration has been integrated at

several pilot and full-scale anaerobic digesters as cost effective tool for in-situ H_2S removal (Rodero et al., 2018).

Jeníček et al. (2017) reported the desulfurization performance of seven full-scale microaerobic digesters with the following specifications: anaerobic reactor volume 1900-3200 m^3, biogas production (520-1000 m^3 d^{-1}), air dose (0.28-1.20 m^3 h^{-1}) and air dose optimization time (4-12 weeks), resulting in H_2S concentrations with (48-72 mg m^{-3}) and without (890-7580 mg m^{-3}) microaeration. The H_2S removal efficiency of the five digesters ranged between 95-99%, while the removal efficiency of the remaining two digesters was in the range of 74-88%. Microaeration further improves the digestion process by enhancing the degradability of the digested sludge (Jeníček et al., 2017). Giordano et al. (2019) studied the desulfurization performance of three full-scale thermophilic digesters (in series) under different microaerobic regimes with the following specifications: digester volume 4500 m^3, digester headspace 500 m^3, feedstock containing 90% sewage sludge and 10% digestate with liquid fraction, total solids in the digestate 10.7% and H_2S concentration 1200-2500 ppm. The authors estimated the specific oxygen consumption at 1.49 L O_2/Nm^3 biogas for H_2S removal. Complete biogas desulfurization was achieved for an organic loading rate ~ 1.8 kg VS m^{-3} d^{-1} maintaining $\geq$ 0.2% residual oxygen as the control parameter (Giordano et al., 2019).

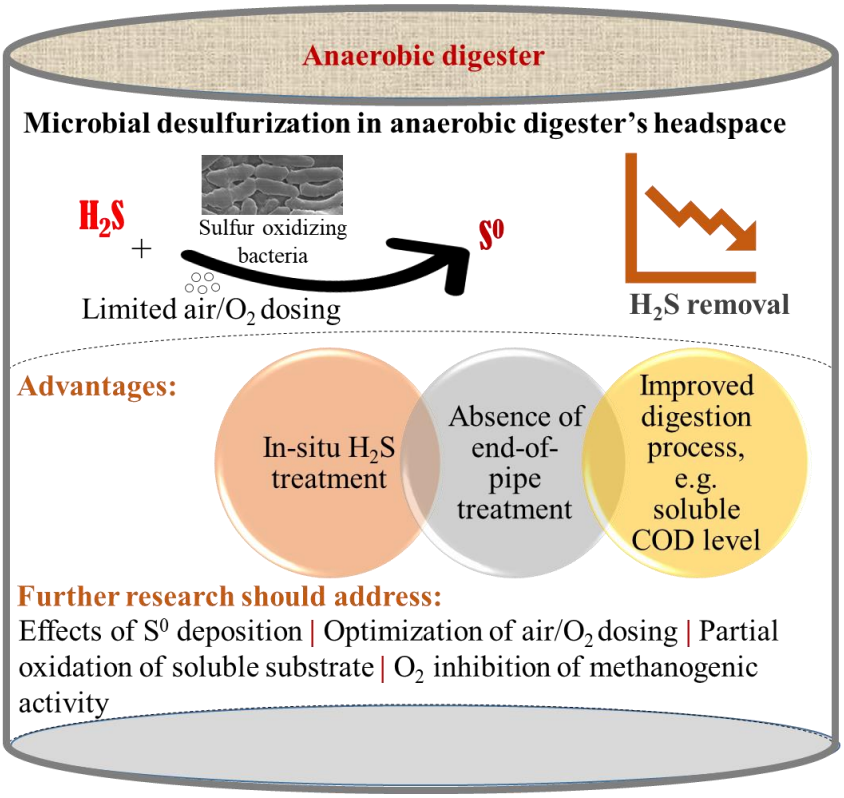

Figure 2.2: Schematic presentation of biogas desulfurization using microaeration.

Accumulation of S^0 on the internal walls of the digester and gas pipes can clog the system and consequently increase the pressure in the digester headspace resulting in biogas leakage. Moreover, excessive S^0 deposition on the ceiling of the anaerobic digester reduces the headspace volume. Consequently, sulfur oxidizing bacteria could have less biogas contact time in the headspace which might affect the H_2S removal performance (Rodero et al., 2018; Toledo-Cervantes et al., 2017). Jeníček et al. (2017) reported nevertheless that there were no clogging problems for operating full-scale digesters installed at the seven municipal wastewater treatment plants investigated.

Though the microaeration technique is an efficient desulfurization method, further research can improve the desulfurization efficiency at industrial scale. Concerns to be addressed are: (i) S^0 deposition in the anaerobic digester headspace, and (ii) effect of excess air or O_2 on the anaerobic digestion process, especially the consequence of aerobic biodegradation of substrates on CH_4 production.

Biofiltration

Biofiltration (Figure 2.3) represents gas treatment by contacting the gas with a biofilm in a fixed bed bioreactor type (Barbusinski et al., 2017; Rybarczyk et al., 2019).

Biofiltration systems can be broadly categorized into either biofilters (BFs) or biotrickling filters (BTFs). BFs (Table 2.3) and BTFs (Table 2.4) are frequently used for biological waste-gas treatment including H_2S removal under both aerobic and anoxic conditions. In BTFs, the liquid phase is continuously trickled over the filter bed, while in BF systems, a water or nutrient salt solution is used intermittently to prevent the filter bed from drying. Efficient pollutant biodegradation or bioconversion in biofiltration processes depends on key components such as packing or filter bed materials, microbial inoculum, biofilm characteristics and operating conditions (Abubackar et al., 2019; Okoro and Sun, 2019; Rybarczyk et al., 2019).

Selection of a proper packing material is a prerequisite for biofiltration to achieve immobilization of the microbial consortia (Vikrant et al., 2018). In addition, the physico-chemical properties of the packing material (e.g. porosity, water holding capacity, buffering capacity, nutrient availability or mechanical resistance) strongly influence the hydrodynamics and the bioavailability of the pollutant for degradation. Both natural (e.g. wood chips or compost; Taheriyoun et al., 2019) and inert (e.g. polyurethane foam; Khanongnuch et al., 2019a) organic packing materials are used for biofiltration. Low cost and easy availability are the advantages of natural organic packing materials and some materials, e.g. biochar and charcoal, also assist in the biodegradation process (Li et al., 2016; Lin et al., 2018). Inert packing materials such as plastic supports or porous ceramics are mainly used in BTFs (Lin et al., 2018), while natural filter bed materials are generally used in BFs (Allievi et al., 2018; Das et al., 2019) for gas desulfurization. Compaction (that leads to channelling and a significant pressure drop) and shorter life span (usually less than five years) are the main drawbacks of natural organic packing materials compared to inert organic materials (Cheng et al., 2019; Kennes and Veiga, 2002).

There is a wide range of variations in BFs (Table 2.3) and BTFs (Table 2.4) in terms of operating conditions, reactor configuration and pollutant elimination capacity. In most cases, the reactors are used for single pollutant removal, e.g. H_2S removal. Issues that need to be addressed in biofiltration research are: (i) low pollutant removal efficiency for high inlet loading rates (Reddy et al., 2019), (ii) poor microbial density in BFs because of limited access by microorganisms to nutrients (Okoro and Sun, 2019), (iii) filter bed clogging problems due to S^0 accumulation (Le Borgne and Baquerizo, 2019), and (iv) sustained growth of the microbial community (Okoro and Sun, 2019).

Several commercial biological biogas desulfurization technologies using the BTF configuration are employed globally (Choudhury et al., 2019; Lin et al., 2018). BTF based commercial technologies include Biopuric™ (Veolia, France; Lin et al., 2018), BIOSULFEX® (Promis Company, Poland; Choudhury et al., 2019), SulfurexBF® (DMT Environmental Technology, The Netherlands; Lin et al., 2018), and BiogasCleaner® (Biogasclean, Denmark; Lin et al., 2018).

Table 2.3: Performance of biofilters (BFs) for H_2S removal from biogas (Reference list updated from Abubackar et al., 2019).

OT, days	IS and/or remarks	Predominant microbes	Packing material	Bed volume, L	Conditions and/or notes	IC, ppmv	ILR, g m^{-3} h^{-1}	EC, g m^{-3} h^{-1}	MILR, g m^{-3} h^{-1}	MEC, g m^{-3} h^{-1}	RE, %	pH of the LM	EBRT, s	Reference
110	Activated sludge from WWTP	NR	Compost and biochar (3:1)	~ 4.5	Aerobic, lab-scale	~ 780 ~ 630	~ 33 ~ 39	~ 33 ~27	34 40	34 28	> 99 70	NR	119 80	Das et al., 2019
21	Domestic waste composting, no additional microbial inoculation	NR	Pretreated compost product	31	Aerobic, pilot-scale, mixed pollutants (H_2S, CH_3SH, CS_2, NH_3)	~ 300	~ 1.4	~ 1.4	1.7	1.4	90-97	NR	~ 750	Yu et al., 2019
5	Sludge, SOB batch activity test of 8 palm oil mill's biofiltration systems	NR	NR	NR	Palm oil mill biogas, anaerobic	2000-3000	NR	7.5-15	NR	~ 15	~ 80	6.4-7.2	NR	Promnuan and O-Thong, 2017
37	Pure culture of *A. thiooxidans*	*Acidithiobacillus thiooxidans*	wood chips	~ 1.5	Aerobic, lab-scale, temperature ~ 30°C	10000	174	130	174	169	75	4.4	289	Aita et al., 2016

Note: EBRT - empty bed residence time; EC - elimination capacity; IC - inlet concentration; ILR - inlet loading rate; IS - inoculum source; LM - liquid medium; MEC - maximum elimination capacity; MILR - maximum inlet loading rate; NR - not reported; OT - operating time; RE - removal efficiency

Table 2.4: Performance of aerobic and anoxic biotrickling filters (BTFs) for H_2S removal from biogas.

OT, days	IS and/or remarks	Predominant microbes	Packing materials	Bed volume, L	Condition	IC, ppmv	ILR, g m^{-3} h^{-1}	EC, g m^{-3} h^{-1}	MILR, g m^{-3} h^{-1}	MEC, g m^{-3} h^{-1}	RE, %	pH of the LM	EBRT, s	Reference
14	Acid acclimatized inoculum from a pilot scale bioreactor	*Acidithiobacillus caldus*	Polypropylene material (pall ring type)	5.0	Semi-pilot scale, aerobic, temperature 33°C, LRR 7.2 L h^{-1}	~ 1800	18-38	NR	38.5	~ 30	~ 95 ~ 70	2.0	1200 300	Reddy et al., 2019
10	A pure stain of *Paracoccus pantotrophus* NTV02	*Paracoccus pantotrophus*	High-density polyethylene	1.0	Aerobic, LRR 0.5 and 3.6 L h^{-1}	100-2000	NR	NR	83.6	83.0	> 98	~ 8.0	120	Juntranaporn et al., 2019
138	*Thiobacillus* dominated lab-scale MBBR	*Thiobacillus*	Polyurethane foam cubes	2.1	Anoxic; autotrophic and mixotrophic condition; temperature 24ºC; N/S ratios of 1.2-1.7 mol mol^{-1}; C/N ratio of 0.2; HRT 115 min	~ 450	NR	NR	~ 20	19.2	~ 99	~ 7.0	210	Khanongnuch et al., 2019a
78	Previously operated BTF (Khanongnuch et al., 2019a), Bioaugmentation with *Paracoccus* MAL 1HM19	*Thiobacillus* sp., *Paracoccus* sp.	Polyurethane foam cubes	2.1	Anoxic, transient state (i.e. effect of liquid flow rate, wet–dry bed operations, H_2S shock loads), HRT 19 min	~ 950 (during shock loads)	~ 35	NR	NR	38	> 93	~ 7.0	180	Khanongnuch et al., 2019b
224	Mesophilic microbial consortium enriched	*Thioalkalivibrio*	Open pore polyurethane foam	3.0	Aerobic; simultaneous removal of organic and inorganic sulfur compounds	96	12	NR	NR	16.8	~ 98	10	40	Arellano-García et al., 2018

	from soils and sediments of a lake												
80	Anoxic sludge; integration of biogas desulfurization and biogas slurry (BS) denitrification	*Thiobacillus*, *Sulfurimonas*, *Methanosaeta*	Pall rings	5.0	Anoxic; temperature ~ 30ºC,	2000	36 36	~ 25 30 22 (BS)	NR	NR	84 62	7.0	420 420	Zeng et al., 2018
105	Nitrate-reducing and sulfide oxidizing bacteria (NR-SOB)	NR	Polypropylene pall rings	2.4	Anoxic; temperature 28-30ºC, nitrate limiting conditions (N/S ratio ~ 0.7 mol mol^{-1}); TLV 15 m h^{-1}	1400-14600	~ 200 < 120	~ 170	201	NR	~ 85 99	7.5	144	Fernández et al., 2013
270	Activated sludge from WWTP, a full scale prototype of MBBTF treated 8000 m^3 h^{-1} of waste gas stream	*Acidithiobacillus*	Polyurethane foam and polypropylene pall rings	8000	Aerobic; optimum temperature25-27ºC; biodiscs rotation velocity 0.1 rpm; rotation frequency 5 min in every 12 h	~ 125	NR	~ 60	NR	90	> 80	3.0	3.5	Spennati et al., 2017; Giordano et al., 2018
220	Activated sludge from WWTP	NR	3D-printed mesh honeycomb monolith	NR	Aerobic; preferred H_2S/O_2 ratio 1:2; temperature 20-25ºC; TLV 13 m h^{-1}	1000	~ 125	122	NR	NR	95	~ 7.0	41	Qiu and Deshusses, 2017

~ 6	Full-scale activated sludge system	*Halothiobacillus neapolitanus* NTV01	High-density polyethylene	1	Aerobic; temperature~ 32ºC	~ 2000 ~ 1500	~ 65 ~ 70	~ 60 ~ 35	NR	78	~ 88 ~ 40	~ 7.0	120 40	Vikromvarasiri et al., 2017
~ 8	Full-scale activated sludge system	*Halothiobacillus neapolitanus* NTV01	High-density polyethylene	0.5	Aerobic; temperature 30-32ºC	255	NR	NR	NR	NR	~ 98	7.0	60	Vikromvarasiri and Pisutpaisal, 2016;
~ 500	Lab scale BTF, same reactor as described in Montebello et al., 2012	*Acidithiobacillus* sp.	Stainless steel and pall rings	2.4	Aerobic; limited supply of O_2 (O_2/H_2S ratio ~ 8 v/v); TLV 7 m h^{-1}	2000 10000	263	100	NR	223	> 99	~ 2.5	~ 75 130	Montebello et al., 2014
~ 365	Aerobic sludge from municipal WWTP	NR	Stainless steel and pall rings (aerobic) open pore polyurethane foam cubes (anoxic)	2.0 (aerobic) 2.4 (anoxic)	Aerobic and anoxic; simultaneous removal of organic and inorganic sulfur compounds; TLV 7 m h^{-1}	~ 2000	~ 155 (aerobic) ~ 155 (anoxic)	~ 95 ~ 125	~ 300 ~ 300	~ 95 ~ 140	~ 62 ~ 80	~ 6.5 ~ 7.5	60 60	Montebello et al., 2012

Note: BTF- biotrickling filter; EBRT - empty bed residence time; EC - elimination capacity; HRT - hydraulic retention time; IC - inlet concentration; ILR - inlet loading rate; IS - inoculum source; LM - liquid medium; LRR - liquid recirculation rate; MBBR - moving bed biofilm reactor; MBBTF - moving bed biotrickling filter; MEC - maximum elimination capacity; MILR - maximum inlet loading rate; NR - not reported; OT - operating time; RE - removal efficiency; TLV - trickling liquid velocity; WWTP- wastewater treatment plant

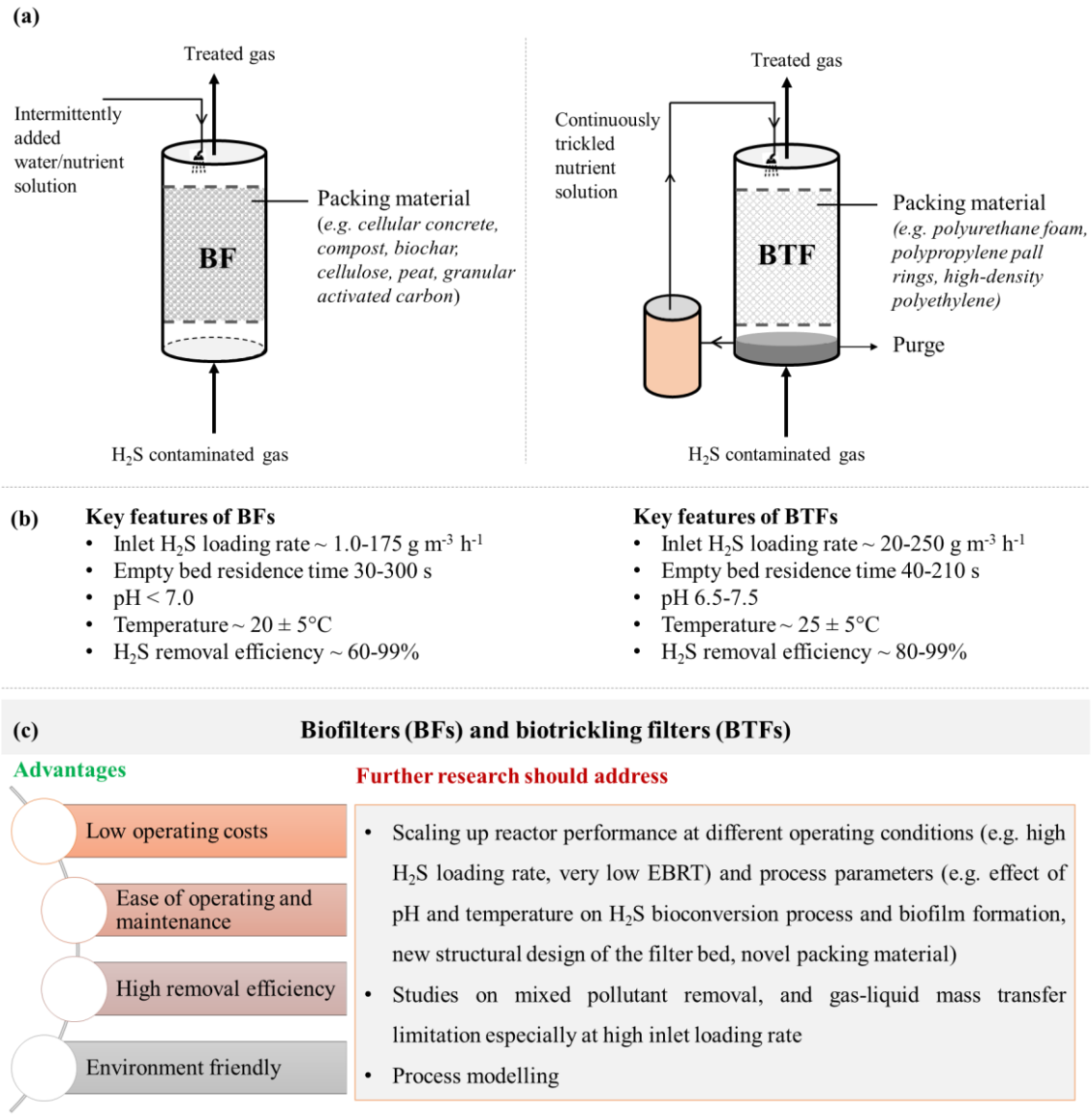

Figure 2.3: Overview of biofiltration processes applied for H_2S removal: (a) schematic representation of biofilter (BF) and biotrickling filter (BTF), (b) key features of biofiltration processes used for desulfurization, and (c) advantages and future research requirements.

Bioscrubber

A bioscrubber (Figure 2.4) consists of two operational units: (i) absorption tower, i.e. a unit that absorbs pollutants, i.e. H_2S, in an aqueous phase, and (ii) bioreactor unit wherein microorganisms convert the dissolved pollutant into end products, i.e. SO_4^{2-}, H_2O and biomass. Bioscrubbers (BSs) are mainly reported for water soluble single pollutant (e.g. H_2S, NH_3 or fatty acids) removal (Ren et al., 2019). BSs can also be used for mixed pollutant removal by modifying the reactor design, e.g. two-liquid phases (water and

organic solvent; Mudliar et al., 2010), spray columns (Ren et al., 2019) or two-stage systems (consists of two bioreactor units: a liquid impelled loop reactor unit and an airlift loop reactor unit; Mudliar et al., 2010). A high efficiency for removal of water soluble pollutants and capability to operate under a wide range of conditions (e.g. pH, temperature or nutrients) are the main advantages of BSs compared to BTFs (Abubackar et al., 2019; Ren et al., 2019). The main drawbacks of BSs are secondary pollution generation from the liquid waste stream as well as operational and maintenance complexity (Le Borgne and Baquerizo, 2019).

Biogas desulfurization using BSs has been studied on lab-scale and pilot scale (San-Valero et al., 2019; Esmaeili-Faraj et al., 2019). San-Valero et al. (2019) studied a lab-scale bioscrubber (bioreactor working volume of ~ 1 L) for H_2S rich biogas desulfurization using synthetic biogas (0.5% H_2S in N_2) and achieved removal efficiencies of > 80% for 80 days operation with the following process parameters: aerobic; biogas/air ratio of 1:1(*v/v*) in the bioreactor unit; pH of ~ 8.0; inlet H_2S concentration of 5000 ppm_v; applied inlet H_2S loading rates of ~ 40-100 g m^{-3} h^{-1}; gas residence times of 6.6, 4.1 and 2.4 min (in the absorption column) and liquid phase recirculation (counter-currently, from bioreactor unit to the absorption column) velocities of 2.5 and 3.7 m h^{-1}.

Nanofluids (colloids of nanoparticles, e.g. SiO_2-water, CuO-water, Al_2O_3-methanol) can promote the absorption of a gaseous pollutant, e.g. NH_3 or CO_2 (Ashrafmansouri and Esfahany, 2014). The H_2S absorption efficiency of a pilot-scale bioscrubber increased from 23-38% to 52-61% after addition of silica nanoparticles (~ 20 nm, 0.1% wt) in the scrubbing liquid (i.e. water) and achieved a H_2S removal efficiency of ~ 97% for 32 days operation with the following operational parameters: aerobic; pH ~ 8.0; inlet H_2S concentration of 3500-4000 ppm_v; no recirculation of the liquid phase (from bioreactor unit to absorption column); biogas residence times of 27 and 12 s (in the absorption column) and absorbent residence time of ~ 3 h in the bioreactor unit (Esmaeili-Faraj et al., 2019).

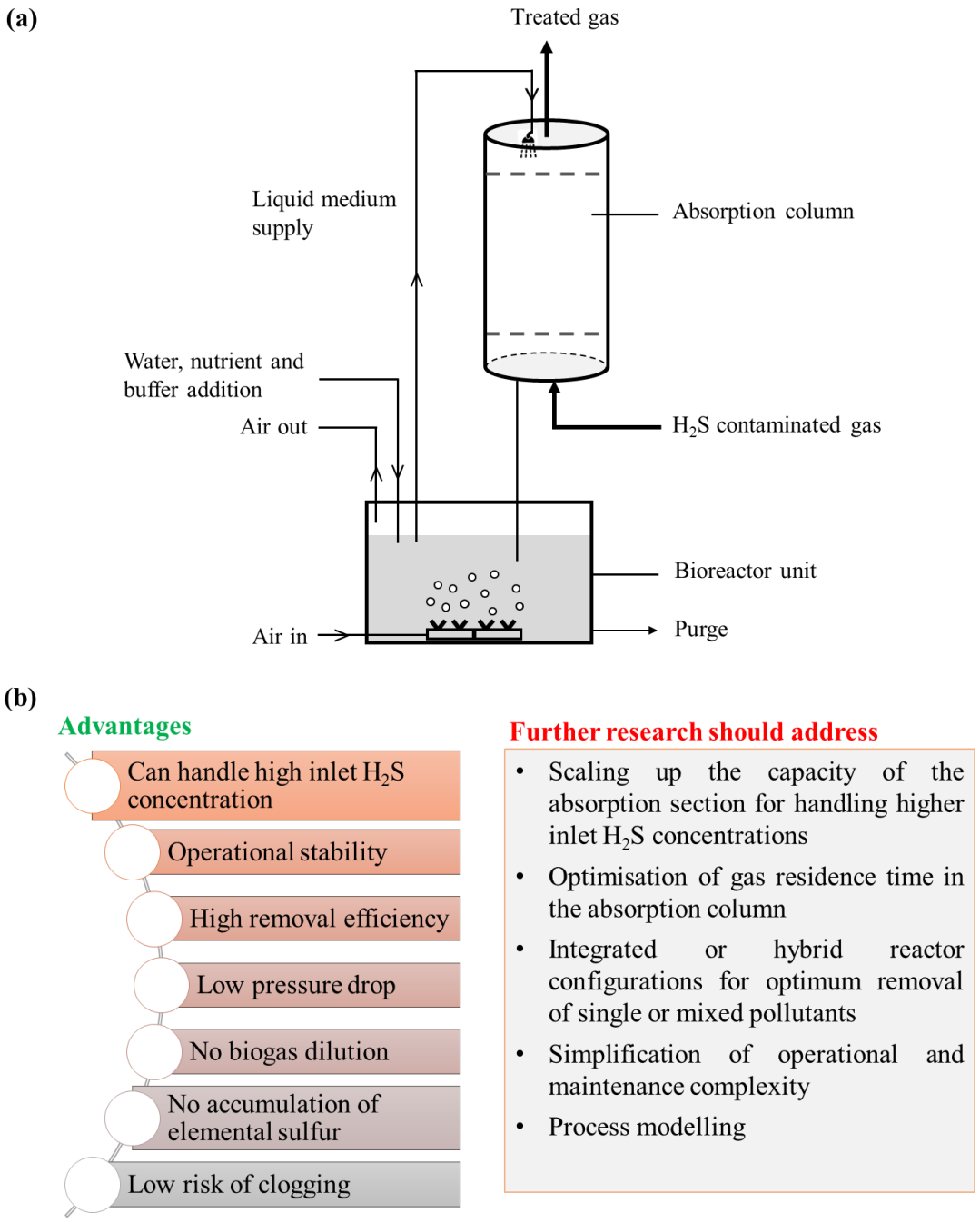

Figure 2.4: Overview of the bioscrubbing process applied for H_2S removal: (a) schematic representation of a bioscrubber (BS) and (b) advantages and future research requirements.

There are several BS based commercial technologies including THIOPAQ® (Paques, the Netherlands; López et al., 2013; San-Valero et al., 2019), Sulfothane™ (Veolia, France; Lin et al., 2018) and Biogasclean ECO (Biogasclean, Denmark; Piñas et al., 2019; Biogasclean, 2020). These commercial desulfurization technologies treat H_2S from a wide range of raw biogas in terms of inlet H_2S concentration and loading rate. For

example, THIOPAQ® can handle biogas flow rates of 50-2500 $Nm^3\ h^{-1}$ and a sulfur load up to 600 kg S day^{-1} (López et al., 2013; San-Valero et al., 2019). Biogasclean ECO (installed in Sika Farm in Philippines) has a capacity to clean raw biogas having a H_2S concentration of 2500 ppm_v with a flow rate of 250 $m^3\ h^{-1}$ (Biogasclean, 2020; Piñas et al., 2019).

2.2.2. NH_3 removal

Biological NH_3 removal mechanisms

Prior to NH_3 removal in a bioreactor, gas-liquid mass transfer occurs in a scrubber. Allowing sufficient contact time between gas-phase NH_3 and the scrubbing liquid allows NH_3 to dissolve as NH_4^+ in aqueous medium (Eq. 2.1), which is subsequently oxidized by nitrifying bacteria present in the bioreactor.

Bioconversion of NH_3 takes place in two steps as shown in equations 2.2 and 2.3. In a first step, ammonia oxidizing bacteria (AOB) oxidize NH_3 to nitrite (NO_2^-) and then, nitrite oxidizing bacteria (NOB) further oxidize NO_2^- to nitrate (NO_3^-). In these bioconversion processes, NH_3 and NO_2^- acts as electron donor, whereas CO_2 and O_2 are the carbon source and electron acceptor, respectively. pH is a key parameter for microbial growth and efficient NH_3 conversion through mass transfer from the gaseous to liquid phase (Joshi et al., 2000; Gerrity et al., 2016; Van der Heyden et al., 2019a). The overall nitrification process of NH_3 and biomass formation is shown in Eq. 2.4 (Wang et al., 2019b). Another NH_3 removal process (Eq. 2.5) is the biological ammonium oxidation in the presence of NO_2^- (Anammox). This process is strictly anaerobic and exothermic, and widely accepted for NH_3 rich wastewater treatment (Pal, 2017). However, aerobic processes are commonly used for gas-phase NH_3 removal (Van der Heyden et al., 2019a).

$$NH_3 + H^+ \rightleftharpoons NH_4^+ \quad (2.1)$$

$$NH_3 + 1.5O_2 \rightarrow NO_2^- + H^+ + H_2O \quad (2.2)$$

$$NO_2^- + 0.5O_2 \rightarrow NO_3^- \quad (2.3)$$

$$NH_3 + 1.86O_2 + 1.98HCO_3^- \rightarrow 0.02C_5H_7NO_2 + 1.04H_2O + 0.98NO_3^- + 1.88H_2CO_3 \quad (2.4)$$

$$NH_4^+ + NO_2^- \rightarrow N_2 + H_2O \quad (2.5)$$

The following bacteria (at genus level) can be present in NH_3 removing biofiltration systems, AOB: *Nitrosococcus* (family *Chromatiaceae*) and NOB: *Nitrobacter* (family

Bradyrhizobiaceae), *Nitrococcus* (family *Ectothiorhodospiraceae*) and *Nitrospina* (family *Nitrospinaceae*). Apart from nitrifiers, also denitrifiers (e.g. *Comamonas nitrativorans*) can be present, as the denitrification process can also take place to reduce NO_2^-, NO_3^- and nitrous oxide (N_2O) into nitrogen (N_2), thus ensuring complete nitrogen removal (Van der Heyden et al., 2019b).

Bioreactor systems for NH_3 removal

Biofiltration (BFs and BTFs) techniques are mainly applied for treating exhaust air having high NH_3 emissions from agricultural and livestock farms (Blázquez et al., 2017; Joshi et al., 2000; Kafle et al., 2015; Tsang et al., 2015; Van der Heyden et al., 2019a). The removal performance of BFs and BTFs depended on process parameters. A biofilter inoculated with the marine bacterium *Vibrio alginolyticus* was used for treating a high NH_3 load (~ 23 g N kg^{-1} dry packing material d^{-1}) with a RE > 85% (Kim et al., 2000). Kafle et al. (2015) evaluated the effectiveness of (wood bark based) BFs handling NH_3 and H_2S emissions, and found that BFs can achieve a removal efficiency of > 95% at an EBRT of 2-3 s. Similar mixed gas treatment, i.e. simultaneous removal of NH_3 and H_2S in BFs systems was carried out by Malhautier et al. (2003) who found high H_2S inlet concentrations (140-280 mg m^{-3}) induce environmental stress on the nitrifying bacterial community. Lee et al. (2013) studied biofiltration of a complex gas mixture of inorganic (ammonia) and organic (methane, ethylene, acetone, n-butanol) compounds. All bioreactors (4 BFs and 2 BTFs) tested achieved a nearly 100% removal efficiency for the water-soluble compounds, i.e. ammonia, acetone and n-butanol.

Apart from biofiltration techniques, a few other types of biological reactors have been used for NH_3 removal (Figure 2.5). Wang et al. (2019b) studied the application of a 'biological folded non-aerated filter reactor (BFNAF)' for ammonium nitrogen (NH_4^+-N) removal from wastewater to overcome the main drawbacks (e.g. high energy consumption for aeration) of a biologically aerated filter (BAF). This folded structure based BFNAF operated for 135 days and achieved ~ 94% RE with an EC of ~ 100 g NH_4^+ m^{-3} d^{-1}. Chen et al. (2018) tested an airlift bioreactor (AB) system to treat simultaneously H_2S and NH_3 from waste gases. The reactor was effective for simultaneous removal of both gases with > 98% removal efficiency. The removal performance depended on a number of process parameters such as gas retention time, inoculum dilution ratio,

fluorescent light intensity, addition of Fe_2O_3 catalyst, and H_2S concentration. Gerrity et al. (2016) showed the possibility of the horizontal flow biofilm reactor (HFBR) system for treating gas-phase NH_3. The HFBR achieved ~99% RE with a maximum loading rate of ~ 115 g m^{-3} d^{-1} for 90 days operation at 10ºC. *Nitrosomonas* and *Nitrosospira* were the most abundant genera. The design of the HFBR ensured a sufficient contact time (EBRT of 120 and 60 s) for gas-liquid mass transfer. The integrated approach (e.g. nitrification in a continuous stirred tank bioreactor integrated with anoxic desulfurization in a BTF or gas-lift bioreactor) demonstrated the possibility of simultaneous treatment of ammonium-rich wastewater and biogas desulfurization (Cano et al., 2021; González-Cortés et al., 2021).

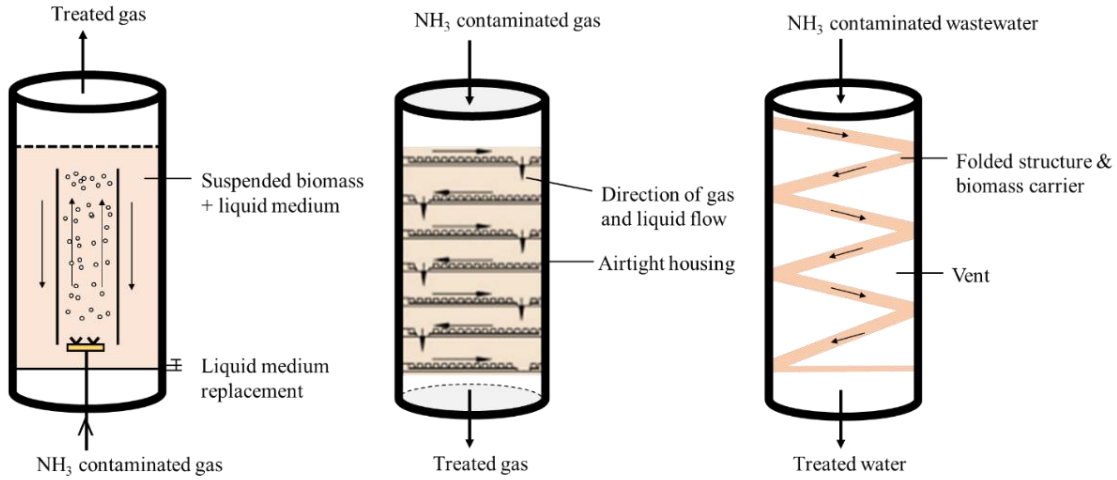

Note: Schematics of the biofiltration systems, i.e. biofilter (BF) and biotrickling filter (BTF) are shown in Figure 3
Reference: Chen et al., 2018; Gerrity et al., 2016; Wang et al., 2019b

Figure 2.5: Overview of NH_3 removal in a bioreactor: (a) schematic of the bioreactors, and (b) NH_3 removal mechanism.

2.2.3. Siloxanes removal

Types of siloxanes in biogas

Organosiloxanes represent organosilicone polymers containing Si-O-Si bonds, wherein organic groups (e.g. methyl or ethyl) are bound to the Si atom (Wang et al., 2019c). Organosiloxanes are extensively used in industries as cleaning agents, fuel additives, surface treatment agents and additives (for manufacturing personal care products such as shaving foams and shampoo) because of their excellent physico-

chemical properties, e.g. low surface tension, high thermal stability and high resistance to environmental oxidation (Shen et al., 2018; Wang et al., 2019c). A fraction of organosiloxanes ends up in the waste streams, especially in sewage and industrial waste (Shen et al., 2018). During anaerobic digestion of organosiloxanes contaminated waste (e.g. secondary wastewater treatment sludge), the organosiloxanes volatilize and enter into the biogas as volatile methyl siloxanes (VMS). VMS are typically classified into two types, linear and cyclic, based on their structures. These are abbreviated as Ln and Dn, respectively, wherein n depicts the number of silicon (Si) atoms. The following VMS types are commonly found in raw biogas (Shen et al., 2018; Wang et al., 2019c): L2 (Hexamethyldisiloxane), L3 (Octamethyltrisiloxane), L4 (Decamethyltetrasiloxane), L5 (Dodecamethylpentasiloxane), D3 (Hexamethylcyclotrisiloxane), D4 (Octamethylcyclotetrasiloxane), D5 (Decamethylcyclopentasiloxane), D6 (Dodecamethylcyclohexasiloxane).

VMS removal mechanisms

VMS is a potential carbon source for microorganisms and can be degraded by various microorganisms including *Arthrobacter*, *Agrobacterium*, *Fusarium oxysporum*, *Methylibium* sp., *Pseudomonas* sp., *Phyllobacterium myrsinacearum, Rhodanobacter* and *Xanthomonadacea* (Accettola et al., 2008; Boada et al., 2020; Li et al., 2014; Shen et al., 2018; Wang et al., 2014). In addition, VMS can be degraded into several metabolites, which are further mineralized to CO_2 and silica (Popat and Deshusses, 2008; Santos-Clotas et al., 2019; Wang et al., 2019c). VMS biodegradation pathways and formation of VMS metabolites during microbial degradation are not yet fully elucidated. Li et al. (2014) and Wang et al. (2014) proposed several degradation pathways of D4 in BTF systems including the metabolites, wherein the metabolite formation followed three key reaction routes: hydrolysis, oxidation and rearrangement (Figure 2.6).

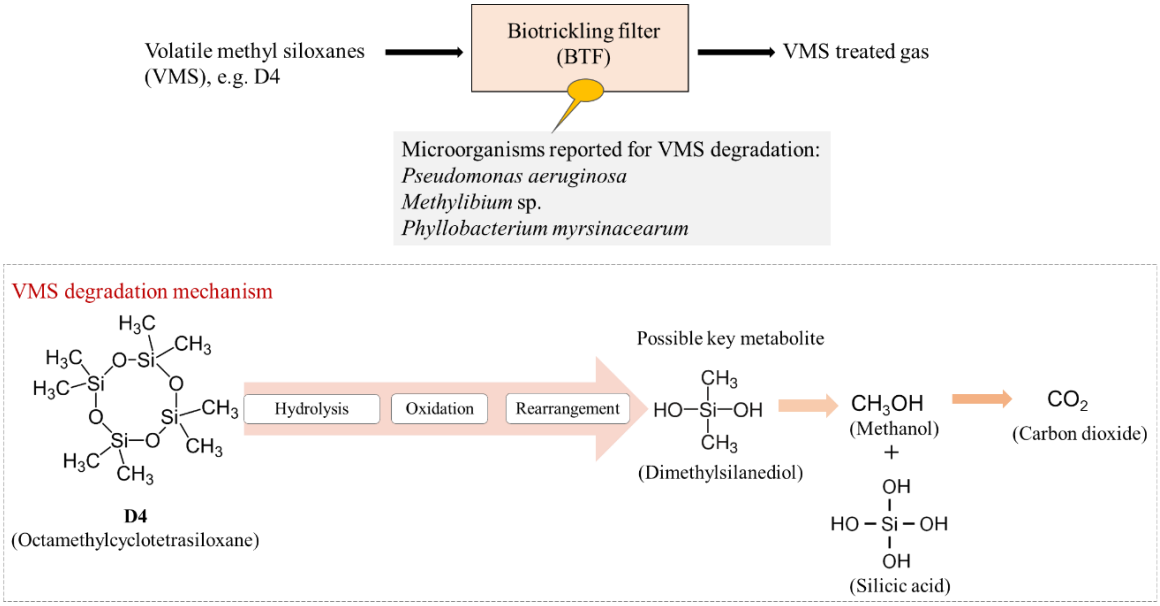

Figure 2.6: Schematic of VMS biodegradation mechanism in BTF (Reference: Boada et al., 2020; Li et al., 2014; Wang et al., 2014).

Approaches for VMS removal from biogas

Physico-chemical methods such as activated carbon adsorption, phosphoric acid absorption, water scrubbing or membrane separation are commonly used for VMS removal while biological methods have been tested mainly at lab scale (Santos-Clotas et al., 2019; Yang and Corsolini, 2019). Table 2.5 summarizes the bioreactors used for VMS removal and their key features. BTFs are mainly used for VMS treatment, although only a few types of VMS have been studied. The bioreactors achieved a low RE in most cases with long gas residence times. Yang and Corsolini (2019) evaluated the performance of a biofilter integrated with an activated carbon filter (ACF) in order to justify the technical feasibility of a biofilter for VMS removal from biogas and compare the performance of the two stage 'biofilter + ACF' with that of an ACF only. The authors reported that the biofilter + ACF system increased the removal efficiency of D3, D4 and D5 by ~ 7, 15 and 9%, respectively, compared to the ACF only. The improved removal performance was due to either direct capture of VMS by the biofilter or the biofilter partially removed water vapour from the biogas which enhanced subsequent VMS removal in the ACF.

Pascual et al. (2021) studied a two-phase partitioning BTF system to improve the VMS removal efficiency where the total VMS (L2, L3, D4 and D5) removal increased from 35 to 52% by increasing the share of the organic fraction (silicone oil) from 5 to 45% in the

aqueous-organic recirculation mixture. In addition, the linear VMS (L2) demonstrated lower solubility in the organic phase compared to the cyclic VMS (D4, D5) due to the higher vapour pressure of L2. The authors also reported that a sharp decline in gas residence time (from 60 min to 15 min) triggered gas-liquid mass transfer limitation. Further research to improve the VMS removal efficiencies needs to be carried out, especially to overcome gas-liquid mass transfer limitations, to identify and utilize suitable microbial consortia for VMS degradation, and to depict the VMS biodegradation pathways.

Table 2.5: Comparison of bioreactor performance for the removal of VMS from biogas.

Bioreactors type	OT, days	Types of VMS	IC, mg m^{-3}	EBRT, s	EC, g m^{-3} h^{-1}	RE, %	Remarks and/or key parameters	Reference
BTF (two-phase partitioning)	172	Mixed (L2, L3, D4 and D5)	~ 700-900	3600 900	0.56 1.80	76 49	EBRT, fraction of silicone oil, types of VMS	Pascual et al., 2021
BTF (anoxic, PM -lava rock)	50	D4	62	900	0.21-0.24	~ 10-15	Mixed pollutants (VMS + VOCs), *Methylibium* sp. and *Pseudomonas aeruginosa* dominated, biodegradability trend: D5 > D4	Boada et al., 2020
		D5			0.10-0.20	~ 25-45		
BTF (anoxic, PM - lava rock)	152	D4	~ 60	870	~ 0.03	13	Mixed pollutants (VMS + VOCs), addition of activated carbon (20%) influenced gas-liquid mass transfer	Santos-Clotas et al., 2019
		D5		870	~ 0.14	37		
Biofilter + activated carbon filter (ACF)	42	D3 D4 D5	330-1190 73-170 13-38	NR	NR	~ 98 ~ 92 ~ 80	RE of biofilter + ACF and ACF only showed similar trend	Yang and Corsolini, 2019
BTF (aerobic, PM - polypropylenering)	120	D4	50 150	1440 480	~ 0.15	60 ~ 15	Optimum pH 4.0-6.0, *Phyllobacterium myrsinacearum* dominated, main metabolite: $Me_3Si\text{-}O\text{-}SiMe_2\text{-}O\text{-}SiMe_3$	Wang et al., 2014
BTF (aerobic, PM - porous lava rock)	275	D4	20-140 50	198	~ 0.44	48	pH: 6.7-7.2, *Pseudomonas aeruginosa* S240 dominated, metabolites: dimethylsilane-diol, methanol and silicic acid	Li et al., 2014
				792	~ 0.17	74		
BTF aerobic	240	D4	~ 45	50-120 1170	0.03-0.10	~ 10 ~ 40	Very slow gas-liquid mass transfer	Popat and Deshusses, 2008
anaerobic	180	D4		240		< 16		
BTF (aerobic, PM - pall ring)	60	D3	45-77	126-216	~ 0.20	10-20	*Pseudomonas* sp. dominated	Accettola et al., 2008

Note: VMS - volatile methyl siloxanes; PM - packing material; BTF- Biotrickling filter; D3 - Hexamethylcyclotrisiloxane; D4 - Octamethylcyclotetrasiloxane; D5 - Decamethylcyclopentasiloxane; L2 - Hexamethyldisiloxane, L3 - Octamethyltrisiloxane, OT - Operating time; IC - inlet concentration; EC - elimination capacity; RE - removal efficiency; EBRT - empty bed residence time; NR - not reported

2.2.4. VOCs removal

Types of VOCs in biogas

Different types of VOCs including monoaromatic hydrocarbons (e.g. toluene and p-cymene; concentration range ~ 3.0-225 µg m^{-3}), linear hydrocarbons (generally C_9-C_{13}, e.g. undecane; concentration range ~ 2.0-1540 µg m^{-3}), terpenes (e.g. α-pinene and D-limonene; concentration range ~ 10-65 µg m^{-3}), halogenated compounds (e.g. iodomethane and tetrachloroethylene; concentration range ~ 1.0-185 µg m^{-3}) and organosulfur compounds (e.g. carbon disulfide; concentration range ~ 1.0-115 µg m^{-3}) have been identified in raw biogas from municipal and sewage sludge digestion (Paolini et al., 2018).

VOCs removal mechanisms

VOCs are converted to CO_2 and water as metabolic end products during the biodegradation process according to the stoichiometric equations (Kennes et al., 2009) considering biomass growth as shown in Eq. 2.6 (biodegradation of toluene) and Eq. 2.7 (biodegradation of monochlorobenzene):

$$1.55C_7H_8 + 12.9O_2 + 0.2NH_4Cl \rightarrow CH_{1.8}N_{0.2}O_{0.5} + 9.85CO_2 + 5.6H_2O + 0.2HCl \quad (2.6)$$

$$C_6H_5Cl + 3.69O_2 + 0.265NH_4NO_3 \rightarrow 2.65CH_{1.8}N_{0.2}O_{0.5} + 3.35CO_2 + 0.15H_2O + HCl \quad (2.7)$$

The following predominate bacterial strains support VOCs biodegradation in BTFs: *Pseudomonas putida*, *Rhodococcus erythropolis* and *Cladosporium sphaerospermum* for benzene, toluene, ethylbenzene and xylene (BTEX); *Burkholderia* sp. strain T3 and *Bacillus cereus* S1 and S2 for toluene*; Pseudomonas oleovorans* DT4 for ethylbenzene; *Ralstonia pickettii* L2 for chlorobenzene; *Ralstonia eutropha* for styrene; and *Bacillus cereus* GIGAN2, *Pseudomonas putida* and *Pseudomonas acidovorans* for dimethyl disulfide degradation (Wu et al., 2018). Fungi can also degrade VOCs and still have effective mass transfer of hydrophobic VOCs at low humidity (Wu et al., 2018). In addition, the filamentous structure of fungi (e.g. *Scedosporium* sp.) favours VOCs absorption.

The biodegradability of VOCs depends on several factors: (i) presence of an acclimatized microbial community capable to utilize VOCs as carbon source, (ii) gas-

liquid and liquid-biofilm mass transfer which can be influenced by VOCs characteristics such as solubility, molecular size and compounds having different biodegradation order (e.g. oxygenated > aromatic > halogenated compounds), and (iii) interactions between compounds, i.e. the presence of one compound can affect the removal of other pollutants (Cheng et al., 2016; Guieysse et al., 2008; Malhautier et al., 2005).

Approaches for biological VOCs removal

Several bioreactor configurations such as BFs, BTFs and BSs have been used for VOCs removal. Biofiltration (BFs and BTFs) for VOCs treatment has been comprehensively reviewed in recent publications wherein the source of VOCs was either a waste gas stream (mainly from industries) or synthetic VOCs used for lab-scale research (Wu et al., 2018; Yang et al., 2018). Though these bioreactors are applied for single or mixed VOCs removal, very few publications reported biological VOCs removal from raw biogas (Franco-Morgado et al., 2018; Lakhouit et al., 2016). Santos-Clotas et al. (2019) used BTF systems for efficient removal of VOCs such as toluene, hexane and limonene from sewage biogas in the presence of VMS (D4 and D5).

Three types of interactions, i.e. antagonistic, neutral and synergistic, can occur during VOCs removal in BFs (Yang et al., 2018). Competitive inhibition between hydrophilic and hydrophobic VOCs are the main obstacles towards effective biodegradation in BFs (antagonistic effect). Substrate interactions can significantly enhance the metabolism of other co-substrates by promoting microbial growth (synergistic effect). Alternatively, biodegradation of hydrophobic VOCs can increase significantly with the addition of hydrophilic VOCs in BFs (Yang et al., 2018).

Among the mentioned bioreactor configurations, BTFs have a better VOCs removal capacity, especially for recalcitrant VOCs. In addition, BTFs allow good control regarding nutrient supply, pH, and removal of toxic metabolites. Moreover, the biodegradability can be enhanced by formation of extracellular polymeric substances (EPS) that allow VOCs adsorption, followed by microbial degradation. Integration of BTF systems with other biological methods and innovations in bioreactor configuration are the future scope of BTFs for VOCs removal (Wu et al., 2018). In addition, interactions among multiple VOCs during their degradation and the metabolic pathways involved are recommended for future investigation (Yang et al., 2018).

2.3. Biogas upgradation to biomethane

Removal of biogas contaminants, mainly CO_2 and H_2S, significantly increases its quality, though getting a suitable methane enrichment technology is a challenging task in terms of cost, energy consumption and environmental impact (Awe et al., 2017). In this section, biological CO_2 removal technologies for biogas upgrading and key process parameters that enhance process stability in AD and minimize biogas impurities are discussed.

2.3.1. Bioconversion of CO_2 for enrichment of the CH_4 content

In-situ and ex-situ H_2 assisted biogas upgrading

Table 2.6 compares the H_2 assisted biogas upgrading performance of several types of bioreactors. H_2 assisted biological conversion of CO_2 to CH_4 is shown in Eqs. 2.8-2.11 including the growth of hydrogenotrophic methanogens (Eq. 2.11):

$$4H_2 + 2CO_2 \rightarrow CH_3COOH + 2H_2O \quad (2.8)$$

$$CH_3COOH \rightarrow CH_4 + CO_2 \quad (2.9)$$

$$CO_2 + 4H_2 \rightarrow CH_4 + 2H_2O \quad (2.10)$$

$$0.131CO_2 + 0.004HCO_3^- + 0.004NH_4^+ + 0.5H_2 \rightarrow 0.115CH_4 + 0.004C_5H_7O_2N + 0.266H_2O \quad (2.11)$$

In these bioconversion processes, homoacetogenic bacteria convert CO_2 to CH_3COO^- (Eq. 2.8), acetoclastic methanogenic archaea convert CH_3COOH to CH_4 (Eq. 2.9), and hydrogenotrophic methanogenic archaea convert CO_2 to CH_4 (Eq. 2.10). Hydrogenotrophic methanogens consume CO_2 as the carbon source and electron acceptor, and H_2 as electron donor (Angelidaki et al., 2018; Dupnock and Deshusses, 2017). CH_4 enrichment can be done either *in-situ* or *ex-situ*. In the *in-situ* upgrading process, CO_2 conversion to CH_4 takes place inside the anaerobic digester and H_2 is provided into the reactor from an external source which stimulates hydrogenotrophic methanogenic activity (Alfaro et al., 2019; Lai et al., 2021; Xu et al., 2020). The *ex-situ* upgrading process takes place in a separate anaerobic reactor containing enriched hydrogenotrophic cultures, with H_2 and CO_2 being externally supplied (Kougias et al., 2017; Tang et al., 2019).

In-situ and *ex-situ* concepts for H_2 assisted biological biogas upgrading are applied for over a decade and are promising biological biogas upgrading tools (Table 2.6). The *in-situ* upgrading process does not require any extra infrastructure, consequently it requires

lower capital investment compared to the *ex-situ* process (Lai et al., 2021). The bioreactor performance regarding H_2 assisted CH_4 enrichment depends on process parameters including temperature, pH, dominated microbial community, optimum CO_2:H_2 ratio and H_2 partial pressure (Table 2.6). A hybrid concept to scale up the upgrading performance by integrating *in-situ* and *ex-situ* reactors has also been proposed (Lai et al., 2021; Voelklein et al., 2019).

Table 2.6: Comparison of H_2 assisted biological biogas upgrading technologies.

Bioreactor type	Key features	Composition of enriched biogas	Remarks	Reference
Two-stage UASB reactor inoculated with AGS	*In-situ:* ▪ OLR: 1-5 gCOD L^{-1} d^{-1} ▪ H_2 feeding rate: 0.1-0.6 g L^{-1} d^{-1} ▪ Temperature 35°C ▪ *Anaerolineae* sp. dominated ▪ Syntrophic partnerships with methanogens ▪ OT 75 days	CH_4 > 90%, H_2 < 5%, CO_2 < 5%	▪ AGS can promote high OLR for higher biomass retention and methanogenic activity	Xu et al., 2020
Anaerobic digester of sewage sludge	*In-situ:* ▪ Submerged HFM module to provide H_2 ▪ H_2 flow rate: 0.87 L $L_{reactor}^{-1}$ d^{-1} ▪ OLR: 1.3-1.8 gVS L^{-1} d^{-1} ▪ Temperature 35°C ▪ Dominant hydrogenotrophic archaea: *Methanoculleus* sp., *Methanospirillum* sp., *Methanolinea* sp. and *Methanobacterium* sp. ▪ OT 240 days	CH_4 ~ 70-75%, H_2 ~ 7-18%, CO_2 ~ 11-20%	▪ Hydrogenotrophic methanogens outcompeted homoacetogens	Alfaro et al., 2019
Fed-batch biogas reactor	*In-situ:* ▪ OLR: 0.23-0.05 gCOD L^{-1} d^{-1} ▪ Optimum molar ratio of H_2 and CO_2: 4:1 ▪ Temperature 37°C ▪ Dominant hydrogenotrophic methanogen: *Methanobacterium* ▪ OT 80 days	Control: CH_4 ~ 67%, CO_2 ~ 33% H_2 assisted: CH_4 ~ 94%, CO_2 ~ 3%, H_2 ~ 3%	▪ Process stability was negatively influenced by pH increase ▪ High H_2 partial pressure can reduce CH_4 yield	Wahid et al., 2019
CSTR	*In-situ:* ▪ OLR: 2 gVS L^{-1} d^{-1} ▪ Dominant hydrogenotrophic methanogens: *Methanoculleus*, *Methanobrevibacter* and *Methanobacterium* ▪ Temperature 55°C ▪ OT 63 days	Relative CH_4 content ~ 80%	▪ Continuous mixing favored thermophilic biogas upgrading ▪ Sodium formate, an interspecies electron carrier, influenced propionate degradation during acetogenesis	Zhu et al., 2019a
CSTR	*In-situ:* ▪ Mesophilic vs thermophilic upgrading ▪ OLR: 2 gVS L^{-1} d^{-1}	Mesophilic digestion: H_2 consumption ~ 0.9 L d^{-1} CH_4 yield ~ 200 L kg^{-1} VS	▪ Temperature had a critical role in succession of microbial community structure	Zhu et al., 2019b

	▪ HRT: 25 days ▪ Temperature 35°C and 55°C ▪ OT 49 days	Relative CH_4 content ~ 65% Thermophilic digestion: H_2 consumption ~ 1.9 L d^{-1} CH_4 yield ~ 242 L kg^{-1} VS Relative CH_4 content ~ 68%	▪ Continuous stirring had negative effect on mesophilic system	
Fed-batch reactor	*Ex-situ:* ▪ Gas injection: CH_4 (53-55%), CO_2 (12-21%), H_2 (~ 98-170 mL) ▪ pH ~ 8.0 ▪ Temperature 37°C ▪ Dominated genus: *Methanoculleus* ▪ OT 31 days	CH_4 ~ 77-91%, CO_2 ~ 5-8%	▪ H_2 was completely consumed	Tang et al., 2019
Batch reactor and modified CSTR	*In-situ and ex-situ:* ▪ Grass silage selected as substrate ▪ Substrate retention time 46 days ▪ OLR: 4 gVS L^{-1} d^{-1} ▪ Gas injection (*ex-situ*): CH_4 (32%), CO_2 (14%), H_2 (54%) ▪ Temperature 55°C	*In-situ*: Productivity ~ 2.5 L CH_4 $L_{RV}^{-1}d^{-1}$ *Ex-situ*: Productivity ~ 3.7 LCH_4 $L_{RV}^{-1}d^{-1}$ Continuous *ex-situ*: CH_4 ~ 61%, CO_2 ~ 9%, H_2 ~ 30%	▪ Conversion of CO_2 to CH_4 decreased drastically when CO_2 level was below 9% ▪ Adequate level of H_2 required to ensure a balanced *in-situ* system	Voelklein et al., 2019
BTF	*Ex-situ*: ▪ Gas injection: H_2 (62%), CH_4 (23%), CO_2 (15%) ▪ BTF fed in co-current mode to avoid stripping of dissolved H_2 ▪ Temperature 35°C ▪ EBRT 32-47 min	*Ex-situ*: CH_4 production rates 10-20 m^3 $m^{-3}_{reactor}$ d^{-1} CH_4 > 97% H_2 removal 99% CO_2 removal 96%	▪ Increasing gas velocity lowered the upgrading capacity ▪ Linear relationship exist between methane concentration and the log average EBRT	Dupnock and Deshusses, 2019
Three different reactors: (i) two upflow reactors in series, (ii) CSTR and (iii) bubble column reactor	*Ex-situ:* ▪ Gas injection: CH_4 (23%), CO_2 (15%), H_2 (62%) ▪ Gas recirculation rate 12 L h^{-1} ▪ Temperature 52°C ▪ OT 51 days	Upflow reactors in series: CH_4 ~ 98%, CO_2 ~ 3%, H_2 < 0.1 % CSTR: CH_4 ~ 50%, CO_2 ~ 12%, H_2 ~ 38% Bubble column reactor: CH_4 ~ 95%, CO_2 ~ 3%, H_2 ~ 2%	▪ Biogas upgrading efficiency increased with an increase of gas recirculation rate ▪ Novel phylotypes resided in the reactors	Kougias et al., 2017

BTF	*Ex-situ*: ▪ Gas injection: H_2 (80%), CO_2 (20%), N_2 (17%) ▪ BTF fed in co-current mode ▪ Temperature 35°C ▪ EBRT 11 min ▪ OT ~ 180 days	CH_4 production rates 38 $m^3\ m^{-3}_{reactor}\ d^{-1}$ CH_4 production 44% H_2 removal 83% CO_2 removal 96%	▪ Methanogen density and activity needs to be optimized for higher upgrading rates	Dupnock and Deshusses, 2017
Hollow fibre membrane biofilm reactor	*Ex-situ:* ▪ Gas injection: H_2 (80%), CO_2 (20%) ▪ Temperature 37°C ▪ OT ~ 70 days	CH_4 production 60% (at pH 6.5-7.5) CH_4 production 80-90% (at pH 4.2-5.5)	▪ Gas injection through HFM ▪ CH_4 ratio of the produced gas depended on the pH condition	Ju et al., 2008

Note: AGS - anaerobic granular sludge; BTF - biotrickling filter; COD - chemical oxygen demand; CSTR - continuous stirred tank reactor; EBRT - empty bed residence time; HFM - hollow fibre membrane; OLR - organic loading rate; OT - operating time; RV - reactor volume; UASB - upflow anaerobic sludge blanket; VS - volatile solid

Photosynthetic biogas upgrading

Photobioreactors (PBs) are used in wastewater treatment for nutrient (e.g. nitrogen and phosphorus) and COD removal (Vo et al., 2019). There are several types of PB configurations such as high rate algal ponds, flat plates, tubular and hybrid PB (Figure 2.7). Different microalgae-based cultivation methods (e.g. monoculture, microalgae + fungi, microalgae + activated sludge) have been tested in photobioreactors and achieved a similar CH_4 and CO_2 composition of the upgraded biogas (Sun et al., 2019a). Compared to physico-chemical methods, the investment cost for photosynthetic biogas upgrading is higher. However, other associated costs such as operating costs and energy requirements of photosynthetic processes are comparatively lower (Rodero et al., 2019a). Moreover, the performance of the photosynthetic process was best compared to other physico-chemical methods (Ferella et al., 2019).

The application of PBs for biogas upgrading is relatively new and makes use of microalgae that use CO_2, thus upgrading the CH_4 content of biogas to biomethane. CO_2 uptake by microalgae can be through (Bose et al., 2019): (i) direct uptake (through cell membrane), (ii) bicarbonate assimilation (through active transporters in the cell membrane), and (iii) enzymatic catalysis (e.g. microalgae use extracellular carbonic anhydrase to accelerate bicarbonate formation). The main advantage of this system is simultaneous removal of H_2S and CO_2 from biogas. High concentrations of dissolved oxygen (DO) generated in the photobioreactor during photosynthesis accelerate the H_2S oxidation to SO_4^{2-} (Meier et al., 2018).

Scale-up and validation of photosynthetic biogas upgrading systems at both lab-scale and semi-industrial scale occurred in the last two years (Bose et al., 2021; Rodero et al., 2019a; Rodero et al., 2019b; Marín et al., 2019). Based on the reported studies, liquid to biogas (L/G) ratio, pH and alkalinity were identified as key regulatory parameters for higher biogas-liquid mass transfer with efficient H_2S and CO_2 removal from raw biogas. Controlling the O_2 level in upgraded biogas, optimum microalgae growth irrespective of seasonal temperature variations and CO_2 mass transfer are the main challenges of photosynthetic biogas upgrading (Bose et al., 2019). Future studies on multiple operational parameters (e.g. pH, L/G ratio, algae concentration, algae productivity, light or alkalinity) and reactor design emphasizing ‘individual sub-systems’ (the interaction

between reactor design factors (e.g. pH and L/G ratio) and their contribution to the overall photosynthetic biogas upgrading performance can be considered as an individual subsystem) of the entire photosynthetic biogas upgrading system are recommended to minimise the variabilities of CO_2 in the upgraded biogas as well as to achieve grid-standard biomethane (Bose et al., 2021).

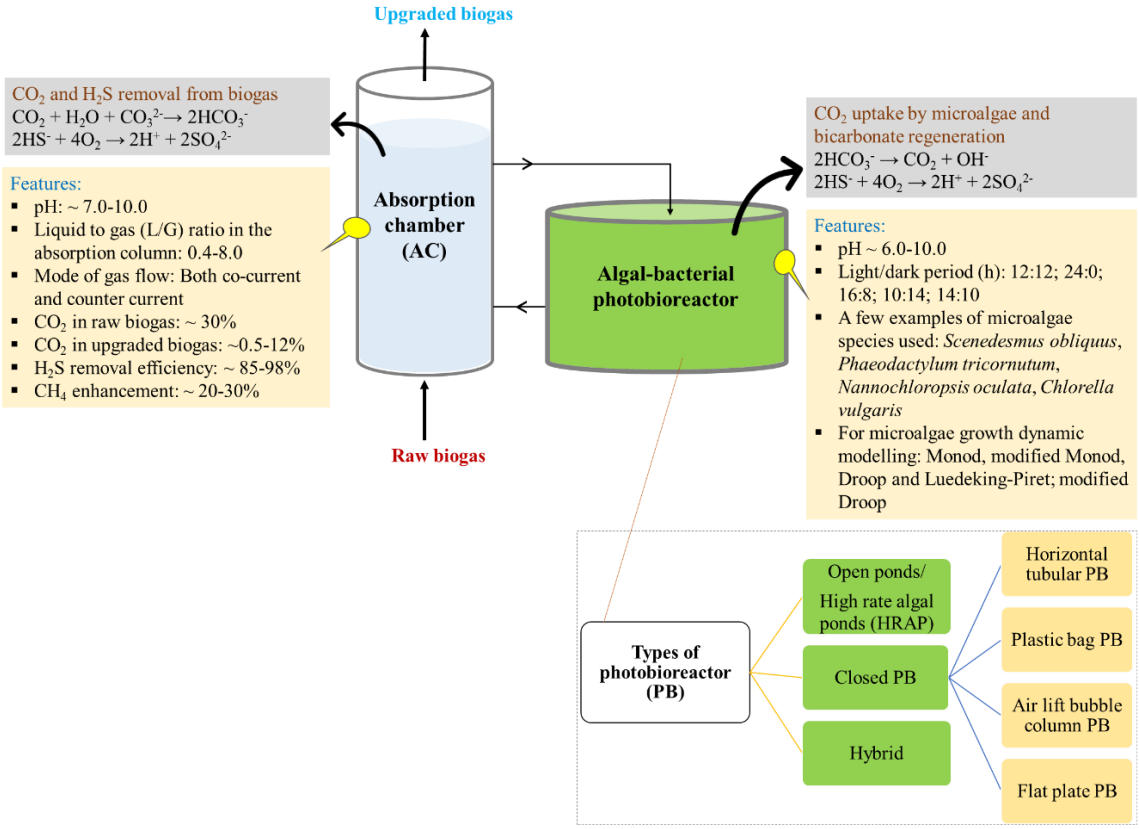

Figure 2.7: Overview of photosynthetic biogas upgrading process (Reference: Bose et al., 2019; Rodero et al., 2019a; Rodero et al., 2019b; Ferella et al., 2019; Meier et al., 2018; Marín et al., 2019; Sun et al., 2019a; Vo et al., 2019).

2.3.2. Process stability in AD to avoid biogas impurities

Feedstock and process optimization

The composition of biogas and its impurities varies with different feedstock (dairy manure, food waste and municipal solid waste) and biogas production process (Table 2.7). For example, (i) easily digestible food waste can result in process instability through generation of excess volatile fatty acids (VFAs) at an early stage of AD which further leads to a decrease in pH (Masebinu et al., 2019), and (ii) organic waste containing a high protein and lipid content increases the NH_3, H_2S and long chain fatty acids concentration

(Xu et al., 2018). Selection of appropriate feedstock (Peu et al., 2012), co-digestion (Choudhury and Lansing, 2019) and process optimization such as pre-treatment (Wang et al., 2019c), e.g. enzymatic (Koupaie et al., 2019) or electrochemical (Zeng et al., 2019), and addition of catalytic materials such as iron oxide (Cao et al., 2019), nanoparticles (Farghali et al., 2019) or biochar (Lee et al., 2021; Masebinu et al., 2019) can enhance process stability in the AD and mitigate biogas impurities. Systematic data-driven modelling of AD, e.g. NARX-BP hybrid neural network, can be useful for process stability and simulation of complex AD system (Xiao et al., 2021).

Proper dosing of nitrogen-rich organic substrates (e.g. livestock manures) is important in the AD process to avoid formation and accumulation of NH_3, because free NH_3 can cause microbial inhibition in AD processes. NH_4^+ concentrations exceeding 3000 mg L^{-1} are toxic to microbial consortia (Jiang et al., 2019), consequently decreasing the biogas quality and quantity. To overcome NH_3 inhibition in AD processes, different strategies can be adopted including dilution of the nitrogen-rich substrates, microbial acclimatization or long term adaptation (Krakat et al., 2017), bioaugmentation (Jiang et al., 2019), co-digestion, pre-treatment including NH_3 stripping (Jiang et al., 2019), air stripping combined with gas washing (Busato et al., 2020) and addition of zeolites (Krakat et al., 2017).

By maintaining elevated ammonium concentrations in AD, H_2S production in raw biogas can be significantly decreased by reducing the abundance of sulfate reducing bacteria (SRB) in mesophilic and thermophilic anaerobic digesters, e.g. ammonium nitrogen levels ~ 3.5 g NH_4^+-N /kg digestate decreased the H_2S production by ~ 50% (Giordano et al., 2019). Hence, the H_2S concentration in the biogas can be limited by maintaining an optimum total ammonia nitrogen (TAN) and free ammonia nitrogen (FAN) level in the digester (Han et al., 2019; Giordano et al., 2019). Moreover, a rapid decrease in CH_4 production (~ 25%) can occur due to the synergistic toxic effect of TAN and sulfide on methanogens (Sürmeli et al., 2019).

Table 2.7: Comparison of raw biogas composition produced from different feedstocks.

Feedstock	Temperature, ºC	Retention time, days	Biogas production process	Raw biogas composition or remarks	Reference
Flushed cow manure collection (1200 cows in total)	20-30	100	Covered lagoon system	CH_4 ~ 70%, CO_2 ~ 20%, N_2 ~ 9% TSC* < 1 ppm VMS 0.0002 ppm (mainly D4) BTEX 0.14 ppm	Li et al., 2019
Flushed cow manure (1200 cows in total)	35-40	50	Single continuously stirred digester	CH_4 ~ 50%, CO_2 ~ 42%, N_2 ~ 7% TSC* ~ 50 ppm VMS 0.0002 ppm (mainly D4) BTEX 0.43 ppm	Li et al., 2019
Food waste (25 Ton/day)	50-55	21	Three-stage digester	CH_4 ~ 55%, CO_2 ~ 35%, N_2 ~ 9% TSC* ~ 140 ppm VMS 0.06 ppm (mainly D5) BTEX 0.18 ppm	Li et al., 2019
Mixture of food waste, animal bedding waste and municipal organic waste	50-55	21	Three-stage digester	CH_4 ~ 50%, CO_2 ~ 46%, N_2 ~ 3% TSC* ~ 15 ppm VMS 1.56 ppm (mainly L2) BTEX 2.25 ppm	Li et al., 2019
Co-digestion (addition of gummy vitamin waste dairy manure)	35	67	Batch digesters	CH_4 yield was increased by 126-151% (336-374 mL CH_4/gVS) H_2S concentration was decreased by 66-83% (35.1–71.9 mL H_2S/kg VS)	Choudhury and Lansing, 2019
High solid anaerobic digestion (HSAD)	35 55	20 20 (operating time ~ 200 days)	Borosilicate glass reactor	H_2S concentration was decreased over 80% in HSAD compared to conventional AD NH_4Cl dosage (optimum ~ 2.50 g L^{-1}) inhibited H_2S generation significantly	Han et al., 2019
Chicken manure and eggs (to maintain higher nitrogen and total sulfur content)	36	30 (operating time ~ 375 days)	Lab-scale anaerobic mono digester (continuously stirred)	TAN (> 4000 mg L^{-1}) and total sulfide (> 100 mg L^{-1}) load increased acetate production rapidly (from 130 to 1700 mg L^{-1}). Consequently, methanogens exceeded acetate inhibition threshold and CH_4 yield dropped by 25%	Sürmeli et al., 2019

Note: TSC - total sulfur containing compound including hydrogen sulfide, mercaptans, sulfur dioxide, sulfides (excluding H_2S), disulfides; * - air (at a rate of 2-6%) was injected into the anaerobic digester to inhibit H_2S formation; VMS - volatile methyl siloxanes; D4- octamethylcyclotetrasiloxane; D5 - decamethylcyclopentasiloxane; L2 – hexamethyldisiloxane; BTEX - Benzene, toluene, ethylbenzene, and xylene; VS - volatile solids; AD - anaerobic digestion; TAN - total ammonia nitrogen

CO_2 and sulfide removal in AD

Biogas upgrading to increase the CH_4 content can be achieved in AD by controlling the production of CO_2 and H_2S or by sequestering these in a post-treatment. In mineral CO_2 sequestration for biogas upgrading, CO_2 is converted into carbonate when reacting with alkaline silicate (Zhang et al., 2019). Addition of magnesium silicate (40 g L^{-1}) combined with wollastonite ($CaSiO_3$, 20 g L^{-1}) in AD increased the CH_4 content in biogas from ~ 70% to ~80% and decreased the CO_2 content from ~ 28% to ~ 18% (Liu et al., 2019). Stepwise sludge ash addition increased the CH_4 content from ~ 69% to ~ 79% in biogas by inhibiting acidifying and hydrolytic enzyme activities and promoting CO_2 capture (Yin et al., 2019). CO_2 can also be removed by integrating a microbial electrosynthesis system (MES) in the AD process, wherein the biocathode in the MES uses the supplied electrons and protons to convert CO_2 into CH_4 (Nelabhotla and Dinamarca, 2019). This integration of MES in AD can achieve an upgraded biogas quality with ~ 90% CH_4 and < 15% CO_2.

Sulfide sequestration can be performed by mineral immobilization, e.g. steel slag fines addition induces the dissociation of H_2S into HS^- and S^{2-} and consequently immobilizes sulfide as metal sulfide (Caicedo-Ramirez et al., 2019). Moreover, the steel slags also catalyse H_2S oxidation to S^0. Alternatively, microbial electrolysis cells coupled to the AD process can minimize the toxic effect of unionized H_2S on the methanogenesis step by converting unionized H_2S to ionized HS^- (Yuan et al., 2020).

2.4. Future prospects

The Driver-Pressure-Stress-Impact-Response (DPSIR) framework and Strengths-Weaknesses-Opportunities-Threats (SWOT) analysis are two important tools that are applied for assessing environmental risks and associated factors (D'Adamo et al., 2020; Miranda et al., 2019; Wang et al., 2020; Zorpas, 2020). The DPSIR framework is used to assess environmental problems or risks by identifying causal relations (Rasool et al., 2021; Zorpas, 2020). DPSIR has been used for strategy development in different application fields, e.g. waste management (Zorpas, 2020), micro-plastic pollution (Miranda et al., 2019), forest management (Zandebasiri et a., 2021), and land use and land cover changes (Rasool et al., 2021). Alternatively, a SWOT analysis is carried out to understand the internal and external factors for a specific objective. The internal factors

identify the strengths and weaknesses, while the external factors illustrate the opportunities and threats (Chen et al., 2014). A SWOT analysis is applied for several applications including the renewable energy sector (D'Adamo et al., 2020) for selection of renewable energy resources in a region (Wang et al., 2020), to compare renewable energy policies among countries (Chen et al., 2014), to evaluate the share of biomethane in the transport sector (D'Adamo et al., 2020) and to develop strategies for waste management (Zorpas, 2020).

Figure 2.8a shows a conceptual model based on the DPSIR framework for biological biogas purification. The SWOT analysis (Figure 2.8b) of the responses in the DPSIR framework was done to demonstrate the present situation of biological biogas purification and future prospects. From a technology point of view, most of the biological approaches demonstrated efficient biogas purification. Several bioreactor configurations were used for both upstream and downstream purification processing. However, each type of purification process has its own limitations. Research is being carried out globally to overcome existing limitations, to optimize the process parameters and to design new bioreactor configurations to accelerate the biological biogas upgrading. Future studies should also focus on the sustainability features of biological biogas upgrading technologies using advanced sustainability assessment tools such as exergy-based approaches that can evaluate both economic and environmental aspects (Aghbashlo et al., 2019a; Aghbashlo et al., 2019b; Rosen, 2018).

Integration of both upstream and downstream responses, inclusion of the AD process in the policy framework, and implementation of a strategic plan for raw biogas to biomethane production are the key responses in the DPSIR framework (Figure 2.8a). However, adoption of green technologies in the future may depend on the conversion of the identified weaknesses in the SWOT analysis (e.g. lack of source segregation of waste, lack of optimization of process parameters or lack of integration among biological methods) into strengths as well as decreasing the threats (e.g. lack of appropriate feedstock composition in AD or lack of policy framework and financial incentives to promote biogas production and upgradation) for the biogas sector.

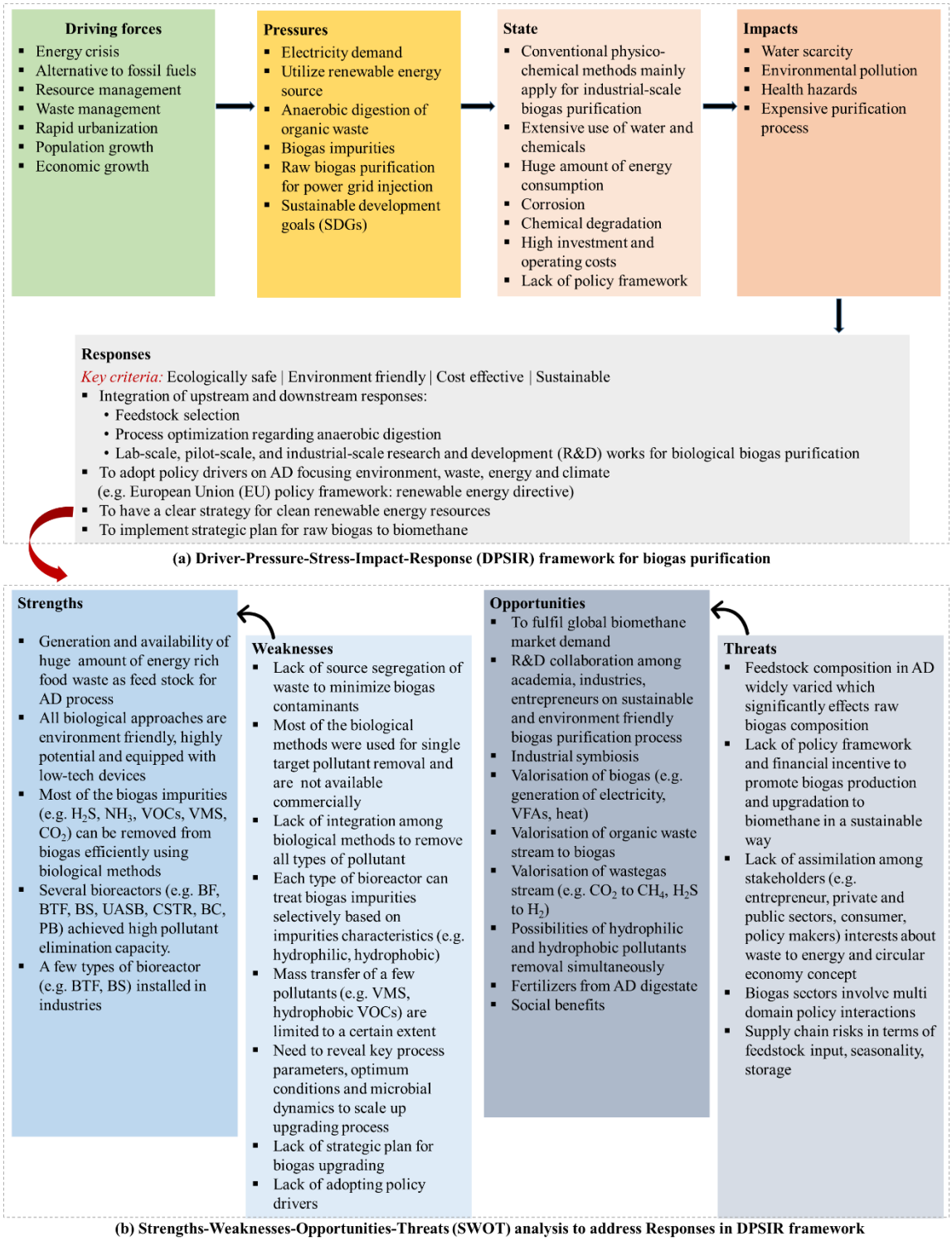

(a) Driver-Pressure-Stress-Impact-Response (DPSIR) framework for biogas purification

(b) Strengths-Weaknesses-Opportunities-Threats (SWOT) analysis to address Responses in DPSIR framework

Note: The information was summarized here based on all the references reviewed in this manuscript.

Abbreviation: AD - anaerobic digestion; SDGs – sustainable development goals; R&D - research and development; BF - biofilter; BTF - biotrickling filter; BS - bioscrubber; UASB - upflow anaerobic sludge blanket; CSTR - continuous stirred tank reactor; BC - bubble column; PB - photo bioreactor; VMS - volatile methyl siloxanes; VOCs - volatile organic compounds; VFAs - volatile fatty acids

Figure 2.8: Conceptual model combining (a) Driver-Pressure-Stress-Impact-Response (DPSIR) and (b) Strengths-Weaknesses-Opportunities-Threats (SWOT) to define and prioritise future prospects of biological biogas purification.

Biogas production through AD can significantly contribute to the global bioenergy production. However, sustainable biogas purification is a key step for biogas applications. Feedstock and process parameters in AD can significantly affect the raw biogas composition. Zhu et al. (2019c) identified the availability of quality feedstock as critical risk for the biogas sector. These authors also emphasized the need of a better understanding of the policies and clear strategic vision to promote agricultural biomethane production. All the weaknesses (Figure 2.8b) can be turned into strengths and all threats can be opportunities through right initiatives. However, this DPSIR-SWOT model is inadequate to describe a complete scenario as there are other factors depending on the implementing country, geographical conditions, present status of waste management practices and stakeholders.

Valorisation of waste and biomass to generate energy, fuel and other valuable materials is a sustainable approach towards a circular economy. It also significantly reduces human health hazard and environmental pollution by avoiding traditional approaches such as landfilling or incineration which generate toxic gases. With rapid urbanisation, tremendous stress is laid on our resources along with concerns over extensive waste generation. Research is conducted globally on waste valorisation by exploiting conventional physico-chemical and biological techniques (Foong et al., 2020; Kanani et al., 2020; Nzihou, 2010; Sharma et al., 2020). For example, poultry waste streams from egg and broiler industries are currently disposed either through landfill dumping or as a fertilizer. This poultry waste can be potentially valorised using well established waste valorisation technologies such as anaerobic mono-digestion or co-digestion (Kanani et al., 2020).

Valorisation of raw biogas and its impurities using a biological approach can be an important aspect as a renewable energy source, for example, generation of biological H_2 through bioconversion of H_2S by green sulfur bacteria. Biological H_2 production has been reported through (i) dark anaerobic production via either the 'water-gas shift-reaction' or fermentation and (ii) photo-production by cyanobacteria or green algae (De Crisci et al., 2019; Markov, 2012). So far, no technology is available for bioconversion of H_2S to generate H_2 and S^0 (De Crisci et al., 2019).

Particulate matter emitted from upgraded biogas, i.e. from biomethane combustion, is in the ultrafine particle (UFP) range compared to other fuels such as gasoline, diesel, coal, fuel oil and solid biomass (Xue et al., 2018). These particles are toxic to human health (Li et al., 2019). Combustion of natural gas and biomethane with similar sulfur and siloxanes content give similar UFP emissions (Li et al., 2019; Xue et al., 2018). Further studies require evaluating the UFP emissions with variations in concentration of sulfur containing compounds and siloxanes in biomethane. Moreover, research should focus on advanced combustion technologies to reduce the ultrafine particles emissions from biogas.

2.5. Conclusions

The working principles, advantages, limitations and future scope of biological approaches for both upstream and downstream treatment of biogas have been reviewed. From a cleaner production approach, selection of appropriate feedstock and process optimization in AD is very important to control pollutant concentrations in raw biogas. In downstream processing, several bioreactor configurations such as BFs, BTFs, BSs and PBs have been used to remove pollutants from biogas. In general, several factors such as bioreactor configuration, process parameters, pollutants characteristics, inhibitory effects and microbial community composition determine the efficiency of the gaseous pollutants removal. In upstream processing, microaeration in AD can be an important aspect of biogas purification, especially for controlling the H_2S concentration in raw biogas. The DPSIR-SWOT analysis demonstrates the present situation and future scope of biogas purification processes. The responses in the DPSIR framework incorporate both upstream and downstream responses, the policy framework and strategic planning. Conversion of identified weaknesses and threats in a SWOT analysis into strengths and opportunities, respectively, could be challenging. However, it is important to implement sustainable biogas upgrading knowledge and to adopt green technologies in the biogas sector.

2.6. References

Abatzoglou, N., Boivin, S., 2009. A review of biogas purification processes. Biofuels, Bioproducts and Biorefining. 3, 42-71.

Abdeen, F.R., Mel, M., Jami, M.S., Ihsan, S.I., Ismail, A.F., 2016. A review of chemical absorption of carbon dioxide for biogas upgrading. Chinese Journal of Chemical Engineering. 24, 693-702.

Abubackar, H.N., Veiga, M.C., Kennes, C., Das, J., Rene, E.R., van Hullebusch, E.D., 2019. Gas-Phase Bioreactors, in: Moo-Young, M. (Eds.), Comprehensive Biotechnology. Elsevier, United Kingdom, pp. 446-463.

Accettola, F., Guebitz, G.M., Schoeftner, R., 2008. Siloxane removal from biogas by biofiltration: biodegradation studies. Clean Technologies and Environmental Policy. 10, 211-218.

Aghbashlo, M., Tabatabaei, M., Soltanian, S., Ghanavati, H., 2019b. Biopower and biofertilizer production from organic municipal solid waste: an exergoenvironmental analysis. Renewable Energy. 143, 64-76.

Aghbashlo, M., Tabatabaei, M., Soltanian, S., Ghanavati, H., Dadak, A., 2019a. Comprehensive exergoeconomic analysis of a municipal solid waste digestion plant equipped with a biogas genset. Waste Management. 87, 485-498.

Aita, B.C., Mayer, F.D., Muratt, D.T., Brondani, M., Pujol, S.B., Denardi, L.B., Hoffmann, R., Da Silveira, D.D., 2016. Biofiltration of H_2S-rich biogas using *Acidithiobacillus thiooxidans*. Clean Technologies and Environmental Policy. 18, 689-703.

Alfaro, N., Fdz-Polanco, M., Fdz-Polanco, F., Díaz, I., 2019. H_2 addition through a submerged membrane for in-situ biogas upgrading in the anaerobic digestion of sewage sludge. Bioresource Technology. 280, 1-8.

Allievi, M.J., Silveira, D.D., Cantão, M.E., Filho, P.B. 2018. Bacterial community diversity in a full scale biofilter treating wastewater odor. Water Science and Technology. 77, 2014-2022.

Angelidaki, I., Treu, L., Tsapekos, P., Luo, G., Campanaro, S., Wenzel, H., Kougias, P.G., 2018. Biogas upgrading and utilization: Current status and perspectives. Biotechnology Advances. 36, 452-466.

Angelidaki, I., Xie, L., Luo, G., Zhang, Y., Oechsner, H., Lemmer, A., Munoz, R., Kougias, P.G., 2019. Biogas Upgrading: Current and Emerging Technologies, in: Pandey, A., Larroche, C., Gnansounou, E., Khanal, S.K., Dussap, C.G., Ricke, S., (Eds.), Biofuels: Alternative Feedstocks and Conversion Processes for the Production of Liquid and Gaseous Biofuels. Academic Press, pp. 817-843.

Arellano-García, L., Le Borgne, S., Revah, S., 2018. Simultaneous treatment of dimethyl disulfide and hydrogen sulfide in an alkaline biotrickling filter. Chemosphere. 191, 809-816.

Ashrafmansouri, S.S., Esfahany, M.N., 2014. Mass transfer in nanofluids: A review. International Journal of Thermal Sciences. 82, 84-99.

Awe, O. W., Zhao, Y., Nzihou, A., Minh, D.P., Lyczko, N., 2017. A review of biogas utilisation, purification and upgrading technologies. Waste and Biomass Valorization. 8, 267-283.

Baena-Moreno, F.M., Rodríguez-Galán, M., Vega, F., Vilches, L.F., Navarrete, B., 2019a. Review: recent advances in biogas purifying technologies. International Journal of Green Energy. 16, 401-412.

Baena-Moreno, F.M., Rodríguez-Galán, M., Vega, F., Vilches, L.F., Navarrete, B., Zhang, Z., 2019b. Biogas upgrading by cryogenic techniques. Environmental Chemistry Letters. 1-11.

Barbusinski, K., Kalemba, K., Kasperczyk, D., Urbaniec, K., Kozik, V., 2017. Biological methods for odor treatment - A review. Journal of Cleaner Production. 152, 223-241.

Biogasclean, 2020. Biogasclean Brochure. https://www.biogasclean.com/CustomerData/Files/Folders/6-pdf-er/147_biog-sheet-eco18-screen.pdf. Last accessed on 21 June 2020.

Blázquez, E., Bezerra, T., Lafuente, J., Gabriel, D., 2017. Performance, limitations and microbial diversity of a biotrickling filter for the treatment of high loads of ammonia. Chemical Engineering Journal. 311, 91-99.

Boada, E., Santos-Clotas, E., Bertran, S., Cabrera-Codony, A., Martín, M.J., Bañeras, L., Gich, F., 2020. Potential use of *Methylibium* sp. as a biodegradation tool in organosilicon and volatile compounds removal for biogas upgrading. Chemosphere. 240, 124908.

Bose, A., Lin, R., Rajendran, K., O'Shea, R., Xia, A., Murphy, J.D. 2019. How to optimise photosynthetic biogas upgrading: a perspective on system design and microalgae selection. Biotechnology Advances. 37, 107444.

Bose, A., O'Shea, R., Lin, R., Murphy, J., 2021. A comparative evaluation of design factors on bubble column operation in photosynthetic biogas upgrading. Biofuel Research Journal. 30, 1351-1373.

Busato, C.J., Da Ros, C., Pellay, R., Barbierato, P., Pavan, P., 2020. Anaerobic membrane reactor: Biomethane from chicken manure and high-quality effluent. Renewable Energy. 145, 1647-1657.

Caicedo-Ramirez, A., Laroco, N., Bilgin, A.A., Shiokari, S., Grubb, D.G., Hernandez, M., 2019. Engineered addition of slag fines for the sequestration of phosphate and sulfide during mesophilic anaerobic digestion. Water Environment Research. 1-10.

Cano, P.I., Almenglo, F., Ramírez, M., Cantero, D., 2021. Integration of a nitrification bioreactor and an anoxic biotrickling filter for simultaneous ammonium-rich water treatment and biogas desulfurization. Chemosphere. 284, 131358.

Cao, J., Zhang, L., Hong, J., Sun, J., Jiang, F., 2019. Different ferric dosing strategies could result in different control mechanisms of sulfide and methane production in sediments of gravity sewers. Water Research. 164, 114914.

Capua, F.D., Pirozzi, F., Lens, P.N., Esposito, G., 2019. Electron donors for autotrophic denitrification. Chemical Engineering Journal. 362, 922-937.

Carriero, G., Neri, L., Famulari, D., Di Lonardo, S., Piscitelli, D., Manco, A., Esposito, A., Chirico, A., Facini, O., Finardi, S., Tinarelli, G., Prandi, R., Zaldei, A., Vagnoli, C., Toscano, P., Magliulo, V., Ciccioli, P., Baraldi, R., 2018. Composition and emission of VOC from biogas produced by illegally managed waste landfills in Giugliano (Campania, Italy) and potential impact on the local population. Science of the Total Environment. 640, 377-386.

Chen, C.Y., Tsai, T.H., Chang, C.H., Tseng, C.F., Lin, S.Y., Chung, Y.C., 2018. Airlift bioreactor system for simultaneous removal of hydrogen sulfide and ammonia from synthetic and actual waste gases. Journal of Environmental Science and Health, Part A. 53, 694-701.

Chen, W.M., Kim, H., Yamaguchi, H., 2014. Renewable energy in eastern Asia: Renewable energy policy review and comparative SWOT analysis for promoting renewable energy in Japan, South Korea, and Taiwan. Energy Policy. *74*, 319-329.

Cheng, Y., He, H., Yang, C., Zeng, G., Li, X., Chen, H., Yu, G., 2016. Challenges and solutions for biofiltration of hydrophobic volatile organic compounds. Biotechnology Advances. 34, 1091-1102.

Cheng, Z., Feng, K., Xu, D., Kennes, C., Chen, J., Chen, D., Zhang, S., Ye, J., Dionysiou, D.D., 2019. An innovative nutritional slow-release packing material with functional microorganisms for

biofiltration: Characterization and performance evaluation. Journal of hazardous materials. 366, 16-26.

Choudhury, A., Lansing, S., 2019. Methane and Hydrogen Sulfide Production from Co-Digestion of Gummy Waste with a Food Waste, Grease Waste, and Dairy Manure Mixture. Energies. 12, 4464.

Choudhury, A., Shelford, T., Felton, G., Gooch, C., Lansing, S., 2019. Evaluation of hydrogen sulfide scrubbing systems for anaerobic digesters on two US dairy farms. Energies. 12, 4605.

D'Adamo, I., Falcone, P.M., Gastaldi, M., Morone, P., 2020. RES-T trajectories and an integrated SWOT-AHP analysis for biomethane. Policy implications to support a green revolution in European transport. Energy Policy. 138, 111220.

Das, J., Rene, E.R., Dupont, C., Dufourny, A., Blin, J., van Hullebusch, E.D., 2019. Performance of a compost and biochar packed biofilter for gas-phase hydrogen sulfide removal. Bioresource Technology. 273, 581-591.

De Crisci, A.G., Moniri, A., Xu, Y., 2019. Hydrogen from hydrogen sulfide: towards a more sustainable hydrogen economy. International Journal of Hydrogen Energy. 44, 1299-1327.

Dupnock, T.L., Deshusses, M.A., 2017. High-performance biogas upgrading using a biotrickling filter and hydrogenotrophic methanogens. Applied Biochemistry and Biotechnology. 183, 488-502.

Dupnock, T.L., Deshusses, M.A., 2019. Detailed investigations of dissolved hydrogen and hydrogen mass transfer in a biotrickling filter for upgrading biogas. Bioresource Technology. 290, 121780.

Esmaeili-Faraj, S.H., Esfahany, M.N., Darvanjooghi, M.H.K., 2019. Application of water based nanofluids in bioscrubber for improvement of biogas sweetening in a pilot scale. Chemical Engineering and Processing-Process Intensification. 143, 107603.

Farghali, M., Andriamanohiarisoamanana, F.J., Ahmed, M.M., Kotb, S., Yamashiro, T., Iwasaki, M., Umetsu, K., 2019. Impacts of iron oxide and titanium dioxide nanoparticles on biogas production: Hydrogen sulfide mitigation, process stability, and prospective challenges. Journal of Environmental Management. 240, 160-167.

Ferella, F., Cucchiella, F., D'Adamo, I., Gallucci, K., 2019. A techno-economic assessment of biogas upgrading in a developed market. Journal of Cleaner Production. 210, 945-957.

Fernández, M., Ramírez, M., Pérez, R.M., Gómez, J.M., Cantero, D., 2013. Hydrogen sulphide removal from biogas by an anoxic biotrickling filter packed with Pall rings. Chemical Engineering Journal. 225, 456-463.

Foong, S.Y., Liew, R.K., Yang, Y., Cheng, Y.W., Yek, P.N.Y., Mahari, W.A.W., Aghbashlo, M., 2020. Valorization of biomass waste to engineered activated biochar by microwave pyrolysis: Progress, challenges, and future directions. Chemical Engineering Journal. 389, 124401.

Franco-Morgado, M., Toledo-Cervantes, A., González-Sánchez, A., Lebrero, R., Muñoz, R., 2018. Integral (VOCs, CO_2, mercaptans and H_2S) photosynthetic biogas upgrading using innovative biogas and digestate supply strategies. Chemical Engineering Journal. 354, 363-369.

García, S.P., Rodríguez, L.Á.G., Martínez, D.B., Córdova, F.D.J.C., Regalado, E.S., Giraudet, S., Guzmán, N.E.D., 2021. Siloxane removal for biogas purification by low cost mineral adsorbent. Journal of Cleaner Production. 286, 124940.

Gerrity, S., Clifford, E., Kennelly, C., Collins, G., 2016. Ammonia oxidizing bacteria and archaea in horizontal flow biofilm reactors treating ammonia-contaminated air at 10° C. Journal of Industrial Microbiology & Biotechnology. 43, 651-661.

Giordano, A., Di Capua, F., Esposito, G., Pirozzi, F., 2019. Long-term biogas desulfurization under different microaerobic conditions in full-scale thermophilic digesters co-digesting high-solid sewage sludge. International Biodeterioration & Biodegradation. 142, 131-136.

Giordano, C., Spennati, F., Mori, G., Munz, G., Vannini, C., 2018. The microbial community in a moving bed biotrickling filter operated to remove hydrogen sulfide from gas streams. Systematic and Applied Microbiology. 41, 399-407.

González-Cortés, J.J., Almenglo, F., Ramírez, M., Cantero, D., 2021. Simultaneous removal of ammonium from landfill leachate and hydrogen sulfide from biogas using a novel two-stage oxic-anoxic system. Science of The Total Environment. 750, 141664.

Guieysse, B., Hort, C., Platel, V., Munoz, R., Ondarts, M., Revah, S., 2008. Biological treatment of indoor air for VOC removal: Potential and Challenges. Biotechnology Advances. 26, 398-410.

Guo, X.J., Tak, J.K., Johnson, R.L., 2009. Ammonia removal from air stream and biogas by a H_2SO_4 impregnated adsorbent originating from waste wood-shavings and biosolids. Journal of Hazardous Materials, 166, 372-376.

Han, Y., Qu, Q., Li, J., Zhuo, Y., Zhong, C., Peng, D., 2019. Performance of ammonium chloride dosage on hydrogen sulfide in-situ prevention during waste activated sludge anaerobic digestion. Bioresource Technology. 276, 91-96.

Hosseinipour, S.A., Mehrpooya, M., 2019. Comparison of the biogas upgrading methods as a transportation fuel. Renewable Energy. 130, 641-655.

IRENA (2020). Global renewables outlook: energy transformation 2050. International Renewable Energy Agency, Abu Dhabi. https://www.irena.org/-/media/Files/IRENA/Agency/Publication/2020/Apr/IRENA_Global_Renewables_Outlook_2020.pdf. Last accessed on 14 June 2020.

Jeníček, P., Horejš, J., Pokorná-Krayzelová, L., Bindzar, J., Bartáček, J., 2017. Simple biogas desulfurization by microaeration-full scale experience. Anaerobe. 46, 41-45.

Jiang, Y., McAdam, E., Zhang, Y., Heaven, S., Banks, C., Longhurst, P., 2019. Ammonia inhibition and toxicity in anaerobic digestion: a critical review. Journal of Water Process Engineering. 32, 100899.

Joshi, J.A., Hogan, J.A., Cowan, R.M., Strom, P.F., Finstein, M.S., 2000. Biological removal of gaseous ammonia in biofilters: space travel and earth-based applications. Journal of the Air & Waste Management Association. 50, 1647-1654.

Ju, D.H., Shin, J.H., Lee, H.K., Kong, S.H., Kim, J.I., Sang, B.I., 2008. Effects of pH conditions on the biological conversion of carbon dioxide to methane in a hollow-fiber membrane biofilm reactor (Hf–MBfR). Desalination. 234, 409-415.

Juntranapaporn, J., Vikromvarasiri, N., Soralump, C., Pisutpaisal, N., 2019. Hydrogen sulfide removal from biogas in biotrickling filter system inoculated with *Paracoccus pantotrophus*. International Journal of Hydrogen Energy. 44, 29554-29560.

Kadam, R., Panwar, N.L., 2017. Recent advancement in biogas enrichment and its applications. Renewable and Sustainable Energy Reviews. 73, 892-903.

Kafle, G.K., Chen, L., Neibling, H., He, B.B., 2015. Field evaluation of wood bark-based down-flow biofilters for mitigation of odor, ammonia, and hydrogen sulfide emissions from confined swine nursery barns. Journal of Environmental Management. 147, 164-174.

Kanani, F., Heidari, M.D., Gilroyed, B.H., Pelletier, N., 2020. Waste valorization technology options for the egg and broiler industries: A review and recommendations. Journal of Cleaner Production. 121129.

Kapoor, R., Ghosh, P., Kumar, M., Vijay, V.K., 2019. Evaluation of biogas upgrading technologies and future perspectives: a review. Environmental Science and Pollution Research. 26, 11631-11661.

Kennes, C., Rene, E.R., Veiga, M.C., 2009. Bioprocesses for air pollution control. Journal of Chemical Technology and Biotechnology. 84, 1419-1436.

Kennes, C., Veiga, M.C., 2002. Inert filter media for the biofiltration of waste gases–characteristics and biomass control. Reviews in Environmental Science and Bio/Technology. 1, 201-214.

Khalil, M., Berawi, M.A., Heryanto, R., Rizalie, A., 2019. Waste to energy technology: The potential of sustainable biogas production from animal waste in Indonesia. Renewable and Sustainable Energy Reviews. 105, 323-331.

Khan, M.U., Lee, J.T.E., Bashir, M.A., Dissanayake, P.D., Ok, Y.S., Tong, Y.W., Shariati, M.A., Wu, S., Ahring, B. K., 2021. Current status of biogas upgrading for direct biomethane use: A review. Renewable and Sustainable Energy Reviews. 149, 111343.

Khanongnuch, R., Di Capua, F., Lakaniemi, A.M., Rene, E.R., Lens, P.N.L., 2019b. Transient-state operation of an anoxic biotrickling filter for H_2S removal. Journal of Hazardous Materials, 377, 42-51.

Khanongnuch, R., Di Capua, F., Lakaniemi, A-Maija., Rene E.R., Lens, P.N.L., 2019a. H_2S removal and microbial community composition in ananoxic biotrickling filter under autotrophic and mixotrophic conditions. Journal of Hazardous Materials. 367, 397-406.

Kim, N. J., Sugano, Y., Hirai, M., Shoda, M., 2000. Removal of a high load of ammonia gas by a marine bacterium, Vibrio alginolyticus. Journal of Bioscience and Bioengineering. 90, 410-415.

Kougias, P.G., Treu, L., Benavente, D.P., Boe, K., Campanaro, S., Angelidaki, I., 2017. Ex-situ biogas upgrading and enhancement in different reactor systems. Bioresource Technology. 225, 429-437.

Koupaie, E.H., Dahadha, S., Lakeh, A.B., Azizi, A., Elbeshbishy, E., 2019. Enzymatic pretreatment of lignocellulosic biomass for enhanced biomethane production- a review. Journal of Environmental Management. 233, 774-784.

Krakat, N., Demirel, B., Anjum, R., Dietz, D., 2017. Methods of ammonia removal in anaerobic digestion: a review. Water Science and Technology. 76, 1925-1938.

Lai, C.Y., Zhou, L., Yuan, Z., Guo, J., 2021. Hydrogen-Driven Microbial Biogas Upgrading: Advances, Challenges and Solutions. Water Research. 117120.

Lakhouit, A., Cabral, A.R., Cabana, H., 2016. Two novel biofilters to remove volatile organic compounds emitted by landfill sites. Water, Air, & Soil Pollution. 227, 113.

Le Borgne, S., Baquerizo, G., 2019. Microbial ecology of biofiltration units used for the desulfurization of biogas. ChemEngineering. 3, 72.

Lee, J.T., Ok, Y.S., Song, S., Dissanayake, P.D., Tian, H., Tio, Z.K., Cui, R., Lim, E.Y., Jong, M.C., Hoy, S.H., Lum, T.Q.H., Tsui, T.H., Yoon, C.S., Dai, Y., Wang, C.H., Tan, H.T.W., Tong, Y.W., 2021. Biochar utilisation in the anaerobic digestion of food waste for the creation of a circular economy via biogas upgrading and digestate treatment. Bioresource Technology. 333, 125190.

Lee, S.H., Li, C., Heber, A.J., Ni, J., Huang, H., 2013. Biofiltration of a mixture of ethylene, ammonia, n-butanol, and acetone gases. Bioresource Technology. 127, 366-377.

Li, W., Loyola-Licea, C., Crowley, D.E., Ahmad, Z., 2016. Performance of a two-phase biotrickling filter packed with biochar chips for treatment of wastewater containing high nitrogen and phosphorus concentrations. Process Safety and Environmental Protection. 102, 150-158.

Li, Y., Alaimo, C.P., Kim, M., Kado, N.Y., Peppers, J., Xue, J., Wan, C., Green, P.G., Zhang, R., Jenkins, B.M., Vogel, C.F.A., Wuertz, S., Young, T.M., Kleeman, M.J., 2019. Composition and toxicity of biogas produced from different feedstocks in California. Environmental Science & Technology. 53, 11569-11579.

Li, Y., Zhang, W., Xu, J., 2014. Siloxanes removal from biogas by a lab-scale biotrickling filter inoculated with Pseudomonas aeruginosa S240. Journal of Hazardous Materials. 275, 175-184.

Lin, S., Mackey, H.R., Hao, T., Guo, G., van Loosdrecht, M.C.M., Chen, G., 2018. Biological sulfur oxidation in wastewater treatment: A review of emerging opportunities. Water Research. 143, 399-415.

Liu, H., Gong, L., Zhang, Y., Jiang, Q., Cui, M., Zhang, J., Fu, B., Liu, H., 2019. Silicate mediated simultaneous in-situ CO_2 sequestration and nutrients removal in anaerobic digestion. Bioresource Technology. 282, 125-132.

López, M.E., Rene, E.R., Veiga, M.C., Kennes, C., 2013. Biogas upgrading, in: Kennes, C., Veiga, M.C., (Eds.), Air Pollution Prevention and Control: Bioreactors and Bioenergy. John Wiley & Sons, Ltd., pp. 293-318.

Malhautier, L., Gracian, C., Roux, J.C., Fanlo, J.L., Le Cloirec, P., 2003. Biological treatment process of air loaded with an ammonia and hydrogen sulfide mixture. Chemosphere. 50, 145-153.

Malhautier, L., Khammar, N., Bayle, S., Fanlo, J.L., 2005. Biofiltration of volatile organic compounds. Applied Microbiology and Biotechnology. 68, 16-22.

Marín, D., Ortíz, A., Díez-Montero, R., Uggetti, E., García, J., Lebrero, R., Muñoz, R., 2019. Influence of liquid-to-biogas ratio and alkalinity on the biogas upgrading performance in a demo scale algal-bacterial photobioreactor. Bioresource Technology. 280, 112-117.

Markov, S.A., 2012. Hydrogen production in bioreactors: current trends. Energy Procedia, 29, 394-400.

Masebinu, S.O., Akinlabi, E.T., Muzenda, E., Aboyade, A.O., 2019. A review of biochar properties and their roles in mitigating challenges with anaerobic digestion. Renewable and Sustainable Energy Reviews. 103, 291-307.

Maurya, R., Tirkey, S.R., Rajapitamahuni, S., Ghosh, A., Mishra, S., 2019. Recent Advances and Future Prospective of Biogas Production, in: Hosseini, M. (Ed.), Advances in Feedstock Conversion

Technologies for Alternative Fuels and Bioproducts: New Technologies, Challenges and Opportunities. Woodhead Publishing, pp. 159-178.

Meier, L., Stará, D., Bartacek, J., Jeison, D., 2018. Removal of H_2S by a continuous microalgae-based photosynthetic biogas upgrading process. Process Safety and Environmental Protection. 119, 65-68.

Miranda, M.N., Silva, A.M., Pereira, M.F.R., 2019. Microplastics in the environment: a DPSIR analysis with focus on the responses. Science of the Total Environment. 134968.

Montebello, A.M., Fernández, M., Almenglo, F., Ramírez, M., Cantero, D., Baeza, M., Gabriel, D., 2012. Simultaneous methylmercaptan and hydrogen sulfide removal in the desulfurization of biogas in aerobic and anoxic biotrickling filters. Chemical Engineering Journal. 200-202, 237-246.

Montebello, A.M., Mora, M., López, L.R., Bezerra, T., Gamisans, X., Lafuente, J., Baeza, M., Gabriel, D., 2014. Aerobic desulfurization of biogas by acidic biotrickling filtration in a randomly packed reactor. Journal of Hazardous Materials. 280, 200-208.

Mudliar, S., Giri, B., Padoley, K., Satpute, D., Dixit, R., Bhatt, P., Pandey, R., Juwarkar, A., Vaidya, A., 2010. Bioreactors for treatment of VOCs and odours-A review. Journal of Environmental Management. 91, 1039-1054.

Mulu, E., M'Arimi, M.M., & Ramkat, R.C., 2021. A review of recent developments in application of low cost natural materials in purification and upgrade of biogas. Renewable and Sustainable Energy Reviews. 145, 111081.

Nelabhotla, A.B.T., Dinamarca, C., 2019. Bioelectrochemical CO_2 reduction to methane: MES integration in biogas production processes. Applied Sciences. 9, 1056.

Noorain, R., Kindaichi, T., Ozaki, N., Aoi, Y., Ohashi, A., 2019. Biogas purification performance of new water scrubber packed with sponge carriers. Journal of Cleaner Production. 214, 103-111.

Nzihou, A., 2010. Toward the valorization of waste and biomass. Waste and Biomass Valorization. 1, 3-7.

Okoro, O.V., Sun, Z., 2019. Desulphurisation of Biogas: A Systematic Qualitative and Economic-Based Quantitative Review of Alternative Strategies. ChemEngineering. 3, 76.

Pal, P., 2017. Biological Treatment Technology, in: Pal, P. (Ed.), Industrial Water Treatment Process Technology. Elsevier (Butterworth-Heinemann), pp. 65-144.

Paolini, V., Petracchini, F., Carnevale, M., Gallucci, F., Perilli, M., Esposito, G., Segreto, M., Occulti, L.G., Scaglione, D., Ianniello, A., Frattoni, M., 2018. Characterisation and cleaning of biogas from sewage sludge for biomethane production. Journal of Environmental Management. 217, 288-296.

Pascual, C., Cantera, S., Muñoz, R., Lebrero, R., 2021. Siloxanes removal in a two-phase partitioning biotrickling filter: Influence of the EBRT and the organic phase. Renewable Energy. 177, 52-60.

Peu, P., Picard, S., Diara, A., Girault, R., Béline, F., Bridoux, G., Dabert, P., 2012. Prediction of hydrogen sulphide production during anaerobic digestion of organic substrates. Bioresource Technology. 121, 419-424.

Piñas, J.A.V., Venturini, O.J., Lora, E.E.S., del Olmo, O.A., Roalcaba, O.D.C., 2019. An economic holistic feasibility assessment of centralized and decentralized biogas plants with mono-digestion and co-digestion systems. Renewable Energy. 139, 40-51.

Pokorna, D., Zabranska, J., 2015. Sulfur-oxidizing bacteria in environmental technology. Biotechnology Advances. 33, 1246-1259.

Popat, S.C., Deshusses, M.A., 2008. Biological removal of siloxanes from landfill and digester gases: opportunities and challenges. Environmental Science & Technology. 42, 8510-8515.

Promnuan, K., O-Thong, S., 2017. Efficiency evaluation of biofilter for hydrogen sulfide removal from palm oil mill biogas. Energy Procedia. 138, 564-568.

Prussi, M., Padella, M., Conton, M., Postma, E.D., Lonza, L., 2019. Review of technologies for biomethane production and assessment of Eu transport share in 2030. Journal of Cleaner Production. 222, 565-572.

Qiu, X., Deshusses, M.A., 2017. Performance of a monolith biotrickling filter treating high concentrations of H_2S from mimic biogas and elemental sulfur plugging control using pigging. Chemosphere. 186, 790-797.

Rasool, R., Fayaz, A., ul Shafiq, M., Singh, H., Ahmed, P., 2021. Land use land cover change in Kashmir Himalaya: Linking remote sensing with an indicator based DPSIR approach. Ecological Indicators. 125, 107447.

Reddy, C.N., Bae, S., Min, B., 2019. Biological removal of H_2S gas in a semi-pilot scale biotrickling filter: Optimization of various parameters for efficient removal at high loading rates and low pH conditions. Bioresource technology. 285, 121328.

Ren, B., Zhao, Y., Lyczko, N., Nzihou, A., 2019. Current status and outlook of odor removal technologies in wastewater treatment plant. Waste and Biomass Valorization. 10, 1443-1458.

Rodero, M.R., Ángeles, R., Marín, D., Díaz, I., Colzi, A., Posadas, E., Lebrero, R., Muñoz, R., 2018. Biogas Purification and Upgrading Technologies, in: Tabatabaei, M., Ghanavati, H. (Eds.), Biogas, Biofuel and Biorefinery Technologies 6. Springer, Cham, pp. 239-276.

Rodero, M.R., Carvajal, A., Castro, V., Navia, D., de Prada, C., Lebrero, R., Muñoz, R., 2019b. Development of a control strategy to cope with biogas flowrate variations during photosynthetic biogas upgrading. Biomass and Bioenergy. 131, 105414.

Rodero, M.R., Lebrero, R., Serrano, E., Lara, E., Arbib, Z., García-Encina, P. A., Muñoz, R., 2019a. Technology validation of photosynthetic biogas upgrading in a semi-industrial scale algal-bacterial photobioreactor. Bioresource Technology. 279, 43-49.

Rosen, M.A., 2018. Environmental sustainability tools in the biofuel industry. Biofuel Research Journal. 17, 751-752.

Rybarczyk, P., Szulczyński, B., Gębicki, J., Hupka, J., 2019. Treatment of malodorous air in biotrickling filters: A review. Biochemical Engineering Journal. 141, 146-162.

Sahota, S., Shah, G., Ghosh, P., Kapoor, R., Sengupta, S., Singh, P, Vijay, V., Sahay, A., Vijay, V.K., Thakur, I.S., 2018. Review of trends in biogas upgradation technologies and future perspectives. Bioresource Technology Reports. 1, 79-88.

Santos-Clotas, E., Cabrera-Codony, A., Boada, E., Gich, F., Muñoz, R., Martín, M.J., 2019. Efficient removal of siloxanes and volatile organic compounds from sewage biogas by an anoxic biotrickling filter supplemented with activated carbon. Bioresource Technology. 294, 122136.

San-Valero, P., Penya-Roja, J.M., Álvarez-Hornos, F.J., Buitrón, G., Gabaldón, C., Quijano, G., 2019. Fully aerobic bioscrubber for the desulfurization of H_2S-rich biogas. Fuel. 241, 884-891.

Sharma, P., Gaur, V.K., Kim, S.H., Pandey, A., 2020. Microbial strategies for bio-transforming food waste into resources. Bioresource Technology. 299, 122580.

Shen, M., Zhang, Y., Hu, D., Fan, J., Zeng, G., 2018. A review on removal of siloxanes from biogas: with a special focus on volatile methylsiloxanes. Environmental Science and Pollution Research. 25, 30847-30862.

Spennati, F., Mannucci, A., Mori, G., Giordano, C., Munz, G., 2017. Moving bed biotrickling filters: an innovative solution for hydrogen sulphide removal from gas streams. Desalination Water Treatment. 61, 215-221.

Struk, M., Kushkevych, I., Vítězová, M., 2020. Biogas upgrading methods: recent advancements and emerging technologies. Reviews in Environmental Science and Bio/Technology. 19, 651-671.

Sun, S., Hu, C., Gao, S., Zhao, Y., Xu, J., 2019a. Influence of three microalgal-based cultivation technologies on different domestic wastewater and biogas purification in photobioreactor. Water Environment Research. 91, 679-688.

Sun, Z., Pang, B., Xi, J., Hu, H.Y., 2019b. Screening and characterization of mixotrophic sulfide oxidizing bacteria for odorous surface water bioremediation. Bioresource Technology. 290, 121721.

Sürmeli, R.Ö., Bayrakdar, A., Molaey, R., Çalli, B., 2019. Synergistic effect of sulfide and ammonia on anaerobic digestion of chicken manure. Waste and Biomass Valorization. 10, 609-615.

Syed, M., Soreanu, G., Falletta, P., Béland, M., 2006. Removal of hydrogen sulfide from gas streams using biological processes- A review. Canadian Biosystems Engineering. 48, 2.1-2.14.

Tabatabaei, M., Aghbashlo, M., Valijanian, E., Panahi, H.K.S., Nizami, A.S., Ghanavati, H., Sulaiman, A., Mirmohamadsadeghi, S., Karimi, K., 2020a. A comprehensive review on recent biological innovations to improve biogas production, part 1: upstream strategies. Renewable Energy. 146, 1204-1220.

Tabatabaei, M., Aghbashlo, M., Valijanian, E., Panahi, H.K.S., Nizami, A.S., Ghanavati, H., Sulaiman, A., Mirmohamadsadeghi, S., Karimi, K., 2020b. A comprehensive review on recent biological innovations to improve biogas production, part 2: mainstream and downstream strategies. Renewable Energy. 146, 1392-1407.

Taheriyoun, M., Salehiziri, M., Parand, S., 2019. Biofiltration performance and kinetic study of hydrogen sulfide removal from a real source. Journal of Environmental Health Science and Engineering. 1-12.

Tang, Q., Xu, J., Liu, Z., Huang, Z., Zhao, M., Shi, W., Ruan, W., 2019. Optimal the ex-situ biogas biological upgrading to biomethane and its combined application with the anaerobic digestion stage. Energy Sources, Part A: Recovery, Utilization, and Environmental Effects. 1-13.

Toledo-Cervantes, A., Lebrero, R., Cavinato, C., Muñoz, R., 2017. Biogas upgrading using algal-bacterial processes, in: Gonzalez-Fernandez, C., Muñoz, R. (Eds.), Microalgae-Based Biofuels and Bioproducts. Woodhead Publishing, pp. 283-304.

Tsang, Y.F., Wang, L., Chua, H., 2015. Simultaneous hydrogen sulphide and ammonia removal in a biotrickling filter: Crossed inhibitory effects among selected pollutants and microbial community change. Chemical Engineering Journal, 281, 389-396.

Van der Heyden, C., De Mulder, T., Volcke, E. I., Demeyer, P., Heyndrickx, M., Rasschaert, G., 2019b. Long-term microbial community dynamics at two full-scale biotrickling filters treating pig house exhaust air. Microbial Biotechnology. 12, 775-786.

Van der Heyden, C., Volcke, E.I., Brusselman, E., Demeyer, P., 2019a. Comparative 1-year performance study of two full-scale biotrickling filters for ammonia removal including nitrous oxide emission monitoring. Biosystems Engineering. 188, 178-189.

Vikrant, K., Kailasa, S.K., Tsang, D.C., Lee, S.S., Kumar, P., Giri, B.S., Singh, R.S., Kim, K. H., 2018. Biofiltration of hydrogen sulfide: trends and challenges. Journal of Cleaner Production. 187, 131-147.

Vikromvarasiri, N., Champreda, V., Boonyawanich, S., Pisutpaisal, N., 2017. Hydrogen sulfide removal from biogas by biotrickling filter inoculated with *Halothiobacillus neapolitanus*. International Journal of Hydrogen Energy. 42, 18425-18433.

Vikromvarasiri, N., Pisutpaisal, N., 2016. Hydrogen sulfide removal in biotrickling filter system by *Halothiobacillus neapolitanus*. International Journal of Hydrogen Energy. 41, 15682-15687.

Vo, H.N.P., Ngo, H.H., Guo, W., Nguyen, T.M.H., Liu, Y., Liu, Y., Nguyen, D.D., Chang, S. W., 2019. A critical review on designs and applications of microalgae-based photobioreactors for pollutants treatment. Science of the Total Environment. 651, 1549-1568.

Voelklein, M.A., Rusmanis, D., Murphy, J.D., 2019. Biological methanation: strategies for in-situ and ex-situ upgrading in anaerobic digestion. Applied Energy. 235, 1061-1071.

Wahid, R., Mulat, D.G., Gaby, J.C., Horn, S.J., 2019. Effects of H_2: CO_2 ratio and H_2 supply fluctuation on methane content and microbial community composition during in-situ biological biogas upgrading. Biotechnology for Biofuels. 12, 104.

Wang, G., Zhang, Z., Hao, Z., 2019c. Recent advances in technologies for the removal of volatile methylsiloxanes: A case in biogas purification process. Critical Reviews in Environmental Science and Technology. 49, 2257-2313.

Wang, J., Zhang, W., Xu, J., Li, Y., Xu, X., 2014. Octamethylcyclotetrasiloxane removal using an isolated bacterial strain in the biotrickling filter. Biochemical Engineering Journal. 91, 46-52.

Wang, Y., Chang, M., Pan, Y., Zhang, K., Lyu, L., Wang, M., Zhu, T., 2019b. Performance analysis and optimization of ammonium removal in a new biological folded non-aerated filter reactor. Science of the Total Environment. 688, 505-512.

Wang, Y., Xu, L., Solangi, Y.A., 2020. Strategic renewable energy resources selection for Pakistan: based on SWOT-Fuzzy AHP approach. Sustainable Cities and Society. 52, 101861.

Wang, Z., Wang, F., Zhu, Y., Gong, B., 2019a. Method of desulfurization process selection based on improved fuzzy comprehensive evaluation: a case study of papermaking desulfurization in China. Processes. 7, 446.

Wasajja, H., Lindeboom, R.E., van Lier, J.B., Aravind, P.V., 2020. Techno-economic review of biogas cleaning technologies for small scale off-grid solid oxide fuel cell applications. Fuel Processing Technology. 197, 106215.

Wu, H., Yan, H., Quan, Y., Zhao, H., Jiang, N., Yin, C., 2018. Recent progress and perspectives in biotrickling filters for VOCs and odorous gases treatment. Journal of Environmental Management. 222, 409-419.

Xiao, J., Liu, C., Ju, B., Xu, H., Sun, D., Dang, Y., 2021. Estimation of in-situ biogas upgrading in microbial electrolysis cells via direct electron transfer: Two-stage machine learning modeling based on a NARX-BP hybrid neural network. Bioresource Technology. 330, 124965.

Xu, F., Li, Y., Ge, X., Yang, L., Li, Y., 2018. Anaerobic digestion of food waste-Challenges and opportunities. Bioresource Technology. 247, 1047-1058.

Xu, H., Wang, K., Zhang, X., Gong, H., Xia, Y., Holmes, D.E., 2020. Application of in-situ H_2-assisted biogas upgrading in high-rate anaerobic wastewater treatment. Bioresource Technology, 299, 122598.

Xue, J., Li, Y., Peppers, J., Wan, C., Kado, N.Y., Green, P.G., Young, T.M., Kleeman, M.J., 2018. Ultrafine particle emissions from natural gas, biogas, and biomethane combustion. Environmental Science & Technology. 52, 13619-13628.

Yang, C., Qian, H., Li, X., Cheng, Y., He, H., Zeng, G., Xi, J., 2018. Simultaneous removal of multicomponent VOCs in biofilters. Trends in Biotechnology. 36, 673-685.

Yang, L., Corsolini, S.I., 2019. Online removal of volatile siloxanes in solid-state anaerobic digester biogas using a biofilter and an activated carbon filter. Journal of Environmental Chemical Engineering. 7, 103284.

Yin, C., Shen, Y., Yu, Y., Yuan, H., Lou, Z., Zhu, N., 2019. In-situ biogas upgrading by a stepwise addition of ash additives: methanogen adaption and CO_2 sequestration. Bioresource Technology. 282, 1-8.

Yu, Y., Hou, J., Li, M., Meng, F., Xi, B., Liu, D., Ye, M., 2019. Selection and optimization of composting packing media for biofiltration of mixed waste odors. Waste and Biomass Valorization. 1-9.

Yuan, Y., Cheng, H., Chen, F., Zhang, Y., Xu, X., Huang, C., Chen, C., Liu, W., Ding, C., Li, Z., Chen, T., Wang, A., 2020. Enhanced methane production by alleviating sulfide inhibition with a microbial electrolysis coupled anaerobic digestion reactor. Environment International. 136, 105503.

Zandebasiri, M., Groselj, P., Azadi, H., Serio, F., Shureshjani, R.A., 2021. DPSIR framework priorities and its application to forest management: a fuzzy modeling. Environmental Monitoring and Assessment, 193, 1-16.

Zeng, Q., Hao, T., Sun, B., Luo, J., Chen, G., Crittenden, J.C. 2019. Electrochemical pretreatment for sludge sulfide control without chemical dosing: a mechanistic study. Environmental Science & Technology. 53, 14559-14567.

Zeng, Y., Xiao, L., Zhang, X., Zhou, J., Ji, G., Schroeder, S., Liu, G., Yan, Z., 2018. Biogas desulfurization under anoxic conditions using synthetic wastewater and biogas slurry. International Biodeterioration & Biodegradation. 133, 247-255.

Zhang, Y., Zhang, L., Liu, H., Gong, L., Jiang, Q., Liu, H., Fu, B., 2019. Carbon dioxide sequestration and methane production promotion by wollastonite in sludge anaerobic digestion. Bioresource Technology. 272, 194-201.

Zhu, T., Curtis, J., Clancy, M., 2019c. Promoting agricultural biogas and biomethane production: Lessons from cross-country studies. Renewable and Sustainable Energy Reviews. 114, 109332.

Zhu, X., Cao, Q., Chen, Y., Sun, X., Liu, X., Li, D., 2019a. Effects of mixing and sodium formate on thermophilic in-situ biogas upgrading by H_2 addition. Journal of Cleaner Production. 216, 373-381.

Zhu, X., Chen, L., Chen, Y., Cao, Q., Liu, X., Li, D., 2019b. Differences of methanogenesis between mesophilic and thermophilic in situ biogas-upgrading systems by hydrogen addition. Journal of Industrial Microbiology & Biotechnology. 46, 1569-1581.

Zhuo, Y., Han, Y., Qu, Q., Li, J., Zhong, C., Peng, D., 2019. Characteristics of low H_2S concentration biogas desulfurization using a biotrickling filter: Performance and modeling analysis. Bioresource Technology. 280, 143-150.

Zorpas, A.A., 2020. Strategy development in the framework of waste management. Science of the Total Environment. 137088.

Chapter 3

Biological removal of gas-phase H_2S in hollow fibre membrane bioreactors

A modified version of this chapter has been published as:

Das, J., Ravishankar, H., Lens, P.N.L., 2022. Biological removal of gas-phase H_2S in hollow fibre membrane bioreactors. Journal of Chemical Technology & Biotechnology. Early View. https://doi.org/10.1002/jctb.6999

Abstract

Hydrogen sulfide (H_2S) must be treated from its emission sources to avoid health risks, odour and corrosion. Conventional physico-chemical H_2S removal technologies, e.g. membrane contactors or chemical scrubbers, have several limitations such as requirement of high amounts of absorption chemicals and energy. In contrast, biological H_2S removal technologies are environment friendly, easy to operate and less expensive due to low energy requirements. In this study, the feasibility of a porous hydrophilic polyethersulfone hollow fibre membrane bioreactor (HFMB) was tested for biological removal of gas-phase H_2S employing three lab-scale reactors (two biotic and one abiotic). The HFMBs were operated at ~ 20°C for ~ 3 months employing different H_2S inlet loading rates (ILR) and an empty bed residence time of 187 s. Biotic performance of the HFMBs demonstrated that the removal efficiency (RE) varied for using different inoculum, in the range 80-100% for the applied H_2S ILR of ~ 5.0-7.5 g m^{-3} h^{-1}. The RE reached to a constant value of ~ 100% in both biotic reactors at an ILR of ~ 17.0 g m^{-3} h^{-1} for using acclimatized inoculum. The biotic HFMBs demonstrated ~5-9 times higher H_2S flux and ~20-26 times higher mass transfer compared to the abiotic control. Surface morphology revealed microbial attached growth on the outer surface of the membranes, while the high throughput sequencing confirmed the richness of H_2S oxidizing microbial communities on the shell side. The obtained results confirm that the HFMB configuration is suitable for biological treatment of H_2S laden waste gas.

3.1. Introduction

Hydrogen sulfide (H_2S) is a highly toxic, corrosive and odorous gas. It is predominantly present in waste gas streams released from industries such as pulp and paper manufacturing, rayon production, biogas production and crude petroleum refineries (Kailasa et al., 2020; Rodero et al., 2018). Physico-chemical and biological treatment processes are commonly employed to treat H_2S (Fernández et al., 2013). Although physico-chemical technologies (e.g. water scrubbing or chemical scrubbing) are widely applied, generation of secondary pollution and requirement of high amounts of chemicals and energy limit their application (Wu et al., 2018). On the contrary, the biological processes (e.g. biofiltration and bioscrubbing) are environment friendly and easy to operate under a wide range of conditions that can significantly reduce the energy

requirement, and generate ecologically safe end products (Lin et al., 2018; Wu et al., 2018).

Several bioreactor configurations such as the biofilter (Das et al., 2019; Yuan et al., 2019), biotrickling filter (Arellano-García et al., 2018; Khanongnuch et al., 2019a; Rodero et al., 2018; Spennati et al., 2017; Vikromvarasiri et al., 2017; Wu et al., 2018; Wu et al., 2020) and bioscrubber (Lin et al., 2018; San-Valero et al., 2019) are frequently used for biological H_2S removal. The bioreactors are operated either under aerobic or anoxic conditions, where sulfur-oxidizing bacteria convert sulfide (S^{2-}) into elemental sulfur (S^0) and sulfate (SO_4^{2-}) as end products during the bioconversion process. However, each bioreactor configuration has some limitations compared to the other bioreactor types, for example, poor buffering capacity of biofilters (Lin et al., 2018), filter bed clogging at high loading rates in biotrickling filters (Spennati et al., 2017), as well as generation of excess waste (Wu et al., 2018) and higher operational costs (Lin et al., 2018) in bioscrubbers compared to biofilters or biotrickling filters. Therefore, studies focus on overcoming the issues through improvements in bioreactor design, operating conditions and use of better packing materials that can augment the pollutant removal performance. Hollow fibre membrane reactors, which were initially developed for the microbial reduction of nitrate and perchlorate from water by diffusing H_2 (as an electron donor) through the hollow fibres (Rittmann et al., 2004), can be such a technology.

Hollow fibre membrane (HFM) based technologies have been employed for several biological applications (Aoi et al., 2009; Alfaro et al., 2019; Shen et al., 2018; Wang et al., 2018). HFM modules were tested for physico-chemical applications as membrane contactors for gas separation (Bao and Lipscomb, 2003) owing to their large surface area per apparatus volume and selective mass transfer (Bazhenov et al., 2018). Non-porous hydrophobic membrane modules are generally preferred in membrane contactors as they eliminate issues around pore blocking caused due to fouling, leaking and pore wetting, which is observed in hydrophilic membranes. However, hydrophilic porous membranes offer better mass transfer characteristics and can facilitate faster reaction kinetics as opposed to non-porous hydrophobic membranes. A few studies on the application non-porous hydrophobic polydimethylsiloxane (PDMS) membrane-based reactor configurations such as bio-membrane unit (Pokorna-Krayzelova et al., 2017) and hybrid bioscrubber using chemical extractant (Tilahun et al., 2018) have been reported for H_2S

removal. Till date, to the best of our knowledge, no work has thus far reported on the application of porous hydrophilic polyethersulfone hollow fibre membrane bioreactor (HFMB) for removal of H_2S through biological desulfurization.

The aim of this study was to test the use of hydrophilic polyethersulfone (H-PES) based bioreactor configuration for biological desulfurization of gas-phase H_2S. To fabricate the HFMB, H-PES membrane was chosen for its high chemical and thermal stability during operation (Zhao et al., 2013), and hydrophilicity that helps to be less prone to fouling (Ahmad et al., 2013). A lab-scale HFMB reactor was fabricated and investigated for treatment of H_2S at ambient (20 ± 2°C) temperature. The reactor's performance for continuous operation was assessed by evaluating the flux, gas-liquid mass transfer, removal efficiency, elimination capacity and microbial community composition of the attached and suspended biomass in the reactor. The study presents a proof of concept of the H-PES membrane based HFMB configuration for the biological treatment of H_2S laden gas.

3.2. Materials and methods

3.2.1. Source of biomass

Activated sludge (total suspended solids (TSS) of ~ 2.90 g L^{-1} and volatile suspended solids (VSS) of ~ 2.30 g L^{-1}) collected from a dairy wastewater treatment plant (Kilconnell, Ireland) was used as a source of autotrophic sulfur oxidizing bacteria (ASOB). The sludge was stored at 4°C prior to its use.

Batch studies of the inoculum

Prior to inoculation of the HFMBs, batch studies with the inoculum were carried out in three cycles to test the suitability of sludge inoculum, i.e. to determine the activity of ASOB for the conversion of S^{2-} into SO_4^{2-}. The end of each cycle of sequential culturing was determined based on the SO_4^{2-} profile of each cycle, i.e. when nearly constant SO_4^{2-} concentrations were achieved. Successive transfer of the enrichment (10%) to the next cycle was carried out at the end of each cycle. The inoculum to mineral medium ratio in each transfer of sequential culturing was 1:9 (*v/v*). The change in SO_4^{2-} concentration in each cycle of sequential culturing was normalized by subtracting the SO_4^{2-} concentration of the control, i.e. sample blank. The first two cycles of enrichment were carried out under

controlled laboratory conditions (at 120 rpm and atmospheric condition using an orbital shaker, model: Innova® 42: SHA4135, Germany). The third cycle of culturing was done at ambient temperature (~ 20°C) without shaking.

Inoculum used for continuous operation of HFMB

At the start of the continuous operation, the first HFMB (R_1) was inoculated with the ASOB enrichment (end of the third cycle of the batch culture) with an inoculum to mineral medium ratio of 1:9 (*v/v*). The second HFMB (R_2) was inoculated with raw activated sludge without any prior enrichment.

3.2.2. Mineral medium

The mineral medium (MM) used for enrichments contained (composition in g L^{-1}): K_2HPO_4 - 1.0, KH_2PO_4 - 1.0; $NaHCO_3$ - 1.0, $MgSO_4 \cdot 7H_2O$ - 0.30, NH_4Cl - 0.35, $MnSO_4 \cdot H_2O$ - 0.02, $CaCl_2 \cdot 2H_2O$ - 0.03 and $Na_2S \cdot 9H_2O$ - 1.0. $Na_2S \cdot 9H_2O$ was added as a source of sulfide in the aqueous salt medium resulting in an initial S^{2-} concentration of 130-140 mg L^{-1} (Cheng et al., 2018). The MM used for the HFMB had the following composition (in g L^{-1}): KH_2PO_4 - 2.0; NH_4Cl - 1.0, $NaHCO_3$ - 1.0, $FeCl_3 \cdot 6H_2O$ - 0.02, $CuCl_2 \cdot 2H_2O$ - 0.02, H_3BO_3 - 0.02, $MnCl_2 \cdot 4H_2O$ - 0.02, $Na_2MoO_4 \cdot 2H_2O$ - 0.02, $MgCl_2 \cdot 6H_2O$ - 0.05, $CaCl_2 \cdot 2H_2O$ - 0.02 and $ZnCl_2$ - 0.02. The MM composition used for the HFMB was modified from the composition used for batch studies by adding trace elements (Zou et al., 2016) to enhance ASOB enrichment during continuous operation of the HFMB. In addition, Cl^- salts instead of SO_4^{2-} salts were used in the MM to avoid interference with the SO_4^{2-} generated by the H_2S bioconversion.

3.2.3. Experimental set-up

Membrane module fabrication

Hydrophilic polyethersulfone (H-PES) hollow fibre membranes (Senuofil Co., China) having an outer diameter - 2.0 mm, inner diameter - 1.65 mm, and thickness - 0.02 mm were used in the hollow fibre membrane bioreactor (HFMB). Table 3.1 summarizes the membrane characteristics volumetric porosity, water flux and permeability at different operation conditions. HFM modules were fabricated with ten fibres in each module, with an effective membrane length, area and surface area/volume ratio of 2.2 m, 0.0138 m^2 and 2000 m^2 m^{-3}, respectively. The fibres in each HFM module lay parallel to each other.

Table 3.1: Characterization of hydrophilic polyethersulfone (H-PES) hollow fibre membrane.

Peristaltic pump water flow rate, L/h	Membrane porosity, %	Mean pore radius, nm	Operational pressure, bar	Permeate flux, L m^{-2} h^{-1}	Water permeability, L m^{-2} h^{-1} bar^{-1}
4	62.93	4.63	0.060	1.06	113.35
8	69.92	10.84	0.124	14.32	
12	69.17	11.11	0.234	27.85	

HFMB set-up

Figure 3.1 shows the schematic of the laboratory scale HFMB set-up used for H_2S removal. Two HFMB reactors (R_1 and R_2) were tested for biological removal of H_2S, whereas a third reactor (R_3) was used as an abiotic control. In each HFMB, a HFM module was placed in a glass column (inner diameter 0.06 m; height 0.25 m) filled with the liquid phase (either with reactor mixed liquor or deionized water). The liquid phase of the HFMB was kept static. The liquid phase of the HFMB, i.e. the changes of pH as well as S^{2-} and sulfur species (e.g. S^{2-}, SO_4^{2-} or $S_2O_3^{2-}$) concentration, were sampled regularly for analysis. The temperature inside the reactors was maintained at 20 (± 2)°C using a temperature controlled water jacket outside of each reactor.

Gas-phase H_2S was supplied to the HFMB by mixing $Na_2S{\cdot}9H_2O$ (0.01-0.03 M) and HCl (0.02-0.03 M) in a mixing chamber using a peristaltic pump (Masterflex, USA) at different flow rates, depending on the desired H_2S concentration (~ 50-650 ppm_v). A variable area flow meter (flow range 0.06-1.7 L min^{-1}, Brooks, USA) was used to control the air flow rate into the gas mixing chamber. Gas bags (10 L Tedlar® SCV gas sampling bag w/Thermogreen® LB-2 Septa) were used to collect the generated H_2S containing synthetic gas (H_2S+CO_2+O_2+N_2) and feed the reactors. The CO_2 concentration in the inlet H_2S containing synthetic gas was adjusted to ~ 0.7-1.5% by adding a certain volume (~ 70-150 mL) of pure CO_2 (~ 100%) into the inlet gas bag. The synthetic gas was passed through the lumen side of the hollow fibres in the membrane module at atmospheric pressure. H_2S, CO_2 and O_2 transferred from the gas-phase through the membrane pores and diffused into the bioreactor mixed liquor, while the non-diffused gas stream left the HFM module and accumulated in the outlet gas bag.

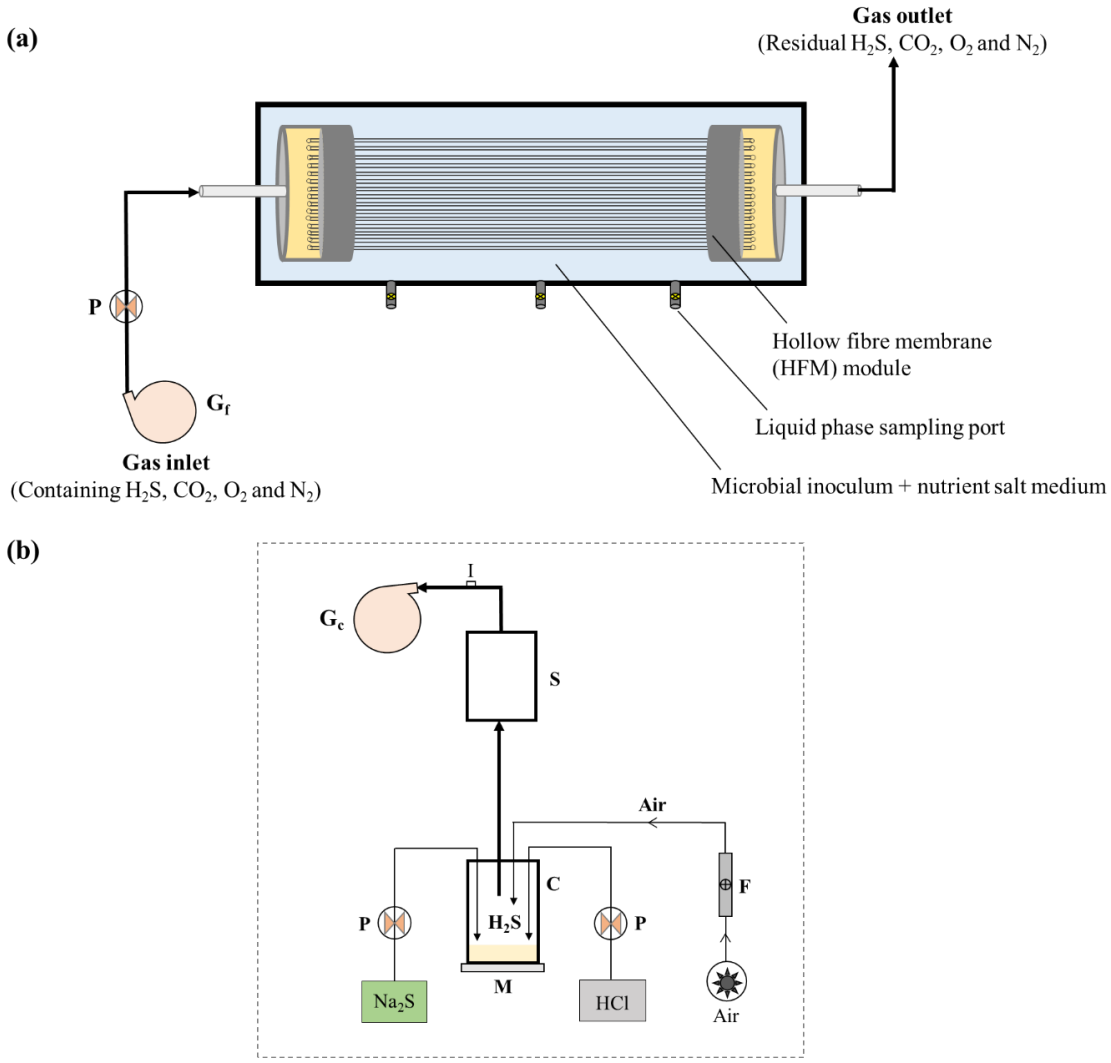

Figure 3.1: Overview of the HFMB set-up used in this study: (a) schematic of the HFMB applied for H_2S removal and (b) H_2S generation and collection unit [Note: C - Chemical mixing and H_2S generation chamber; F - Flow meter; G_c - Collection of H_2S containing synthetic polluted gas in tedlar gas bag; G_f - Continuous feeding of H_2S containing synthetic polluted gas; I - Port to measure inlet gas; M - Magnetic stirrer; P - Peristaltic pump; S - Moisture free gas collecting glass vessel].

3.2.4. Experimental design to evaluate the HFMB performance

Table 3.2 summarizes the different operating conditions of the three reactors. The HFMBs R_1 and R_2 operated continuously for 83 days in five phases. The inlet H_2S concentration was maintained at low values (0.07-0.08 g m^{-3}) in both R_1 and R_2 during Phase 1 (i.e. start-up and acclimatization phase) and was subsequently increased at the start of a new phase. The H_2S removal performance of R_1 and R_2 in Phase 1-3 was tested to observe if there were differences in removal performance by the two inocula. At the

end of Phase 3 operation, sludge from R_2 was homogeneously mixed with freshly prepared MM at a ratio of 7:3 (*v/v*) and used as inoculum for both reactors R_1 and R_2 to evaluate the HFMBs performance when operated with the same inoculum. The control HFMB reactor (R_3) was filled with deionized water only. The inlet gas flow rate was kept constant (~ 0.14 L h^{-1}) throughout operation of R_1 - R_3 and the corresponding empty bed residence time (EBRT) was estimated to be 187 s.

Table 3.2: Operating conditions employed for continuous operation of the HFMB.

Phase	Operating time, days	EBRT, s	Inlet H_2S[c] concentration, ppm_v	Inlet H_2S concentration, g m^{-3}	Inlet loading rate, g m^{-3} h^{-1}
Biotic operation of HFMB (R_1)					
Phase 1	0-24 (24)	187	47±15	0.07±0.02	1.28±0.41
Phase 2	25-48 (24)	187	184±14	0.26±0.02	5.01±0.37
Phase 3	49-64 (16)	187	194±14	0.27±0.02	5.27±0.38
Phase 4[b]	65-74 (10)	187	323±20	0.46±0.03	8.78±0.54
Phase 5	75-83 (9)	187	613±28	0.87±0.04	16.68±0.75
Biotic operation of HFMB (R_2)					
Phase 1[a]	0-15 (15)	187	56±08	0.08±0.01	1.53±0.21
Phase 2	16-39 (24)	187	184±15	0.26±0.02	5.01±0.42
Phase 3	40-55 (16)	187	287±09	0.41±0.01	7.81±0.23
Phase 4[b]	56-65 (10)	187	322±17	0.46±0.02	8.77±0.46
Phase 5	66-74 (9)	187	621±32	0.88±0.05	16.90±0.87
Abiotic operation of HFMB (R_3)					
Phase 1	0-22 (22)	187	166±33	0.23±0.05	4.51±0.89
Phase 2	23-28 (6)	187	305±18	0.43±0.03	8.31±0.48

Note: [a] - R_2 started its operation 9 days after the start-up of R_1; [b] - Phase 4 was started using the same inoculum in both reactors; [c] - the detection limit of gas-phase H_2S was 1 ppm_v.

The inlet and outlet concentration of gas-phase H_2S was monitored daily to determine the H_2S removal performance of the HFMB. To quantify the H_2S bioconversion process and identify the main sulfur species (either S^0 or SO_4^{2-}) in the HFMB, the S^{2-}, $S_2O_3^{2-}$ and SO_4^{2-} concentrations in the shell side were periodically monitored during each phase. The pH was also periodically monitored. The H_2S flux through the hollow fibre membrane module and the gas-liquid mass transfer coefficient for all three HFMBs were determined to compare the biotic and abiotic performance of the HFMB. Apart from H_2S, the inlet

and outlet concentration of CO_2 was also monitored to observe whether gas-phase CO_2 is diffused through the membrane to the liquid phase or not, and to identify if the inorganic carbon source of the ASOB is from the gas phase CO_2 supplied through the HFM or bicarbonate (HCO_3^-) supplied via the MM.

Microbial community analysis of the suspended biomass from both R_1 and R_2 was carried out at the end of Phase 3 to identify the microbial population in both reactors, especially the presence of ASOB species. The morphology of the membrane surface (collected from R_2 on day 75) was studied at the end of Phase 5 to assess attached microbial growth onto the membranes.

3.2.5. Calculations

Membrane characterization

The volumetric porosity (Eq. 3.1) and the mean pore radius (Eq. 3.2) of the membranes were determined using gravimetric analysis (Tan et al., 2001) and the Guerout-Elford-Ferry equation (Guo and Kim, 2017), respectively. The water flux (Eq. 3.3) and permeability (Eq. 3.4) were estimated using permeation tests (Ravishankar et al., 2018).

$$\varepsilon = \frac{(W_{wet} - W_{dry})/\rho H_2O}{(1/4)\pi L(D_o^2 - D_i^2)} \quad (3.1)$$

$$r_m = \sqrt{\frac{(2.9 - 1.75\varepsilon)8\eta l Q}{\varepsilon A \Delta P}} \quad (3.2)$$

$$J_v = \frac{Q}{A} \quad (3.3)$$

$$L_p = \frac{J_v}{\Delta P} \quad (3.4)$$

where ε is the volumetric porosity, W_{wet} and W_{dry} are respectively the wet and dry weight of the membrane (kg), ρH_2O is the density of deionized water (kg m^{-3}), L is the membrane length (m), D_o and D_i are respectively the outer and inner diameter of the membrane (m), r_m is the membrane mean pore radius (nm), η is the water viscosity (Pa.s), l is the thickness of the membrane (m), Q is the permeate flow rate (m^3 s^{-1}), A is the effective membrane area (m^2), ΔP is the operational pressure bar (Pa), J_v is the permeate flux (L m^{-2} h^{-1}), and L_p is the water permeability (L m^{-2} h^{-1} bar^{-1}).

HFMB performance parameters

The HFMB's operating parameters and performance were evaluated in terms of EBRT, inlet loading rate (ILR), removal efficiency (RE) and elimination capacity (EC), according to Jaber et al. (2017):

$$\text{EBRT (s)} = \frac{V}{Q} \quad (3.5)$$

$$\text{ILR } (g/m^3h) = \frac{Q}{V} C_{in} \quad (3.6)$$

$$\text{RE (\%)} = \frac{(C_{in} - C_{out})}{C_{in}} 100 \quad (3.7)$$

$$\text{EC } (g/m^3h) = \frac{Q}{V}(C_{in} - C_{out}) \quad (3.8)$$

where Q is the gas flow rate ($m^3\ h^{-1}$), V is the bed volume (m^3), C_{in} and C_{out} are respectively the inlet and outlet H_2S concentration ($g\ m^{-3}$).

Experimental data were used to determine the H_2S flux (J) and overall mass transfer coefficient (K_G) of gas-phase H_2S in each reactor according to Tilahun et al. (2017):

$$J\ (g\ m^{-2}\ h^{-1}) = \frac{Q}{A}(C_{in} - C_{out}) \quad (3.9)$$

$$K_G (m\ h^{-1}) = \frac{Q}{A} \ln \frac{C_{in}}{C_{out}} \quad (3.10)$$

where Q is the gas flow rate ($m^3\ h^{-1}$), A is the surface area of the membrane (m^2), C_{in} and C_{out} are respectively the inlet and outlet H_2S concentration ($g\ m^{-3}$).

3.2.6. Analytical methods

Gas phase

A portable multi-gas analyzer (Biogas 5000, Geotech, UK) calibrated by QED environmental system limited (Coventry, UK) was used for simultaneous analysis of H_2S, NH_3, CH_4, CO_2, and O_2. To check for consistency with the analysis, another multi-gas detection device (Dräger X-am 8000, Germany) was used in regular intervals (once in a week). The ideal gas law (PV = nRT) was used to convert the H_2S concentration unit from ppm_v to $g\ m^{-3}$, wherein the temperature (T), pressure (P) and molar gas constant (R) were 294 K, 101.325 kPa and 8.314 L kPa K^{-1} mol^{-1}, respectively.

Liquid phase

The liquid microbial suspensions from the HFMBs were periodically (generally once a week) collected and filtered through a 0.2 μm filter (Sartorius™ cellulose acetate membrane filters, Fisher Scientific, UK) prior to analysis of sulfate (SO_4^{2-}), thiosulfate

($S_2O_3^{2-}$) and sulfide (S^{2-}). The pH of the solutions was measured using a pH meter (Mettler Toledo™ 30266626, Fisher Scientific, UK). The total suspended solids and volatile suspended solids of the activated sludge were determined in triplicates according to the protocol described in Standard Methods (APHA, 2012).

SO_4^{2-} and $S_2O_3^{2-}$ were measured using an ion chromatograph (Thermo Scientific™ Dionex™, USA) fitted with a guard column (Dionex™ IonPac™ AS14A IC Column, 4mm, catalog number 056897) and an analytical column (Dionex™ IonPac™ AS14A IC Column, 4mm, catalog number 056904). The ion chromatograph was also used to determine the concentration of PO_4^{3-}, NO_3^-, SO_4^{2-} and $S_2O_3^{2-}$ in the liquid phase of the aerobic sludge. The S^{2-} concentration was determined using a colorimetric method (Allen et al., 1993) where the absorbance (λ_{max} 670 nm) was measured in a UV/Vis spectrophotometer (Shimadzu UV-1900, Germany).

Surface morphology

The morphology of the fresh and used (sampled from R_2 on day 75) membranes surface were observed by scanning electron microscopy (SEM) (Hitachi S-4700, Germany; Fuller et al., 2016). Membrane samples were air dried, fixed onto a stub using carbon tape and gold coated (Fuller et al., 2016) to prevent charging effects on the surface and to minimize the thermal damage.

Microbial community analysis

The inoculum and suspended biomass (from both HFMBs R_1 and R_2) were collected in triplicates at the end of Phase 3 operation (i.e. on day 64 in R_1 and day 55 in R_2) for microbial community analysis. Each sample was centrifuged at 10,000×g for 5 minutes. The pellet was retained for total genome DNA extraction using DNeasy PowerSoil Kit (Qiagen, Germany). Extracted DNA was visualised by UV excitation after electrophoresis in 1% agarose gels (w/v) 1× TAE buffer (40 mM Tris-base, 1 mM EDTA, 1.14 mM glacial acetic acid; pH 8) containing 1 mg L^{-1} GelRed™ (Bioscience) with Hyperladder IV (Bioline) as a molecular weight marker. The DNA concentration was analysed using a Qubit™ 2.0 Fluorometer.

The obtained DNA samples were then sent to Novogene Institute (Beijing, China) for sequencing library construction and Illumina high-throughput sequencing on the HiSeq 2500 platform (Illumina, USA). Amplicon generation was carried out using specific

primers (341F-806R) to amplify the V3-4 region. Both sequencing preparation (e.g. PCR reactions and purification, sequencing libraries and assessing the library qualities) and bioinformatics analysis (e.g. sequencing data processing, OTU cluster and taxonomic annotation, alpha and beta diversity) was provided by Novogene Institute as described in detail by Jiang et al. (2019).

3.3. Results

3.3.1. Batch activity of the inoculum

Figure 3.2 shows that the activated sludge converted the supplied S^{2-} to SO_4^{2-} at a rate of ~ 100 mg S^{2-}/g VSS·d. The pH dropped from ~ 8.5 to ~ 7.5 at the end of each incubation. Considering the initial (at 0 hr) SO_4^{2-} concentration and stoichiometry of the bioconversion process (from S^{2-} to SO_4^{2-}), the SO_4^{2-} concentration could reach ~ 250-270 mg L^{-1} after complete bioconversion. Figure 3.2 shows the estimated and observed SO_4^{2-} concentrations for each of the three incubations were nearly similar. However, a longer period for complete conversion of S^{2-} to SO_4^{2-} was observed when the incubation was at outdoor temperature (Cycle 3).

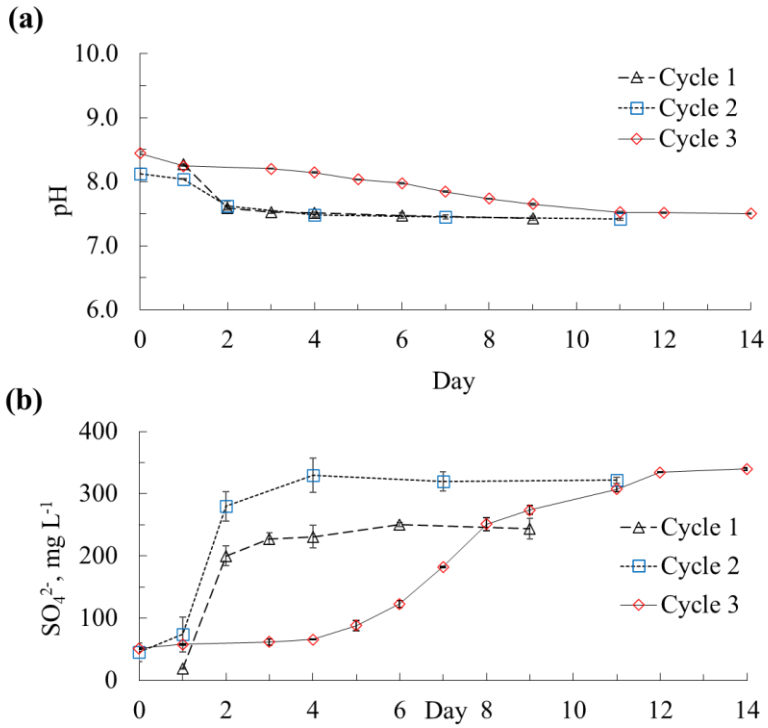

Figure 3.2: Batch activity test of ASOB during sequential culturing: (a) change of pH

and (b) change of sulfate concentration. [Note: error bars represent the standard deviations of triplicate analysis].

3.3.2. Performance of the HFMB

Biotic performance

Figures 3.3 and 3.4 show the H_2S removal efficiency (RE) and elimination capacity (EC), respectively, of R_1 and R_2. During Phase 1, the RE of R_1 varied for the first 10 days of operation around a mean value of ~ 38% and achieved ~100% RE from day 11 for an inlet loading rate (ILR) of 1.50 (±0.21) g m^{-3} h^{-1}. The R_2 achieved ~ 100% RE for an ILR of 1.53 (±0.21) g m^{-3} h^{-1} within 24 h.

The RE of R_1 varied from ~ 80 to 100% where the EC was 4.50 (±0.54) and 5.03 (±0.53) g m^{-3} h^{-1} in Phase 2 and 3, respectively. In contrast, R_2 achieved ~ 100% RE in both Phase 2 and 3 with an EC of 5.01 (±0.42) and 7.81 (±0.23) g m^{-3} h^{-1}, respectively. In Phase 4, the RE of R_1 increased from ~ 90 to 100% within 5 days of operation, while the RE of R_2 was ~ 100% from the starting of Phase 4 operation. The EC of R_1 and R_2 were 8.51 (±0.71) and 8.77 (±0.46) g m^{-3} h^{-1}, respectively. In Phase 5, both R_1 and R_2 achieved ~ 100% RE corresponding to an EC of 16.68 (±0.75) and 16.90 (±0.87) g m^{-3} h^{-1}, respectively (Figure 3.4).

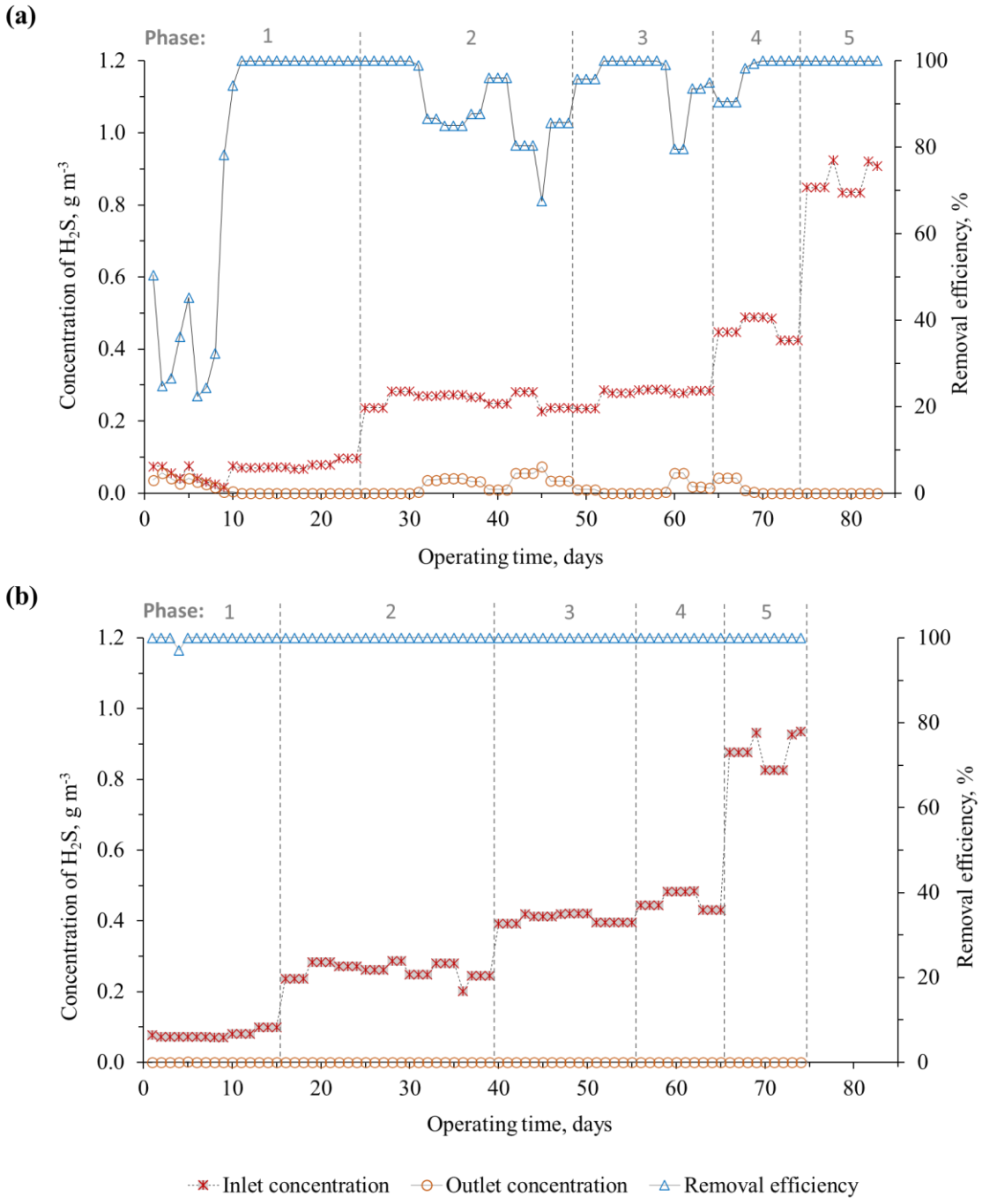

Figure 3.3: H_2S removal performance of HFMB: (a) R_1 and (b) R_2.

The initial pH on day 0 was ~ 7.00 and 7.84 for R_1 and R_2, respectively. The values slightly changed during operation, and the mean pH was 7.06 (±0.04) and 7.23 (±0.22) for R_1 and R_2, respectively, at the end of Phase 3. During Phase 4, the pH was 7.01 for both reactors, which slightly dropped at the end of Phase 5 to around 6.83 (±0.16).

The S^{2-} and $S_2O_3^{2-}$ concentrations of the reactor mixed liquor were below the detection limit in both R_1 and R_2, suggesting the complete bioconversion of S^{2-} into S^0 and SO_4^{2-}. The theoretical and experimental values of cumulative SO_4^{2-}-S in the liquid medium were 30.99 and 19.32 mg, respectively, after 64 days of operation of R_1, suggesting that SO_4^{2-} (62%) was the main sulfur species of the S^{2-} bioconversion. However, a much larger gap was observed for R_2 where the theoretical and experimental values were 43.17 and 7.00 mg SO_4^{2-}-S, respectively, after 56 days of operation, suggesting that S^0 (84%) was the main sulfur species in R_2.

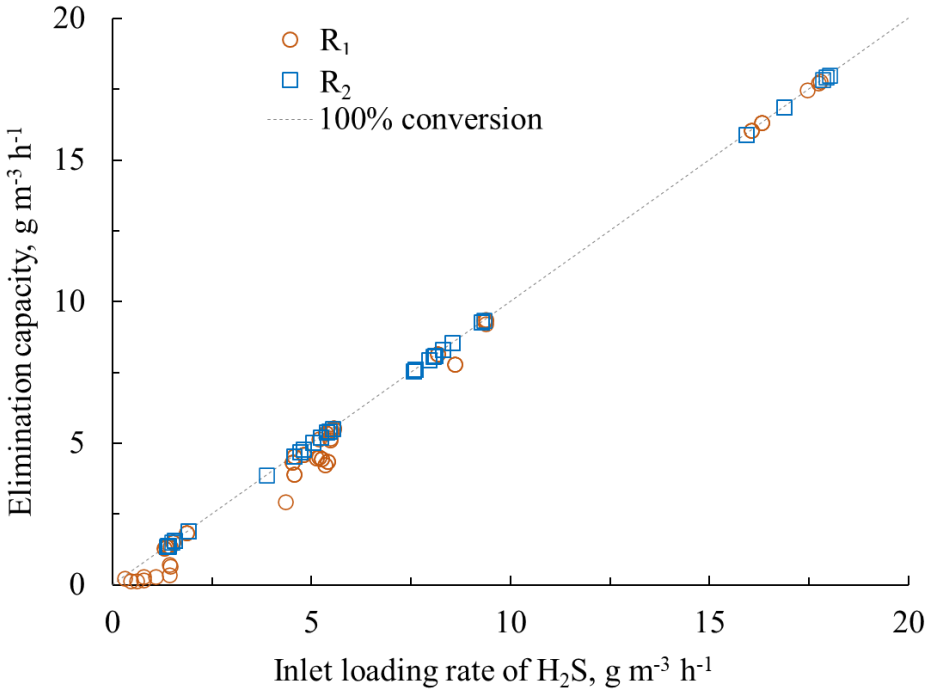

Figure 3.4: Influence of H_2S inlet loading rate on the elimination capacity of the HFMBs (R_1 and R_2).

Abiotic performance

Figure 3.5 shows the inlet and outlet concentration profiles of H_2S and CO_2 during continuous operation of the abiotic reactor (R_3). The S^{2-} concentration in R_3 was < 0.10 mg L^{-1} for an inlet H_2S concentration of 0.23 (±0.05) g m^{-3} in Phase 1 and 0.43 (±0.03) g m^{-3} in Phase 2. The outlet/inlet concentration ratio of H_2S reached ~ 0.70 (Figure 3.5a) within the first 3 days of operation and then increased with time till a constant value of 0.80 in Phase 2. The outlet/inlet concentration ratio of CO_2 (Figure 3.5b) was nearly constant for the entire period at a value of ~ 1.00.

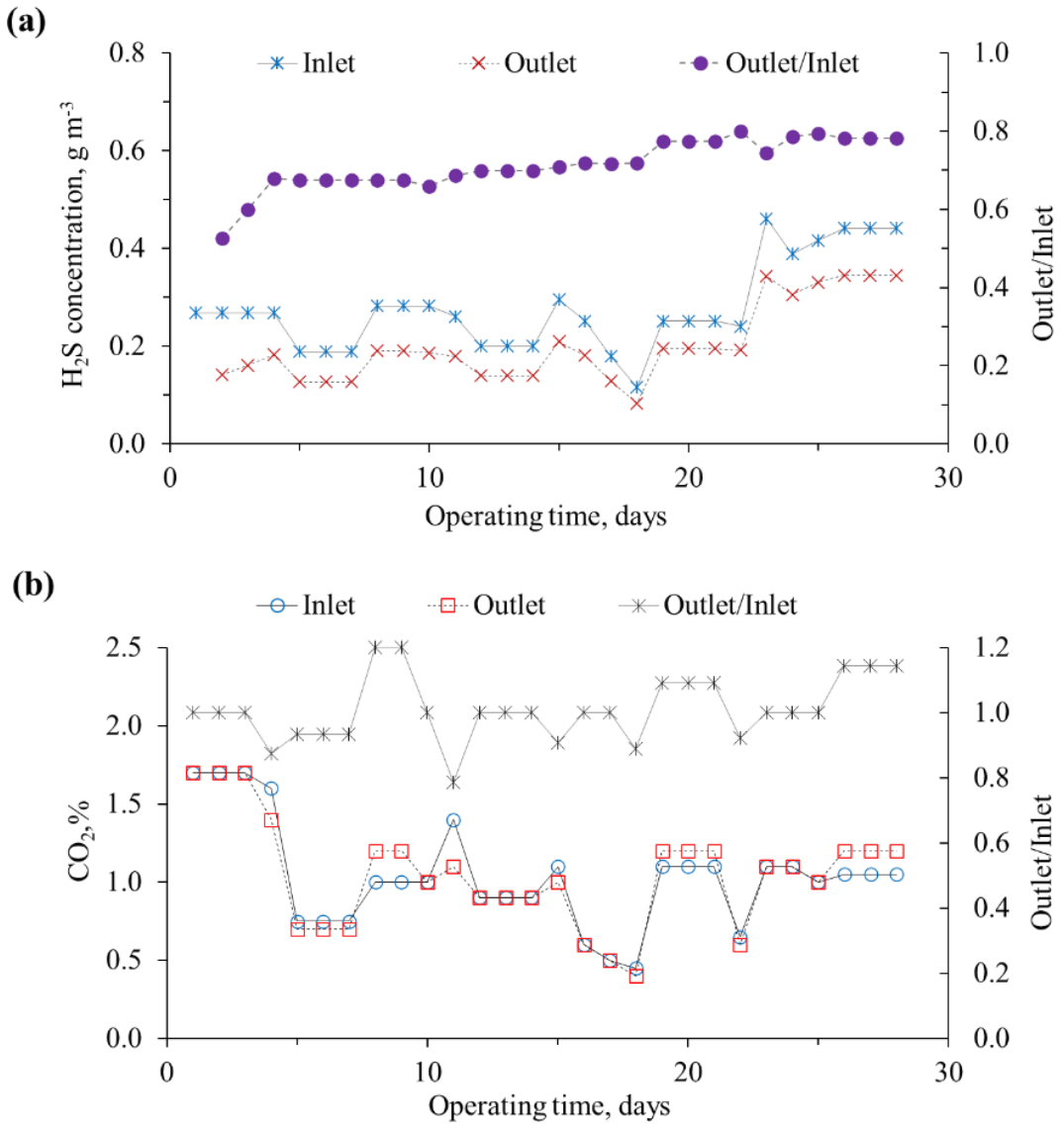

Figure 3.5: Inlet and outlet concentration profiles of: (a) H_2S and (b) CO_2 during abiotic operation of the HFMB (R_3).

Comparison of biotic and abiotic performance of HFMB

Table 3.3 summarizes the H_2S flux and gas-liquid mass transfer during biotic and abiotic operation of the HFMBs. A small quantity (~ 20%) of the applied inlet H_2S concentration diffused through the hollow fibres in R_3 for similar operating conditions applied to R_1 and R_2. The H_2S flux of R_1 and R_2 was ~ 5-9 times higher than that of the abiotic reactor (R_3) for the applied inlet concentrations. The overall mass transfer coefficient (K_G) values for the biotic process (R_1 and R_2) were ~ 20-26 times higher than that of the abiotic process (R_3).

Table 3.3: Comparison of H_2S flux and mass transfer through the HFMB during biotic and abiotic operation.

HFMBs	Inlet H_2S concentration, g m^{-3}	H_2S flux, g m^{-2} day^{-1}	Overall mass transfer coefficient (K_G), µm s^{-1}
R_1 *(Biotic operation)*	0.26	0.06	13.68
	0.46	0.10	12.04
	0.87	0.20	17.15
R_2 *(Biotic operation)*	0.27	0.06	13.99
	0.46	0.11	15.43
	0.88	0.20	17.19
R_3 *(Abiotic operation)*	0.25	0.01	0.98
	0.43	0.02	0.67

Note: Arithmetic mean was used for all parameters

3.3.3. Surface morphology

Figure 3.6 shows the SEM images of the fresh and used hollow fibre membranes. The cross-sectional image revealed the micro-porous structure of the hollow fibre membranes (Figure 3.6c). Microbial attached growth on the outer surface of the used membranes was observed (Figure 3.6d-f).

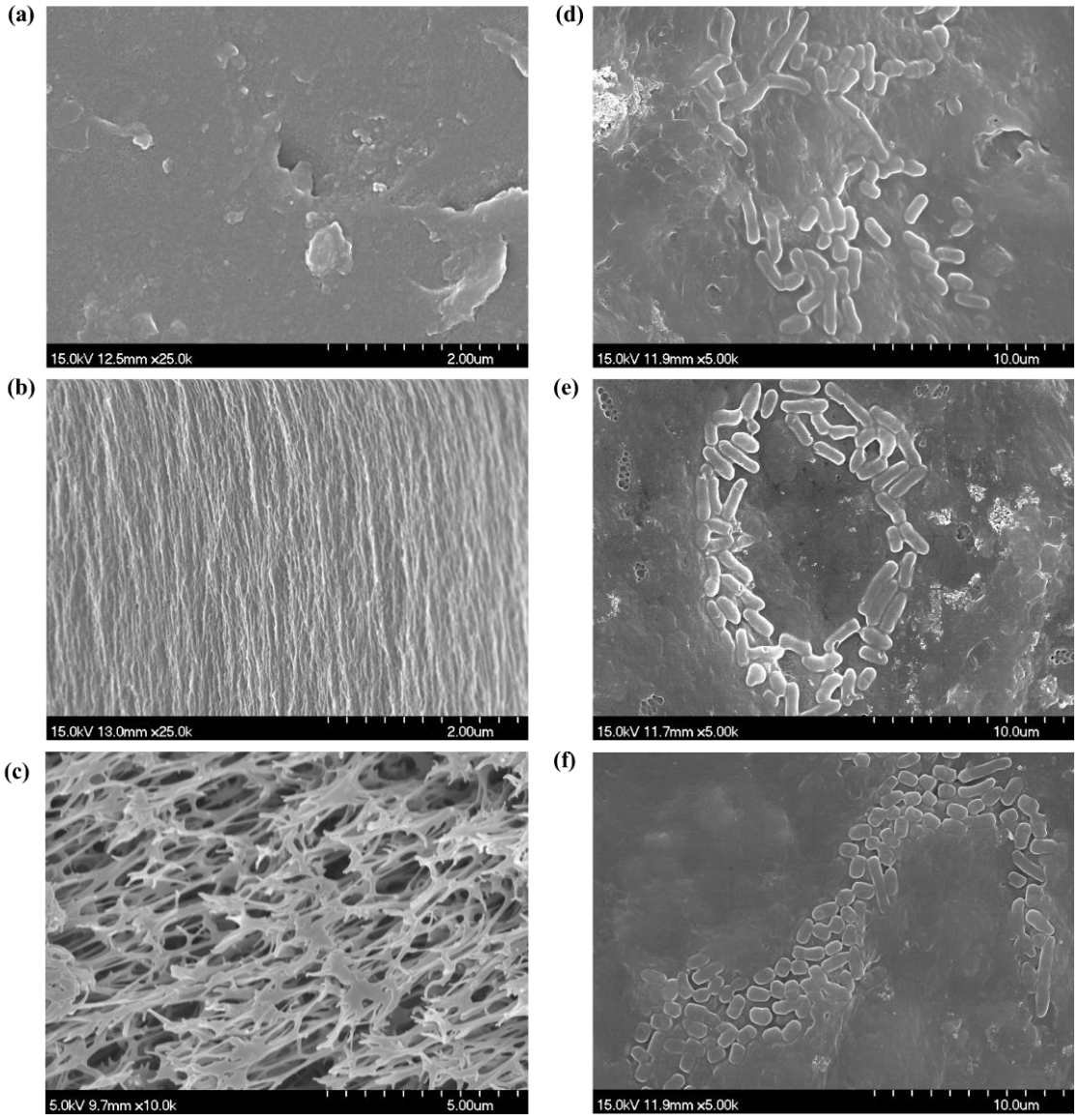

Figure 3.6: SEM image of the membranes: (a) outer surface of pristine membrane, (b) inner surface of pristine membrane and (c) cross section of the HFM of pristine membrane; (d) used membrane image 1, (e) used membrane image 2 and (f) used membrane image 3 of the attached biofilm on outer surface of HFM.

3.3.4. Microbial community in HFMB

High throughput sequencing indicated the richness of the microbial community in the inoculum and reactors R_1 (after 64 days of operation) and R_2 (after 55 days of operation). Figure 3.7 shows the relative abundance of the top 10 taxa in the phylum, Venn diagram and Rarefaction curves demonstrating the number of species present in the samples. *Proteobacteria*, *Bacteroidetes*, *Firmicutes* and *Actinobacteria* were the abundant phyla in both HFMB. Nearly 82000 were sequenced and the number of species (i.e. the number

OTUs) varied from ~ 1100 to 1400. The sequenced number of species in the samples was in the rank of $R_2 > R_1 >$ Inoculum (Figure 3.7c).

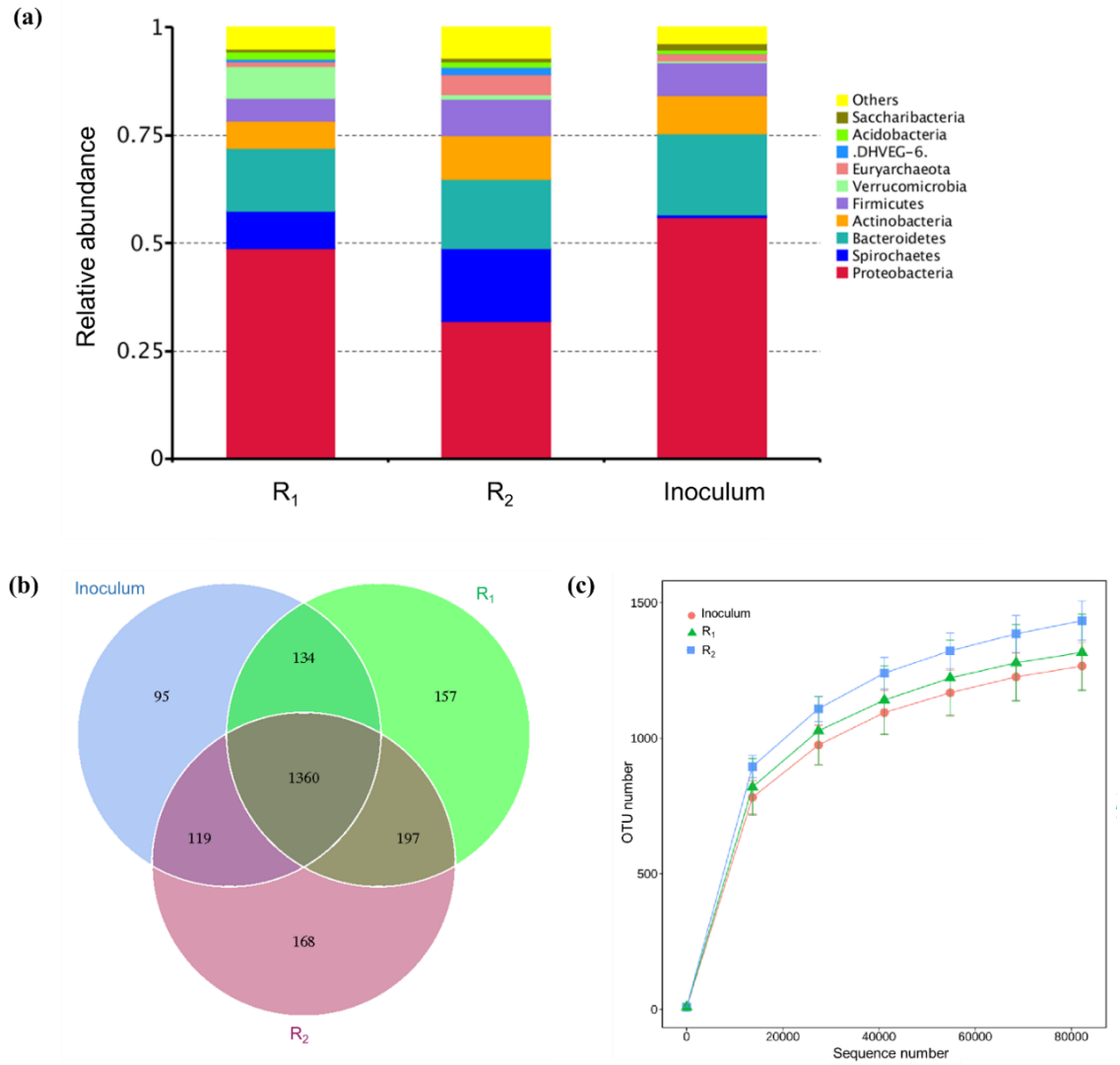

Figure 3.7: Composition of the microbial community analysis: (a) taxa relative abundance in phyla, (b) Venn diagram and (c) Rarefaction curves demonstrating the number of species present in the inoculum and HFMBs (R_1 & R_2).

The ASOB genera *Acinetobacter*, *Bacillus*, *Rhodanobacter* and *Thioclava* were enriched in R_1, while *Chlorobium*, *Dechloromonas* and *Hydrogenophaga* dominated in R_2 (Figure 3.8). The abundance of other ASOB genera such as *Arcobacter*, *Pseudomonas*, *Rhodopseudomonas*, *Sulfuricurvum* and *Sulfurospirillum* was nearly similar in both R_1 and R_2 (Figure 3.8). Apart from ASOB, the presence of other bacterial genera such as sulfur-reducing (e.g. *Desulfovibrio*), ammonia oxidizing (e.g. *Nitrosospira*), organic

matter degrading (e.g. *Trichococcus*) bacteria, and methanogenic (e.g. *Methanosaeta*) archaea were observed in both HFMB (Figure 3.8).

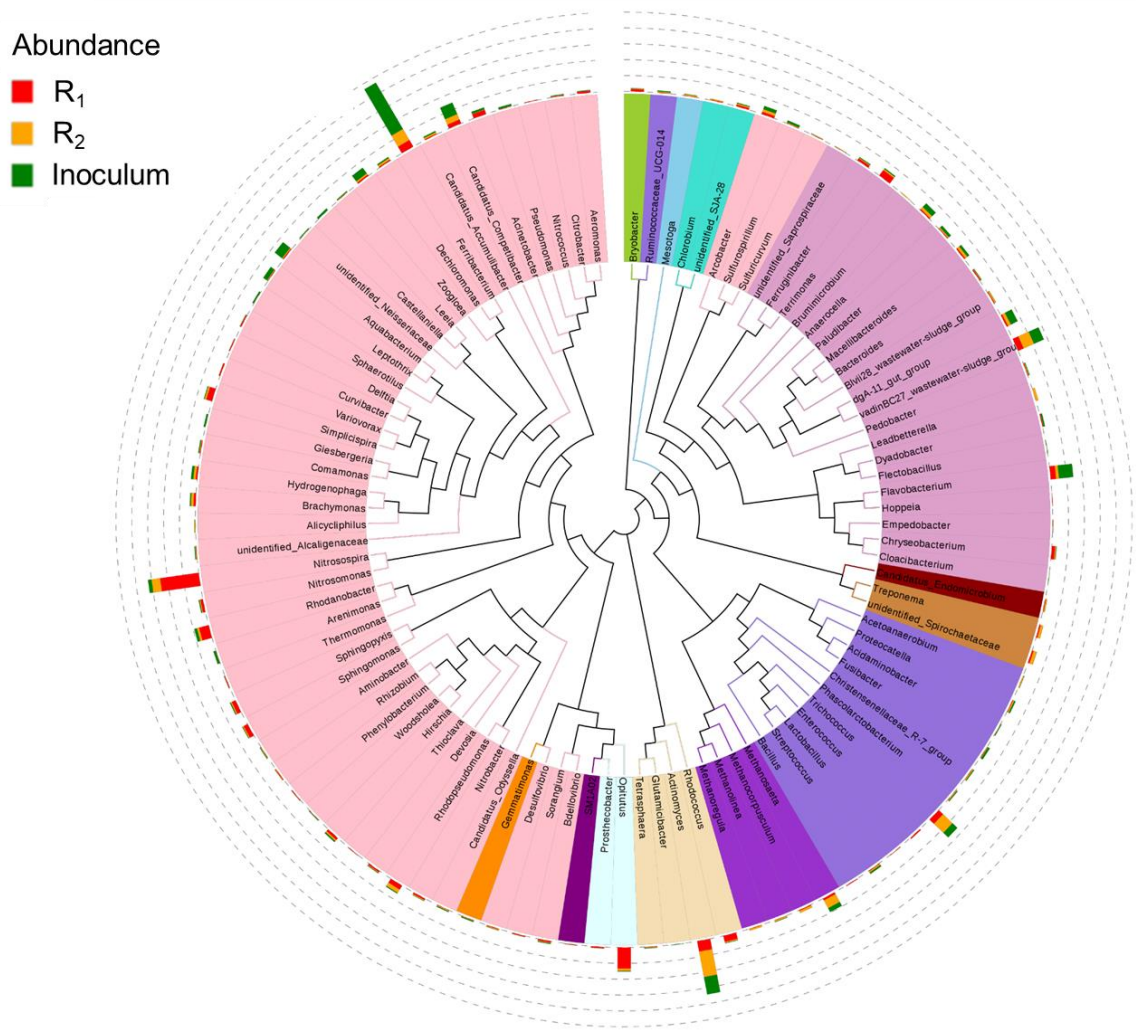

Figure 3.8: Evolutionary tree of the top 100 genera present in the inoculum and HFMBs (R_1 & R_2).

3.4. Discussion

3.4.1. Use of H-PES HFMBs for H_2S removal

This study showed that the HFMB reactor configuration can efficiently treat gas-phase H_2S up to an ILR of ~ 17.0 g m^{-3} h^{-1} at an EBRT of 187 s (Figures 3.3 and 3.4). Efficient H_2S removal in a bioreactor depends on some key components: packing material for microbial attached growth (Wu et al., 2018), gas-liquid mass transfer (Fernández et al., 2013), biofilm characteristics and microbial community composition (Lin et al., 2018),

and operating conditions such as inlet concentration and loading rate (Fernández et al., 2013; Wu et al., 2020), gas flow rate corresponding to EBRT (Das et al., 2019; Wu et al., 2020), pH and temperature (Abubackar et al., 2019).

This is, to the authors knowledge, the first report on the use of a submerged HFM module based HFMB configuration for H_2S gas treatment. In contrast, hollow fibre membrane contactors (HFMCs) are well known in H_2S treatment. HFMCs separate H_2S from an acidic gaseous mixture (e.g. raw biogas) by selective gas-liquid mass transfer, wherein H_2S diffuses through a membrane and dissolves in an alkaline absorption medium (Bazhenov et al., 2018; Nakhjiri et al., 2018). The HFMB can be a cost-effective biological approach for H_2S treatment compared to conventional physico-chemical methods such as membrane contactors or scrubbing processes. This is mainly because a HFMB does not require absorption chemicals (Alinezhad et al., 2019), scrubbing water or operational pressure (Noorain et al., 2019).

3.4.2. H_2S removal performance comparison

The H_2S removal performance of a bioreactor can vary depending on the reactor type (e.g., biofilter, biotrickling filter or bioscrubber) and its operating conditions (Table 3.4). The performance of a biotrickling filter (BTF), most frequently used for treating H_2S contaminated gases, strongly depends on the operating conditions (Table 3.4). Anoxic BTF system inoculated with *Paracoccus versutus* strain MAL 1HM19 achieved a maximum elimination capacity (EC_{max}) of ~ 16 and 120 g m^{-3} h^{-1} under steady-state and transient-state operation, respectively at an EBRT of 180 s (Watsuntorn et al., 2020). A similar BTF system dominated by *Thiobacillus* sp. achieved an EC_{max} of ~ 19 g m^{-3} h^{-1} at an EBRT of 210 s under steady-state (Khanongnuch et al., 2019a) and ~ 38 g m^{-3} h^{-1} at an EBRT of 180 s under transient-state operation (Khanongnuch et al., 2019b). The wide variation of EC_{max} (38-120 g m^{-3} h^{-1}) in the BTF system demonstrates the importance of operating conditions and process parameters. The H_2S removal performance of the HFMBs (~ 100% RE with an EC of 17.0 g m^{-3} h^{-1}) was similar to the steady-state performance of the BTFs reported by Watsuntorn et al. (2020) and Khanongnuch et al. (2019a), and better than a hybrid membrane bioscrubber (MBS), where the MBS fabricated with PDMS tubular membrane (non-porous, dense and hydrophobic in nature) and achieved ~ 80% RE with a maximum EC of ~ 8.0 g m^{-3} h^{-1} (Tilahun et al., 2018).

However, similar (~ 20 g m^{-3} h^{-1}, Zhang et al., 2021) or higher (~ 85 g m^{-3} h^{-1}, Huan et al., 2021) EC have also been reported for the BTF system even with lower EBRT (~ 30-60 s).

Table 3.4: H_2S removal performance of different bioreactor configurations treating H_2S contaminated gases.

Bioreactor type	OT, days	pH	EBRT, s	ILR, g m^{-3} h^{-1}	EC, g m^{-3} h^{-1}	RE, %	Reference
Biotrickling filter (BTF)							
BTF	75	NR	~ 32-43	~ 85	~ 85	~ 99	Huan et al., 2021
BTF	150	1.0-4.0	60	17-24	17-24	100	Zhang et al., 2021
BTF	189	7.0-8.0	180	~ 2.0-120	~ 1.0-115	17-100	Watsuntorn et al., 2020
BTF	10	~ 8.0	120	~ 83^{MLR}	~ 83^{MEC}	> 98	Juntranapaporn et al., 2019
BTF	108	7.0-9.0	210	3-20	~ 19	>99	Khanongnuch et al., 2019a
BTF	78	~ 7.0	180	~ 35	~ 32	> 90	Khanongnuch et al., 2019b
BTF	14	2.0	1200	< 40	< 38	~ 95	Reddy et al., 2019
BTF	105	~ 7.5	144	~ 200	~ 170	~ 85	Fernández et al., 2013
Biofilter (BF)							
BF	90	~ 7.5	60	~ 1.7	~ 1.7	> 98	Taheriyoun et al., 2019
BF	10	~ 7.5	600	~ 0.2	~ 0.1	~ 60	Yuan et al., 2019
BF	190	4.5	85	150	> 140	> 98	Ramírez-Sáenz et al., 2009
Bioscrubber (BS)							
BS	80	~ 8.0	144-396	~ 40-100	< 80	> 80	San-Valero et al., 2019
BS	32	~ 8.0	12-27	1800-7200	~1800-4320	~ 40- 98	Esmaeili-Faraj et al., 2019
Hybrid membrane bioscrubber (MBS)							
MBS	180	7.0 8.5	NR	~ 10.5 ~ 10.2	~ 8.4 ~ 7.9	~ 80 ~ 77	Tilahun et al., 2018
Hollow fibre membrane bioreactor (HFMB)							
HFMB	83	~ 7.0	187	~ 17.0	~ 17.0	> 99	This study

Note: HFMB - hollow fibre membrane bioreactor; EBRT - empty bed residence time; EC - elimination capacity; ILR - inlet loading rate; MILR - maximum loading rate; MEC - maximum elimination capacity; NR - not reported; OT - operating time; RE - removal efficiency

Comparatively a longer gas contact time (EBRT of 187 s) has been chosen in this feasibility study of the HFMB to allow adequate time to the functional microorganisms for the H_2S bioconversion, and to test the HFMB performance in the absence of possible limiting factors such as a shorter gas contact time (e.g. 40 s, Zhuo et al., 2019) that can affect the H_2S mass-transfer and removal performance. A wide range of EBRTs (~ 30-1200 s) and ILR (~ 1-200 g m^{-3} h^{-1}) are employed in different bioreactor configurations (Table 3.4). Further research is also being carried out to optimize the H_2S removal performance of the bioreactors. For example, Bu et al. (2021) employed different trickling strategies and a shorter EBRT (6 s) to handle low H_2S (< 200 ppm_v) concentrations in a

BTF. This study suggests that the HFMB can be employed for treating H_2S (up to ~ 650 ppm_v) from several H_2S emission sources, including sewage and wastewater treatment plants. However, future studies on process optimization in terms of EBRT and ILR can be useful to adopt the HFMB for full-scale application.

The variation of the main H_2S oxidation product (i.e. SO_4^{2-} in R_1 and S^0 in R_2) during the H_2S bioconversion is likely related to the dissolved oxygen (DO) concentration of the HFMB liquid suspension. The inlet H_2S contaminated gas-stream contained ~ 21% of O_2 and a certain fraction (~ 0.1-1.0%) of O_2 diffused into the liquid phase of the HFMB. Hence, the O_2 concentration in the liquid is expected to exceed the stoichiometric amount required for the complete bioconversion of H_2S to SO_4^{2-} (Pokorna and Zabranska, 2015), as shown in Eq. (3.11), for the employed H_2S concentrations (Table 3.2).

$$H_2S + 2O_2 \rightarrow SO_4^{2-} + 2H^+ \qquad \Delta G^0 = -798.2 \text{ kJ/reaction} \qquad (3.11)$$

$$H_2S + 0.5O_2 \rightarrow S^0 + H_2O \qquad \Delta G^0 = -209.4 \text{ kJ/reaction} \qquad (3.12)$$

However, no stirrer was used to mix the gas diffused through the membranes in the shell side of the HFMB. Hence, improper mixing of oxygen (that was diffusing through the membrane) could have resulted in a lack of availability of oxygen for the complete oxidation of H_2S to SO_4^{2-} by the ASOB, resulting in S^0 formation (Eq. 3.12). The O_2 supply to the ASOB could be increased by mixing of the HFMB mixed liquor or by increasing the inlet gas flow rate through the hollow fibres.

3.4.3. H_2S flux and gas-liquid mass transfer in HFMB

The higher H_2S flux and gas-liquid mass transfer (Table 3.3) in the HFMB during biotic operation (in R_1 and R_2) compared to abiotic operation (in R_3) is likely due to the continuous dissociation of H_2S in the liquid phase followed by bioconversion of sulfides by ASOB genera immobilized on the membranes (Qureshi et al., 2005) and present in the liquid suspension. The outlet/inlet concentration ratio of H_2S during the abiotic operation of the HFMB (Figure 3.5) suggests the importance of continuous bioconversion of H_2S (by ASOB) to continue rapid diffusional transport of H_2S and maintain a high H_2S flux and mass transfer through the HFM. The main mechanisms of H_2S diffusion through the H-PES membranes are Knudsen diffusion (that occurs inside the narrow membrane pores due to molecular collisions with the pore walls; Ismail et al., 2015) and surface diffusion (that occurs due to the adsorption gradient of the permeating gases; Ismail et al., 2015).

The abiotic operation (R_3) of the HFMB gave an insight about a membrane contactor performance in the absence of microorganisms, absorption chemicals and high operation pressure.

The H_2S flux and overall mass transfer coefficient obtained in this study (Table 3.3) was lower than the values reported for physico-chemical separation using HFMCs (Table 3.5). High operational pressure and different concentrations of absorption chemicals are employed to enhance the H_2S flux in HFMCs for separating H_2S from a gas mixture (Table 3.5). An increase in the H_2S gas/absorbent liquid flow ratio can decrease the gas-liquid contact time, i.e. limit the reaction time between H_2S and absorbent liquid, and consequently decrease the H_2S removal performance (Mirfendereski et al., 2019).

Table 3.5: Effect of operational pressure and absorption liquid on H_2S flux in HFMCs.

Absorption liquid	Operational pressure, bar	H_2S flux in HFMC, mol m^{-2} min^{-1} (g m^{-2} day^{-1})	Overall mass transfer coefficient (K_G) of H_2S, µm s^{-1}	H_2S removal efficiency, %	Reference
2.0 M KCO_3	50	0.0225 (1104)	~ 30[a]	> 99	Al-Marzouqi et al., 2017
1.0 M KCO_3 + 1.0 M $KHCO_3$	50	0.0195 (~ 957)		~ 96	
0.8-2.0 M Methyldiethanolamine	0.3-0.6	NR	~ 220 ~ 290	~ 85[b] ~ 58[c]	Hedayat et al., 2011
Water	1	0.0015 (~ 74)	NR	~ 15	Marzouk et al., 2010
	20	0.0052 (~ 255)		~ 50	
0.1M NaOH	1	0.0055 (~ 270)		~ 55	
	20	0.0080 (~ 393)		~ 80	
0.5M NaOH	1	6.8×10^{-3} (~ 333)		~ 70	
	20	9.1×10^{-3} (~ 447)		~ 90	
2 M Na_2CO_3	0.2-0.6	NR	13000[d] 9000[e]	> 99	Wang et al., 2004

Note: NR - not reported; [a]- poly(tetrafluoroethylene-co-perfluorinated alkyl vinyl ether (PFA) HFM Module 300; [b] - The polyvinylidene fluoride (PVDF) HFM was used; [c] - The polysulfone (PSf) HFM was used; [d] - The flow ratio of H_2S gas and absorption liquid was 600; [e] - The flow ratio of H_2S gas and absorption liquid was 1800

Membrane wetting was not observed during the HFMB operation. The SEM images confirm that a biofilm was formed on the membrane surface (Figure 3.6d-f). A biofilm on the membrane surface can significantly influence the bioreactor performance (Chung et al., 2005; Shen et al., 2018; Wang et al., 2018). H_2S removal in a biofilter (Sologar et al., 2003) and BTF (Kim and Deshusses, 2003) reported a very thin biofilm having a thickness of 10 µm and 23 µm, respectively. The thickness of the biofilm could, however, not be determined during HFMB operation as this would damage the fibres of the HFM module and thus negatively affect the HFMB operation.

3.4.4. Microbial community composition

The longer start-up and acclimatization phase of R_1 (~ 11 days) and its variation of RE (between ~ 80 and 100%) until Phase 3 (Figure 3.3a) compared to R_2 (Figure 3.3b) can be attributed to the differences in microbial population (Lin et al., 2018). Indeed, different inocula were used in R_1 and R_2 which had a different bacterial diversity (Figure 3.7) and dominant sulfur-oxidizing genera (Figure 3.8). The removal performance of the HFMB was not associated with any nutrient limitation as mineral medium was provided in R_1, but still the RE varied until Phase 3, while R_2 was capable to achieve ~ 100% RE for the same period where mineral medium was not provided.

The initial variation of the RE of R_1 in Phase 4 (on day 65-69; Figure 3.3a) followed by a ~ 100% RE suggests that the change of inoculum (at the end of Phase 3) enhanced the removal performance of R_1. The change in microbial diversity on the shell side mainly contributed to improve the removal performance of R_1. Moreover, the pH was not the limiting factor for the initial variation of the RE in Phase 4 as the pH was in a similar range (~ 6.8-7.0) in both R_1 and R_2 during that period (Phase 4-5).

The microbial community in R_1 and R_2 (Figure 3.8) was diverse, which can be related to the inoculum and the microbial enrichment in the HFMBs. The microbial community changes depending on the substrate utilization under both aerobic and anaerobic conditions (Luo et al., 2013). The presence of diverse ASOB genera including *Sulfuricurvum, Hydrogenophaga, Arcobacter, Rhodopseudomonas, Dechloromonas, Pseudomonas* and *Chlorobium* mainly contributed to H_2S oxidation in the HFMBs R_1 and R_2 (Haosagul et al., 2020a; Luo et al., 2013; Tian et al., 2017). However, the oxidation ability of different ASOB species can vary as different species use different enzymes, electron transport mechanisms and energy conservation pathways for S^{2-} oxidation (Haosagul et al., 2020b).

The performance of R_2 during the start-up indicates the presence of a diverse ASOB population in the activated sludge inoculum which acclimatized in the HFMB within 24 h of operation (Figure 3.3b). Moreover, it also shows that activated sludge can be used directly as an inoculum for the start-up of H_2S treating HFMB without the need for prior enrichment in batch (R_2 versus R_1) or other pretreatment. Activated sludge is commonly

employed as inoculum during start-up of different bioreactor configurations (e.g. biofilter or bioscrubber) for treating H_2S (Fan et al., 2020).

The relative abundance of functional microorganisms, i.e. ASOB, plays a key role in the biological desulfurization process (Wang et al., 2015; Wu et al., 2018). ASOB communities utilize H_2S and CO_2 as their energy and carbon source, respectively (Haosagul et al., 2020b). The most abundant phylum in the HFMB, *Proteobacteria* (Figure 3.7a), was similar to a BTF system used for H_2S removal from biogas (Wu et al., 2020) and an airlift bioreactor used for simultaneous removal of H_2S and NH_3 from waste gases (Chen et al., 2018). Chemolithotrophic ASOB (e.g. *Thiobacillus* sp.) are very suitable for biological desulfurization because of their high sulfide oxidation rate with considerable affinity to sulfide and oxygen and minimum nutrient requirements compared to photoautotrophic sulfide oxidizers, e.g. *Chlorobium* sp. (Pokorna and Zabranska, 2015).

3.5. Conclusions

The proof of concept of the use of a H-PES hollow fibre membrane bioreactor (HFMB) for biological removal of gas-phase H_2S was established in the present study. The HFMBs R_1 and R_2 showed ~ 9 times higher H_2S flux through the membrane module and ~ 25 times higher mass transfer coefficient for an inlet H_2S concentration of ~ 0.9 g m^{-3} compared to the abiotic control (R_3). HFMBs inoculated with acclimatized inoculum achieved a ~ 100% removal efficiency with an elimination capacity of ~ 17.0 g m^{-3} h^{-1} at an EBRT of 187 s. Microbial community analysis showed the conversion of H_2S to S^0 and SO_4^{2-} which was carried out by a diverse ASOB genera, including *Sulfuricurvum, Hydrogenophaga, Arcobacter, Rhodopseudomonas, Dechloromonas* and *Pseudomonas*.

3.6. References

Abubackar, H.N., Veiga, M.C., Kennes, C., Das, J., Rene, E.R., van Hullebusch, E.D., 2019. Gas-Phase Bioreactors, in: Moo-Young, M. (Eds.), Comprehensive Biotechnology. Elsevier, United Kingdom, pp. 446-463.

Ahmad, A.L., Abdulkarim, A.A., Ooi, B.S., Ismail, S., 2013. Recent development in additives modifications of polyethersulfone membrane for flux enhancement. Chemical Engineering Journal. 223, 246-267.

Alfaro, N., Fdz-Polanco, M., Fdz-Polanco, F., Díaz, I., 2019. H_2 addition through a submerged membrane for in-situ biogas upgrading in the anaerobic digestion of sewage sludge. Bioresource Technology. 280, 1-8.

Alinezhad, E., Haghighi, M., Rahmani, F., Keshizadeh, H., Abdi, M., Naddafi, K., 2019. Technical and economic investigation of chemical scrubber and bio-filtration in removal of H_2S and NH_3 from wastewater treatment plant. Journal of Environmental Management. 241, 32-43.

Allen, H.E., Fu, G., Deng, B., 1993. Analysis of acid-volatile sulfide (AVS) and simultaneously extracted metals (SEM) for the estimation of potential toxicity in aquatic sediments. Environmental Toxicology and Chemistry. 12, 1441-1453.

Al-Marzouqi, M.H., Marzouk, S.A., Abdullatif, N., 2017. High pressure removal of acid gases using hollow fiber membrane contactors: Further characterization and long-term operational stability. Journal of Natural Gas Science and Engineering. 37, 192-198.

Aoi, Y., Kinoshita, T., Hata, T., Ohta, H., Obokata, H., Tsuneda, S., 2009. Hollow-fiber membrane chamber as a device for in situ environmental cultivation. Applied and Environmental Microbiology. 75, 3826-3833.

APHA, 2012. In Rice, E.W., Baird, R.B., Eaton, A.D., Clesceri, L.S., (Eds.), Standard methods for the examination of water and wastewater (22nd ed.). American Public Health Association (APHA), Washington.

Arellano-García, L., Le Borgne, S., Revah, S., 2018. Simultaneous treatment of dimethyl disulfide and hydrogen sulfide in an alkaline biotrickling filter. Chemosphere. 191, 809-816.

Bao, L., Lipscomb, G.G., 2003. Mass transfer in axial flows through randomly packed fiber bundles, in: Bhattacharyya, D., Butterfield D.A. (Eds.), Membrane Science and Technology. Elsevier, United Kingdom, pp. 5-26.

Bazhenov, S.D., Bildyukevich, A.V., Volkov, A.V., 2018. Gas-liquid hollow fiber membrane contactors for different applications. Fibers. 6, 76.

Bu, H., Carvalho, G., Huang, C., Sharma, K.R., Yuan, Z., Song, Y., Jiang, G., 2021. Evaluation of continuous and intermittent trickling strategies for the removal of hydrogen sulfide in a biotrickling filter. Chemosphere, 132723.

Chen, C.Y., Tsai, T.H., Chang, C.H., Tseng, C.F., Lin, S.Y., Chung, Y.C., 2018. Airlift bioreactor system for simultaneous removal of hydrogen sulfide and ammonia from synthetic and actual waste gases. Journal of Environmental Science and Health, Part A. 53, 694-701.

Cheng, Y., Yuan, T., Deng, Y., Lin, C., Zhou, J., Lei, Z., Shimizu, K., Zhang, Z., 2018. Use of sulfur-oxidizing bacteria enriched from sewage sludge to biologically remove H_2S from biogas at an industrial-scale biogas plant. Bioresource Technology Reports. 3, 43-50.

Chung, T.P., Wu, P.C., Juang, R.S., 2005. Use of microporous hollow fibers for improved biodegradation of high-strength phenol solutions. Journal of Membrane Science. 258, 55-63.

Das, J., Rene, E.R., Dupont, C., Dufourny, A., Blin, J., van Hullebusch, E.D., 2019. Performance of a compost and biochar packed biofilter for gas-phase hydrogen sulfide removal. Bioresource Technology. 273, 581-591.

Esmaeili-Faraj, S.H., Esfahany, M.N., Darvanjooghi, M.H.K., 2019. Application of water based nanofluids in bioscrubber for improvement of biogas sweetening in a pilot scale. Chemical Engineering and Processing-Process Intensification. 143, 107603.

Fan, F., Xu, R., Wang, D., Meng, F., 2020. Application of activated sludge for odor control in wastewater treatment plants: Approaches, advances and outlooks. Water Research. 181, 115915.

Fernández, M., Ramírez, M., Pérez, R.M., Gómez, J.M., Cantero, D., 2013. Hydrogen sulphide removal from biogas by an anoxic biotrickling filter packed with Pall rings. Chemical Engineering Journal. 225, 456-463.

Fuller, K.P., Gaspar, D., Delgado, L.M., Pandit, A., Zeugolis, D.I., 2016. Influence of porosity and pore shape on structural, mechanical and biological properties of poly ε-caprolactone electro-spun fibrous scaffolds. Nanomedicine. 11, 1031-1040.

Guo, J., Kim, J., 2017. Modifications of polyethersulfone membrane by doping sulfated-TiO_2 nanoparticles for improving anti-fouling property in wastewater treatment. RSC Advances. 7, 33822-33828.

Haosagul, S., Prommeenate, P., Hobbs, G., Pisutpaisal, N., 2020a. Sulfide-oxidizing bacteria community in full-scale bioscrubber treating H_2S in biogas from swine anaerobic digester. Renewable Energy. 150, 973-980.

Haosagul, S., Prommeenate, P., Hobbs, G., Pisutpaisal, N., 2020b. Sulfur-oxidizing bacteria in full-scale biogas cleanup system of ethanol industry. Renewable Energy. 150, 965-972.

Hedayat, M., Soltanieh, M., Mousavi, S.A., 2011. Simultaneous separation of H_2S and CO_2 from natural gas by hollow fiber membrane contactor using mixture of alkanolamines. Journal of Membrane Science. 377, 191-197.

Huan, C., Fang, J., Tong, X., Zeng, Y., Liu, Y., Jiang, X., Yan, Z., 2021. Simultaneous elimination of H_2S and NH_3 in a biotrickling filter packed with polyhedral spheres and best efficiency in compost deodorization. Journal of Cleaner Production. 284, 124708.

Ismail, A.F., Khulbe, K.C., Matsuura, T., 2015. Fundamentals of gas permeation through membranes, in: Ismail, A.F., Khulbe, K.C., Matsuura, T., (Eds.), Gas Separation Membranes. Springer, Cham, pp. 11-35.

Jaber, M.B., Couvert, A., Amrane, A., Le Cloirec, P., Dumont, E., 2017. Removal of hydrogen sulfide in air using cellular concrete waste: Biotic and abiotic filtrations. Chemical Engineering Journal. 319, 268-278.

Jiang, L., Chen, X., Qin, M., Cheng, S., Wang, Y., Zhou, W., 2019. On-board saline black water treatment by bioaugmentation original marine bacteria with *Pseudoalteromonas* sp. SCSE709-6 and the associated microbial community. Bioresource Technology. 273, 496-505.

Juntranapaporn, J., Vikromvarasiri, N., Soralump, C., Pisutpaisal, N., 2019. Hydrogen sulfide removal from biogas in biotrickling filter system inoculated with *Paracoccus pantotrophus*. International Journal of Hydrogen Energy. 44, 29554-29560.

Kailasa, S.K., Koduru, J.R., Vikrant, K., Tsang, Y.F., Singhal, R.K., Hussain, C.M., Kim, K.H., 2020. Recent progress on solution and materials chemistry for the removal of hydrogen sulfide from various gas plants. Journal of Molecular Liquids. 297, 111886.

Khanongnuch, R., Di Capua, F., Lakaniemi, A.M., Rene, E.R., Lens, P.N.L., 2019b. Transient-state operation of an anoxic biotrickling filter for H_2S removal. Journal of Hazardous Materials, 377, 42-51.

Khanongnuch, R., Di Capua, F., Lakaniemi, A-Maija., Rene E.R., Lens, P.N.L., 2019a. H_2S removal and microbial community composition in ananoxic biotrickling filter under autotrophic and mixotrophic conditions. Journal of Hazardous Materials. 367, 397-406.

Kim, S., Deshusses, M.A., 2003. Development and experimental validation of a conceptual model for biotrickling filtration of H2S. Environmental Progress. 22, 119-128.

Lin, S., Mackey, H.R., Hao, T., Guo, G., van Loosdrecht, M.C.M., Chen, G., 2018. Biological sulfur oxidation in wastewater treatment: A review of emerging opportunities. Water Research. 143, 399-415.

Luo, J., Tian, G., Lin, W., 2013. Enrichment, isolation and identification of sulfur-oxidizing bacteria from sulfide removing bioreactor. Journal of Environmental Sciences. 25, 1393-1399.

Marzouk, S.A., Al-Marzouqi, M.H., Abdullatif, N., Ismail, Z.M., 2010. Removal of percentile level of H_2S from pressurized H_2S-CH_4 gas mixture using hollow fiber membrane contactors and absorption solvents. Journal of Membrane Science. 360, 436-441.

Mirfendereski, S.M., Niazi, Z., Mohammadi, T., 2019. Selective removal of H_2S from gas streams with high CO_2 concentration using hollow-fiber membrane contractors. Chemical Engineering & Technology. 42, 196-208.

Nakhjiri, A.T., Heydarinasab, A., Bakhtiari, O., Mohammadi, T., 2018. Influence of non-wetting, partial wetting and complete wetting modes of operation on hydrogen sulfide removal utilizing monoethanolamine absorbent in hollow fiber membrane contactor. Sustainable Environment Research. 28, 186-196.

Noorain, R., Kindaichi, T., Ozaki, N., Aoi, Y., Ohashi, A., 2019. Biogas purification performance of new water scrubber packed with sponge carriers. Journal of Cleaner Production. 214, 103-111.

Pokorna, D., Zabranska, J., 2015. Sulfur-oxidizing bacteria in environmental technology. Biotechnology Advances, 33, 1246-1259.

Pokorna-Krayzelova, L., Bartacek, J., Vejmelkova, D., Alvarez, A.A., Slukova, P., Prochazka, J., Volcke, E.I.P., Jenicek, P., 2017. The use of a silicone-based biomembrane for microaerobic H_2S removal from biogas. Separation and Purification Technology, 189, 145-152.

Qureshi, N., Annous, B.A., Ezeji, T.C., Karcher, P., Maddox, I.S., 2005. Biofilm reactors for industrial bioconversion processes: employing potential of enhanced reaction rates. Microbial Cell Factories. 4, 24.

Ramírez-Sáenz, D., Zarate-Segura, P.B., Guerrero-Barajas, C., Garcia-Peña, E.I., 2009. H_2S and volatile fatty acids elimination by biofiltration: Clean-up process for biogas potential use. Journal of Hazardous Materials. 163, 1272-1281.

Ravishankar, H., Christy, J., Jegatheesan, V., 2018. Graphene oxide (GO)-blended polysulfone (PSf) ultrafiltration membranes for lead ion rejection. Membranes. 8, 77.

Reddy, C.N., Bae, S., Min, B., 2019. Biological removal of H_2S gas in a semi-pilot scale biotrickling filter: Optimization of various parameters for efficient removal at high loading rates and low pH conditions. Bioresource Technology. 285, 121328.

Rittmann, B.E., Nerenberg, R., Lee, K.C., Najm, I., Gillogly, T.E., Lehman, G.E., Adham, S. S., 2004. Hydrogen-based hollow-fiber membrane biofilm reactor (MBfR) for removing oxidized contaminants. Water Science and Technology: Water Supply. 4, 127-133.

Rodero, M.R., Ángeles, R., Marín, D., Díaz, I., Colzi, A., Posadas, E., Lebrero, R., Muñoz, R., 2018. Biogas Purification and Upgrading Technologies, in: Tabatabaei, M., Ghanavati, H. (Eds.), Biogas, Biofuel and Biorefinery Technologies 6. Springer, Cham, pp. 239-276.

San-Valero, P., Penya-Roja, J.M., Álvarez-Hornos, F.J., Buitrón, G., Gabaldón, C., Quijano, G., 2019. Fully aerobic bioscrubber for the desulfurization of H_2S-rich biogas. Fuel. 241, 884-891.

Shen, N., Dai, K., Xia, X.Y., Zeng, R.J., Zhang, F., 2018. Conversion of syngas (CO and H_2) to biochemicals by mixed culture fermentation in mesophilic and thermophilic hollow-fiber membrane biofilm reactors. Journal of Cleaner Production. 202, 536-542.

Sologar, V.S., Lu, Z., Allen, D.G., 2003. Biofiltration of concentrated mixtures of hydrogen sulfide and methanol. Environmental Progress. 22, 129-136.

Spennati, F., Mannucci, A., Mori, G., Giordano, C., Munz, G., 2017. Moving bed bio trickling filters: an innovative solution for hydrogen sulphide removal from gas streams. Desalination Water Treatment. 61, 215-221.

Taheriyoun, M., Salehiziri, M., Parand, S., 2019. Biofiltration performance and kinetic study of hydrogen sulfide removal from a real source. Journal of Environmental Health Science and Engineering. 17, 645-656.

Tan, X., Liu, S., Li, K., 2001. Preparation and characterization of inorganic hollow fiber membranes. Journal of Membrane Science. 188, 87-95.

Tian, H., Gao, P., Chen, Z., Li, Y., Li, Y., Wang, Y., Zhou, J., Li, G., Ma, T., 2017. Compositions and abundances of sulfate-reducing and sulfur-oxidizing microorganisms in water-flooded petroleum reservoirs with different temperatures in China. Frontiers in Microbiology. 8, 143.

Tilahun, E., Bayrakdar, A., Sahinkaya, E., Çalli, B., 2017. Performance of polydimethylsiloxane membrane contactor process for selective hydrogen sulfide removal from biogas. Waste Management. 61, 250-257.

Tilahun, E., Sahinkaya, E., Çalli, B., 2018. A hybrid membrane gas absorption and bio-oxidation process for the removal of hydrogen sulfide from biogas. International Biodeterioration & Biodegradation. 127, 69-76.

Vikromvarasiri, N., Champreda, V., Boonyawanich, S., Pisutpaisal, N., 2017. Hydrogen sulfide removal from biogas by biotrickling filter inoculated with *Halothiobacillus neapolitanus*. International Journal of Hydrogen Energy. 42, 18425-18433.

Wang, D., Teo, W.K., Li, K., 2004. Selective removal of trace H_2S from gas streams containing CO_2 using hollow fibre membrane modules/contractors. Separation and Purification Technology. 35, 125-131.

Wang, H.J., Dai, K., Xia, X.Y., Wang, Y.Q., Zeng, R.J., Zhang, F., 2018. Tunable production of ethanol and acetate from synthesis gas by mesophilic mixed culture fermentation in a hollow fiber membrane biofilm reactor. Journal of Cleaner Production. 187, 165-170.

Wang, L., Wei, B., Chen, Z., Deng, L., Song, L., Wang, S., Zheng, D., Liu, Y., Pu, X., Zhang, Y., 2015. Effect of inoculum and sulfide type on simultaneous hydrogen sulfide removal from biogas and nitrogen removal from swine slurry and microbial mechanism. Applied Microbiology and Biotechnology. 99, 10793-10803.

Watsuntorn, W., Khanongnuch, R., Chulalaksananukul, W., Rene, E.R., Lens, P.N., 2020. Resilient performance of an anoxic biotrickling filter for hydrogen sulphide removal from a biogas mimic: Steady, transient state and neural network evaluation. Journal of Cleaner Production, 249, 119351.

Wu, H., Yan, H., Quan, Y., Zhao, H., Jiang, N., Yin, C., 2018. Recent progress and perspectives in biotrickling filters for VOCs and odorous gases treatment. Journal of Environmental Management. 222, 409-419.

Wu, J., Jiang, X., Jin, Z., Yang, S., Zhang, J., 2020. The performance and microbial community in a slightly alkaline biotrickling filter for the removal of high concentration H_2S from biogas. Chemosphere. 249, 126127.

Yuan, J., Du, L., Li, S., Yang, F., Zhang, Z., Li, G., Wang, G., 2019. Use of mature compost as filter media and the effect of packing depth on hydrogen sulfide removal from composting exhaust gases by biofiltration. Environmental Science and Pollution Research. 26, 3762-3770.

Zhang, Y., Oshita, K., Takaoka, M., Kawasaki, Y., Minami, D., Inoue, G., Tanaka, T., 2021. Effect of pH on the performance of an acidic biotrickling filter for simultaneous removal of H_2S and siloxane from biogas. Water Science and Technology. 83, 1511-1521.

Zhao, C., Xue, J., Ran, F., Sun, S., 2013. Modification of polyethersulfone membranes-a review of methods. Progress in Materials Science. 58, 76-150.

Zhuo, Y., Han, Y., Qu, Q., Li, J., Zhong, C., Peng, D., 2019. Characteristics of low H_2S concentration biogas desulfurization using a biotrickling filter: Performance and modeling analysis. Bioresource technology. 280, 143-150.

Zou, G., Papirio, S., Lakaniemi, A.M., Ahoranta, S.H., Puhakka, J.A., 2016. High rate autotrophic denitrification in fluidized-bed biofilm reactors. Chemical Engineering Journal. 284, 1287-1294.

Chapter 4

Resilience of hollow fibre membrane bioreactors for treating H_2S under steady state and transient conditions

Abstract

H_2S removal performance by hollow fibre membrane bioreactors (HFMBs) was investigated for 271 days at ambient (20 ± 2°C) temperature employing an inlet H_2S concentrations up to ~ 3600 ppm_v and empty bed residence time (EBRT) of 187, 92 and 62 s. Different operating conditions including pH control (with or without), famine period, shock loads (4-72 h) and different biomass types (presence or absence of suspended biomass) were investigated. The H_2S flux and mass-transfer coefficient were significantly higher for the biotic HFMBs (R_1 and R_2) compared to the abiotic control (R_3) at all employed EBRTs. Significant differences in H_2S removal efficiency (RE) and elimination capacity (EC) were noted for different inlet H_2S concentrations, EBRTs, pH and biomass type. The HFMB achieved ~ 100% RE at steady-state for biotic operation with an EC of 33.8, 30.0 and 30.9 g m^{-3} h^{-1} at an EBRT of 187, 92 and 62 s, respectively. Sulfate (~ 92-93%) was the main sulfur species in the H_2S bioconversion process. The HFMB showed a good resilience to shock loads and showed quick recovery (< 24 h) after withdrawal of the shock loads. The HFMB had a critical load of H_2S ~ 135 g m^{-3} h^{-1} under transient-state.

4.1. Introduction

Hydrogen sulfide (H_2S) is a highly toxic and odorous gas which is produced through natural and industrial processes such as geo-thermal sources or crude petroleum refining (Kailasa et al., 2020). It results in environmental pollution, human health issues, corrosion and odor issues at various treatment processes, e.g. sewer networks, wastewater treatment plants or raw biogas upgrading units, due to its pernicious nature (Ren et al., 2021). The raw biogas generated during anaerobic digestion may contain ~ 50-10000 ppm_v of H_2S (Zhang et al., 2021) which corrodes biogas fired appliances and other metallic accessories, thereby restricting its end-use application such as electricity generation (Valdebenito-Rolack et al., 2021).

Biological odor removal technologies are more efficient, cost-effective and environment friendly than conventional physical-chemical methods such as chemical scrubbing or membrane separation (Liu et al., 2021; Valdebenito-Rolack et al., 2021). Different reactor configurations have been reported to treat H_2S laden gas, including biofilter (Zheng et al., 2021), biotrickling filter (Wu et al., 2020) and integrated reactors

such as a scrubbing unit coupled with a biochemical treatment pond (Li et al., 2021) or polydimethylsiloxane (PDMS) membrane contactors coupled with a bioscrubber (Tilahun et al., 2018).

The H_2S removal performance of these bioreactors varies depending on the applied operating conditions. For example, the biotrickling filter (Reddy et al., 2019) and biofilter (Zheng et al., 2021) performance varies with high H_2S loading rates. Most of the bioreactor configurations deal with several operational issues, e.g. filter bed clogging or poor microbial density, resulting into poor biofilter performance (Okoro and Sun, 2019). Innovations are being carried out to overcome existing limitations and integrate other aspects, for example, simultaneous treatment of wastewater and gas-phase H_2S in an alum sludge (a residual by-product of water treatment plants) based biofilter (Ren et al., 2021).

Hollow fibre membrane bioreactors (HFMBs) were used for several applications such as: phenolic wastewater treatment through membrane aerated biofilm formation (Tian et al., 2020), production of value-added products (e.g. volatile fatty acids) through syngas fermentation (Shen et al., 2018; Wang et al., 2018), H_2 assisted biogas upgrading by feeding H_2 through the membrane module (Alfaro et al., 2019), and immobilization carrier of enzymes and cells (Łabęcki et al., 1996). However, limited research has reported on the application of HFMBs for biological desulfurization of H_2S laden gases (Das et al., 2022a; Das et al., 2022b).

Feasibility of the hydrophilic polyethersulfone hollow fibre membrane bioreactor (HFMB) configuration was tested for biological removal of gas-phase H_2S in our earlier study (Das et al., 2022b), where the HFMB treated H_2S up to a loading rate of ~ 17.0 g m^{-3} h^{-1} (corresponding to an inlet H_2S concentration of ~ 650 ppm_v) at an empty bed residence time (EBRT) of 187 s under steady-state. To adopt the HFMB as a biological approach for H_2S removal, long-term performance evaluation of the HFMB is important as well, especially to test the resilience of the HFMB at various operating conditions, i.e. pH changes, elevated H_2S concentrations and shock loads. Moreover, the effect of membrane fouling and operation after a period of non-use on the performance of the HFMB also needs to be investigated. The long-term performance evaluation of the HFMB is essential as industries often observe fluctuation of process parameters such as the substrate concentration or gas flow rates.

This study, therefore, aimed to (i) evaluate long-term (~ 9 months) performance of the HFMB under different operating conditions including different H_2S concentrations (from ~ 200 to 1255 ppm_v) during steady state, different gas contact times (187, 92 and 62 s), pH control (with and without), famine period and shock loads (from 4 to 72 h) by increasing H_2S concentrations (up to ~ 3600 ppm_v), (ii) determine if there are significant correlations between the employed operating parameters and the performance parameters (H_2S flux, gas-liquid mass-transfer, removal efficiency and elimination capacity), and (iii) identify the ideal mode of operation (batch or semi-batch mode) of the liquid phase (shell side of the HFMB configuration). Furthermore, a biokinetic analysis of the HFMB was performed.

4.2. Materials and methods

4.2.1. Experimental set-up of HFMB

Figure 4.1 shows an overview of the HFMB set-up used for H_2S removal. Hydrophilic polyethersulfone (H-PES) membranes (Senuofil Co., China) having an inner diameter, outer diameter and thickness of 1.65 mm, 2.0 mm and 0.02 mm, respectively, were used to fabricate a HFM module. Each HFMB consists of a submerged HFM module (with an effective membrane length, area and surface area/volume ratio of 2.2 m, 0.0138 m^2 and 2000 $m^2\ m^{-3}$, respectively) in a glass column (inner volume of ~ 970 mL, surrounded by a temperature-controlled water jacket) as described in our earlier study (Das et al., 2022b).

In this HFMB set-up, an H_2S contaminated air stream was passed through the lumen side of the hollow fibre membranes at atmospheric pressure where H_2S diffused through the membrane pores into the liquid phase (shell side). Other predominant constituents (e.g. O_2 and N_2) of the gas stream mainly left the HFM module and accumulated in the outlet gas bag. The shell side of the HFMB was kept static and the liquid profile was regularly monitored to do the sulfur mass balance and determine the effects of other parameters (e.g. pH and SO_4^{2-} concentration) on the H_2S removal performance. Two HFMB reactors (R_1 and R_2) were used for biotic operation, while the third HFMB (R_3) was used for abiotic operation.

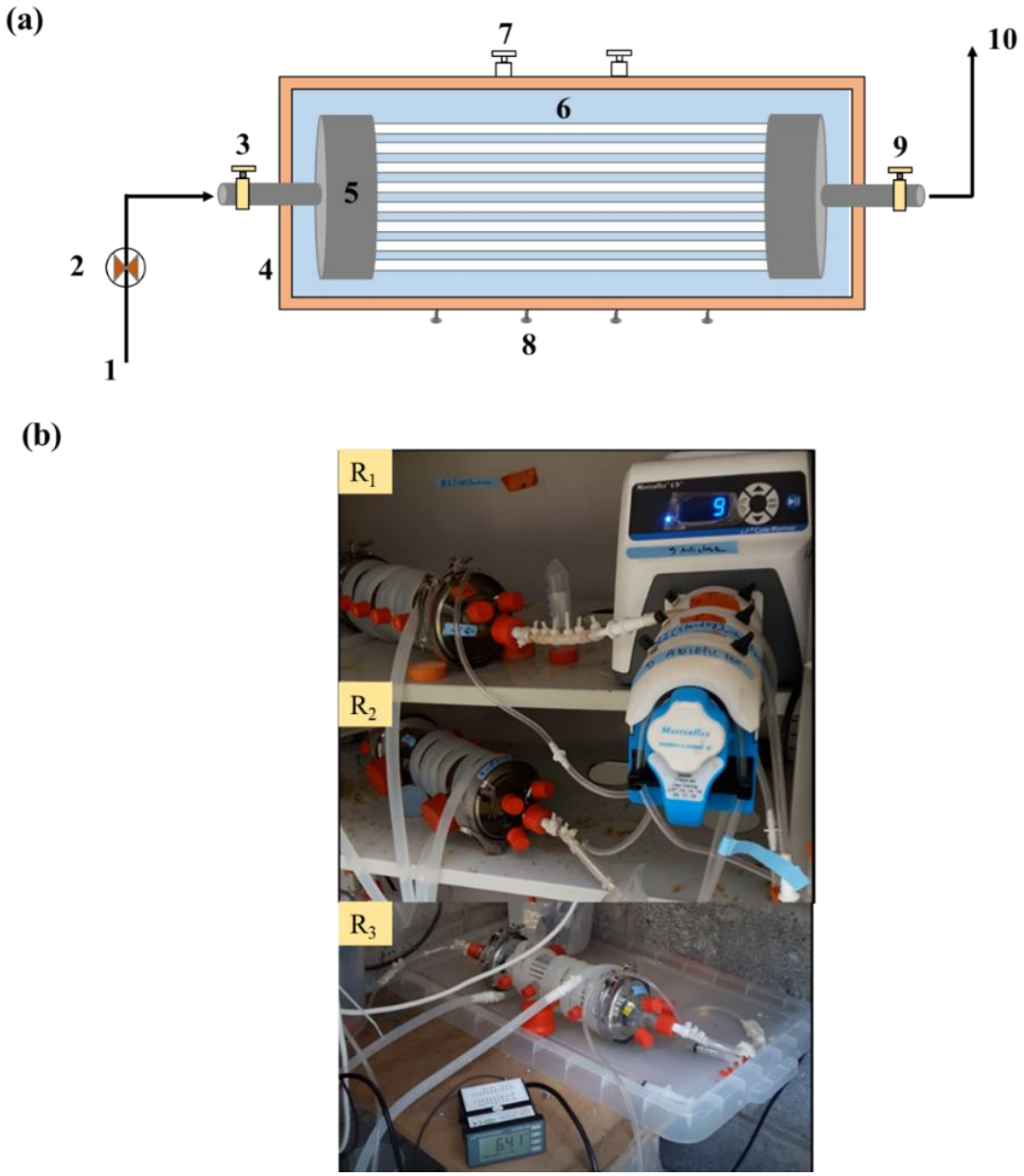

Figure 4.1: Overview of the HFMBs set-up used in this study: (a) schematic of a laboratory scale HFMB and (b) photographs of the three HFMB reactors R_1, R_2 and R_3 used for biotic and abiotic operation. 1) gas inlet containing H_2S, CO_2, O_2 and N_2, 2) peristaltic pump, 3) inlet sampling point to measure gas-phase H_2S and pressure, 4) glass column surrounded by a temperature-controlled water jacket outside, 5) hollow fibre membrane module, 6) liquid phase containing microbial inoculum and nutrient salt medium, 7) port to monitor pH, temperature and dissolved oxygen, 8) liquid phase sampling port, 9) outlet sampling point to measure gas-phase H_2S and pressure, 10) gas outlet with residual H_2S, CO_2, O_2 and N_2.

The first HFMB (R_1), previously operated for 83 days to test the feasibility of the HFMB configuration (Das et al., 2022b), was continued for long-term H_2S removal performance evaluation under different operating conditions. The second HFMB (R_2) was

newly fabricated, inoculated with fresh activated sludge and operated to compare the H_2S removal performance with that of R_1. The activated sludge from a dairy wastewater treatment plant (Kilconnell, Ireland) was used as an inoculum source. The mineral medium (Das et al., 2022b) was added to the sludge inoculum at a ratio of 3:7 (*v/v*) to ensure macronutrients and trace elements that are required for the enrichment of sulfur oxidizing bacteria. $NaHCO_3$ salt was used in the medium as an inorganic carbon source for sulfur oxidizing bacteria.

The third HFMB (R_3) was filled with deionized water and operated to compare the H_2S flux and mass-transfer for biotic and abiotic operation. The temperature inside each of the HFMB was maintained at 20 (± 2) °C and the dissolved oxygen (DO) concentration in the liquid phase was periodically monitored. The inlet and outlet pressure were observed regularly to check the pressure drop in the HFMB. Gas-phase H_2S generated in the lab under aerobic conditions (Das et al., 2022b) was fed in each HFMB using gas bags (10 L Tedlar® SCV gas sampling bag w/Thermogreen® LB-2 Septa). The inlet gas flow rates were set to ~ 0.14, 0.27 and 0.41 L h^{-1} during continuous operation of the HFMBs and the corresponding empty bed residence times (EBRTs) were estimated to be 187, 92 and 62 s, respectively.

4.2.2. Continuous operation of HFMB

Table 4.1 summarizes the operational strategies of the HFMBs used in this study where the experiments were categorized into three main sections: steady-state, transient-state and process parameters associated tests. The H_2S removal performance of the HFMB was tested under both steady and transient-state conditions employing variations of the inlet H_2S concentrations at three different EBRTs of 187, 92 and 62 s. The steady-state and transient-state operation was categorized with the following assumptions: (i) the inlet H_2S concentrations can fluctuate at an employed EBRT during the steady-state operation but the corresponding inlet loading rates (ILRs) of H_2S were not too high to prevent shock loads for functional microorganisms and (ii) the H_2S concentrations can suddenly (within 24 h) increase to a certain extent that can lead to shock loads of H_2S to the microbial consortia during the transient-state operation.

Table 4.1: Operating conditions applied during the continuous operation of the HFMB for treating H_2S contaminated gas.

HFMB	Remarks	OT, days	Operating conditions				
			EBRT, s	IC, ppm_v	IC, g m^{-3}	ILR, g m^{-3} h^{-1}	pH control (Yes/No)
Steady-state operation							
R_1	Biotic	84-310	187 *	974 ± 22 *	1.38 ± 0.03 *	26.48 ± 0.59 *	No *
			187	705 ± 280	1.00 ± 0.40	19.18 ± 7.60	No
			92	393 ± 272	0.56 ± 0.38	21.64 ± 15.00	No
			62	298 ± 75	0.42 ± 0.11	24.62 ± 6.16	Yes
R_2	Biotic	1-220	187 *	690 ± 60 *	0.98 ± 0.09 *	18.88 ± 1.64 *	Yes *
			187	556 ± 172	0.79 ± 0.24	15.11 ± 4.69	Yes
			92	426 ± 79	0.60 ± 0.11	23.49 ± 4.38	Yes
			62	253 ± 45	0.36 ± 0.06	20.91 ± 3.72	Yes
R_3	Abiotic	1-49	187	650 ± 278	0.92 ± 0.39	17.69 ± 7.57	No
	1st cycle		92	589 ± 328	0.83 ± 0.46	32.43 ± 18.08	
	2nd cycle	1-14	92	279 ± 60	0.39 ± 0.09	15.38 ± 3.33	No
			187	323 ± 8	0.46 ± 0.01	8.77 ± 0.22	
	3rd cycle	1-43	92	316 ± 225	0.45 ± 0.32	17.42 ± 12.39	Yes
			62	384 ± 140	0.54 ± 0.20	31.70 ± 11.60	
			187	581 ± 150	0.82 ± 0.21	15.81 ± 4.08	
Transient-state operation							
R_1	4 h shock loads at an EBRT of 92 and 62 s, 7-72 h shock loads at an EBRT 187 s	310-333	62	143 ± 10 (low) 1553 ± 758 (high)	0.20 ± 0.01 2.19 ± 1.07	11.85 ± 0.80 128.29 ± 62.65	No
			92	229 ± 102 (low) 2206 ± 554 (high)	0.32 ± 0.14 3.12 ± 0.78	12.60 ± 5.60	No
			187	635 ± 263 (low) 2787 ± 700 (high)	0.90 ± 0.37 3.94 ± 0.99	121.52 ± 30.53 17.27 ± 7.16 75.82 ± 19.05	No
Effect of biofilm and suspended biomass**							
R_1	1st cycle	339-345	187	628 ± 177	0.89 ± 0.25	17.08 ± 4.80	No
	2nd cycle	346-360	187	675 ± 175	0.95 ± 0.25	18.37 ± 4.77	No

Note: * - Shutdown of HFMB operation (from day 96 to 205 in R_1 and day 6 to 116 in R_2) considered as starvation period for the microbial consortia of HFMB; ** - steady-state performance of HFMB with and without suspended biomass was tested in two cycles; OT - operating time; IC - inlet H_2S concentration; ILR - inlet loading rate.

The steady-state experiment of the HFMB was started at an EBRT of 187s and stopped (from day 96 to 205 in R_1 and day 6 to 116 in R_2) unexpectedly within the first two weeks of operation. The HFMBs were kept at ambient temperature (~ 5-10°C) during this non-use (COVID) period. This shutdown period was considered as a starvation period for the microbial consortia present in the HFMB. Continuous operation of the HFMB was resumed after 110 days by employing similar operating conditions as used before the

shutdown period. The EBRT was switched from 187 s to 92 s followed by 62 s. The EBRT of either 92 s or 62 s was employed for the first four days in a week and changed back to 187s for the remaining three days, i.e. the gas flow rates were periodically changed to test simultaneously the effect of H_2S concentrations and loading rates. This was continued for a certain period (8 weeks operation at EBRT of 92 s followed by 4 weeks operation at EBRT of 62 s). A high inlet H_2S concentration was employed in R_1 during the entire steady-state operation compared to R_2 to assess the optimum H_2S removal capacity of the HFMB (for the applied conditions in R_1) and to test the possibility of achieving 100% H_2S removal consistently at the same time (in R_2).

To test the effect of pH on HFMB performance, R_1 was operated at both conditions: without controlling the pH during operation at EBRT of 187 and 92 s, and with controlling the pH (~ 7.0) during operation at an EBRT of 62 s. The pH of R_2 was controlled (~ 7.0) for the entire period of steady-state operation to test the combined effect of ILR and EBRT on HFMB performance, and to compare the H_2S removal performance with that of R_1. To control pH of the HFMB, a portion of the supernatant (~ 10-30%) from the shell side was replaced periodically by freshly prepared mineral medium (MM) solution. The abiotic operation of HFMB (R_3) was performed in three cycles including both a long (~ 50 days) and short (~ 15 days) term period by replacing the existing liquid phase at the end of each cycle to test the consistency in H_2S flux, mass transfer coefficient and outlet/inlet ratio of H_2S. The first and second cycle was carried out at an EBRT of 182 and 92 s without any pH adjustment. The third cycle was tested at EBRT of 187, 92 and 62 s with initial pH adjustment (~ 6.5) using a $NaHCO_3$ solution (0.05 M).

Transient-state experiments were carried out using R_1 to assess the resilience of the HFMB during shock loads with continuous fluctuation of the inlet H_2S concentration at each gas contact time. The effect of different shock load periods: 4 h (at an EBRT of 62 s and 92 s), 7 h, 16 h and 72 h (at an EBRT of 187 s) were also tested to identify differences in HFMB performance. At the end of the transient-state experiments, R_1 was operated in the absence of suspended biomass (i.e. mixed suspended liquor) and its operation continued for two cycles (first cycle for 7 days followed by a second cycle for 15 days) to reveal the contribution of the attached biofilm (on the outer surface of the membrane) and microbial consortia present in the suspended biomass on the HFMB's performance. To start the first cycle of operation, the suspended biomass was removed

from R_1. Then R_1 was filled with mineral solution (30% MM and 70% demineralized water). The same procedure was repeated for the second cycle.

4.2.3. Biokinetic modelling

A kinetic analysis of the HFMB was performed using a modified Michaelis-Menten equation (Dumont, 2017; Kim et al., 2008) as shown in Eq. (4.1) to test the suitability of the Michaelis-Menten model to predict the H_2S removal performance of the HFMB:

$$\frac{1}{EC} = \frac{K_s + C_{ln}}{EC_{max} C_{ln}} \quad (4.1)$$

With:

$$C_{ln} = \frac{C_{in} - C_{out}}{\ln\left(\frac{C_{in}}{C_{out}}\right)} \quad (4.2)$$

where C_{in} and C_{out} are, respectively, the inlet and outlet concentration (g m^{-3}), EC - elimination capacity (g m^{-3} h^{-1}), EC_{max} - maximum elimination capacity (g m^{-3} h^{-1}), K_s - half saturation constant (g m^{-3}). Eq. (4.1) was valid with the assumption of $C_{out} > 0$.

The EC_{max} and K_s were estimated from the intercept (C) and slope (m) of the linear relationship (Y = mX + C) where Y represents 1/EC and X represents $1/C_{ln}$. Experimental data of both steady and transient state operation was used to project the kinetic parameters K_s and EC_{max}.

4.2.4. Calculations

The operational parameters: EBRT and ILR, and the performance parameters: removal efficiency (RE) and elimination capacity (EC) of the HFMB were measured according to Jaber et al. (2017):

$$\text{EBRT (s)} = \frac{V}{Q} \quad (4.3)$$

$$\text{ILR (g } m^{-3}\ h^{-1}) = \frac{Q}{V} C_{in} \quad (4.4)$$

$$\text{RE (\%)} = \frac{(C_{in} - C_{out})}{C_{in}} 100 \quad (4.5)$$

$$\text{EC (g } m^{-3}\ h^{-1}) = \frac{Q}{V} (C_{in} - C_{out}) \quad (4.6)$$

where V is the bed volume (m^3), Q is the gas flow rate (m^3 h^{-1}), C_{in} and C_{out} are, respectively, the inlet and outlet concentration (g m^{-3}).

To compare the biotic and abiotic performance of the HFMB, the H_2S flux (J) through

the hollow fibre membrane and overall mass-transfer coefficient (K_G) were determined using the experimental data according to Tilahun et al. (2017):

$$\mathrm{J}\ (\mathrm{g}\ m^{-2}\ h^{-1}) = \frac{Q}{A}(C_{in} - C_{out}) \quad (4.7)$$

$$\mathrm{K_G}(\mathrm{m}\ h^{-1}) = \frac{Q}{A}\ln\frac{C_{in}}{C_{out}} \quad (4.8)$$

where A is the surface area of the membrane (m^2).

4.2.5. Analytical methods

The inlet and outlet H_2S concentrations were measured using a calibrated (QED environmental system limited, Coventry, UK) H_2S sensor (Biogas 5000, Geotech, UK). The sulfate (SO_4^{2-}) and thiosulfate ($S_2O_3^{2-}$) concentrations were measured using an ion chromatograph (Thermo Scientific™ Dionex™, USA) where the liquid samples were filtered through 0.2 μm filter (Sartorius™ cellulose acetate membrane filters, Fisher Scientific, UK) prior to analysis. A colorimetric method (Allen et al., 1993) was used to measure sulfide (S^{2-}) in the liquid using a UV/Vis spectrophotometer (Shimadzu UV-1900, Germany). A pH meter (Cole-Parmer 300 pH/ORP/Temperature 1/8-DIN Controller) was used to measure the pH of the liquid. A dissolved oxygen (DO) meter (HACH HQ 40d, USA) was used to monitor the DO of the liquid. The inlet and outlet pressure of the HFMB were measured using a digital manometer (measuring range of -1 to 3 bar; Model: Keller LEO1, Switzerland).

4.2.6. Statistical analysis

One-way and two-way analysis of variance (ANOVA) were performed using OriginLab (OriginPro 2018, OriginLab Corporation, USA) to observe the statistical differences (at the p-value of ≤ 0.05 level) in H_2S removal performance for (i) the HFMB operations with and without suspended biomass (one-way ANOVA) and (ii) changing the operating parameters pH, EBRT and ILR (two-way ANOVA).

4.3. Results

4.3.1. Steady-state performance of the HFMB

Biotic performance

Figures 4.2 and 4.3 demonstrate the H_2S removal efficiency (RE) and elimination

capacity (EC), respectively, during steady-state operation of the HFMBs (R_1 and R_2). The RE of both R_1 and R_2 were varied from its usual trend (~ 100% RE) to some extent (Figure 4.2) depending on the employed inlet H_2S concentrations and flow rates corresponding to EBRT of 187 s, 92 s and 62 s. The EC of the HFMB was increased with some fluctuations (Figure 4.3) when the EBRT was changed from 187 s to 92 s followed by 62 s, i.e. with the increase of H_2S flow rates.

At the start of the experiments, the RE of R_1 was ~ 100% with an inlet H_2S concentration of 1.38 (± 0.03) g m^{-3} (974 ± 22 ppm_v), corresponding to an ILR of ~ 27 (± 0.59) g m^{-3} h^{-1} at an EBRT of 187 s. The RE of R_2 was in the range of ~ 83-86% during the start-up and acclimatization phase with an inlet H_2S concentration of 0.98 (± 0.09) g m^{-3} (~ 694 ± 60 ppm_v), corresponding to an ILR of ~ 19 (± 1.64) g m^{-3} h^{-1}. Both R_1 and R_2 demonstrated the re-acclimatization capability and efficient H_2S removal profile after the starvation period, i.e. after the non-use period of ~ 110 days, and achieved ~ 100% RE at an EBRT of 187 s, where the inlet H_2S concentrations in R_1 and R_2 were 1.27 (± 0.22) g m^{-3} (902 ± 152 ppm_v) and 0.62 (± 0.18) g m^{-3} (435 ± 124 ppm_v), respectively. At an EBRT of 187 s, R_1 and R_2 achieved a maximum elimination capacity (EC_{max}) of 33.8 and 21.8 g m^{-3} h^{-1}, respectively, for an ILR of 34.1 g m^{-3} h^{-1} (inlet H_2S concentration of 1.77 g m^{-3} or 1255 ppm_v) and 21.8 g m^{-3} $h^{-1\ 1}$ (inlet H_2S concentration of 1.13 g m^{-3} or 800 ppm_v), respectively.

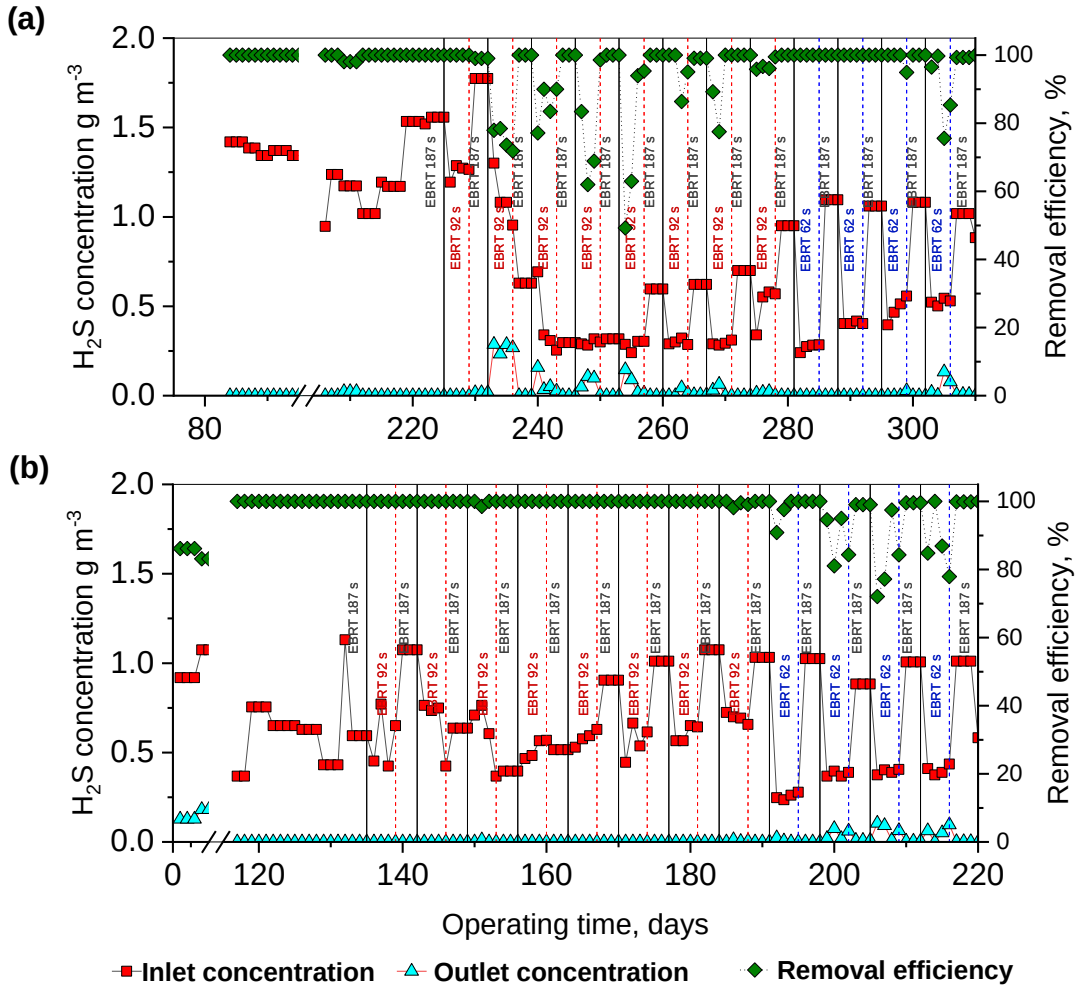

Figure 4.2: H_2S removal performance of HFMB: (a) R_1 and (b) R_2 under steady-state operation at an empty bed residence time of 187, 92 and 62 s.

At an EBRT of 92 s, the RE of R_1 was gradually decreased from 100% to ~ 72% and achieved an average EC of 41 (± 9.45) g m^{-3} h^{-1} for employing an inlet H_2S concentration of ~ 1.18 (± 0.13) g m^{-3} (834 ± 90 ppm_v), corresponding to an ILR of 46 (± 4.93) g m^{-3} h^{-1}. The removal performance of R_1 did not improve even though the inlet H_2S concentrations were kept lower (with a mean value of 0.29 g m^{-3} or 208 ppm_v) compared to earlier operation and the RE varied between ~ 50% and 95%. Thereafter, the removal performance of R_1 gradually improved and achieved a ~ 95% RE for an ILR of 14.3 (± 4.73) g m^{-3} h^{-1}. The RE of R_2 was ~ 100% during the entire experiment at an EBRT of 92 s for an average inlet H_2S concentration of 0.60 (± 0.11) g m^{-3} (426 ± 79 ppm_v), corresponding to an ILR of ~ 24 (± 4.38) g m^{-3} h^{-1}. The EC_{max} of R_2 was 30.0 g m^{-3} h^{-1} at an EBRT of 92 s for an inlet H_2S concentration of 0.77 g m^{-3} (545 ppm_v), corresponding

to an ILR of 30.0 g m^{-3} h^{-1}.

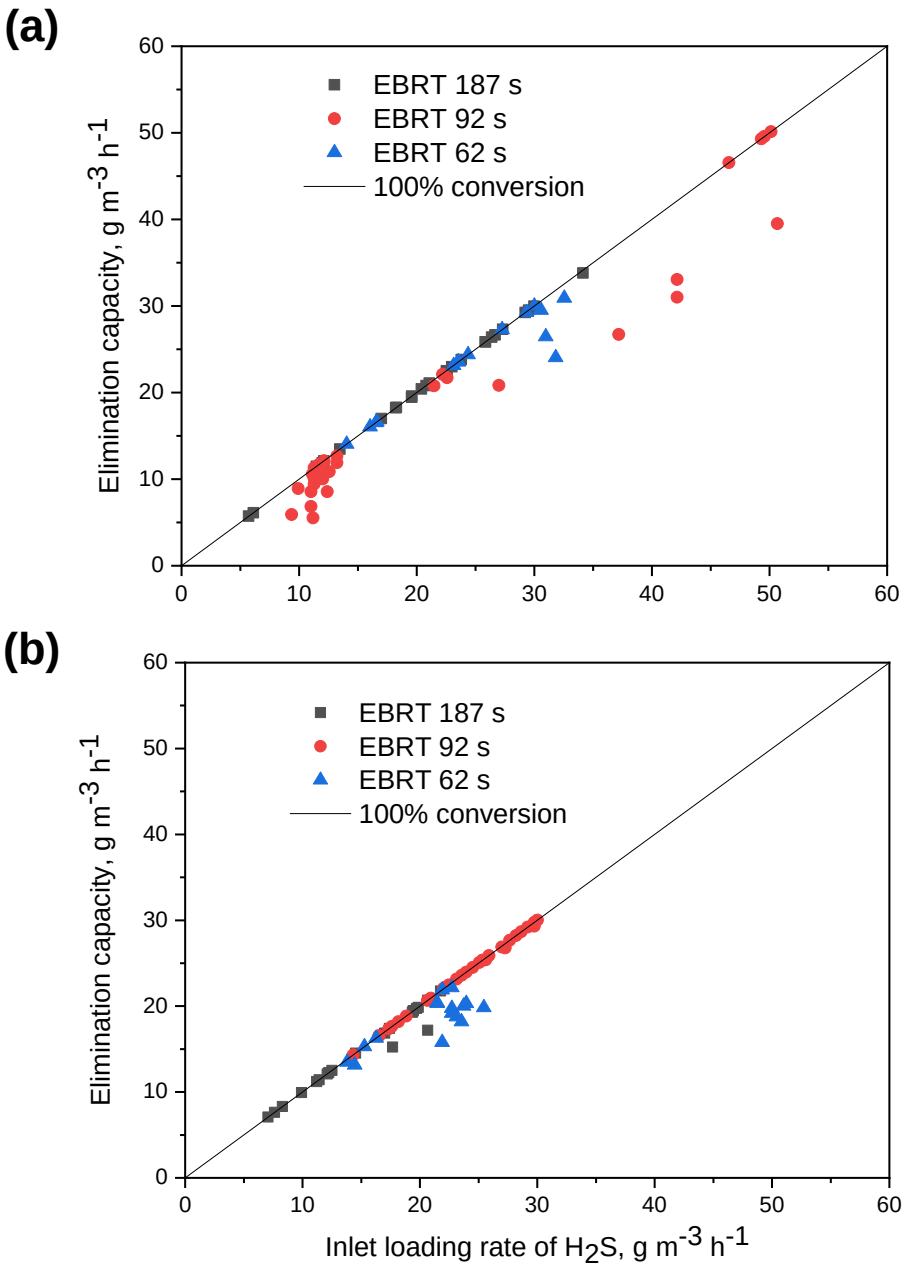

Figure 4.3: Influence of H_2S inlet loading rate on the elimination capacity of HFMB: (a) R_1 and (b) R_2 under steady-state operation at an empty bed residence time of 187, 92 and 62 s.

R_1 achieved ~ 100% RE at an EBRT of 62 s for an inlet H_2S concentration of 0.27 (± 0.02) g m^{-3} (191 ± 15 ppm_v) corresponding to an ILR of ~ 16 (± 1.20) g m^{-3} h^{-1}. The removal performance was consistent (~ 100% RE) when the inlet concentrations were further increased with an average value of 0.43 g m^{-3} (303 ppm_v), corresponding to an

ILR of ~ 25 (± 2.59) g m^{-3} h^{-1}. The RE of R_1 varied between ~80 and 100% when inlet H_2S concentration was > 0.51 g m^{-3} (363 ppm_v) at an EBRT of 62 s, and achieved an EC_{max} of 30.9 g m^{-3} h^{-1} for an ILR of 32.6 g m^{-3} h^{-1}. The RE of R_2 varied between ~80 to 100% during the experiments at an EBRT of 62 s and achieved an average RE of ~ 90% for an inlet H_2S concentration of 0.36 (± 0.06) g m^{-3} (253 ± 45 ppm_v), corresponding to an ILR of 20.9 (± 3.72) g m^{-3} h^{-1}. The DO concentration in the HFMB mixed liquor was initially ~ 9.0 mg L^{-1}, which gradually dropped with the HFMB operation and achieved a final concentration of 4.59 mg L^{-1} on day 305 in R_1 and 3.55 mg L^{-1} on day 215 in R_2.

Abiotic performance

Figure 4.4 shows the inlet and outlet concentration profiles of H_2S in three cycles during abiotic operation of the HFMB (R_3). All three cycles of R_3 suggests that a certain percentage (13-30%) of the inlet H_2S was diffused through the hollow fibre membranes. The outlet/inlet (O/I) ratio of H_2S reached 0.68 within the first 3 days of the first operation cycle of R_3 at an EBRT of 187 s. The O/I ratio varied between 0.68 and 0.77 for 28 days operation and achieved a mean O/I ratio of 0.70 (± 0.05) for an inlet H_2S concentration of 1.03 (± 0.33) g m^{-3} (725 ± 230 ppm_v), suggesting that ~ 30% of the employed inlet H_2S was diffused through the hollow fibres at an EBRT of 187 s. The mean O/I ratio was increased from ~ 0.70 to 0.83 (Figure 4.4a) during the next 16 days of the operation at an inlet concentration of 0.83 (± 0.46) g m^{-3} (589 ± 328 ppm_v) when the gas flow rate increased, corresponding to an EBRT of 92 s. The mean O/I ratio was 0.68 for the remaining 5 days of operation at an EBRT of 187 s even though a lower inlet H_2S concentration (0.33 ± 0.08 g m^{-3} or 232 ± 58 ppm_v) was employed compared to earlier operation.

The performance of R_3 during its second cycle operation was similar to its first cycle even though the second cycle was operated for a shorter period (8 days at an EBRT of 92 s followed by 6 days at an EBRT of 187 s). The mean O/I ratio in the second cycle was 0.82 (± 0.01) and 0.63 (± 0.01) at an EBRT of 92 s and 187 s, respectively (Figure 4.4b). The abiotic performance of R_3 during its third cycle operation (Figure 4.4c) was similar to both the first and second cycle even though the initial pH was adjusted to ~ 6.5 in the third cycle. The O/I ratio was increased with the increase in gas flow rates and achieved the highest O/I ratio of 0.87 (± 0.03) at an EBRT of 62 s for an inlet H_2S concentration of

0.54 (± 0.20) g m^{-3} (384 ± 140 ppm_v). The DO concentration in R_3 was ~ 10.5 mg L^{-1} initially and achieved a final concentration of 9.6 mg L^{-1} on day 37 of the third cycle.

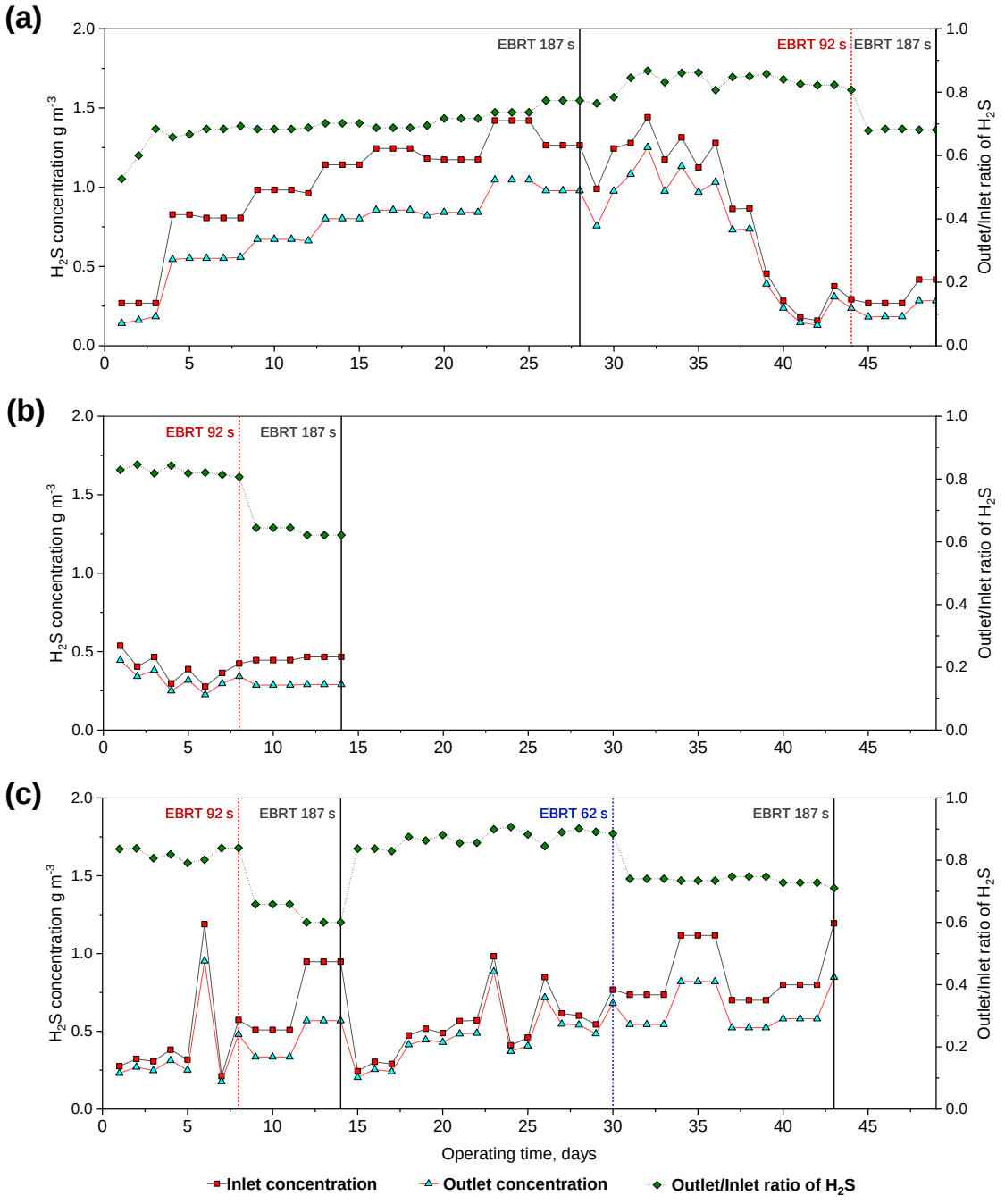

Figure 4.4: Inlet and outlet concentration profiles of H_2S during abiotic operation of the HFMB (R_3): (a) 1st cycle, (b) 2nd cycle and (c) 3rd cycle.

4.3.2. Transient-state performance of HFMB

Figure 4.5 shows the RE and EC of the HFMB (R_1) during its transient-state operation.

The RE gradually dropped from ~ 100 to 54% (Figure 4.5a) depending on the scale of the shock loads, duration of each shock load and the gas flow rates applied (corresponding to EBRT). The RE restored rapidly to 100% with the withdrawal of the shock loads, suggesting the resilience of the HFMB. The HFMB achieved an EC_{max} of ~ 147 g m^{-3} h^{-1} during the transient-state operation (Figure 4.5b).

The HFMB retained ~100% RE at an EBRT of 62 s, though ~ 3.5 times higher inlet H_2S concentrations (1.43 g m^{-3} or 1010 ppm_v) were employed compared to the steady-state operation, suggesting that the microbial consortia present in the HFMB can tolerate the ILR of ~ 83 g m^{-3} h^{-1} up to a 4 h period. The RE gradually decreased from ~100% to 89, 75 and 71% when the inlet H_2S concentrations were further increased to 2.16 g m^{-3} (1525 ppm_v), 2.91 g m^{-3} (2060 ppm_v) and 3.56 g m^{-3} (2518 ppm_v), respectively, corresponding to an ILR of ~ 126, 170 and 208 g m^{-3} h^{-1}, respectively. The RE was returned back to 100% when the shock loads were withdrawn.

When the gas flow rate was reduced (corresponding to an EBRT of 92 s) but employed higher H_2S concentrations up to 3.92 g m^{-3} (2770 ppm_v) during a 4 h period of shock load cycle, the RE dropped from ~100% to 87% and the HFMB achieved an EC_{max} of 133 g m^{-3} h^{-1}. At the end of each shock load, the HFMB rapidly regained its ~ 100% RE when it was operated using low inlet H_2S concentrations of 0.32 (± 0.14) g m^{-3} (229 ± 102 ppm_v).

The RE was ~ 100% during the 7 h shock load cycle at an EBRT of 187 s though an inlet H_2S concentration of 4.78 g m^{-3} (3380 ppm_v) was used (which was ~ 4 times higher than steady-state operation). The RE dropped from ~ 100 to 98% when the shock load period was increased from 7 to 16 h with an inlet H_2S concentration of 5.10 g m^{-3} (3606 ppm_v). The HFMB achieved an EC_{max} of ~ 97 g m^{-3} h^{-1} for an ILR of ~ 98 g m^{-3} h^{-1} during that period. The RE further dropped to ~ 54% when the shock load was continued for 72 h continuously, employing an inlet H_2S concentration of 3.39 g m^{-3} (2401 ppm_v). The RE increased from ~ 54% to 100% within 24 h of the withdrawal of the shock load.

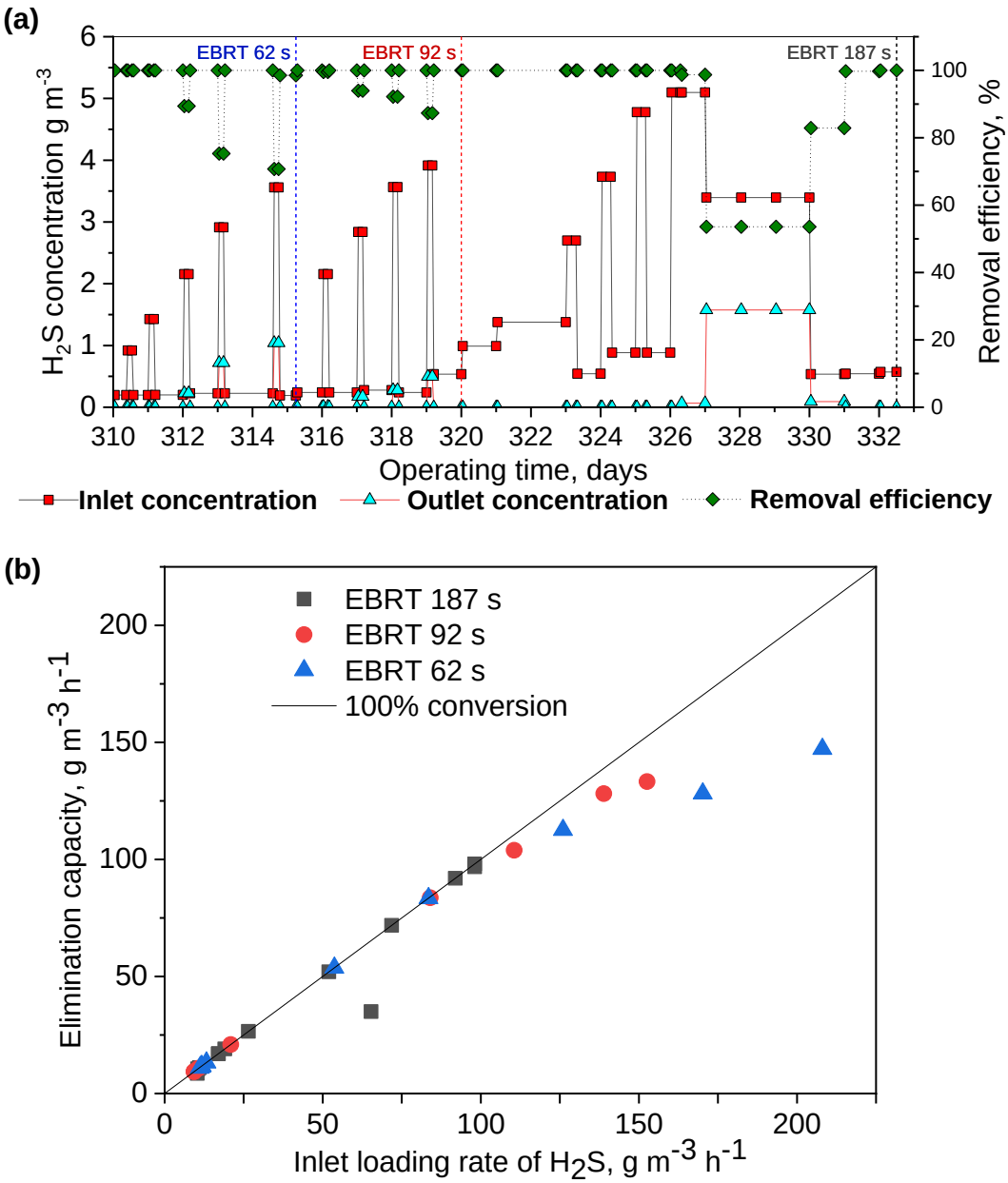

Figure 4.5: H_2S removal performance: (a) removal efficiency and (b) elimination capacity of the HFMB (R_1) under transient-state operation at an empty bed residence time of 187, 92 and 62 s.

4.3.3. Effect of process parameters on H_2S removal in HFMB

Effects of pH, ILR and EBRT

Figure 4.6 shows the significant changes in RE due to the pH drop and variations in ILR and EBRT. Table 4.2 summarizes the two-way ANOVA parameters associated with the effects of pH, ILR and EBRT. The mean RE of R_1 at an EBRT of 92 s was ~ 93% when the pH of the shell side liquid was in the range of 5.6-6.5. There was a significant

(P ≤ 0.05) decrease of RE (by ~ 10%) when the pH was in the range of 4.4-5.5 (Figure 4.6a). However, no significant changes in RE of R_1 were observed during that period for employing an ILR in the rage of 10-30 and 41-50 g m^{-3} h^{-1} (Figure 4.6a).

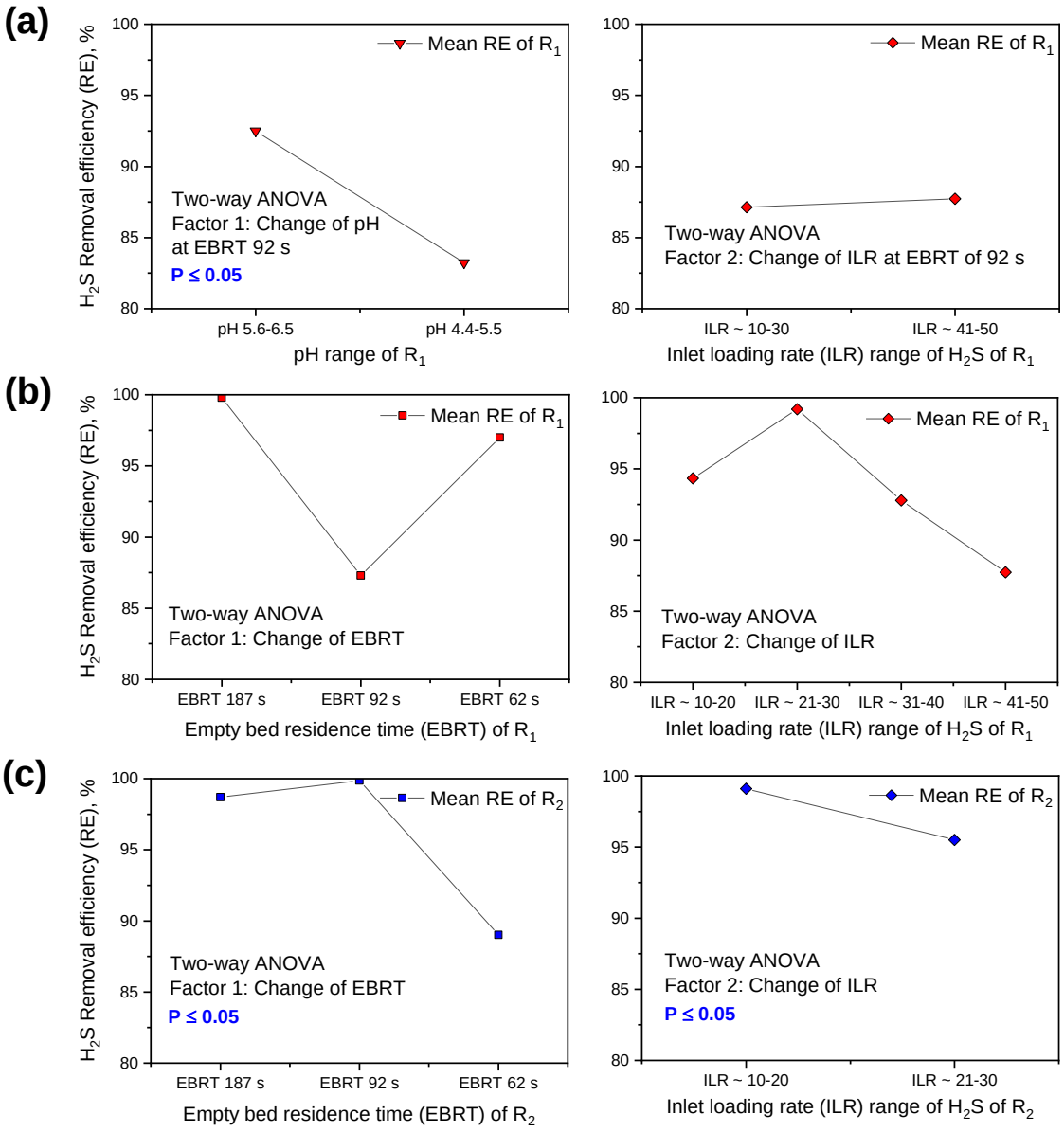

Figure 4.6: Mean comparison of H_2S removal efficiency of HFMB using two-way ANOVA including the factors (a) pH and inlet loading rate (ILR, g m^{-3} h^{-1}) at empty bed residence time (EBRT) of 92 s in R_1, (b) EBRT and ILR in R_1, and (c) EBRT and ILR in R_2.

There were significant differences in the RE of R_2 when changing the ILR and EBRT (Figure 4.6c) while keeping the pH controlled at ~ 7.0. The mean RE of R_2 dropped from ~ 100 to 89% at an EBRT of 62 s. There were no significant differences in mean RE of

R_1 when changing the EBRT and the ILR (Figure 4.6b), suggesting that pH control is required for the entire period of operation to differentiate the effect of EBRT from the ILR on the H_2S removal performance.

Table 4.2: Two-way ANOVA analysis (at significance level of 0.05) to evaluate the H_2S removal efficiency of the HFMB.

HFMB	DF	Sum of Squares	Mean Square	F Value	P Value
R_1					
Factors: pH and ILR					
Effect of pH on RE	1	1218.79	1218.79	7.53	**0.0105**
Effect of ILR on RE	1	0.3692	0.3692	0.0023	0.9622
Factors: EBRT and ILR					
Effect of EBRT on RE	2	0.0306	0.0153	2.53E-04	0.9998
Effect of ILR on RE	3	52.39	17.46	0.28835	0.8337
R_2*					
Factors: EBRT and ILR					
Effect of EBRT on RE	2	523.50	261.75	14.37	**3.1E-06**
Effect of ILR on RE	1	310.94	310.94	17.08	**7.3E-05**

Note: HFMB - hollow fibre membrane bioreactor; DF - degree of freedom; EBRT - empty bed residence time; ILR - inlet loading rate; RE - removal efficiency; * - effect of pH change can not be performed using two-way ANOVA as pH was controlled and maintained up to ~ 7.0 in R_2.

Figure 4.7 shows the pH and sulfate profile of R_1 and R_2. The S^{2-} and $S_2O_3^{2-}$ concentrations were below the detection limit suggesting the complete bioconversion of S^{2-} into S^0 or SO_4^{2-} in both R_1 and R_2. The average SO_4^{2-} generation (due to the S^{2-} bioconversion) on the shell side of the HFMBs was increased by ~ 24% (from 62.6 to 86.6% in R_1 and from ~ 62.4 to 86.8% R_2) when the EBRT was switched from 92 to 62 s. The cumulative theoretical and experimental SO_4^{2-} concentration were 1172 and 1075 mg/L, respectively, in R_1 at the end of day 309 (Figure 4.7a), suggesting that SO_4^{2-} (~ 92%) was the main sulfur species of the S^{2-} bioconversion. A similar S^{2-} to SO_4^{2-} (~ 93%) bioconversion trend was observed in R_2 at the end of day 219, where the theoretical and experimental SO_4^{2-} concentrations were 917 and 850 mg/L, respectively.

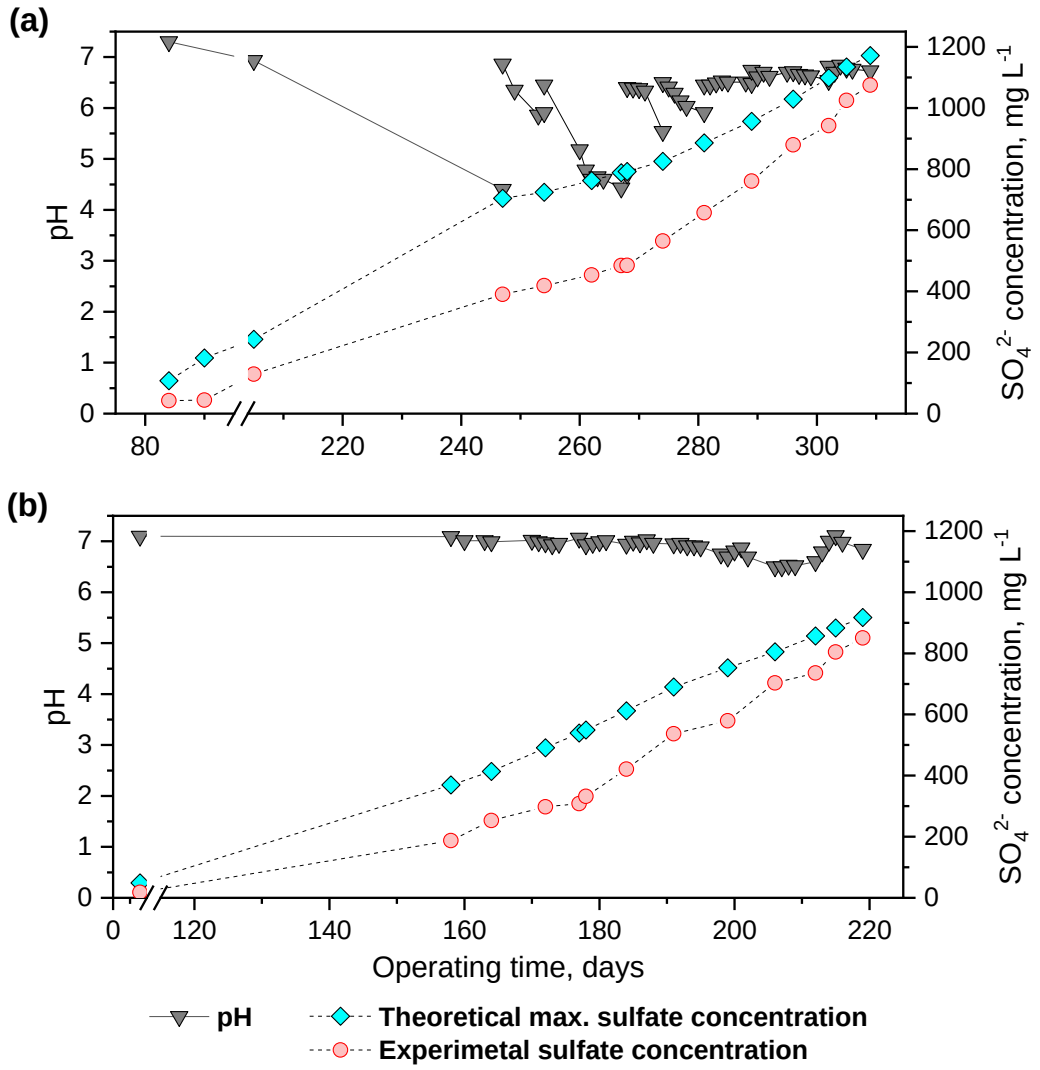

Figure 4.7: pH and sulfate profile of HFMB: (a) R_1 and (b) R_2 during steady-state operation.

Biofilm versus suspended biomass

Figure 4.8 shows the significant differences in H_2S removal performance for operating the HFMB (R_1) either in the presence or absence of suspended biomass (i.e. mixed suspended liquor). The HFMB achieved ~ 100% RE for its usual configuration, i.e. membrane attached biofilm and suspended biomass on the shell side. There were sharp variations in RE (from ~ 100 to 47%, Figure 4.8a) depending on the duration of the operation (7 or 15 days cycle), where the HFMB configuration was modified by replacing the suspended biomass with MM solution, i.e. the shell side was filled with MM solution only.

In the absence of the suspended biomass, the RE of the HFMB was ~ 100% for an ILR

of ~ 17 (± 4.80) g m^{-3} h^{-1} at an EBRT of 187 s during its first cycle (7 days) operation. In the second cycle, the RE was ~ 98 % for an ILR of ~ 18 (± 6.13) g m^{-3} h^{-1} at an EBRT of 187 s during the first 7 days of operation in the absence of the suspended biomass. Then, the RE was varied between 47 and 83% for the remaining 8 days of operation, with an average value of ~ 66% for an ILR of ~ 18 (± 3.64) g m^{-3} h^{-1}, suggesting that the sulfide oxidizing microbial consortia present in both the suspended biomass and membrane attached biofilm contributed to achieve ~ 100% RE in the HFMB.

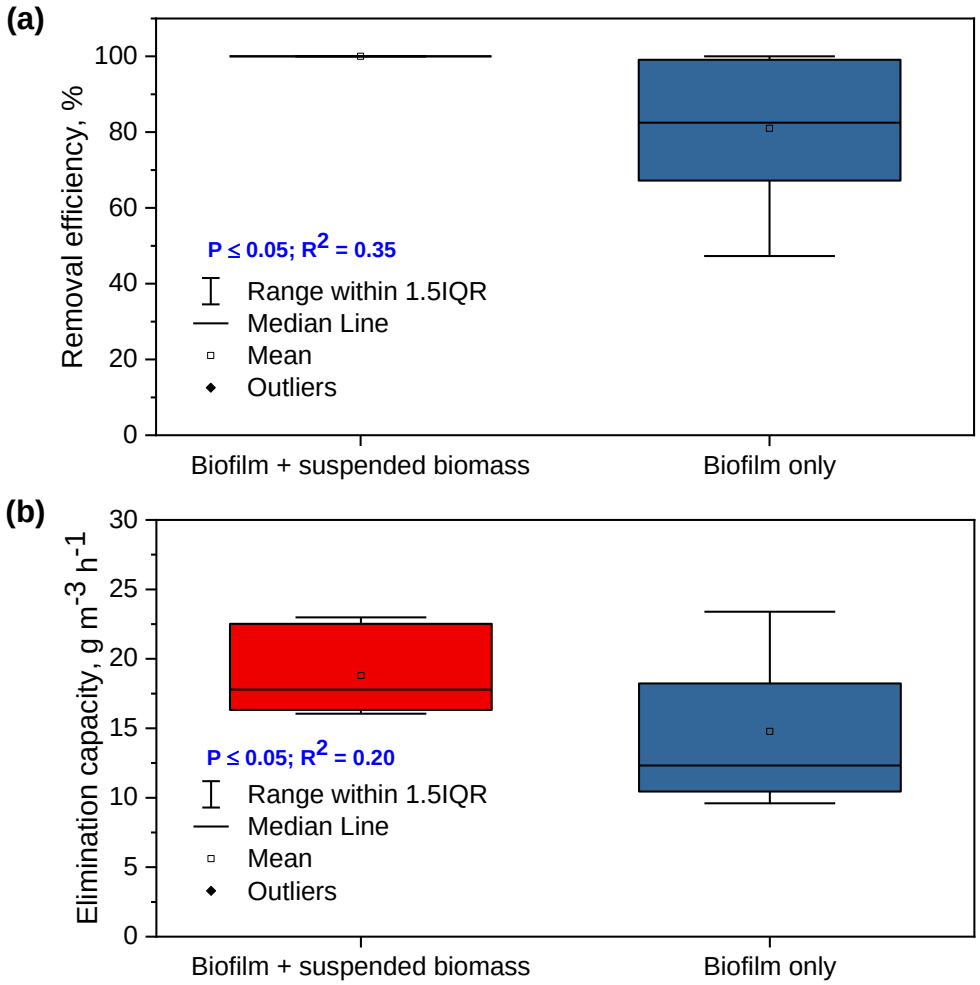

Figure 4.8: Mean comparison in terms of (a) H_2S removal efficiency and (b) elimination capacity of HFMB (R_1) using one-way ANOVA to test the effect of biofilm and suspended biomass.

4.3.4. H_2S flux and mass-transfer through the HFMB

Figure 4.9 demonstrates the significant differences in H_2S flux between biotic and abiotic operation of the HFMB at different EBRTs. The average H_2S flux in the biotic

HFMBs (R_1 and R_2) was ~ 5 times higher than the flux in the abiotic HFMB (R_3), suggesting the nearly complete diffusion of the applied inlet H_2S through the hollow fibres into the liquid phase during biotic operation. R_1 achieved a maximum H_2S flux of 0.41, 0.60 and 0.37 g m^{-2} day^{-1} at an EBRT of 187, 92 and 62 s, respectively, compared to R_2 indicating a positive correlation between the H_2S flux and inlet H_2S concentration. However, the maximum flux of R_3 was between 0.09 and 0.13 g m^{-2} day^{-1} at all employed EBRTs with an average value of 0.05 g m^{-2} day^{-1}, suggesting the influence of the microbial consortia on the H_2S diffusion in the HFMB.

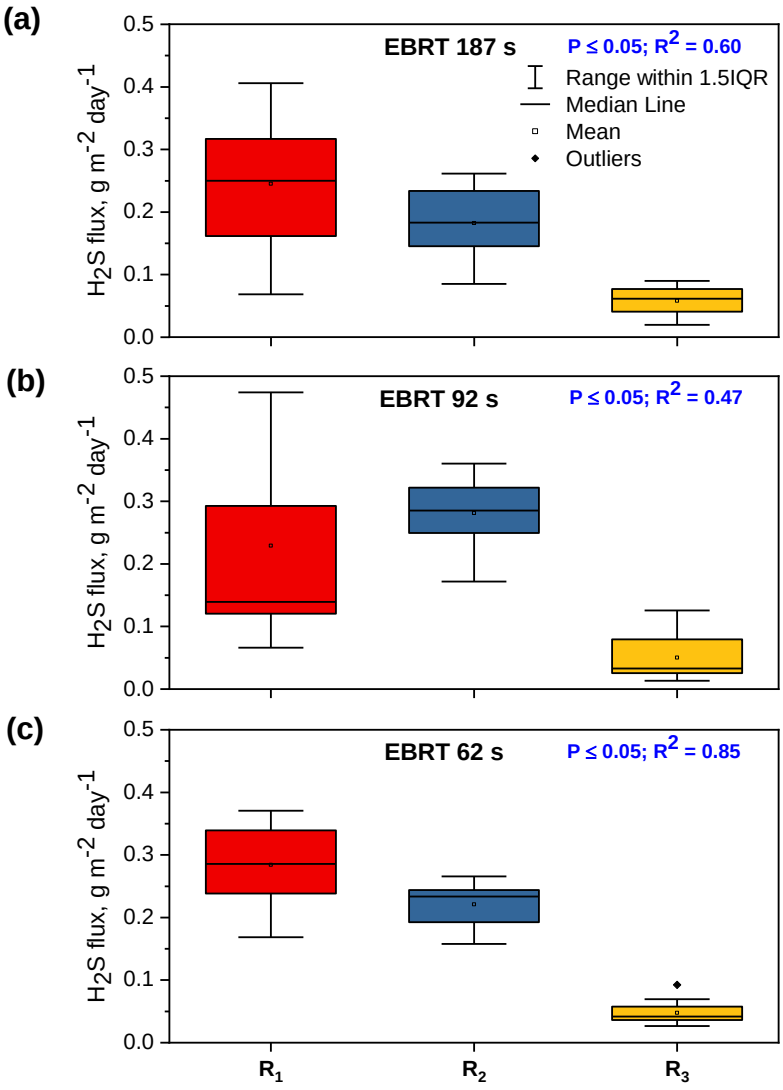

Figure 4.9: Comparison of H_2S flux in HFMB for biotic (R_1 and R_2) and abiotic (R_3) operation under steady-state at an at empty bed residence time (EBRT) of (a) 187 s, (b) 92 s and (c) 62 s.

Figure 4.10 shows the significant differences of the overall mass-transfer coefficient (K_G) of H_2S between biotic (R_1 and R_2) and abiotic (R_3) operation of the HFMB at an employed EBRT of 187 s, 92 s and 62 s. The average K_G of the biotic HFMBs was ~ 16 to 35 times higher than that of the abiotic HFMB depending on the applied gas flow rates (corresponding to EBRTs) and both inlet and outlet H_2S concentrations. The average K_G of R_1 and R_2 at an EBRT of 187s were 16.5 and 15.4 μm s^{-1}, respectively. The K_G of R_1 varied at an EBRT of 92 s where the average K_G was 0.54 times lower than that of R_2 (Figure 4.10b). The average K_G increased by 1.49 to 2.35 times and achieved a maximum value of 38.8 μm s^{-1} when the EBRT was switched from 187 s to 62 s. The maximum K_G of R_1 and R_2 was 47.9 and 45.3 μm s^{-1}, respectively, at an EBRT of 62 s with a RE of > 99%. The average K_G of R_3 (the abiotic HFMB) was ~ 1.0 μm s^{-1} at all employed operating conditions suggesting a positive correlation between K_G and RE of H_2S.

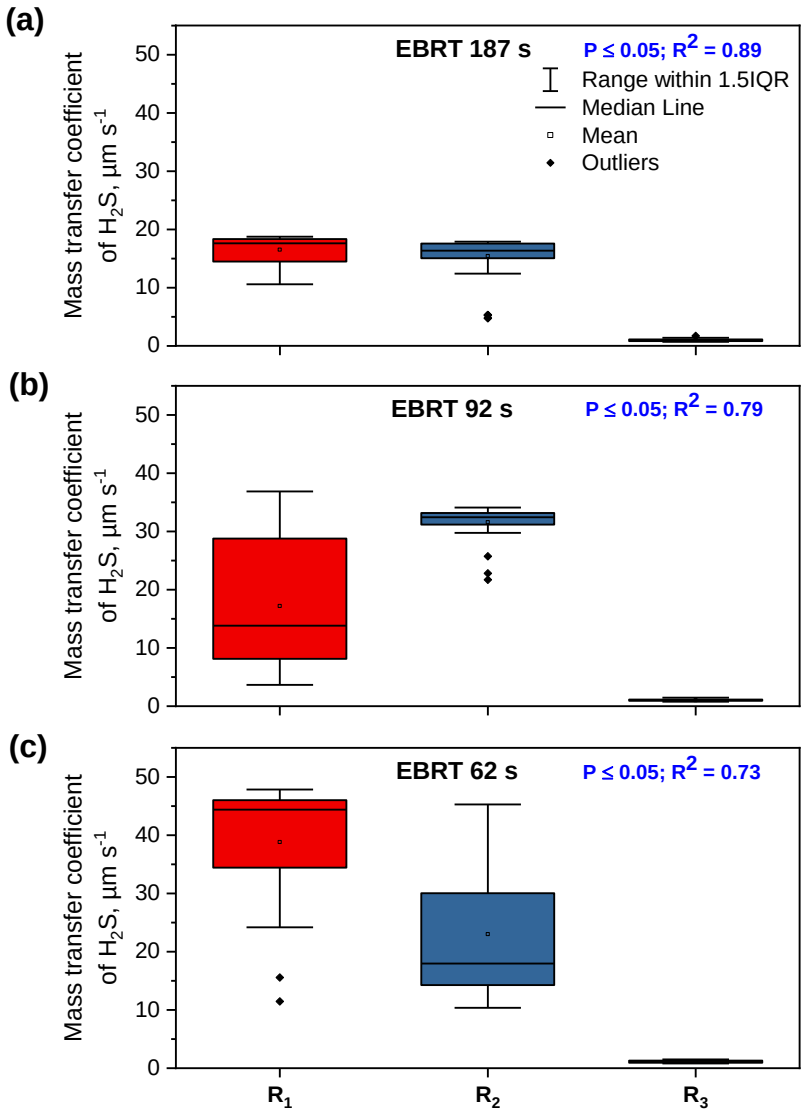

Figure 4.10: Comparison of the overall mass-transfer coefficient of H_2S in the HFMB for biotic (R_1 and R_2) and abiotic (R_3) operation under steady-state at an at empty bed residence time (EBRT) of (a) 187 s, (b) 92 s and (c) 62 s.

4.3.5. Biodegradation kinetics

Table 4.3 summarizes the projected half saturation constant (K_s) and maximum elimination capacity (EC_{max}) of H_2S, obtained from the linear plot (1/EC versus $1/C_{ln}$) of the slope and intercept as shown in Figure 4.11 under different operating conditions of the HFMB, and compares these with the experimental values. The projected EC_{max} of R_1 and R_2 during steady-state operation varied widely (from ~ 20 to 230 g m^{-3} h^{-1}), suggesting that there were differences in H_2S removal performance at an employed EBRT which influenced the model predictions. The average EC_{max} obtained from the Michaelis-

Menten model was ~ 85 g m^{-3} h^{-1} during the steady-state operation of the HFMB (irrespective of EBRT) which was ~ 2.7 times higher than that of the experimental value. The projected EC_{max} was ~ 2.3 times higher with an average value of ~ 300 g m^{-3} h^{-1} during the transient-state operation (irrespective of EBRT) compared to the experimental value.

Table 4.3: Experimental and projected maximum H_2S elimination capacity of the HFMB

HFMB	Operating condition	EBRT, s	Experimental value		Biokinetic modelling prediction*	
			IC_{max}, g m^{-3} (ppm_v)	EC_{max}, g m^{-3} h^{-1}	K_s, g m^{-3} (ppm_v)	EC_{max}, g m^{-3} h^{-1}
R_1	Steady-state	187	1.77 (1255)	33.81	1.26 (890)	128.21
		92	1.30 (920)	50.13	0.04 (30)	16.98
		62	0.56 (394)	30.90	0.08 (58)	44.64
R_2	Steady-state	187	1.13 (800)	21.76	0.52 (365)	71.43
		92	0.77 (545)	30.02	0.93 (660)	232.56
		62	0.44 (308)	22.14	0.02 (15)	20.79
R_1	Transient-state	187	5.10 (3606)	98.06	0.56 (400)	76.34
		92	3.92 (2770)	133.25	1.16 (820)	270.27
		62	3.56 (2518)	147.21	1.83 (1295)	555.56

Note: IC_{max} - maximum inlet H_2S concentration applied; EC_{max}- maximum elimination capacity of H_2S; K_s - half saturation constant of H_2S; * - The projected value of K_s and EC_{max} obtained from the linear plot slope and intercept as shown in Figure 4.11.

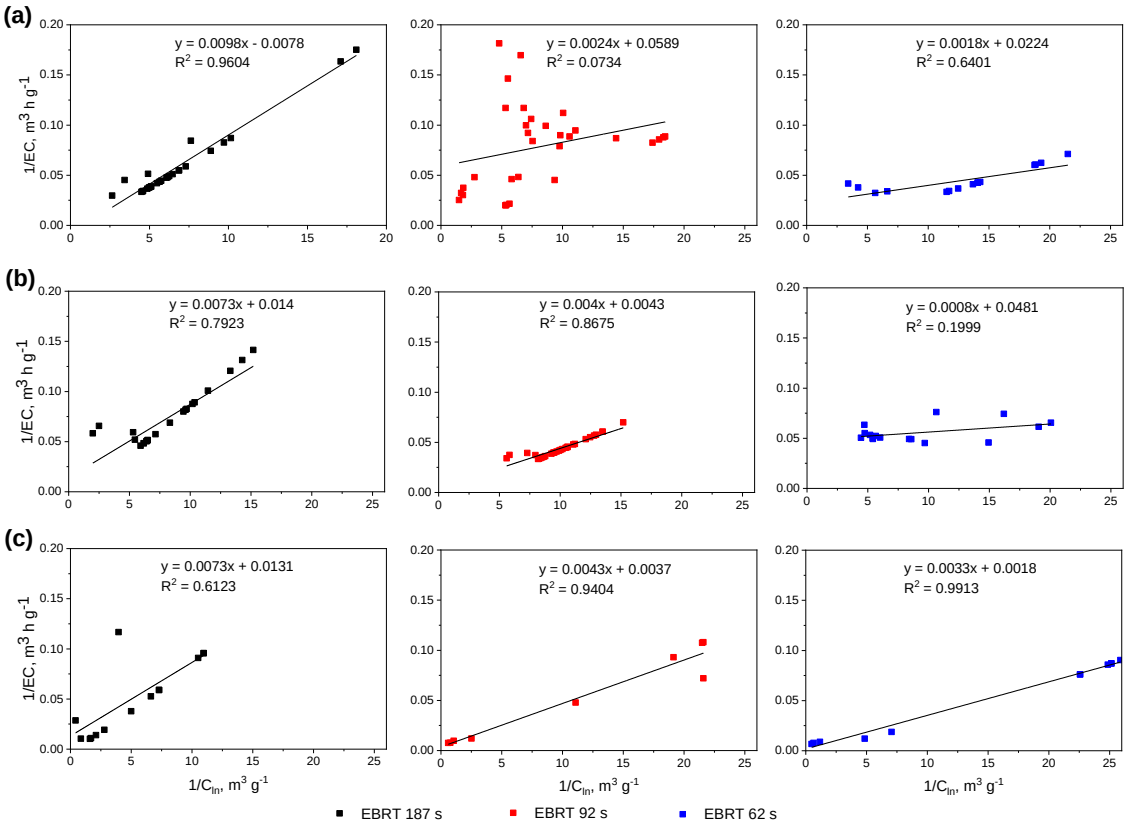

Figure 4.11: Relationship between 1/EC and $1/C_{ln}$ for the removal of H_2S in HFMB: (a) R_1 under steady-state, (b) R_2 under steady-state and (c) R_1 under transient-state operation at an EBRT of 187, 92 and 62 s.

4.4. Discussion

4.4.1. H_2S removal performance of the HFMBs

Effects of H_2S loading rates and pH

The HFMBs used in this study demonstrated efficient H_2S removal during the steady-state operation (Figure 4.2 and 4.3). The inlet H_2S concentrations, loading rates (with respect to EBRTs) and pH influenced the removal performance of the HFMBs. There are many influencing factors (e.g pH change or inlet loading rate) on the biofilm development in a bioreactor that can affect the bioreactor performance (Nhut et al., 2020). Operational aspects such as pH, employed EBRTs or fluctuation of the loading rates need to be considered in a biological desulfurization process (Das et al., 2022a; Montebello et al., 2013).

Though the HFMB (R_1) achieved ~ 100% RE of H_2S for an ILR up to ~ 34 g m^{-3} h^{-1}

(corresponding to inlet H_2S concentration up to ~ 1250 ppm_v) at an EBRT of 187 s, the H_2S removal performance varied when the EBRT was decreased from 187s to 92 s and the inlet H_2S concentration was kept high (~ 900 ppm_v). The main reason for the variations of RE in R_1 at an EBRT of 92 s can be related to the increase of ILR of H_2S prior to acclimatization of existing sulfide oxidizing microbial consortia (Cox and Deshusses, 2002) in R_1 during that period. pH can be another reason as the pH gradually dropped during that period which might not be suitable for the sulfide oxidizers that were responsible for the H_2S bioconversion process. The optimum pH can vary in a biological desulfurization process depending on the type of sulfide oxidizing bacteria (SOB) population (e.g. acidophilic or alkalophilic) present in the bioreactor (Pokorna and Zabranska, 2015). The H_2S removal performance of a biotrickling filter (BTF) increased from ~ 38 to 98% when pH was increased from ~ 7.0 to 9.0 (Zhuo et al., 2019).

Steady and more efficient performance (~ 100% RE with an EC_{max} of 30 g m^{-3} h^{-1}) of R_2 compared to R_1 at an EBRT of 92 s was related to the loading rate and pH, as R_2 was operated employing lower inlet H_2S concentrations (~ 450 ppm_v which was nearly half of the R_1 for the same period) and the pH in R_2 was controlled at ~ 7.0. Controlling the pH is important to avoid microbial inhibition in a bioreactor (Zhuo et al., 2019). The variations in H_2S removal performance of the HFMBs R_1 and R_2 at an EBRT of 92 s emphasized on the importance of controlling pH and H_2S loading rate (with respect to an EBRT) of a HFMB to achieve ~ 100% RE. R_1 improved its performance (~ 100% RE with an EC_{max} of 31 g m^{-3} h^{-1}) at an EBRT of 62 s with controlled pH and inlet H_2S concentrations (up to ~ 360 ppm_v).

As the ILR increases with the increase of gas flow rate in a fixed bed with similar inlet H_2S concentration, it is assumed that the RE will drop gradually if gas flow rates are increased (i.e. the EBRTs are decreased) and the inlet H_2S concentrations are kept constant. A significant decrease of flow rates (from ~ 135 to 60 m^3 h^{-1}) induced a sharp increase of the H_2S RE (from 60 to ~ 95%) in an industrial-scale bioscrubber (Cheng et al., 2018). The RE increased (from ~ 65% to 95%) with an increase of EBRT (from 40 to 100 s) in a BTF treating low H_2S concentrations (~ 200 ppm_v) from biogas (Zhuo et al., 2019). In another study (Montebello et al., 2013), the reduction of the EBRT (from 60 to 30 s), with the variations of ILR rather than a constant ILR, significantly reduced the RE

(from ~100 to 30%) in a BTF treating high H_2S concentrations (~ 2000 ppm_v) from synthetic biogas and achieved a critical EBRT of ~ 90 s.

Resilience of the HFMB

The SOB survived the long starvation period (~ 110 days) and the HFMBs achieved ~ 100% RE when the HFMBs resumed its operation at the end of the non-use period. The resilience of the HFMB after the starvation period can be related to the survival of the SOB through intracellular and extracellular S^0 production supporting energy generation (Li et al., 2020). The SOB generate S^0 in the periplasmic space to reserve energy. When sulfide supply is limited, chemoautotrophic SOB do not discharge most of the S^0, but they store the S^0 in the periplasmic space for further oxidation of S^0 to SO_4^{2-} to gain energy (ΔG^0 = - 587.1 kJ/reaction) (Li et al., 2020). A starvation period is an effective method for sulfur de-accumulation in packed bed bioreactors, e.g. BTF or biofilter (Fasihi et al., 2020).

The HFMB showed a fast recovery time (< 24 h) for the sudden increase of the inlet H_2S concentration in the range of ~ 2400-3600 ppm_v (Figure 4.5a) corresponding to a H_2S shock load up to ~ 208 g m^{-3} h^{-1} (Figure 4.5b). The inlet H_2S concentration applied in this study was ~ 3.6 times higher than that of an anoxic BTF with similar EBRT (180 s), dominated by *Thiobacillus* sp., and subjected to a H_2S shock load of ~ 36 g m^{-3} h^{-1} for a ~ 4 h period (Khanongnuch et al. 2019b). A similar transient-state study of an anoxic BTF inoculated with *Paracoccus versutus* strain MAL 1HM19 applied a H_2S shock load up to ~ 117 g m^{-3} h^{-1} (by sudden increase of the inlet H_2S concentration up to ~ 4000 ppm_v) for a 4 h period at an EBRT of 180 s, where the RE decreased to 61% but recovered its performance immediately after withdrawing the shock loads (Watsuntorn et al., 2020). In contrast, the HFMB (the present study) was capable to tolerate high H_2S concentrations (3606 ppm_v) for a longer period (16 h continuously) at an EBRT of 187 s with 98% RE, suggesting that the functional microorganisms were well adapted to the applied conditions.

The performance of the HFMB was more promising compared to that of anoxic BTFs (Khanongnuch et al., 2019b; Watsuntorn et al., 2020) where the BTFs handled shock loads for only a 4 h period. The HFMB was more resilient to shock loads even after employing continuous shock loads for 72 h and recovered its performance (from ~ 54%

to 100% RE) within 24 h after withdrawing the shock load. The restoration time to achieve 100% RE after withdrawing the shock load in an immobilized cell biofilter was within 96 h (Kim et al., 2008). In sulfide led wastewater treatment, the recovery time of an upflow anaerobic reactor was ~ 30 h for applying a 2 h shock load where the applied S^{2-} concentration was up to 1820 mg L^{-1} (Jing et al., 2009). The critical load of H_2S observed in the HFMB (~ 135 g m^{-3} h^{-1}; Figure 4.5b) was much higher compared to a compost and biochar packed biofilter (~ 81 g m^{-3} h^{-1}) operated at an EBRT of 80 s (Das et al., 2019).

Compared to BTFs or biofilters, the HFMB configuration used in this study can be more suitable to handle shock loads for having a better access to O_2 and nutrients by the SOB present on the membrane attached biofilm and in the mixed suspended liquor. When the SOB population attached onto the membrane surface is affected by a high H_2S load, the SOB present in the suspended biomass could re-build the biofilm.

Mass-transfer in the HFMB

The high outlet/inlet ratio of H_2S during abiotic operation of the HFMB (Figure 4.4), the H_2S flux (Figure 4.9) and mass-transfer coefficient (K_G; Figure 4.10) for both the biotic and abiotic process clearly show that the biological oxidation process mainly contributed to the efficient mass-transfer of H_2S in the HFMB compared to the abiotic HFMB (R_3), i.e. the SOB population present in the HFMB consumed the H_2S (that was diffused through the membranes) to gain energy from H_2S oxidation in the presence of O_2 as shown in Eq. (4.9) to (4.11) (Pokorna and Zabranska, 2015). Microbial community analysis carried out in our earlier proof of concept study (Das et al., 2022b) confirmed the presence of diverse SOB genera, including *Arcobacter*, *Chlorobium*, *Dechloromonas*, *Hydrogenophaga*, *Pseudomonas*, *Rhodopseudomonas*, *Sulfurospirillum* and *Sulfuricurvum* in the HFMB biomass, which mainly contributed to biological H_2S oxidation.

$$H_2S + 0.5O_2 \rightarrow S^0 + H_2O \qquad \Delta G^0 = -209.4 \text{ kJ/reaction} \qquad (4.9)$$

$$S^0 + 1.5O_2 + H_2O \rightarrow SO_4^{2-} + 2H^+ \qquad \Delta G^0 = -587.1 \text{ kJ/reaction} \qquad (4.10)$$

$$H_2S + 2O_2 \rightarrow SO_4^{2-} + 2H^+ \qquad \Delta G^0 = -798.2 \text{ kJ/reaction} \qquad (4.11)$$

The variation of K_G in the biotic process (R_1 and R_2) can be explained from the positive correlation between K_G and the RE, i.e. the K_G dropped when the RE decreased for the

applied operating conditions (Figure 4.6). Hence, it is necessary to ensure optimum conditions in the HFMB to ensure sustained SOB growth that leads to efficient mass-transfer of H_2S.

Wide variations of the H_2S flux (from ~ 74 to 447 g m^{-2} day^{-1}) (Marzouk et al., 2010) and K_G (from 30 to 13000 µm s^{-1}) (Al-Marzouqi et al., 2017; Wang et al., 2004) have been reported for physico-chemical separation using hollow fibre membrane contactors (HFMCs). The mass-transfer of the HFMCs depends on several factors, such as type of the absorption chemical used (Mirfendereski et al., 2019), molarity of the absorption chemicals (Marzouk et al., 2010), operation pressure (Marzouk et al., 2010), gas/absorbent liquid flow ratio (Wang et al., 2004), and membrane type and contactor design (Bazhenov et al., 2018). It is expected that both the H_2S flux and K_G value will be lower in HFMBs (Figures 4.9 and 4.10) compared to HFMCs (Al-Marzouqi et al., 2017; Marzouk et al., 2010; Wang et al., 2004) as the shell side (liquid phase) of the HFMBs was operated in static mode without using absorption chemicals, and the gas stream was passed through the lumen side of the hollow fibres at atmospheric pressure.

Though the H_2S contaminated air stream used in this study contained high O_2 concentration (~ 21%) compared to that of raw biogas (usually < 1% O_2), only a small fraction (~ 0.2-0.9%) of O_2 present in the waste gas stream was diffused through the hollow fibres and dissolved in the reactor mixed liquor of the HFMBs. The feasibility study of the HFMB (Das et al., 2022b) also reported the similar O_2 (~ 0.1-1.0%) diffusion onto the shell side. Periodical change of supernatant of the reactor mixed liquor on the shell side was useful to control both the pH (Figure 4.7) and DO concentrations (~ 3.5-4.5 mg L^{-1}) in a certain range in the biotic HFMBs. The DO concentrations in the biotic HFMBs also suggest that there was sufficient O_2 (Zhuo et al., 2019) onto the shell side for H_2S oxidation. Hence, the HFMB can be suitable for biogas desulfurization, because the O_2 concentration in the reactor mixed liquor of the HFMB should be sufficient for H_2S oxidation by the sulfur oxidizers.

The optimum DO for S^0 generation in a full-scale biogas desulfurization system was 0.8-1.2 mg L^{-1} (Cheng et al., 2018). Periodical changing of supernatant (from the shell side) as well as switching the EBRT (from 92 to 62 s) may equally contribute to the availability of sufficient O_2 in the liquid and shifting the S^{2-} bioconversion trend from S^0

(~ 38%) and SO_4^{2-} (~ 62%) to mainly SO_4^{2-} (~ 92%, Figure 4.7). Elemental sulfur (S^0) could also be produced during H_2S bioconversion as an intermediate and intracellular product which SOB utilize as a substrate for their growth (Nhut et al., 2020). The SO_4^{2-} generation increased from 22% to ~ 200% due to the further oxidation of the S^0 (present in the reactor mixed liquor) when the DO increased from ~ 1.0 to 4.0 mg L^{-1} (Cheng et al., 2018).

Though the liquid phase, i.e. shell side, was kept static in this study, a certain fraction (~ 50%) of the supernatant of the mixed suspended liquor can be replaced periodically (either biweekly or monthly basis) with fresh mineral medium depending on the applied H_2S loading rate to keep the SO_4^{2-} concentrations lower in the HFMB mixed liquor and subsequently increase the pH. Moreover, addition of fresh mineral medium can also improve the DO in the liquid. To avoid inhibition of the functional microorganisms due to the excess salinity generated from sulfate accumulation, ~ 90% supernatant from a biochemical treatment pond was replaced with fresh water in a biochemical treatment unit integrated with the scrubbing process (Li et al., 2021).

Though pH was controlled and lower inlet H_2S concentrations were applied during R_2 operation at an EBRT of 62 s, the possible reason for the variation of RE could be related to the high sulfate concentration (Mahmood et al., 2008) and the different SOB community present (Lin et al., 2018). High sulfate concentrations (> 365 mg L^{-1}) caused excess salinity, resulting in an inhibitory effect on the functional microorganism (Li et al., 2021).

4.4.2. Practical implications of the HFMB

Comparison of biological H_2S removal performance

Several bioreactor configurations (Table 4.4) were used in recent years for biological H_2S removal, where the EC of both aerobic and anoxic bioreactors were varied in a wide range (from ~ 8-166 g m^{-3} h^{-1}) depending on the employed operating conditions such as H_2S concentrations, loading rates, EBRTs, pH and temperature. Various EBRT, from ~ 40 to 120 s, were reported in conventional bioreactors, i.e. biofilters and biotrickling filters, for H_2S removal (Table 3). Three different EBRT of 187, 92 and 62 s have been chosen in this study to optimize the HFMB performance in terms of shorter EBRT and high inlet H_2S concentrations. This study suggests that the HFMB can be used for long-

term continuous operation in industries, e.g. raw biogas purification, for treating a wide range of H_2S (up to ~ 1250 and 3600 ppm_v for steady and transient-state, respectively) where the EBRT can be adjusted depending on the employed inlet H_2S concentration. The HFMB performance could be further increased by increasing the temperature from ~ 20 to 25°C as temperature has a positive correlation with H_2S RE (Zheng et al., 2021).

From a HFMB configuration perspective, diffusion of gas-phase pollutants through the hollow fibres into the bioreactor mixed liquor (shell side) followed by microbial conversion (both membranes attached biofilm and suspended SOB) was the key mechanism for efficient H_2S removal (Das et al., 2022b). Though the gas-phase pollutant was fed continuously through the lumen side of the hollow fibres, the shell side of the HFMB can be operated in semi-batch mode by replacing the supernatant intermittently, e.g. removal of the 50% supernatant once biweekly or monthly depending on the H_2S load. The main benefits of the semi-batch mode operation of the shell side can be: (i) to avoid a pH drop, low DO and sulfate inhibition, (ii) no additional pH controller and chemicals to adjust pH, (iii) sufficient mixing of the diffused gas through the membranes in the shell side at an employed gas flow rate (corresponding to EBRT), (iv) no additional mixing required for complete oxidation of H_2S, and (v) avoid shear stress on the membranes due to the water flux in the shell side. Apart from H_2S removal, further studies should focus on the HFMB application for treating a mixture of corrosive gases, for example, simultaneous removal of H_2S and NH_3 which are major contributors to the malodor index (Huan et al., 2021).

Table 4.4: Comparison on biological H_2S removal performance of different bioreactor configurations treating H_2S laden gases.

Bioreactor type	H_2S laden gas source	PM (remarks)	OT, days	pH	T, ^oC	IC, ppm_v	ILR, $g\ m^{-3}\ h^{-1}$	EBRT, s	RE, %	EC, $g\ m^{-3}\ h^{-1}$	Reference
CSTBR	Synthetic biogas	N/A (Anoxic, HRT 42 h)	53	7.8	30	2500 2000	100 232	119 41	> 98 ~ 72	~ 98 166	González-Cortés et al., 2021
BTF	Raw biogas	PC (aerobic)	150	1.0-4.0	30	~ 400-570	17-24	60	100	17-24	Zhang et al., 2021
BTF	Synthetic biogas	PR (aerobic)	550	2.5-2.7	NR	2000	52	130	> 99	~ 52	Montebello et al., 2014
BTF	Standard gas cylinder	PS (aerobic)	75	NR	NR	0-500	~ 85	~ 32-43	~ 99	~ 85	Huan et al., 2021
BF	Sanitary landfill odour	PUFCs (aerobic)	480	NR	25	10-160	NR	90	> 85	NR	Zheng et al., 2021
BF	Synthetic exhaust gases	PC (aerobic)	205	4.0	22-36	~ 40	~ 8.0	80	> 99	~ 8.0	Liu et al., 2021
BS	Synthetic biogas	N/A (aerobic)	80	~ 8.0	21	5000	~ 40-100	144-396	> 80	< 80	San-Valero et al., 2019
MBS	Synthetic biogas	PDMS membrane (aerobic)	180	7.0 8.5	30	10000	~ 10.5 ~10.2	NR	~ 80 ~ 77	~ 8.4 ~ 7.9	Tilahun et al., 2018
HFMB	Synthetic gas mixture	H-PES HFM (aerobic)	271	~ 7.0	20	167-1255 135-3606*	~ 6-50 ~ 9-208*	62, 92, 187	100 54-100*	30-34 35-147*	This study

Note: BF - biofilters; BTF - biotrickling filters; BSs - bioscrubbers; CSTBR - continuous stirred tank bioreactor; EBRT - empty bed residence time; EC - elimination capacity; HFMB - hollow fibre membrane bioreactor; H-PES HFM- hydrophilic polyethersulfone hollow fibre membrane; IC - inlet concentration of H_2S; ILR - inlet loading rate; OT - operating time; PC - polypropylene carrier; PDMS - polydimethylsiloxane; PM - packing materials; PR - pall ring; PS - polyhedral spheres; PUCFs - polyurethane foam cubes; MBS - hybrid membrane bioscrubber; NA - not applicable; NR - not reported; RE - removal efficiency; T - temperature; * - under transient-state operation of the HFMB

Biofilm formation and fouling

A thin biofilm was formed on the outer surface of the membrane during the biotic operation of the HFMBs (R_1 and R_2). The biofilm favoured the H_2S removal in the HFMBs (Figure 4.8). However, this attached biofilm was not associated with any membrane fouling issues due to the following reasons: (i) there were no pressure differences between inlet and outlet gas, (ii) the inlet and outlet gas volume was nearly the same during the entire operation, (iii) there was no water flux on the lumen side of the membrane, (iv) the outlet H_2S concentration should gradually increase during the biotic operation in case of fouling and (v) sulfate, easily soluble in water, was the main product (> 90% SO_4^{2-}) during H_2S bioconversion which means lower chance (< 10%) of S^0 formation that may influence the membrane clogging.

Excess biomass accumulation resulted into membrane clogging in membrane bioreactors operated for volatile organic compounds (VOCs) removal (Lebrero et al., 2014). The use of the organic carbon source (e.g. glucose) strongly influenced the growth of mixotrophic SOB isolated from activated sludge where biomass growth increased significantly compared to that for using inorganic substances (Sun et al., 2019). Though a mixed culture inoculum (activated sludge) was used, chemolithotrophic SOB can dominate in the HFMBs as only an inorganic carbon ($NaHCO_3$) source was supplied to the SOB growth. The absence of organic carbon can also limit the growth of the heterotrophs and consequently biomass accumulation in the HFMB.

Membrane wetting was not noticed during the entire operation of the HFMB. The reasons can be: (i) the static shell side (i.e. liquid phase was not associated with any turbulence that can create a pressure gradient between shell and lumen side of the membrane module) and (ii) the absence of the absorption chemicals (Mirfendereski et al., 2019) that can change the membrane surface morphology and pore-size.

Biokinetic modelling limitations

The Michaelis-Menten model overestimated the EC_{max} value of the HFMB for both steady and transient-state operation (Table 4.3). Theoretically, the half saturation constant (K_s) in the Michaelis-Menten model indicates the amount of pollutant that has to be treated to achieve $EC_{max}/2$ (Dumont, 2017). A small K_s value indicates the greater affinity of the pollutant (e.g. H_2S) with the microorganisms on the packing material where the

pollutant removal rate shifts towards the EC_{max} with lower inlet concentrations (Dumont, 2017). The main reason for variations between the predicted and experimental values in this study can be the high inlet H_2S concentration employed in the HFMB and related factors, e.g. pH drop, that inhibited the H_2S bioconversion process and consequently, the experimental EC_{max} value was lower than the predicted value.

The predicted EC_{max} (~ 120 g m^{-3} h^{-1}) of xylene in a compost biofilter by the Michaelis-Menten model was ~ 3.0 times higher than the experimental EC_{max} (42 g m^{-3} h^{-1}) where the critical loading rate of xylene was ~ 50 g m^{-3} h^{-1} (Rene et al., 2010). Similar overestimation trends were observed by Huan et al. (2021) and Andriamanohiarisoamanana et al. (2020) for predicting the maximum H_2S removal in a pilot-scale BTF system. In another study (Kim et al., 2008), the predicted K_s obtained from the biokinetic expression for H_2S removal in a biofilter was 3 ppm, though the experimental value was > 50 ppm suggesting the limitation of the modified Michaelis-Menten equation. The main limitation of the Michaelis-Menten model can be not to consider the substrate inhibition (Andriamanohiarisoamanana et al., 2020), which results into overestimation of the EC_{max} value. Further studies on the HFMB should focus on the mathematical modelling of the HFMB bioprocesses and mass transfer to predict the pollutant removal performance, considering the factors that influence the HFMB performance, such as pH change, substrate inhibition and biofilm growth.

4.5. Conclusions

A hollow fibre membrane bioreactor (HFMB) was tested for H_2S removal under different operating conditions. The operating parameters inlet H_2S concentrations, EBRT and pH significantly influenced the steady-state performance of the HFMB. The HFMB achieved ~ 100% RE under steady-state at a pH of ~ 7.0, with an EC of 33.8, 30.0 and 30.9 g m^{-3} h^{-1} at an EBRT of 187, 92 and 62 s, respectively, for an inlet H_2S concentrations up to 1255, 545 and 363 ppm_v, respectively. The H_2S mass-transfer coefficient of the biotic process (R_1 and R_2) was ~ 16-36 times higher than the abiotic process (R_3). The HFMB showed a good resilience to shock loads and a fast recovery time (< 24 h) after withdrawing the shock loads, where the H_2S removal performance varied depending on the duration of the shock load and employed EBRT. During a 4 h period of shock load, the RE dropped to 71 and 87% at an EBRT of 62 s (ILR of 208 g m^{-3} h^{-1}) and 92 s (ILR

of 153 g m^{-3} h^{-1}), respectively. The RE was > 98% for the 7-16 h period of shock load with a H_2S loading rate up to 98 g m^{-3} h^{-1} at an EBRT of 187 s and the RE dropped further to ~ 54% when the shock load increased from 16 to 72 h. From a practical viewpoint, the HFMB can be used for efficient H_2S removal in the industries dealing with H_2S contaminated gas streams with regular fluctuations.

4.6. References

Alfaro, N., Fdz-Polanco, M., Fdz-Polanco, F., Díaz, I., 2019. H_2 addition through a submerged membrane for in-situ biogas upgrading in the anaerobic digestion of sewage sludge. Bioresource Technology. 280, 1-8.

Allen, H.E., Fu, G., Deng, B., 1993. Analysis of acid-volatile sulfide (AVS) and simultaneously extracted metals (SEM) for the estimation of potential toxicity in aquatic sediments. Environmental Toxicology and Chemistry. 12, 1441-1453.

Al-Marzouqi, M.H., Marzouk, S.A., Abdullatif, N., 2017. High pressure removal of acid gases using hollow fiber membrane contactors: Further characterization and long-term operational stability. Journal of Natural Gas Science and Engineering. 37, 192-198.

Andriamanohiarisoamanana, F.J., Yasui, S., Iwasaki, M., Yamashiro, T., Ihara, I., Umetsu, K., 2020. Performance study of a bio-trickling filter to remove high hydrogen sulfide concentration from biogas: a pilot-scale experiment. Journal of Material Cycles and Waste Management. 22, 1390-1398.

Bazhenov, S.D., Bildyukevich, A.V., Volkov, A.V., 2018. Gas-liquid hollow fiber membrane contactors for different applications. Fibers. 6, 76.

Cheng, Y., Yuan, T., Deng, Y., Lin, C., Zhou, J., Lei, Z., Shimizu, K., Zhang, Z., 2018. Use of sulfur-oxidizing bacteria enriched from sewage sludge to biologically remove H_2S from biogas at an industrial-scale biogas plant. Bioresource Technology Reports. 3, 43-50.

Cox, H.H.J., Deshusses, M.A., 2002. Co-treatment of H_2S and toluene in a biotrickling filter. Chemical Engineering Journal. 87, 101-110.

Das, J., Ravishankar, H., Lens, P.N.L., 2022a. Biological biogas purification: recent developments, challenges and future prospects. Journal of Environmental Management. 304, 114198.

Das, J., Ravishankar, H., Lens, P.N.L., 2022b. Biological removal of gas-phase H_2S in hollow fibre membrane bioreactors. Journal of Chemical Technology & Biotechnology. Early View. https://doi.org/10.1002/jctb.6999

Das, J., Rene, E.R., Dupont, C., Dufourny, A., Blin, J., van Hullebusch, E.D., 2019. Performance of a compost and biochar packed biofilter for gas-phase hydrogen sulfide removal. Bioresource Technology. 273, 581-591.

Dumont, E., 2017. Validation of a rapid procedure to determine biofilter performances. Journal of Environmental Chemical Engineering. 5, 2668-2680.

Fasihi, M., Fazaelipoor, M.H., Rezakazemi, M., 2020. H_2S removal from sour water in a combination

system of trickling biofilter and biofilter. Environmental Research. 184, 109380.

González-Cortés, J.J., Torres-Herrera, S., Almenglo, F., Ramírez, M., Cantero, D., 2021. Anoxic biogas biodesulfurization promoting elemental sulfur production in a Continuous Stirred Tank Bioreactor. Journal of Hazardous Materials. 401, 123785.

Huan, C., Fang, J., Tong, X., Zeng, Y., Liu, Y., Jiang, X., Ji, G., Xu, L., Lyu, Q., Yan, Z., 2021. Simultaneous elimination of H_2S and NH_3 in a biotrickling filter packed with polyhedral spheres and best efficiency in compost deodorization. Journal of Cleaner Production. 284, 124708.

Jaber, M.B., Couvert, A., Amrane, A., Le Cloirec, P., Dumont, E., 2017. Removal of hydrogen sulfide in air using cellular concrete waste: Biotic and abiotic filtrations. Chemical Engineering Journal. 319, 268-278.

Jing, C., Ping, Z., Mahmood, Q., 2009. Simultaneous sulfide and nitrate removal in anaerobic reactor under shock loading. Bioresource Technology. 100, 3010-3014.

Kailasa, S.K., Koduru, J.R., Vikrant, K., Tsang, Y.F., Singhal, R.K., Hussain, C.M., Kim, K.H., 2020. Recent progress on solution and materials chemistry for the removal of hydrogen sulfide from various gas plants. Journal of Molecular Liquids. 297, 111886.

Khanongnuch, R., Di Capua, F., Lakaniemi, A.M., Rene, E.R., Lens, P.N.L., 2019. Transient-state operation of an anoxic biotrickling filter for H_2S removal. Journal of Hazardous Materials, 377, 42-51.

Kim, J.H., Rene, E.R., Park, H.S., 2008. Biological oxidation of hydrogen sulfide under steady and transient state conditions in an immobilized cell biofilter. Bioresource Technology. 99, 583-588.

Łabęcki, M., Bowen, B.D., Piret, J.M., 1996. Two-dimensional analysis of protein transport in the extracapillary space of hollow-fibre bioreactors. Chemical Engineering Science. 51, 4197-4213.

Lebrero, R., Gondim, A.C., Pérez, R., García-Encina, P.A., Muñoz, R., 2014. Comparative assessment of a biofilter, a biotrickling filter and a hollow fiber membrane bioreactor for odor treatment in wastewater treatment plants. Water Research. 49, 339-350.

Li, W., Zhang, M., Kang, D., Chen, W., Yu, T., Xu, D., Zeng, Z., Li, Y., Zheng, P., 2020. Mechanisms of sulfur selection and sulfur secretion in a biological sulfide removal (BISURE) system. Environment International. 137, 105549.

Li, X., Zou, J., Zhang, D., Xie, L., Yuan, Y., 2021. A new method for in-situ treatment of waste gas scrubbing liquid containing both NH_3 and H_2S based on sulfur autotrophic denitrification and partial nitrification-Anammox coupling system. Bioresource Technology. 124925.

Lin, S., Mackey, H.R., Hao, T., Guo, G., van Loosdrecht, M.C.M., Chen, G., 2018. Biological sulfur oxidation in wastewater treatment: A review of emerging opportunities. Water Research. 143, 399-415.

Liu, J., Sun, J., Lu, C., Kang, X., Liu, X., Yue, P., 2021. Performance and substance transformation of low-pH and neutral-pH biofilters treating complex gases containing hydrogen sulfide, ammonia, acetic acid, and toluene. Environmental Science and Pollution Research. 1-12.

Mahmood, Q., Zheng, P., Hayat, Y., Islam, E., Wu, D., Ren-Cun, J., 2008. Effect of pH on anoxic sulfide oxidizing reactor performance. Bioresource Technology. 99, 3291-3296.

Marzouk, S.A., Al-Marzouqi, M.H., Abdullatif, N., Ismail, Z.M., 2010. Removal of percentile level of H_2S from pressurized H_2S-CH_4 gas mixture using hollow fiber membrane contactors and absorption solvents. Journal of Membrane Science. 360, 436-441.

Mirfendereski, S.M., Niazi, Z., Mohammadi, T., 2019. Selective removal of H_2S from gas streams with high CO_2 concentration using hollow-fiber membrane contractors. Chemical Engineering & Technology. 42, 196-208.

Montebello, A. M., Bezerra, T., Rovira, R., Rago, L., Lafuente, J., Gamisans, X., Campoy, S., Gabriel, D., 2013. Operational aspects, pH transition and microbial shifts of a H_2S desulfurizing biotrickling filter with random packing material. Chemosphere. 93, 2675-2682.

Montebello, A.M., Mora, M., López, L.R., Bezerra, T., Gamisans, X., Lafuente, J., Baeza, M., Gabriel, D., 2014. Aerobic desulfurization of biogas by acidic biotrickling filtration in a randomly packed reactor. Journal of Hazardous Materials. 280, 200-208.

Nhut, H.H., Thanh, V.L.T., Le, L.T., 2020. Removal of H_2S in biogas using biotrickling filter: Recent Development. Process Safety and Environmental Protection. 144, 297-309.

Okoro, O.V., Sun, Z., 2019. Desulphurisation of Biogas: A Systematic Qualitative and Economic-Based Quantitative Review of Alternative Strategies. ChemEngineering. 3, 76.

Pokorna, D., Zabranska, J., 2015. Sulfur-oxidizing bacteria in environmental technology. Biotechnology Advances, 33, 1246-1259.

Reddy, C.N., Bae, S., Min, B., 2019. Biological removal of H_2S gas in a semi-pilot scale biotrickling filter: Optimization of various parameters for efficient removal at high loading rates and low pH conditions. Bioresource Technology. 285, 121328.

Ren, B., Lyczko, N., Zhao, Y., Nzihou, A., 2021. Simultaneous hydrogen sulfide removal and wastewater purification in a novel alum sludge-based odor-gas aerated biofilter. Chemical Engineering Journal. 129558.

Rene, E.R., Murthy, D.V.S., Swaminathan, T., 2010. Effect of flow rate, concentration and transient-state operations on the performance of a biofilter treating xylene vapors. Water, Air, & Soil Pollution. 211, 79-93.

San-Valero, P., Penya-Roja, J.M., Álvarez-Hornos, F.J., Buitrón, G., Gabaldón, C., Quijano, G., 2019. Fully aerobic bioscrubber for the desulfurization of H_2S-rich biogas. Fuel. 241, 884-891.

Shen, N., Dai, K., Xia, X.Y., Zeng, R.J., Zhang, F., 2018. Conversion of syngas (CO and H_2) to biochemicals by mixed culture fermentation in mesophilic and thermophilic hollow-fiber membrane biofilm reactors. Journal of Cleaner Production. 202, 536-542.

Sun, Z., Pang, B., Xi, J., Hu, H.Y., 2019. Screening and characterization of mixotrophic sulfide oxidizing bacteria for odorous surface water bioremediation. Bioresource Technology. 290, 121721.

Tian, H., Xu, X., Qu, J., Li, H., Hu, Y., Huang, L., He, W., Li, B., 2020. Biodegradation of phenolic compounds in high saline wastewater by biofilms adhering on aerated membranes. Journal of Hazardous Materials. 392, 122463.

Tilahun, E., Bayrakdar, A., Sahinkaya, E., Çalli, B., 2017. Performance of polydimethylsiloxane membrane contactor process for selective hydrogen sulfide removal from biogas. Waste Management. 61, 250-

257.

Tilahun, E., Sahinkaya, E., Çalli, B., 2018. A hybrid membrane gas absorption and bio-oxidation process for the removal of hydrogen sulfide from biogas. International Biodeterioration & Biodegradation. 127, 69-76.

Valdebenito-Rolack, E., Díaz, R., Marín, F., Gómez, D., Hansen, F., 2021. Markers for the comparison of the performances of anoxic biotrickling filters in biogas desulphurisation: A critical review. Processes. 9, 567.

Wang, D., Teo, W.K., Li, K., 2004. Selective removal of trace H_2S from gas streams containing CO_2 using hollow fibre membrane modules/contractors. Separation and Purification Technology. 35, 125-131.

Wang, H.J., Dai, K., Xia, X.Y., Wang, Y.Q., Zeng, R.J., Zhang, F., 2018. Tunable production of ethanol and acetate from synthesis gas by mesophilic mixed culture fermentation in a hollow fiber membrane biofilm reactor. Journal of Cleaner Production. 187, 165-170.

Watsuntorn, W., Khanongnuch, R., Chulalaksananukul, W., Rene, E.R., Lens, P.N.L., 2020. Resilient performance of an anoxic biotrickling filter for hydrogen sulphide removal from a biogas mimic: Steady, transient state and neural network evaluation. Journal of Cleaner Production, 249, 119351.

Wu, J., Jiang, X., Jin, Z., Yang, S., Zhang, J., 2020. The performance and microbial community in a slightly alkaline biotrickling filter for the removal of high concentration H_2S from biogas. Chemosphere. 249, 126127.

Zhang, Y., Oshita, K., Takaoka, M., Kawasaki, Y., Minami, D., Inoue, G., Tanaka, T., 2021. Effect of pH on the performance of an acidic biotrickling filter for simultaneous removal of H_2S and siloxane from biogas. Water Science and Technology. 83, 1511-1521.

Zheng, T., Li, L., Chai, F., Wang, Y., 2021. Factors impacting the performance and microbial populations of three biofilters for co-treatment of H_2S and NH_3 in a domestic waste landfill site. Process Safety and Environmental Protection. 149, 410-421.

Zhuo, Y., Han, Y., Qu, Q., Li, J., Zhong, C., Peng, D., 2019. Characteristics of low H_2S concentration biogas desulfurization using a biotrickling filter: Performance and modeling analysis. Bioresource Technology. 280, 143-150.

Chapter 5

Simultaneous removal of H_2S and NH_3 from raw biogas in hollow fibre membrane bioreactors

Abstract

H_2S and NH_3 are toxic, corrosive and odorous gases that often co-exist in gas streams emitted from industrial processes, including biogas produced in anaerobic digestion plants. A hollow fibre membrane bioreactor (HFMB) was tested for simultaneous biological removal of H_2S and NH_3 from raw biogas. The HFMB achieved ~ 100% removal efficiency (RE) for treating up to 1850, 915 and 1200 ppm_v of H_2S, and 460, 355 and 750 ppm_v of NH_3 at an empty bed residence time (EBRT) of 187, 92 and 46 s, respectively. At an EBRT of 46 s, the RE of H_2S and NH_3 was in the range of 85-97 and 73-95%, respectively, for inlet biogas laden with ~ 1200-1700 ppm_v of H_2S and 750-1050 ppm_v of NH_3. The critical loading rates of H_2S and NH_3 were ~ 150 and 40 g m^{-3} h^{-1}, respectively. S^0 (52%), SO_4^{2-} (48%) and N_2 (92%) were the end products of the H_2S and NH_3 bioconversion. Both aerobic (e.g. *Smithella*, *Sulfuricurvum* and *Thiomonas*) and nitrate reducing (e.g. *Rhodanobacter*, *Sulfuritalea* and *Thiobacillus*) sulfide oxidizing genera contributed to the H_2S bioconversion. Aerobic (e.g. *Pseudomonas*, *Stenotrophomonas* and *Nitrosospira*) and Fe(III) reducing (e.g. *Clostridium_sensu_stricto_12*, *Rhodoferax* and *Dechloromonas*) ammonia oxidizing genera contributed to the NH_3 bioconversion.

5.1. Introduction

Anaerobic digestion (AD) is a sustainable approach to treat organic wastes and generate renewable energy simultaneously (Angelidaki et al., 2018). Raw biogas, an end product of AD, generally consists of methane (CH_4, range: 35-75%), carbon dioxide (CO_2, range: 25-60%) and other undesired constituents such as nitrogen (N_2), water vapour, oxygen (O_2), hydrogen sulfide (H_2S), ammonia (NH_3), volatile organic compounds (VOCs) and siloxanes (Bragança et al., 2020). CH_4 is the only desired constituent in raw biogas for its calorific value. The highest heating value of raw biogas ranges between 15 and 30 MJ/Nm^3 for a CH_4 content of 35-75%. All biogas impurities are a prime concern in the biogas utilization processes, such as electricity generation or natural gas grid injection (Angelidaki et al., 2018; Bragança et al., 2020).

The concentrations of H_2S (generally < 5000 ppm_v) and NH_3 (generally < 1000 ppm_v) in raw biogas can vary depending on the AD conditions and type of substrate used (Kang et al., 2020). The presence of H_2S and NH_3 in raw biogas, even in trace amounts, hinders the end-use application of raw biogas because these gases are toxic to human health, cause corrosion and damage the combined heat and power (CHP) engines and other metallic parts after burning

(Angelidaki et al., 2018; Kang et al., 2020). Conventional physico-chemical methods (e.g. water scrubbing, chemical scrubbing or pressure swing adsorption) are commonly employed for raw biogas purification in industries prior to electricity generation. However, these physico-chemical approaches can have a significant environmental impact and require higher energy consumption compared to biological biogas purification methods (Das et al., 2022a).

Biological H_2S and NH_3 removal methods have several advantages (e.g. more economical, environmental friendly and efficient pollutant removal) compared to the physico-chemical methods (Barbusiński et al., 2021). Several bioreactor configurations such as the biotrickling filter (Huan et al., 2021), biofilter (Gandu et al., 2021) and airlift bioreactor (Chen et al., 2018) have been employed for simultaneous removal of H_2S and NH_3 where the inlet concentrations of both H_2S and NH_3 in the odour emissions were < 500 ppm_v. An integrated two-stage system such as gas-lift bioreactor (González-Cortés et al., 2021) or biotrickling filter (Cano et al., 2021) integrated with a continuously stirred tank bioreactor was also reported for simultaneous removal of H_2S and NH_4^+ from leachate and wastewater. Biological innovations in terms of bioreactor configurations are required for the optimization of downstream raw biogas treatment, especially for mixed pollutant removal (Das et al., 2022a).

In our earlier study (Das et al., 2022b), the feasibility of a hollow fibre membrane bioreactor (HFMB) configuration to treat a H_2S laden biogas mimic has been demonstrated, where the HFMB achieved an elimination capacity (EC) of ~ 17 g m^{-3} h^{-1} for inlet H_2S concentrations up to ~ 650 ppm_v at an empty bed residence time (EBRT) of 187s. However, further studies are recommended to optimize the HFMB performance for full scale application in terms of shorter EBRT and higher EC of H_2S (Das et al., 2022b). To adopt the HFMB as a suitable biological approach for several applications including biogas purification and odour treatment, it is important to test the HFMB performance for mixed pollutant (e.g. H_2S and NH_3) removal under different operating conditions (e.g. different EBRTs or loading rates), and reveal the mass transfer profile of the mixed pollutant and their microbial conversion pathways during long term continuous operation. To date, to the best of our knowledge, no work has been reported on simultaneous biological removal of H_2S and NH_3 from raw biogas employing the HFMB.

The objective of this study was, therefore, to evaluate the long-term HFMB performance for treating H_2S and NH_3 simultaneously from raw biogas, employing different inlet loading rates (ILRs) and EBRTs (187, 92 and 46 s). In addition, the flux and gas-liquid mass transfer profiles

of the biogas constituents through the hollow fibres of the HFMBs were assessed. Apart from the removal performance of the HFMB, the reactor mixed liquor profile (e.g. metabolic end products, mass balance and functional microorganisms for H_2S and NH_3 bioconversion) was investigated for continuous operation (~ 6 months). Finally, a possible bioconversion pathway for simultaneous H_2S and NH_3 removal in the HFMB has been proposed.

5.2. Materials and methods

5.2.1. Inoculum

An enriched activated sludge, collected from a HFMB at the end of H_2S removal studies under different operating conditions (Chapter 4) and stored at 4°C (for ~ 3 months), was used as inoculum in this study.

5.2.2. Nutrient salt medium at shell side of the HFMB

To ensure macro-nutrients, trace elements, and inorganic and organic carbon source for sulfur and ammonia oxidizing bacteria, the nutrient salt medium (NSM) used in the HFMB had the following composition (in g L^{-1}): K_2HPO_4 - 1.2, KH_2PO_4 -1.8, NH_4Cl - 0.35, $NaHCO_3$ - 1.0, $C_6H_{12}O_6$ - 0.02, $FeCl_3 \cdot 6H_2O$ - 0.02, $CuCl_2 \cdot 2H_2O$ - 0.02, H_3BO_3 - 0.02, $MnCl_2 \cdot 4H_2O$ - 0.02, $Na_2MoO_4 \cdot 2H_2O$ - 0.02, $MgCl_2 \cdot 6H_2O$ - 0.05, $CaCl_2 \cdot 2H_2O$ - 0.02 and $ZnCl_2$ - 0.02. The NSM composition used in this study was modified from previously reported studies (Cheng et al., 2018; Huan et al., 2021). The inoculum to NSM ratio was 7:3 (*v/v*).

5.2.3. Raw biogas from anaerobic digester

The raw biogas used in this study was collected from an AD plant (Kildare, Ireland), where agricultural residues (pig and chicken manure), food processing wastes and retail food waste are used as feedstocks. The produced raw biogas is used for electricity and heat generation using a CHP (1.2 MW), with the remainder upgraded to biomethane (> 95% CH_4) using a membrane-based scrubber. Activated carbon (AC) is currently used as the primary method for removing H_2S from raw biogas, i.e. AC filters are used prior to both CHP and membrane-based scrubbing units. The raw biogas was regularly collected from the AD plant in Tedlar® PLV gas sampling bags (25L w/Thermogreen® LB-2 septa, Sigma-Aldrich), transported to the laboratory set-up and fed the HFMBs.

5.2.4. Experimental set-up

Figure 5.1 shows the schematic of the raw biogas purification set-up to treat H_2S and NH_3 simultaneously. Two HFMB reactors, one biotic and an abiotic control, were used in this study. Each HFMB consisted of a submerged hollow fibre membrane (HFM) module having an effective surface area of 0.0138 m^2 and an area to volume ratio of 2000 m^2 m^{-3}. The membrane characteristics, HFM module fabrication and HFMB configuration are detailed in Das et al. (2022b).

The biotic HFMB was filled with the inoculum, while the abiotic control was filled with sterilized (autoclaved using a SANYO, MLS-3020U, Japan) NSM only. The liquid phase on the shell side of the HFMB was kept static and the reactor mixed liquor composition was regularly monitored. The raw biogas collected in the gas bags was continuously supplied through the lumen side of the HFM, where a fraction of the biogas constituents diffused through the hollow fibres into the liquid phase (i.e. NSM on the shell side). The remaining undissociated biogas constituents left the HFM module and accumulated in the outlet gas bags. The HFMBs were operated at controlled temperature (20 ± 2°C) and atmospheric pressure. The biogas composition (both the inlet and outlet) and the pressure were measured regularly.

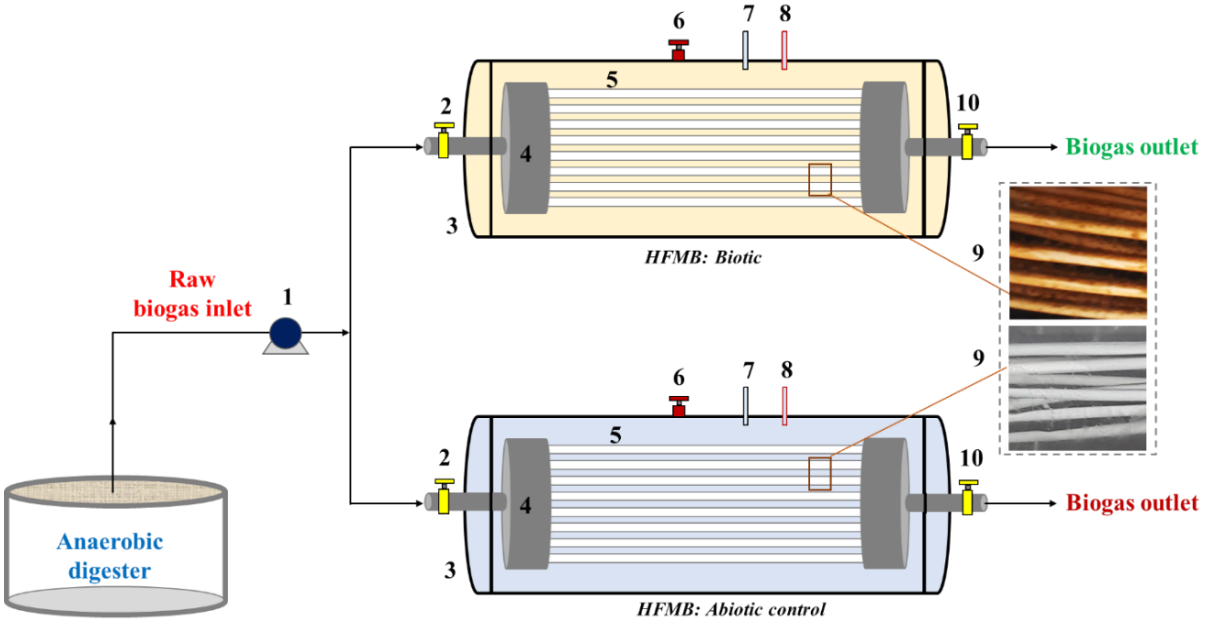

Figure 5.1: Schematic of raw biogas purification using two lab-scale HFMBs (biotic and abiotic control). [Note: HFMB - hollow fibre membrane bioreactor; 1. peristaltic pump; 2. inlet sampling point to measure the raw biogas composition and pressure before passing

through the membrane module; 3. glass column with a temperature-controlled water jacket outside; 4. submerged hollow fibre membrane module; 5. shell side of the membrane module where the abiotic and biotic HFMB contains nutrient salt medium (NSM) and microbial inoculum + NSM, respectively; 6. sampling point for collecting analytical and microbial samples and replacing the supernatant by fresh nutrient salt medium periodically; 7. pH probe; 8. dissolved oxygen (DO) probe; 9. photographs of used membranes for biotic and abiotic operation of HFMBs (on day 126); 10. outlet sampling point to measure biogas composition and pressure after passing through the membrane module].

5.2.5. Experimental design

Table 5.1 summarizes the raw biogas composition and operating conditions applied to the HFMBs. The biogas was continuously fed to the HFMB during its three cycles of operation. Three different flow rates of ~ 0.14, 0.27 and 0.54 L h^{-1}, corresponding to an EBRT of 187, 92 and 46 s, respectively, were applied in this study. The EBRT was kept constant at each cycle of operation, but the biogas composition fluctuated in a wide range (Table 5.1). During the first two cycles, the HFMBs were operated for a 6 week period each, while the biotic HFMB was operated for an extended period (~ 12 weeks) in a third cycle to test the resilience of the HFMB to treat raw biogas with high H_2S and NH_3 concentrations at shorter EBRT (46 s).

The shell side profiles including the pH change, dissolved oxygen (DO) concentrations, functional microorganisms and metabolic end products for the H_2S and NH_3 bioconversion were regularly monitored to investigate the effect of different ILRs and EBRTs. The pH of the reactor mixed liquor on the shell side was not controlled directly, but the supernatant of the liquor was periodically changed after a certain period (Table 5.1) to keep the pH in the ~ 3.5-7.0 range.

Table 5.1: Raw biogas composition and operating conditions applied to the HFMBs.

Operating cycles	Operating time, days	EBRT, s	Inlet raw biogas composition (Min-Max)						Inlet loading rate of		Shell side profile
			CH_4, %	CO_2, %	O_2, %	N_2*, %	H_2S, ppm_v	NH_3, ppm_v	H_2S, $g\ m^{-3}\ h^{-1}$	NH_3, $g\ m^{-3}\ h^{-1}$	Supernatant replacement**
HFMB 1 (Biotic)											
Cycle 1	0-42	187	39-69	28-49	0.2-6	0-26	63-1854	14-460	22 ± 11	4 ± 1	On day 42
Cycle 2	43-84	92	42-62	31-45	0.3-4	2-18	135-915	70-375	32 ± 11	6 ± 2	On day 63 and 84
Cycle 3	85-166	46	41-73	21-36	0.5-5	2-24	107-1687	60-1032	63 ± 47	21 ± 14	On day 93, 103, 126 and 160
HFMB 2 (Abiotic control)											
Cycle 1	0-42	187	41-58	29-45	1-6	5-24	64-1035	28-335	14 ± 4	3 ± 1	On day 42
Cycle 2	43-84	92	42-57	33-41	1-6	5-20	157-627	60-235	21 ± 9	4 ± 2	On day 63
Cycle 3	85-126	46	41-56	28-37	1-5	5-23	117-1905	80-800	58 ± 48	16 ± 10	-

Note: EBRT - empty bed residence time; * - This quantity was to balance gases in the biogas which was mainly N_2 and there was no H_2 present, however, there might have been some moisture and other trace compounds such as VOCs which were not considered in this study; ** - The supernatant from the shell side was replaced (~ 35-45%) with fresh nutrient salt medium (NSM) after a certain period of continuous operation to control the pH (at a certain level without any chemical addition) and to avoid inhibitory factors such as high sulfate concentrations

5.2.6. Calculations

The HFMB's performance parameters, i.e. the removal efficiency and elimination capacity were measured as described in Jaber et al. (2017). The flux (J) and overall mass-transfer coefficient (K_G) of H_2S and NH_3 were determined based on the experimental data using the following equations (Tilahun et al., 2017):

$$\mathrm{J}\ (\mathrm{g}\ m^{-2}\ h^{-1}) = \frac{Q}{A}(C_{in} - C_{out}) \quad (5.1)$$

$$\mathrm{K_G}(\mathrm{m}\ h^{-1}) = \frac{Q}{A}\ln\frac{C_{in}}{C_{out}} \quad (5.2)$$

where A is the surface area of the membrane (m^2), Q is the gas flow rate ($m^3\ h^{-1}$), C_{in} and C_{out} are, respectively, the inlet and outlet concentration ($g\ m^{-3}$).

The elemental sulfur (S^0) selectivity (%) for the bioconversion of H_2S in HFMB was calculated based on the mass balance Eq. (5.3) modified from Li et al. (2020):

$$P_{S^0} = \frac{([I_{H_2S}]-[O_{H_2S}]) - [P_{SO_4^{2-}\text{-}S}]-[P_{SO_3^{2-}\text{-}S}]-[P_{S_2O_3^{2-}\text{-}S}]-[R_{S^{2-}}]}{([I_{H_2S}]-[O_{H_2S}])} \quad (5.3)$$

where P_{S^0} is the elemental sulfur selectivity (%), $([I_{H_2S}] - [O_{H_2S}])$ is the amount of S^{2-} (mg) transferred through HFM and dissolved on the shell side of the HFMB during each cycle of operation; $P_{SO_4^{2-}\text{-}S}$, $P_{SO_3^{2-}\text{-}S}$ and $P_{S_2O_3^{2-}\text{-}S}$ are, respectively, the amount of SO_4^{2-}-S (mg), SO_3^{2-}-S (mg) and $S_2O_3^{2-}$-S (mg) produced for the same period of time and $R_{S^{2-}}$ is the dissolved S^{2-} (mg) remained on the shell side.

The nitrogen (N_2) selectivity (%) for the bioconversion of NH_3 in the HFMB was calculated based on the mass balance Eq. (5.4):

$$P_{N_2} = \frac{([I_{NH_3}]-[O_{NH_3}]) - [P_{NO_3^-\text{-N}}]-[P_{NO_2^-\text{-N}}]-[P_{N_2O-N}]-[R_{NH_4^+\text{-N}}]}{([I_{NH_3}]-[O_{NH_3}])} \quad (5.4)$$

where P_{N_2} is the nitrogen selectivity (%), $([I_{NH_3}] - [O_{NH_3}])$ is the amount of NH_3-N (mg) transferred through the HFM and dissolved on the shell side of the HFMB during each cycle of operation; $P_{NO_3^-\text{-N}}$, $P_{NO_2^-\text{-N}}$ and P_{N_2O-N} are, respectively, the amount of NO_3^--N (mg), NO_2^--N (mg) and N_2O-N (gas-phase, mg) produced for the same period of time and $R_{NH_4^+\text{-N}}$ is the dissolved NH_4^+-N (mg) remaining on the shell side.

5.2.7. Analytical methods

Gas and liquid phase

The inlet and outlet biogas composition was measured using a calibrated (QED Environmental System Limited, Coventry, UK) portable multi-gas analyzer (Biogas 5000, Geotech, UK). A gas chromatograph (GC, Agilent Technologies, USA) equipped with a thermal conductivity detector (TCD) and flame ionization detector (FID) was used to measure the H_2 and N_2O, respectively, in biogas. A digital manometer (measuring range of -1 to 3 bar; Keller LEO1, Switzerland) was used to measure the pressure of inlet and outlet biogas. The concentrations of sulfite (SO_3^{2-}), sulfate (SO_4^{2-}), thiosulfate ($S_2O_3^{2-}$), nitrite (NO_2^-) and nitrate (NO_3^-) in the reactor mixed liquor were measured using an ion chromatograph (Thermo Scientific™ Dionex™, USA). The sulfide (S^{2-}) concentration in the liquid was measured using a colorimetric method (Allen et al., 1993) and a UV/Vis spectrophotometer (Shimadzu UV-1900, Germany). The pH and DO concentrations of the liquid on the shell side were measured using a pH meter (Cole-Parmer 300 pH/ORP/Temperature 1/8-DIN Controller, USA) and DO meter (HACH HQ 40d, USA), respectively.

Electronic microscopy

Suspended biomass samples collected from the reactor on day 126 day were processed for both scanning electron microscopy (SEM, Hitachi S-4700, Germany) with energy dispersive X-ray spectroscopy (EDX) and transmission the electron microscopy (TEM, Hitachi S-4700, Germany), according to the standard operating procedure provided by Electron Microscopy Unit (NUI Galway) as described in detail by Li et al. (2020).

Microbial community analysis

The suspended biomass of the reactor mixed liquor was collected in triplicates with a 6 week interval, i.e. on days 0, 42, 84 and 126. The DNA was extracted from the collected samples using the DNeasy PowerSoil Kit (Qiagen, Germany), following the manufacturer's DNA extraction protocol. The obtained DNA samples were further processed by Novogene Institute (Beijing, China) for amplicon metagenomics sequencing as described in detail by Das et al. (2022b) and Jiang et al. (2019).

5.3. Results

5.3.1. Simultaneous H_2S and NH_3 removal from raw biogas

H_2S removal

Figure 5.2 shows the H_2S removal performance of the HFMBs for biotic and abiotic operation at an EBRT of 187, 92 and 46 s. The biotic HFMB achieved ~ 100% removal efficiency (RE) for inlet H_2S concentrations up to 2.62 g m^{-3} (1854 ppm_v), corresponding to an ILR of ~ 50 g m^{-3} h^{-1}, during the first 42 days operation at an EBRT of 187s. The pH of the reactor mixed liquor gradually dropped from ~ 7.0 to 5.8. In the next 42 days (i.e. days 43-84) operation at an EBRT of 92 s, the removal performance of the biotic HFMB was consistent and achieved ~ 100% RE with a maximum elimination capacity (EC_{max}) of ~ 50 g m^{-3} h^{-1} for an inlet H_2S concentration up to 1.29 g m^{-3} (915 ppm_v). The pH varied in the range of ~ 4.4-6.3 during that period. In the final 82 days (i.e. day 85-166) operation at an EBRT of 46 s, the RE of the biotic HFMB varied between ~ 85 to 97% (Figure 5.2a) when the inlet H_2S concentrations in raw biogas were higher than 1.68 g m^{-3} (1190 ppm_v). The biotic HFMB achieved an EC_{max} of ~ 162 g m^{-3} h^{-1} (Figure 5.2c) for an ILR of ~ 186 g m^{-3} h^{-1}, corresponding to an inlet H_2S concentration of 2.38 g m^{-3} (1687 ppm_v) at an EBRT of 46 s. The pH varied in the range of ~ 3.1-6.3 during that period.

In contrast, the RE of the abiotic HFMB decreased by ~ 10% (from ~ 32% at an EBRT of 187s to ~ 13% at an EBRT of 46s, Figure 5.2b) at each step of reducing the gas contact time, i.e. when the EBRT was switched from 187 s to 92 s followed by 46 s. Though the RE of the abiotic HFMB was usually in the range of ~ 7-14% for inlet H_2S concentrations up to 1.41 g m^{-3} (1000 ppm_v) at an EBRT of 46 s, the RE reached to ~ 19% when the inlet H_2S concentrations were comparatively higher (up to 2.69 g m^{-3} or 1905 ppm_v) and achieved an EC_{max} of ~ 39 g m^{-3} h^{-1} for an ILR up to ~ 210 g m^{-3} h^{-1} (Figure 5.2d). The pH was in the range of ~ 5.9-7.0 during the entire abiotic operation.

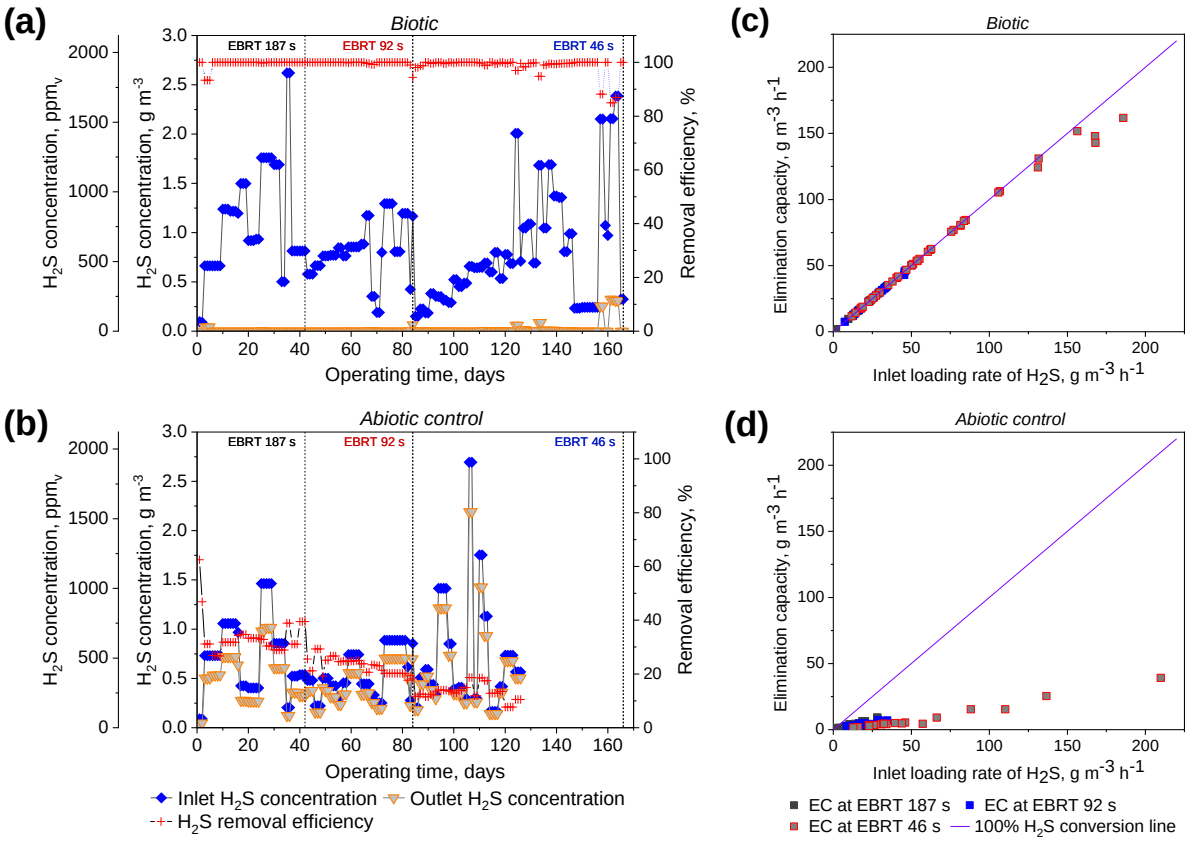

Figure 5.2: H_2S removal from raw biogas in HFMBs: removal efficiency for biotic (a) and abiotic (b) operation as well as elimination capacity for biotic (c) and abiotic (d) operation. [Note: the removal performance was observed at three different empty bed residence times (EBRT) of 187 s, 92 s and 46 s].

NH_3 removal

Figure 5.3 shows the NH_3 removal performance of the HFMBs for biotic and abiotic operation at an EBRT of 187, 92 and 46 s. The biotic HFMB achieved ~ 100% RE at both EBRTs of 187 and 92 s where the supplied biogas contained NH_3 concentrations up to 0.32 g m^{-3} (460 ppm_v), corresponding to an ILR of ~ 10 g m^{-3} h^{-1}. However, the RE varied between ~ 73 and 95% (Figure 5.3a) at an EBRT of 46 s when the inlet NH_3 concentrations in the biogas were in the range of 0.53-0.73 g m^{-3} (750-1032 ppm_v) and achieved an EC_{max} of ~ 45 g m^{-3} h^{-1} (Figure 5.3c).

The RE of the abiotic HFMB was initially ~ 100% for the first 2 days, then the RE was ~ 60% for the next 7 days (i.e. day 3-9) for inlet NH_3 concentrations of ~ 0.21 g m^{-3} (297 ppm_v) at an EBRT of 187 s. Thereafter, the RE gradually dropped and reached a constant value of ~ 30, 13 and 10% (Figure 5.3b) for an EBRT of 187, 92 and 46 s, respectively. The abiotic HFMB

achieved an EC_{max} of ~ 4 g m^{-3} h^{-1} for the employed ILR of 44 g m^{-3} h^{-1} (Figure 5.3d).

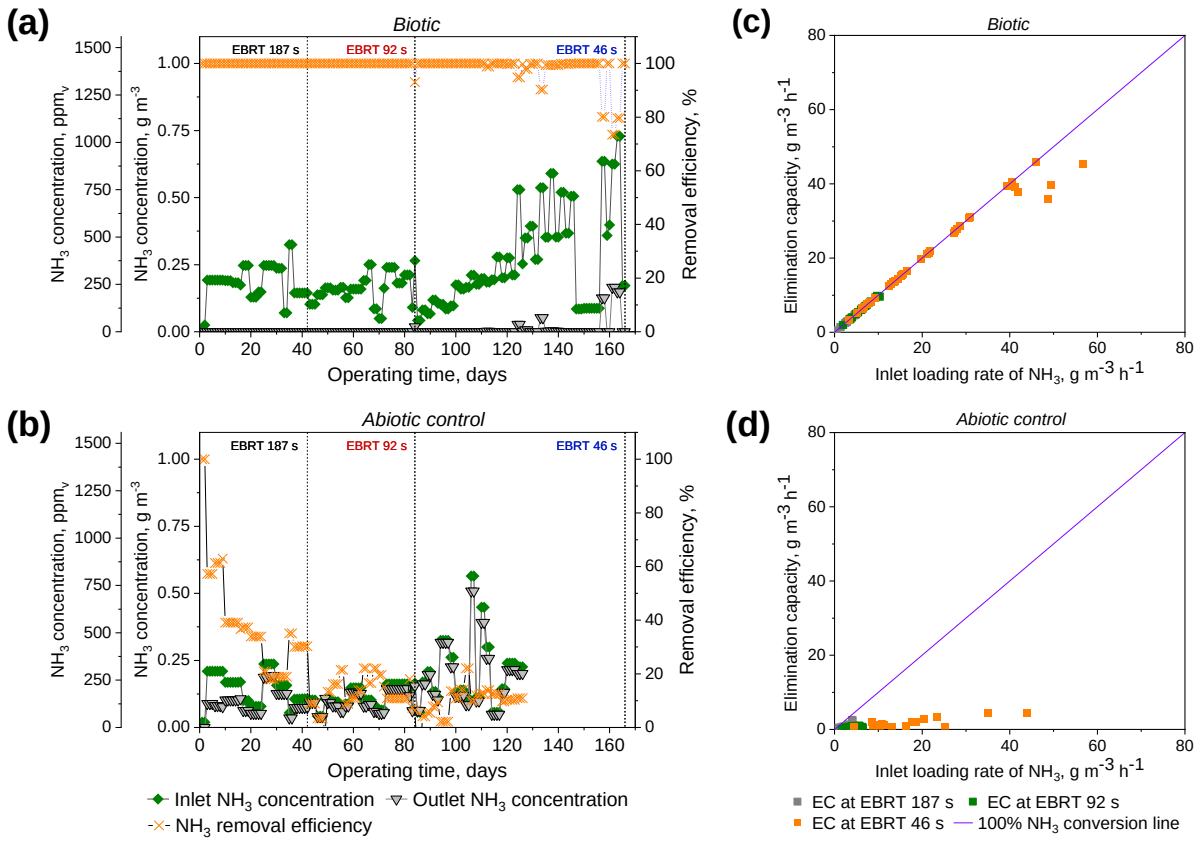

Figure 5.3: NH_3 removal from raw biogas in HFMBs: removal efficiency for biotic (a) and abiotic (b) operation as well as elimination capacity for biotic (c) and abiotic (d) operation. [Note: the removal performance was observed at three different empty bed residence times (EBRT) of 187 s, 92 s and 46 s].

Other biogas constituents

Figure 5.4 shows the CH_4, CO_2, N_2 and O_2 concentrations in the inlet and outlet biogas. The mean value (%) of CH_4: CO_2: N_2: O_2 in the raw biogas were, respectively, 53.97: 32.91: 10.97: 2.11 (inlet) and 53.41: 32.02: 12.34: 2.20 (outlet) for the biotic HFMB, and 49.26: 34.73: 13.13: 2.84 (inlet) and 48.57: 33.82: 14.61: 2.96 (outlet) for the abiotic HFMB, irrespective of the employed EBRTs. The outlet/inlet (O/I) ratio of CH_4, CO_2, N_2 and O_2 during the biotic operation of the HFMB was ~ 0.99, 0.97, 1.18 and 1.10, respectively (Figure 5.4a, 5.4c, 5.4e, and 5.4g). A similar O/I ratio for CH_4 (0.99), CO_2 (0.97), N_2 (1.14) and O_2 (1.06) was also observed for the abiotic operation of the HFMB (Figure 5.4b, 5.4d, 5.4f, and 5.4h).

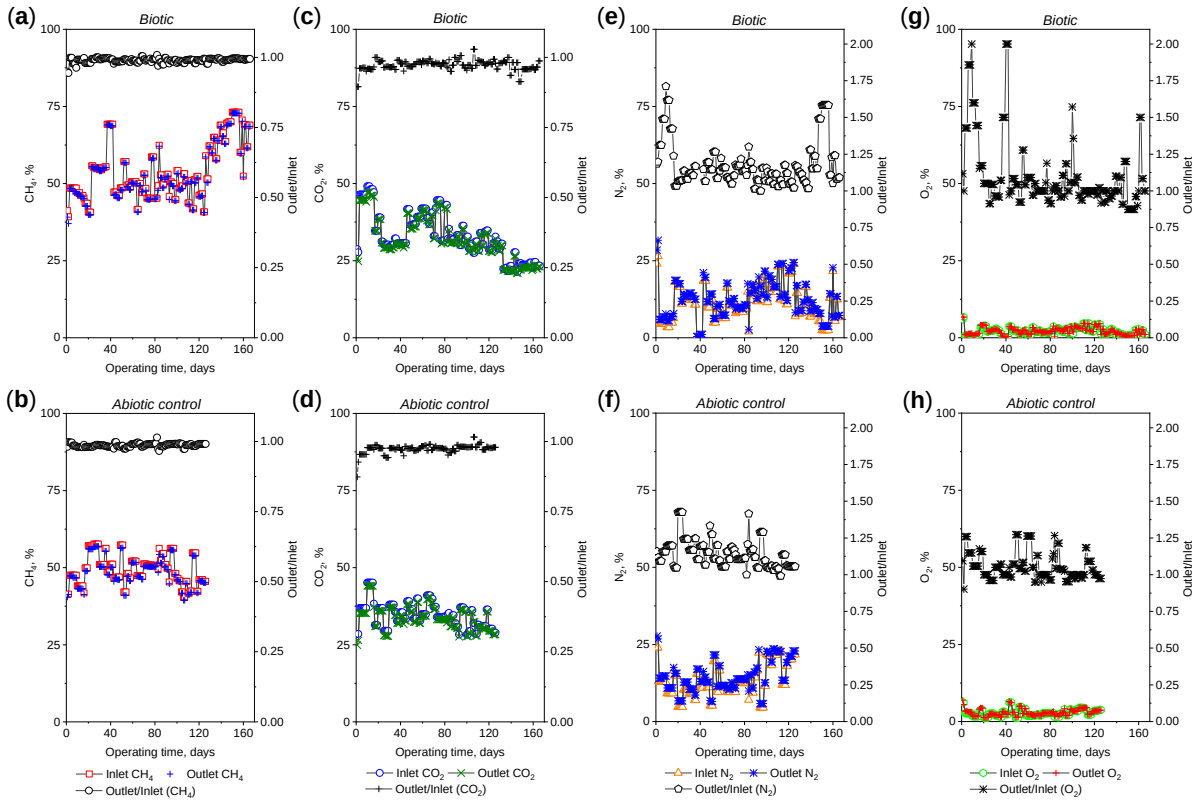

Figure 5.4: Inlet and outlet biogas composition in HFMBs: CH_4 (a), CO_2 (c), N_2 (e) and O_2 (g) profile for biotic operation as well as CH_4 (b), CO_2 (d), N_2 (f) and O_2 (h) profile for abiotic operation.

5.3.2. Flux and mass transfer of H_2S and NH_3 through the HFMBs

Table 5.2 summarizes the flux and gas-liquid mass transfer of H_2S and NH_3 in the HFMBs. Both the H_2S flux and overall mass transfer coefficient (K_G) for the biotic process increased gradually with the decrease in the EBRTs. The biotic HFMB achieved a maximum H_2S flux of 1.94 g m^{-2} day^{-1} and a K_G of 71 µm s^{-1} at an EBRT of 46s. The mean H_2S flux and K_G for the biotic HFMB at an EBRT of 46 s were ~ 7.3 and 36.2 times higher, respectively, compared to the abiotic HFMB. The mean NH_3 flux and K_G for the biotic HFMB were ~ 12 and 49 times higher, respectively, compared to the abiotic control.

Table 5.2: Comparison of flux and mass transfer profile for biotic and abiotic operation of HFMBs for simultaneous removal of H_2S and NH_3 from raw biogas.

Reactor operating time, days	EBRT, s	H_2S profile*		NH_3 profile*	
		H_2S flux, g m^{-2} day^{-1}	Overall mass transfer coefficient (K_G) of H_2S, µm s^{-1}	NH_3 flux, g m^{-2} day^{-1}	Overall mass transfer coefficient (K_G) of NH_3, µm s^{-1}
HFMB 1 (Biotic)					
0-42	187	0.26 (0.61) ± 0.13	17 (20) ± 3	0.04 (0.07) ± 0.02	15 (16) ± 2
43-84	92	0.38 (0.60) ± 0.13	33 (37) ± 4	0.08 (0.12) ± 0.02	29 (32) ± 3
85-166	46	0.73 (1.94) ± 0.51	55 (71) ± 12	0.24 (0.55) ± 0.15	53 (71) ± 14
HFMB 2 (Abiotic control)					
0-42	187	0.05 (0.11) ± 0.03	1.09 (2.62) ± 0.29	0.01 (0.03) ± 0.01	1.60 (2.65) ± 1.76
43-84	92	0.06 (0.09) ± 0.02	1.42 (1.88) ± 0.21	0.01 (0.01) ± 0.003	0.75 (1.35) ± 0.36
85-126	46	0.10 (0.47) ± 0.11	1.52 (2.23) ± 0.35	0.02 (0.05) ± 0.02	1.08 (2.70) ± 0.76

Note: EBRT - empty bed residence time; * - Arithmetic mean (maximum value) ± standard deviation was used for each cycle of HFMBs operation for each employed EBRT.

5.3.3. Metabolic products for H_2S and NH_3 bioconversion

Table 5.3 summarizes the sulfur and nitrogen mass balance for H_2S and NH_3 conversion in the HFMBs. There was no SO_3^{2-} and $S_2O_3^{2-}$ formation, and the residual S^{2-} concentrations were < 0.50 mg L^{-1} at the end of the biotic operation (at an EBRT of 46 s), suggesting a complete bioconversion of S^{2-} (> 99%) into S^0 or SO_4^{2-}. The mean SO_4^{2-} selectivity was 48% for the biotic operation of the HFMB. The DO concentrations (~ 6.50-7.75 mg L^{-1}) of the reactor mixed liquor declined rapidly to 0.30-1.25 mg L^{-1} during each supernatant replacement period (Table 5.1). The S^0 selectivity was ~ 55% at an EBRT of 46 s.

The SEM-EDX and TEM images of the suspended biomass suggest the presence of S^0 in the biomass (Figure 5.5a) and possible S^0 accumulation in the periplasmic space (Figure 5.5b). NO_2^- and NO_3^- were not detected in the reactor liquor, and the biogas (both the inlet and outlet) did not contain any N_2O (Table 5.3). The mean N_2 selectivity was ~ 90% where the remaining 10% was the residual NH_4^+ in the HFMB mixed liquor at the end of each employed EBRT.

Table 5.3: Sulfur and nitrogen mass balance for simultaneous removal of H_2S and NH_3 from raw biogas.

Reactor operating time, days	EBRT, S	Sulfur mass balance							Nitrogen mass balance					
		S^{2-} [a], mg	SO_4^{2-}-S produced, mg	SO_3^{2-}-S produced, mg	$S_2O_3^{2-}$-S produced, mg	S^{2-} [b], mg	SO_4^{2-} selectivity, %	S^0 selectivity, %	NH_4^+-N[c], mg	NO_3^--N, mg	NO_2^--N, mg	NH_4^+-N[d], mg	N_2O-N, mg	N_2 selectivity, %
HFMB 1 (Biotic)														
0-42	187	142	56	BDL	BDL	0.01	39	61	20	BDL	BDL	2	BDL	90
43-84	92	209	127	BDL	BDL	0.23	60	40	36	BDL	BDL	5	BDL	86
85-166	46	749	340	BDL	BDL	0.50	45	55	212	BDL	BDL	19	BDL	91
HFMB 2 (Abiotic control)														
0-42	187	9	BDL	BDL	BDL	5	NA	NA	~ 3	BDL	BDL	BDL	BDL	NA
43-84	92	17	BDL	BDL	BDL	9	NA	NA	~ 1	BDL	BDL	BDL	BDL	NA
85-126	46	8	BDL	BDL	BDL	4	NA	NA	~ 2	BDL	BDL	BDL	BDL	NA

Note: [a] - The amount of gas-phase sulfide transferred through membrane fibres and dissolved on the shell side; [b] - The amount of sulfide remaining on the shell side at the end of each cycle; c - The amount of ammonium-nitrogen on the shell side due to the transfer of gas-phase ammonia through membrane fibres; [d] - The amount of ammonium-nitrogen remaining on the shell side at the end of each cycle; EBRT - empty bed residence time; NA - not applicable; BDL - below detection limit.

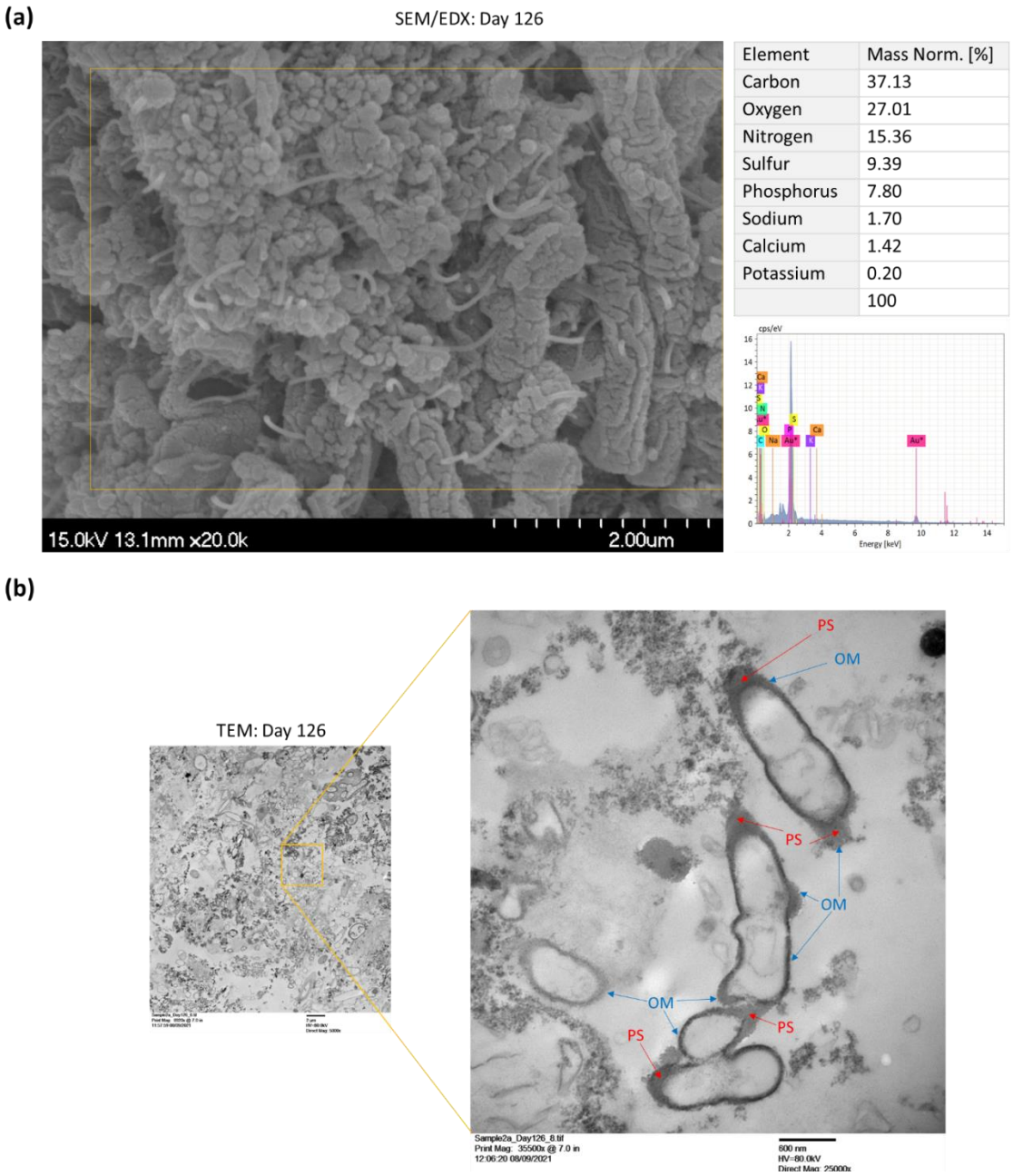

Figure 5.5: Electron microscopic observations of the HFMB sludge biomass sampled on day 126 (after 6 weeks operation at EBRT of 46 s): (a) SEM-EDX analysis and (b) TEM analysis [Note: OM - Outer-membrane (blue arrows), PS - Periplasmic space (red arrows)].

5.3.4. Microbial community in the HFMB

Proteobacteria, *Halobacterota*, *Bacteroidota*, *Firmicutes* and *Actinobacteriota* were the top 5 abundant phyla (with ~ 75% relative abundance) observed in the HFMB during the entire operational period (Figure 5.6a). The biomass contained about 1434-1562 operational taxonomic units (OTUs). The microbial genera *Rhodanobacter*,

Williamwhitmania, *Sulfuricurvum*, *Chlorobium*, *Acinetobacter*, *Clostridium_sensu_stricto_12* and *Methanosaeta* accounted for ~ 40% of the total genus-level microbiota present in the HFMB (Figure 5.6b). With regard to the H_2S and NH_3 bioconversion in the HFMB, diverse functional microorganisms such as aerobic and anoxic sulfur-oxidizers, aerobic ammonium oxidizers, Fe(III) reducing ammonium oxidizers, denitrifiers, and denitrifying phosphorus accumulating organisms were present at genus level (Table 5.4), where the relative abundance of the genera varied among the sampling time.

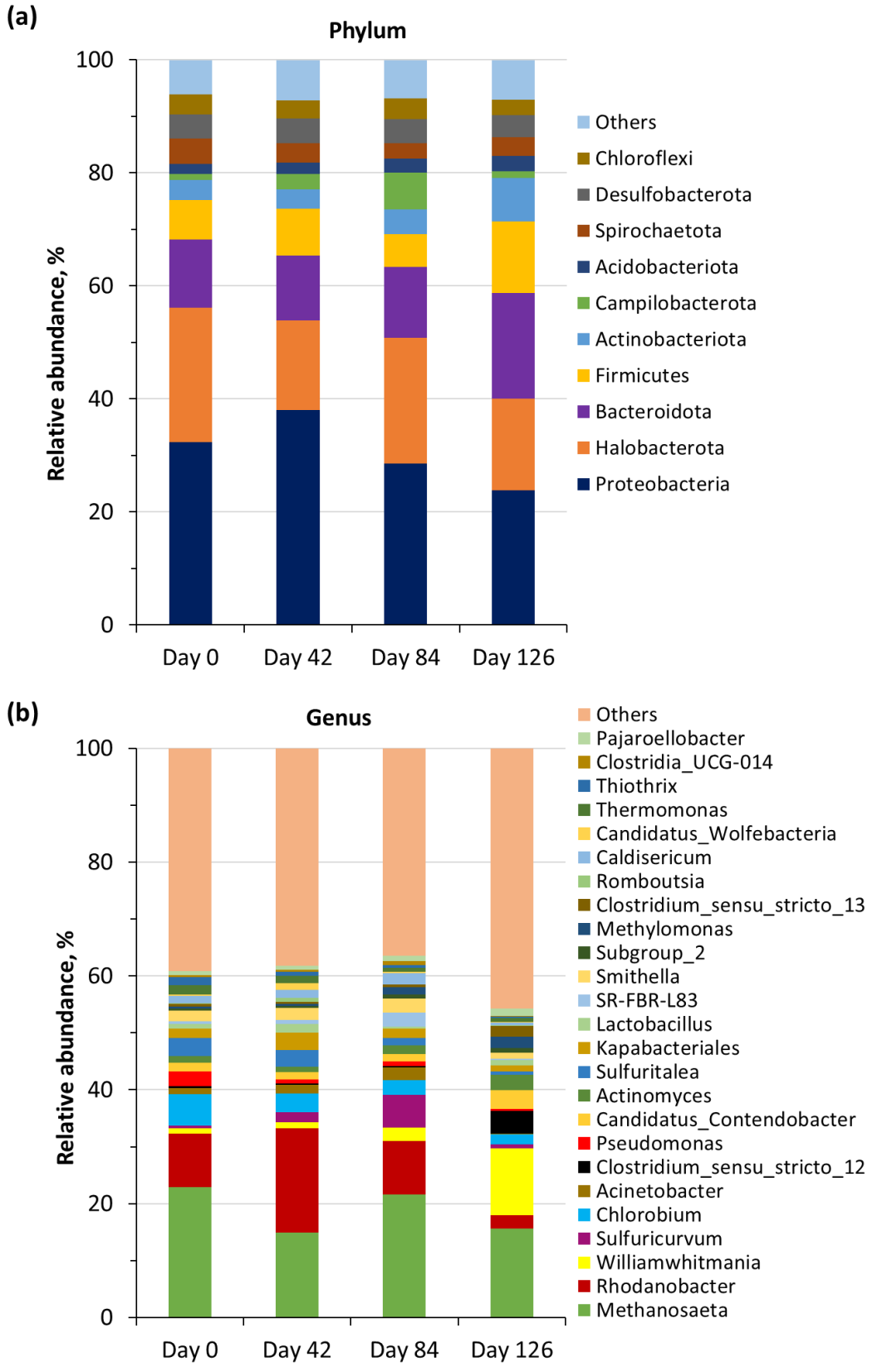

Figure 5.6: Taxa relative abundance of top 10 phyla (a) and top 25 genera (b) present in the suspended biomass of the HFMB sampled at different stages of the HFMB

operation, i.e. at the starting of the operation using acclimatized sludge inoculum (day 0), at the end of EBRT of 187s (on day 42), at the end of EBRT of 92 s (on day 84), and after 6 weeks operation at an EBRT of 46 s (on day 126).

Table 5.4: Predominant functional microbial genera associated with H_2S and NH_3 bioconversion processes observed at different stages of the HFMB operation.

Microbial genera[1]	**Taxa relative abundance, %**				**Reference**[2]
	Day 0	Day 42	Day 84	Day 126	
Sulfide oxidizers: Aerobic chemolithotrophs					
Sulfuricurvum	0.465	1.748	5.783	0.710	Haosagul et al., 2020
Sulfurovum	0.425	0.329	0.273	0.293	
Pseudomonas	2.521	0.670	0.822	0.373	
Smithella	1.965	2.101	2.444	1.028	
Thiomonas	0.161	0.136	0.264	0.733	
Thiovirga	0.008	0.011	0.010	0.028	
Arcobacter	0.018	0.009	0.030	0.048	
Thiothrix	1.467	0.727	0.362	0.293	
Magnetospirillum	0.003	0.005	0.007	0.022	
Sphingobium	0.002	0.002	0.003	0.003	
Novosphingobium	0.007	0.002	0.010	0.007	
Acidithiobacillus	0.002	0.007	0.010	0.005	
Sulfide oxidizers: Anoxic chemolithotrophs (autotrophic denitrification)					
Rhodanobacter	9.490	18.288	9.423	2.374	Cai et al., 2020;
Sulfuritalea	3.147	2.995	1.258	0.531	Kumar et al., 2018;
Hydrogenophaga	0.235	0.163	0.123	0.227	Haosagul et al., 2020;
Thiobacillus	0.194	0.215	0.383	0.183	
Acinetobacter	1.020	1.452	2.251	0.131	
Sulfurimonas	0.075	0.301	0.323	0.076	
Sulfuricella	0.096	0.126	0.147	0.021	
Halothiobacillus	0.001	0.001	0.005	0.000	
Sulfide oxidizers: phototrophs					
Chlorobium	5.531	3.345	2.599	1.709	Haosagul et al., 2020;
Thiobaca	0.004	0.003	0.006	0.002	Aliboni et al., 2015
Rhodopseudomonas	0.236	0.179	0.265	1.104	
Rhodobacter	0.006	0.005	0.008	0.013	
Ammonium oxidizer (aerobic)					
Pseudomonas	RA	RA	RA	RA	Zheng et al., 2021;
Stenotrophomonas	0.011	0.040	0.089	0.043	Wei et al., 2021;
Nitrosospira	0.004	0.004	0.007	0.011	Wu et al., 2011;
Nitrosomonas	0.013	0.012	0.001	0.006	Monteiro et al., 2014
Ammonium oxidizer (Fe(III) reducing)					
Clostridium_sensu_stricto_12	0.450	0.301	0.258	3.978	Rodríguez et al., 2021
Rhodoferax	0.602	0.538	0.268	0.433	
Dechloromonas	0.161	0.179	0.167	0.209	
Anaeromyxobacter	0.000	0.001	0.003	0.025	
Thermoanaerobaculum	0.040	0.041	0.023	0.024	
Geobacter	0.005	0.001	0.002	0.005	
Denitrifiers					
Sphingomonas	0.009	0.016	0.035	0.038	Zheng et al., 2021;
Rhodanobacter	RA	RA	RA	RA	Wang et al., 2021;
Candidatus_Solibacter	0.082	0.123	0.201	0.231	Huang et al., 2020
Haliangium	0.008	0.005	0.007	0.017	
Hyphomicrobium	0.206	0.147	0.198	0.451	
Lentimicrobium	0.008	0.004	0.006	0.006	
Terrimonas	0.030	0.023	0.026	0.029	

Thermomonas	1.594	1.323	0.819	0.699	
Denitrifying phosphorus accumulating organisms (DPAO)					
Candidatus_Contendobacter	1.569	1.240	1.263	3.326	Huang et al., 2020
Candidatus_Accumulibacter	0.032	0.018	0.019	0.014	
Dechloromonas	RA	RA	RA	RA	

Note: [1] - The functional microbial genera listed here have been identified from ~ 705 genera, and more functional microbial genera were present which have not been included in the list but might have contributed to H_2S and NH_3 bioconversion processes; [2] - Functional microbial genera reported in the literature; RA - reported above for other type of activity

5.4. Discussion

5.4.1. Raw biogas purification performance of the HFMB

This study showed that the biotic HFMB can simultaneously treat H_2S (~ 100% RE for inlet H_2S concentrations up to ~ 1850 and 1200 ppm_v at an EBRT of 187 and 46 s, respectively, and an EC_{max} of ~ 162 g m^{-3} h^{-1}, Figure 5.2a and 5.2c) and NH_3 (~ 100% RE for inlet NH_3 concentrations up to ~ 460 and 750 ppm_v at an EBRT of 187 and 46 s, respectively, and an EC_{max} of ~ 45 g m^{-3} h^{-1}, Figure 5.3a and 5.3c) present in raw biogas during its long-term operation (~ 6 months) at different operating conditions (Table 5.1). Achieving a critical load of ~ 150 g m^{-3} h^{-1} of H_2S (Figure 5.2c) and ~ 40 g m^{-3} h^{-1} of NH_3 (Figure 5.3c) demonstrated the resilience of the HFMB to handle the fluctuations in loading rates, mainly for raw biogas with a higher H_2S (~ 1200-1700 ppm_v) and NH_3 (~ 750-1050 ppm_v) concentration at an EBRT of 46s. Although the HFMB can tolerate a higher load of H_2S and NH_3, the removal performance of the HFMB can also be influenced by other operational parameters such as the EBRT (Zhuo et al., 2019) to allow sufficient gas contact time to the functional microorganisms for efficient bioconversion of the contaminants or the type of sulfide oxidizers present in the reactor and their optimum pH (Pokorna and Zabranska, 2015).

The consistent performance of the biotic HFMB suggests that ~ 100% of the supplied H_2S and NH_3 from raw biogas diffused through the hollow fibres and dissolved in the reactor mixed liquor, where the microbial consortia present (Table 5.4) removed the H_2S and NH_3. The O/I ratios of H_2S and NH_3 of the abiotic HFMB suggest that a small quantity of the H_2S (Figure 5.2b) and NH_3 (Figure 5.3b) from raw biogas diffused through the hollow fibres and dissolved in the liquid on the shell side during the abiotic operation. The sulfide and nitrogen mass balance (Table 5.3) confirm that the dissolved H_2S and NH_3 were not involved in bioconversion process in the abiotic reactor. Apart from the

H_2S and NH_3 removal performance of the HFMB, the O/I ratio of CH_4 (Figure 5.4a-b) suggests that there is a little chance (< 1%) of biogas dilution in the HFMBs, in terms of CH_4 content, which is expected due to the lower solubility of CH_4 in water and lack of high operational pressure to diffuse CH_4 through the hollow fibres onto the shell side of the HFMB.

Long-term desulfurization performance of the HFMB (Chapter 4) revealed that the membrane attached biofilm favoured the desulfurization process and there were no membrane fouling or wetting issues. Also in this study, no membrane fouling or wetting occurred. The reason for the absence of membrane wetting can be related to the HFMB features such as static shell side (Chapter 4) and the absence of absorption chemicals (Mirfendereski et al., 2019). A review on biological methods for H_2S and NH_3 removal (Barbusiński et al., 2021) emphasized the need for further research on innovative biotechnologies to handle industrial scale issues (e.g. sudden increases in pollutant concentrations or flow rates) and overcome the limitations (e.g. useful for low concentrations of pollutants) of the commonly used bioreactors such as biofilter. The HFMB can be such a technology for odour treatment and biogas purification with high H_2S and NH_3 concentrations due to its consistent performance for the entire period. To retain ~ 100% RE in the HFMB, especially for higher inlet concentrations of H_2S (> 1700 ppm_v) and NH_3 (> 1000 ppm_v), the EBRT can also be switched between 46 and 92 s.

5.4.2. HFMB for mixed pollutant removal from gases

This is, to the authors knowledge, the first report on the application of a HFMB for treating simultaneously H_2S and NH_3 from raw biogas. The long-term performance of the HFMB in terms of inlet concentrations, RE and EC of both target pollutants, i.e. H_2S (Figure 5.2) and NH_3 (Figure 5.3), and post-treatment biogas composition (Figure 5.4) suggests that the HFMB used in this study is more promising compared to that of other bioreactor types, such as biofilters (Gandu et al., 2021; Malhautier et al., 2003; Zheng et al., 2021), biotrickling filters (Huan et al., 2021; Jiang et al., 2009) and airlift bioreactors (Chen et al., 2018).

The RE of both H_2S and NH_3 in a pilot-scale biofilter were in the range of 90-99% at an EBRT of 55 s where the inlet concentrations of both pollutants in the air stream were in the range of 200-210 ppm_v (Gandu et al., 2021). Huan et al. (2021) reported a semi-

pilot scale biotrickling filter (BTF) that achieved ~ 89% RE of NH_3 (with an EC_{max} of 39 g m^{-3} h^{-1}) and ~ 98% RE of H_2S (with an EC_{max} of 85 g m^{-3} h^{-1}) for inlet concentrations up to 500 ppm_v at EBRTs of ~ 32-43 s under aerobic conditions. However, the RE of both NH_3 and H_2S decreased significantly (by ~ 8% for NH_3 and ~ 31% for H_2S) when the EBRT was switched from ~ 32 to 25 s (Huan et al., 2021). An airlift bioreactor was used for NH_3 and H_2S contaminated waste gas treatment, and achieved ~ 99% RE for inlet concentrations up to 400 ppm_v at an EBRT of 20 s, where Fe_2O_3 was added to improve the RE of H_2S through rapid oxidation of H_2S to S^0 (Chen et al., 2018).

Integration of several bioreactor configurations can help to address simultaneous treatment of wastewater and waste gas. For example, González-Cortés et al. (2021) reported nitrification and anoxic desulfurization in a two-stage system. In the first stage, nitrification of NH_4^+ to NO_2^- and NO_3^- took place in a continuously stirred tank bioreactor (CSTB), then NO_2^-/NO_3^- rich effluents from the CSTB were fed to a gas-lift bioreactor for anoxic desulfurization of H_2S to S^0 by nitrate-reducing and sulfide oxidizing bacteria (NR-SOB) including *Sulfurimonas* sp. (González-Cortés et al., 2021). However, very few studies have reported wastewater and waste gas treatment using a single bioreactor set-up. The bioconversion pathways of H_2S and NH_3 in the HFMB (see below) and enrichment of functional microorganisms in the HFMB biomass (Table 5.4) suggest that the HFMB can be used for nutrient (e.g. NO_3^-, NH_4^+, PO_4^{3-}) recovery from wastewater and gas-phase biological H_2S removal, simultaneously. This requires further research to optimize the operational parameters on shell-side of the HFMB such as optimum substrate concentration, N/S ratio, hydraulic retention time or DO concentration.

5.4.3. Bioconversion of H_2S and NH_3 in the HFMB

The flux and mass transfer profile (Table 5.2) of the HFMBs suggests that biotic processes mainly contributed to the flux and mass-transfer of H_2S and NH_3 through the hollow fibres. The 16S rRNA sequencing confirmed the richness of the microbial community (Figure 5.6) in the HFMB, and both aerobic and anoxic processes contributed to H_2S and NH_3 bioconversion (Table 5.4). The reasons for the variation of the relative abundance (at phylum and genus level) of the functional microorganisms in the HFMB can be associated with the applied operating conditions such as high inlet H_2S concentrations (Haosagul et al., 2020), increase of loading rates when switching EBRT

(from 187 to 46 s) or pH (Pokorna and Zabranska, 2015). *Proteobacteria*, the most abundant phylum in the HFMB (Figure 5.6a), are the predominant phylum in different H_2S treating bioreactor configurations, including microbial fuel cells treating sulfide and nitrate simultaneously (Cai et al., 2020), bioscrubber treating H_2S (Haosagul et al., 2020) and airlift bioreactor treating both H_2S and NH_3 (Chen et al., 2018).

Different sulfide oxidizers such as phototrophs and chemolithotrophs (Table 5.4) contributed to the biological oxidation of H_2S in the HFMB. Phototrophic sulfide oxidizers gain energy utilizing light energy, whereas chemolithotrophic sulfide oxidizers obtain energy from the oxidation of H_2S to S^0 and SO_4^{2-}, using either O_2 or NO_3^- as electron acceptor (Pokorna and Zabranska, 2015). Chemolithotrophs (e.g. *Rhodanobacter* sp. and *Thiobacillus* sp.) are more suitable for biological sulfide oxidation in both natural environments and bioreactors, even with limited O_2 supply, compared to the phototrophs, e.g. *Chlorobium* sp. (Pokorna and Zabranska, 2015). The sulfide oxidizing genera *Rhodanobacter* (~ 10% relative abundance) and *Chlorobium* (~ 2.55% relative abundance) were the most abundant, respectively, chemolithotrophs and phototrophs, present in the HFMB biomass (Figure 5.6b). *Chlorobium limicola*, a photoautotrophic anaerobe and a member of the green sulfur bacteria, has potential for biogas clean-up as it oxidises H_2S to S^0 through an anoxygenic photosynthetic process (Aliboni et al., 2015). The sulfide oxidizing genera *Sulfurovum*, *Sulfuricurvum and Thiothrix* are primary contributors in industrial-scale desulfurization of H_2S from biogas under aerobic conditions (Haosagul et al., 2020). Under anoxic conditions, *Sulfurimonas* and *Rhodanobacter* were the most dominant NR-SOB in microbial fuel cells treating sulfide and nitrate concurrently (Cai et al., 2020).

In the absence of free O_2 (anoxic conditions), the NO_3^- generated from the nitrification of NH_3 (by the ammonia oxidizers) can be utilized by the NR-SOB (López et al., 2017) for the oxidation of H_2S. Nitrification is a key biological process where aerobic oxidation of NH_3 takes place in two steps, i.e. NH_4^+ to NO_2^- and NO_3^-, by the ammonia oxidizers (Monteiro et al., 2014). The RE of both NH_3 and H_2S was positively correlated with the functional bacteria (e.g. *Pseudomonas* sp.) present in the biofilters and negatively correlated with the ILR (Zheng et al., 2021). *Pseudomonas* is one of the top 10 genera present in the HFMB biomass (Figure 5.6b). *Pseudomonas aeruginosa* can perform both nitrification and denitrification depending on the nitrogen species (i.e. NH_4^+, NO_3^- and

NO_2^-) present in the system (Wei et al., 2021). Though *P. aeruginosa* prefers heterotrophic nitrification of NH_4^+, denitrification of NO_3^- and NO_2^- prevails when the NH_4^+ concentration is nearly depleted in the system (Wei et al., 2021).

Enrichment of aerobic ammonia oxidizers (Table 5.4) including *Pseudomonas stutzeri*, *Pseudomonas aeruginosa* and *Nitrosomonas europaea* in the HFMB suggests that nitrification took place in the HFMB. Furthermore, the relative abundance of Fe(III) reducing ammonium oxidizers (e.g. *Clostridium_sensu_stricto_12* sp., *Rhodoferax* sp. and *Dechloromonas* sp.; Table 5.4), especially during the HFMB operation at an EBRT of 46 s, suggests that Fe(III) dependent anaerobic NH_4^+ oxidation to N_2 or NO_3^- and NO_2^- (i.e. Feammox process; Rodríguez et al., 2021) can be another NH_3 bioconversion pathway in the HFMB during that period. As the pH was in the acidic range (~ 3.1-6.3) in the HFMB, bioconversion of NH_4^+ to NO_3^- and NO_2^- can prevail (Rodríguez et al., 2021). The source of Fe(III) in the HFMB was likely the nutrient salt medium used.

Apart from nitrification, also denitrification took place in the HFMB, evidenced by the enrichment of denitrifiers such as *Thermomonas* sp., *Hyphomicrobium* sp. and *Candidatus_Solibacter* sp. (Table 5.4). The presence of dominant denitrifying phosphorus accumulating organisms (DPAO) including *Candidatus_Contendobacter* sp., *Candidatus_Accumulibacter* sp. and *Dechloromonas* sp. in the HFMB suggests that DPAO could have played an important role in the denitrification pathway by utilizing NO_x^--N as an electron acceptor to accumulate phosphorus in the form of polyphosphate (Huang et al., 2020).

The DO concentration in the liquid phase and the O/I ratio of O_2 indicates that a small fraction of O_2 (Figure 5.4g and 5.4h) diffused through the hollow fibres. Hence, both an aerobic (probably adjacent to the submerged membrane module) and an anaerobic/anoxic (probably bottom and edge of the reactor) zone could have developed in the liquid on the shell side of the HFMB. The N_2 and S^0 selectivity, and the absence of NO_3^- and NO_2^- (Table 5.3) in the liquid phase (on the shell side) clearly indicate that nitrification of NH_3 followed by denitrification, and both aerobic and anoxic desulfurization of H_2S from biogas took place in the HFMB. The molar ratio of N/S in the mixed suspended liquor can also have an influence on the selectivity of the H_2S oxidation to S^0 or SO_4^{2-} (Cai et al., 2020). NO_3^-, NO_2^-, S^0 and SO_4^{2-} were the main end products for treating NH_3 and H_2S,

simultaneously, under aerobic conditions in biofilters (Malhautier et al., 2003; Zheng et al., 2021) and biotrickling filters (Huan et al., 2021; Jiang et al., 2009). The competition for O_2 (between the sulfide and ammonia oxidizers in the HFMB) may result in O_2 limitation. End product selectivity (~ 55% S^0 and ~ 90% N_2) and the presence of residual NH_4^+ (Table 5.3) in the biotic HFMB could be the combined effects of the activities of ammonia oxidizers and sulfide oxidizers, including the NR-SOB.

The H_2S and NH_3 bioconversion pathway (Figure 5.7) in the HFMB could thus include the following steps: (i) H_2S oxidation to S^0 and SO_4^{2-} by sulfide oxidizers using O_2 as electron acceptor, (ii) nitrification of NH_3 to NO_2^- and NO_3^- by aerobic as well as Fe(III) reducing ammonia oxidizers, (iii) anoxic desulfurization, i.e. denitrification of NO_3^- to N_2 coupled to oxidation of H_2S to S^0 and SO_4^{2-} by NR-SOB, and (iv) denitrification by the denitrifiers including DPAO. Further research using N^{15} tracing experiments (Zhu et al., 2011) and fluorescence in situ hybridization (FISH) using specific probes (Borgne and Baquerizo, 2019) can further elucidate the bioconversion pathways that took place during simultaneous nitrification and anoxic desulfurization in HFMB.

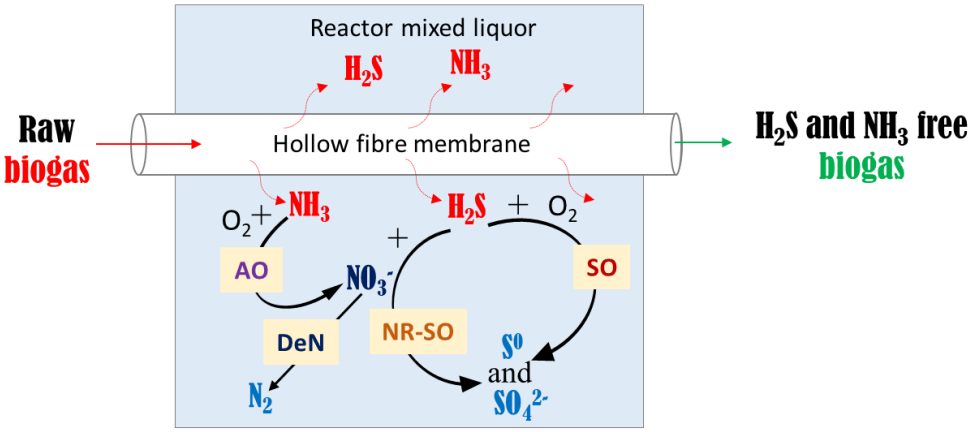

Reaction mechanism

(i) H_2S oxidation by the sulfide oxidizers (SO):

Phototrophs

$2H_2S + CO_2 + light \rightarrow 2S^0 + CH_2O + H_2O$

$H_2S + 2CO_2 + 2H_2O + light \rightarrow SO_4^{2-} + 2CH_2O + 2H^+$

Chemolithotrophs (aerobic)

$2HS^- + O_2 \rightarrow 2S^0 + 2OH^-$

$2S^0 + 3O_2 + 2OH^- \rightarrow 2SO_4^{2-} + 2H^+$

$H_2S + 2O_2 \rightarrow SO_4^{2-} + 2H^+$

(ii) NH_3 oxidation by the ammonia oxidizers (AO)

Aerobic

$NH_3 + H^+ \rightleftharpoons NH_4^+$

$NH_3 + 1.5O_2 \rightarrow NO_2^- + H^+ + H_2O$

$NO_2^- + 0.5O_2 \rightarrow NO_3^-$

Fe (III) reducing

$3Fe(OH)_3 + 5H^+ + NH_4^+ \rightarrow 3Fe^{2+} + 9H_2O + 0.5N_2$

$6Fe(OH)_3 + 10H^+ + NH_4^+ \rightarrow 6Fe^{2+} + 16H_2O + NO_2^-$

$8Fe(OH)_3 + 14H^+ + NH_4^+ \rightarrow 8Fe^{2+} + 21H_2O + NO_3^-$

(iii) H_2S oxidation by nitrate reducing sulfide oxidizers (NR-SO)

Chemolithotrophs (anoxic)

$5S^{2-} + 8NO_3^- + 8H^+ \rightarrow 5SO_4^{2-} + 4N_2 + 4H_2O$

$5S^{2-} + 2NO_3^- + 12H^+ \rightarrow 5S^0 + N_2 + 6H_2O$

$4HS^- + NO_3^- + 6H^+ \rightarrow 4S^0 + NH_4^+ + 3H_2O$

(iv) Denitrification by the denitrifiers (DeN)

Phosphorus accumulating DeN

$2NO_3^- + 12H^+ \rightarrow N_2 + 6H_2O$

Dominant genera

SO (Phototrophs)
Chlorobium, *Rhodopseudomonas*

SO (Aerobic chemolithotrophs)
Smithella, *Sulfuricurvum*, *Thiomonas*

AO
Pseudomonas, *Stenotrophomonas*, *Nitrosospira*

AO (Fe(III) reducing)
Clostridium_sensu_stricto_12, *Rhodoferax*, *Dechloromonas*

NR-SO (Anoxic chemolithotrophs)
Rhodanobacter, *Sulfuritalea*, *Thiobacillus*

DeN
Thermomonas, *Rhodanobacter*, *Hyphomicrobium*
Phosphorus accumulating DeN
Candidatus_Contendobacter, *Dechloromonas*

Figure 5.7: Possible H_2S and NH_3 bioconversion pathways prevailing in the HFMB fed with raw biogas.

5.5. Conclusions

The simultaneous H_2S and NH_3 removal performance of a hollow fibre membrane bioreactor (HFMB) was tested under different operating conditions including different gas contact times and raw biogas composition. The HFMB efficiently treated both H_2S and NH_3 from raw biogas during its ~ 6 months continuous operation without diluting CH_4, the main target ingredient of biogas (O/I ratio of CH_4 ~ 0.99). The RE of H_2S was ~ 100% with an EC of ~ 50, 50 and 131 g m^{-3} h^{-1} at an EBRT of 187, 92 and 46 s, respectively, for inlet H_2S concentrations up to ~ 1850, 915 and 1200 ppm_v, respectively. While the RE of NH_3 was ~ 100% with an EC of ~ 6, 10 and 40 g m^{-3} h^{-1} at an EBRT of 187, 92 and 46 s, respectively, for inlet NH_3 concentrations up to ~ 460, 355 and 750 ppm_v, respectively. The HFMB demonstrated resilience to handle high loading rates of H_2S (~130-186 g m^{-3} h^{-1}, corresponding concentration of ~ 1200-1700 ppm_v) and NH_3 (~ 41-56 g m^{-3} h^{-1}, corresponding concentration of ~ 750-1050 ppm_v) at an EBRT of 46 s, where the mean RE of H_2S and NH_3 was ~ 92 and 86%, respectively. The 16S rRNA gene sequencing along with the sulfur and nitrogen mass balance suggests that nitrification of NH_3, followed by denitrification, and both aerobic and anoxic desulfurization of H_2S mainly contributed to the simultaneous H_2S and NH_3 removal in the HFMB. This study confirms that the HFMB is an excellent bioreactor configuration for H_2S and NH_3 laden biogas purification.

5.6. References

Albinoni, A., Lona, L., Felici, C., Corsaro, N., Izzo, G., De Luca, E., 2015. Analytical protocols for the determination of sulphur compounds characteristic of the metabolism of *Chlorobium limicola*. Analytical Chemistry Research. 5, 9-13.

Aliboni, A., Lona, L., Felici, C., Corsaro, N., Izzo, G., De Luca, E., 2015. Analytical protocols for the determination of sulphur compounds characteristic of the metabolism of *Chlorobium limicola*. Analytical Chemistry Research. 5, 9-13.

Allen, H.E., Fu, G., Deng, B., 1993. Analysis of acid-volatile sulfide (AVS) and simultaneously extracted metals (SEM) for the estimation of potential toxicity in aquatic sediments. Environmental Toxicology and Chemistry. 12, 1441-1453.

Angelidaki, I., Treu, L., Tsapekos, P., Luo, G., Campanaro, S., Wenzel, H., Kougias, P.G., 2018. Biogas upgrading and utilization: Current status and perspectives. Biotechnology Advances. 36, 452-466.

Barbusiński, K., Parzentna-Gabor, A., Kasperczyk, D., 2021. Removal of odors (mainly H_2S and NH_3) using biological treatment methods. Clean Technologies. 3, 138-155.

Bragança, I., Sánchez-Soberón, F., Pantuzza, G.F., Alves, A., Ratola, N., 2020. Impurities in biogas: Analytical strategies, occurrence, effects and removal technologies. Biomass and Bioenergy. 143, 105878.

Cai, J., Qaisar, M., Ding, A., Wang, K., Sun, Y., & Wang, R., 2020. Microbial Fuel Cells Simultaneously Treating Sulfide and Nitrate under Different Influent Sulfide to Nitrate Molar Ratios. Energy & Fuels. 34, 3858-3866.

Cano, P.I., Almenglo, F., Ramírez, M., Cantero, D., 2021. Integration of a nitrification bioreactor and an anoxic biotrickling filter for simultaneous ammonium-rich water treatment and biogas desulfurization. Chemosphere. 284, 131358.

Chen, C.Y., Tsai, T.H., Chang, C.H., Tseng, C.F., Lin, S.Y., Chung, Y.C., 2018. Airlift bioreactor system for simultaneous removal of hydrogen sulfide and ammonia from synthetic and actual waste gases. Journal of Environmental Science and Health, Part A. 53, 694-701.

Cheng, Y., Yuan, T., Deng, Y., Lin, C., Zhou, J., Lei, Z., Shimizu, K., Zhang, Z., 2018. Use of sulfur-oxidizing bacteria enriched from sewage sludge to biologically remove H_2S from biogas at an industrial-scale biogas plant. Bioresource Technology Reports. 3, 43-50.

Das, J., Ravishankar, H., Lens, P.N.L., 2022a. Biological biogas purification: recent developments, challenges and future prospects. Journal of Environmental Management. 304, 114198.

Das, J., Ravishankar, H., Lens, P.N.L., 2022b. Biological removal of gas-phase H_2S in hollow fibre membrane bioreactors. Journal of Chemical Technology & Biotechnology. Early View. https://doi.org/10.1002/jctb.6999

Gandu, B., Palanivel, S., Juntupally, S., Arelli, V., Begum, S., Anupoju, G. R., 2021. Removal of NH_3 and H_2S from odor causing tannery emissions using biological filters: Impact of operational strategy on the performance of a pilot-scale bio-filter. Journal of Environmental Science and Health, Part A. 56, 625-634.

González-Cortés, J.J., Almenglo, F., Ramírez, M., Cantero, D., 2021. Simultaneous removal of ammonium from landfill leachate and hydrogen sulfide from biogas using a novel two-stage oxic-anoxic system. Science of The Total Environment. 750, 141664.

Haosagul, S., Prommeenate, P., Hobbs, G., Pisutpaisal, N., 2020. Sulfide-oxidizing bacteria community in full-scale bioscrubber treating H_2S in biogas from swine anaerobic digester. Renewable Energy. 150, 973-980.

Huan, C., Fang, J., Tong, X., Zeng, Y., Liu, Y., Jiang, X., Ji, G., Xu, L., Lyu, Q., Yan, Z., 2021. Simultaneous elimination of H_2S and NH_3 in a biotrickling filter packed with polyhedral spheres and best efficiency in compost deodorization. Journal of Cleaner Production. 284, 124708.

Huang, W., Gong, B., He, L., Wang, Y., Zhou, J., 2020. Intensified nutrients removal in a modified sequencing batch reactor at low temperature: Metagenomic approach reveals the microbial community structure and mechanisms. Chemosphere. 244, 125513.

Jaber, M.B., Couvert, A., Amrane, A., Le Cloirec, P., Dumont, E., 2017. Removal of hydrogen sulfide in air using cellular concrete waste: Biotic and abiotic filtrations. Chemical Engineering Journal. 319, 268-278.

Jiang, L., Chen, X., Qin, M., Cheng, S., Wang, Y., Zhou, W., 2019. On-board saline black water treatment by bioaugmentation original marine bacteria with *Pseudoalteromonas* sp. SCSE709-6 and the associated microbial community. Bioresource Technology. 273, 496-505.

Jiang, X., Yan, R., Tay, J.H., 2009. Simultaneous autotrophic biodegradation of H_2S and NH_3 in a biotrickling filter. Chemosphere. 75, 1350-1355.

Kang, J.H., Yoon, Y., Song, J., 2020. Effects of pH on the simultaneous removal of hydrogen sulfide and ammonia in a combined absorption and electro-oxidation system. Journal of Hazardous Materials. 382, 121011.

Kumar, S., Herrmann, M., Blohm, A., Hilke, I., Frosch, T., Trumbore, S. E., Küsel, K., 2018. Thiosulfate- and hydrogen-driven autotrophic denitrification by a microbial consortium enriched from groundwater of an oligotrophic limestone aquifer. FEMS microbiology ecology. 94, fiy141.

Le Borgne, S., Baquerizo, G., 2019. Microbial ecology of biofiltration units used for the desulfurization of biogas. ChemEngineering. 3, 72.

Li, W., Zhang, M., Kang, D., Chen, W., Yu, T., Xu, D., Zeng, Z., Li, Y., Zheng, P., 2020. Mechanisms of sulfur selection and sulfur secretion in a biological sulfide removal (BISURE) system. Environment International. 137, 105549.

López, J.C., Porca, E., Collins, G., Pérez, R., Rodríguez-Alija, A., Muñoz, R., Quijano, G., 2017. Biogas-based denitrification in a biotrickling filter: Influence of nitrate concentration and hydrogen sulfide. Biotechnology and bioengineering. 114, 665-673.

Malhautier, L., Gracian, C., Roux, J.C., Fanlo, J.L., Le Cloirec, P., 2003. Biological treatment process of air loaded with an ammonia and hydrogen sulfide mixture. Chemosphere. 50, 145-153.

Mirfendereski, S.M., Niazi, Z., Mohammadi, T., 2019. Selective removal of H_2S from gas streams with high CO_2 concentration using hollow-fiber membrane contractors. Chemical Engineering & Technology. 42, 196-208.

Monteiro, M., Séneca, J., Magalhães, C., 2014. The history of aerobic ammonia oxidizers: from the first discoveries to today. Journal of microbiology. 52, 537-547.

Pokorna, D., Zabranska, J., 2015. Sulfur-oxidizing bacteria in environmental technology. Biotechnology Advances, 33, 1246-1259.

Rodríguez, C., Cisternas, J., Serrano, J., Leiva, E., 2021. Nitrogen Removal by an Anaerobic Iron-Dependent Ammonium Oxidation (Feammox) Enrichment: Potential for Wastewater Treatment. Water, 13, 3462.

Tilahun, E., Bayrakdar, A., Sahinkaya, E., Çalli, B., 2017. Performance of polydimethylsiloxane membrane contactor process for selective hydrogen sulfide removal from biogas. Waste Management. 61, 250-257.

Wang, H., Sun, Y., Zhang, L., Wang, W., Guan, Y., 2021. Enhanced nitrogen removal and mitigation of nitrous oxide emission potential in a lab-scale rain garden with internal water storage. Journal of Water Process Engineering. 42, 102147.

Wei, R., Hui, C., Zhang, Y., Jiang, H., Zhao, Y., Du, L., 2021. Nitrogen removal characteristics and predicted conversion pathways of a heterotrophic nitrification–aerobic denitrification bacterium, *Pseudomonas aeruginosa* P-1. Environmental Science and Pollution Research. 28, 7503-7514.

Wu, L. C., Kuo, C.L., Chung, Y.C., 2011. Removal of high concentrations of NH_3 by a combined photoreactor and biotrickling filter system. Journal of Environmental Science and Health, Part A. 46, 1675-1682.

Zheng, T., Li, L., Chai, F., Wang, Y., 2021. Factors impacting the performance and microbial populations of three biofilters for co-treatment of H_2S and NH_3 in a domestic waste landfill site. Process Safety and Environmental Protection. 149, 410-421.

Zhu, T., Zhang, J., Cai, Z., 2011. The contribution of nitrogen transformation processes to total N_2O emissions from soils used for intensive vegetable cultivation. Plant and Soil. 343, 313-327.

Zhuo, Y., Han, Y., Qu, Q., Li, J., Zhong, C., Peng, D., 2019. Characteristics of low H_2S concentration biogas desulfurization using a biotrickling filter: Performance and modeling analysis. Bioresource Technology. 280, 143-150.

Chapter 6

General Discussion and future perspectives

6.1. Introduction

In this thesis, a novel hollow fibre membrane bioreactor (HFMB) was successfully used for treating both single (H_2S from air stream) and mixed (H_2S and NH_3 from raw biogas) gaseous pollutants. Prior to study of the HFMB's performance, a comprehensive review identified the challenges and future prospects of biological biogas purification technologies for treating H_2S, CO_2, NH_3, siloxanes and volatile organic compounds (VOCs) from raw biogas (**Chapter 2**). Several factors such as bioreactor configuration, process parameters, pollutant characteristics, inhibitory effects and microbial community composition determine the efficiency of the gaseous pollutant removal in a bioreactor system (**Chapter 2**). The Driver-Pressure-Stress-Impact-Response (DPSIR) framework and Strengths-Weaknesses-Opportunities-Threats (SWOT) analysis identified a holistic approach for biological biogas purification (**Chapter 2**).

As a proof of concept study, the hydrophilic polyethersulfone (H-PES) based HFMBs were successfully used for the biological treatment of H_2S laden gas (**Chapter 3**). Considering the importance of operating conditions and process parameters, especially in industries where fluctuation of substrate concentrations and gas flow rates are often observed, the long-term performance of the HFMBs was investigated where the HFMBs demonstrated efficient H_2S removal during both steady and transient state operation (**Chapter 4**). Thereafter, for the first time, the HFMBs were successfully used for treating H_2S and NH_3 simultaneously from raw biogas (**Chapter 5**). This research provides valuable insights into long-term performance of the HFMB under different operating conditions and confirms that the HFMB is suitable for simultaneous removal of H_2S and NH_3 from various waste gas emission sources including raw biogas produced in anaerobic digestion (AD) plants, sewage and wastewater treatment plants.

6.2. Prospects of biological biogas purification and upgrading

Lack of source segregation of waste (prior to its use as a feedstock), wide variation of feedstock composition and lack of optimum operating conditions in AD cause a wide

variation in raw biogas composition and process instability in AD systems (Li et al., 2018; Xu et al., 2018). Suitable feedstock selection and process optimization is important to achieve sustainable AD and minimise biogas impurities (**Chapter 2**). Small-scale AD plants are becoming more popular, especially in low population communities and in the absence of central waste treatment facilities, to convert organic waste streams into resources (heat and electricity generation) with financial benefits (O'Connor et al., 2021). It is expected that installation of small-scale (CHP electrical output 15-99 kW_e) AD plants will gradually increase in the European agricultural sector, especially in small to medium-sized farms, because insufficient feedstock is a big concern for large-scale (CHP electrical output > 300 kW_e) AD plants (O'Connor et al., 2021).

Though large-scale AD plants use conventional physico-chemical biogas upgrading methods, adoption of these technologies is financially not feasible for small-scale AD plants because of high investment, maintenance and operating costs (O'Connor et al., 2021). Pre-treatment (H_2S removal) is recommended for most of the commonly used biogas upgrading (CO_2 removal) methods, such as organic solvent scrubbing or membrane separation (Golmakani et al., 2022). High CH_4 loss (including the CH_4 needed to generate the required electrical energy for each biogas upgrading process) is another concerning factor in these biogas upgrading methods, e.g. water scrubbing (17-18%), membrane separation (12-15%) or adsorption (14%) processes, as the CH_4 loss contributes to a much higher global warming potential (Golmakani et al., 2022).

Recent advancements in biological technologies for biogas purification as well as the limitations of those technologies have been described in **Chapter 2**. Bioreactors can efficiently remove CO_2, H_2S, NH_3, siloxanes and VOCs from biogas, for example, the H_2 assisted biogas upgrading process can achieve ~70-98% CH_4 in the enriched biogas. Adopting a policy framework and providing financial incentives could be effective to adopt environment friendly biogas clean-up technologies and promote biogas production as a clean and renewable energy resource (**Chapter 2**).

6.3. Application of HFMB for biological waste gas treatment

Figure 6.1 shows the major findings and bioconversion mechanism regarding the application of HFMB for the removal of H_2S and NH_3 from gas stream (**Chapters 3-5**). This research was carried out in three experimental steps, where the first step of the

experiments was about the feasibility study of the HFMB for treating H_2S laden gas (**Chapter 3**). The second step of the experiments investigated the effects of operating conditions and process parameters to test the resilience of the HFMB during its long-term (~ 9 months) operation (**Chapter 4**). The third step of the experiments tested the mixed pollutant (e.g. H_2S and NH_3) removal performance of the HFMB under different operating conditions (**Chapter 5**).

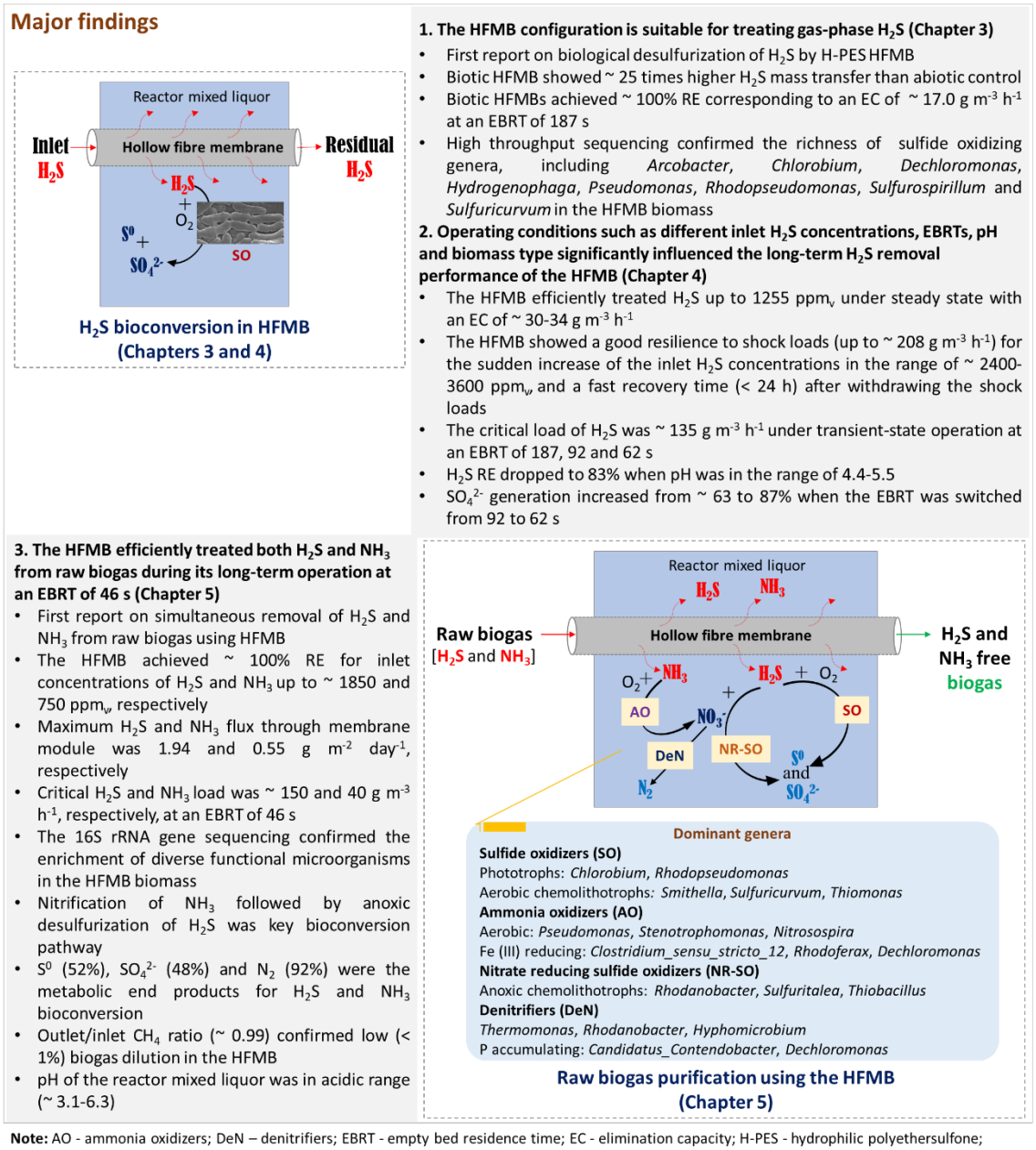

Note: AO - ammonia oxidizers; DeN – denitrifiers; EBRT - empty bed residence time; EC - elimination capacity; H-PES - hydrophilic polyethersulfone; HFMB - hollow fibre membrane bioreactor; RE - removal efficiency; NR-SO - nitrate-reducing sulfide oxidizers; SO - sulfide oxidizers;

Figure 6.1: Major findings of this PhD dissertation on the application of HFMB for

treating H_2S and NH_3, including process parameters and bioconversion processes.

6.3.1. H_2S removal

Gas-phase H_2S was passed through the lumen side of the hollow fibres attached to a submerged hollow fibre membrane module of the HFMB. Continuous dissociation of H_2S in the liquid on the shell side of the HFMB followed by bioconversion of the dissolved sulfides by autotrophic sulfur oxidizing bacteria (ASOB) immobilized on the membranes and present in the liquid suspension is the main mechanism of the HFMB for treating H_2S from waste gas streams (**Chapter 3 and 4**). In contrast, conventional physico-chemical methods such as hollow fibre membrane contactors (HFMCs) require alkaline absorption chemicals and high operational pressure to remove H_2S from a gaseous mixture by selective mass transfer (Bazhenov et al., 2018).

The variation of the removal efficiency (RE) of H_2S (in the range of 80-100%, corresponding to an elimination capacity (EC) of 4.50-5.03 g m^{-3} h^{-1}) for using different inocula, followed by a consistent RE (i.e. ~ 100% RE with an EC of ~ 17.0 g m^{-3} h^{-1}) for using acclimatized inoculum in both biotic HFMBs, clearly suggests the importance of the relative abundance of functional microorganisms, i.e. ASOB. The high throughput sequencing confirmed the richness of ASOB genera including *Sulfuricurvum*, *Hydrogenophaga*, *Arcobacter*, *Rhodopseudomonas*, *Dechloromonas*, *Pseudomonas* and *Chlorobium*, which mainly contributed to the H_2S bioconversion in the HFMBs (**Chapter 3**).

Different bioreactor configurations such as the biotrickling filter or the bioscrubber have different operational requirements wherein the performance of those bioreactor configurations vary in a wide range depending on the operating conditions such as pH, pollutant concentration, empty bed residence time (EBRT) and loading rate (Khanongnuch et al., 2022). Though the HFMB efficiently treated H_2S concentrations up to ~ 650 ppm_v at an EBRT of 187 s (**Chapter 3**), it is important to reveal the operational aspects and shell side profile of the HFMB to justify the suitability of the HFMB for long-term H_2S removal (**Chapter 4**) compared to the conventional bioreactor configurations such as biofilters or biotrickling filters. The long-term H_2S removal performance of the HFMBs (**Chapter 4**) suggests that the operating parameters such as inlet H_2S concentration, EBRT, pH, shock loads at different EBRT, duration of the shock load and

different biomass types significantly influenced the H_2S removal performance of the HFMB.

Optimum pH for efficient H_2S bioconversion varies in a wide range (1-9) depending on the ASOB genera present in a system (Pokorna and Zabranska, 2015). The HFMB used in this study achieved ~ 100% RE of H_2S with an EC of 33.8, 30.0 and 30.9 g m^{-3} h^{-1} at an EBRT of 187, 92 and 62 s, respectively, during the steady state operation at pH ~ 7.0. The variation of RE at an EBRT of 92 s in the biotic HFMB can be related to the operational factors, such as gradual pH drop or increasing the inlet loading rate (ILR) immediate after switching the EBRT from 187 to 92 s, that affected the ASOB activity. Survival of a famine period (i.e. in the absence of H_2S) by the ASOB consortia in the HFMB could be related to the utilization of S^0 (accumulated in the periplasmic space during the feast period) for energy generation (ΔG^0 = - 587.1 kJ/reaction) through the complete oxidation of S^0 to SO_4^{2-} (Li et al., 2020). The H_2S removal performance (~ 100% RE for an inlet concentration up to ~ 900 ppm_v at an EBRT of 187 s) of the HFMB after the starvation period (~ 110 days) suggests the re-acclimatization capability of the ASOB (**Chapter 4**).

Achieving ~ 100% RE in the presence of both suspended biomass and membrane attached biofilm in the HFMB while varying the RE (from 47 to 83%) in the absence of suspended biomass, i.e. when the suspended biomass on the shell side was replaced with mineral solution only, confirms that suspended biomass along with membrane attached biofilm contributed to H_2S bioconversion in the HFMB. In addition, changing the supernatant of the reactor mixed liquor periodically on the shell side of the HFMB has been identified as an important operational aspect to maintain the pH, dissolved oxygen and sulfate concentration in a certain range, consequently, to retain efficient H_2S removal performance (**Chapter 4**).

The HFMB achieved an EC of ~ 97 g m^{-3} h^{-1} (corresponding RE of 98% during 16 h shock load employing an inlet H_2S concentration of ~ 3600 ppm_v at an EBRT of 187s), 133 g m^{-3} h^{-1} (corresponding RE of 87% during 4 h shock load employing an inlet H_2S concentration of ~ 2700 ppm_v at an EBRT of 92 s) and 147 g m^{-3} h^{-1} (corresponding RE of 71% during 4 h shock load employing an inlet H_2S concentration of ~ 2500 ppm_v at an EBRT of 62 s) g m^{-3} h^{-1} during transient-state operation. The HFMB rapidly recovered ~

100% RE when the shock loads were withdrawn. Though the HFMB was capable to handle inlet H_2S concentrations up to ~ 3600 ppm_v for a 16 h period at an EBRT of 187 s and achieved ~ 98% RE, the removal performance dropped rapidly (54% RE) when the HFMB operated with high H_2S concentrations (~ 2400 ppm_v) for a longer period (72 h). Variation of RE depending on the scale of the shock load and its duration, and fast recovery time (< 24 h) after withdrawing the successive shock loads clearly suggest the resilience of the HFMB configuration (**Chapter 4**).

6.3.2. Simultaneous removal of H_2S and NH_3 from raw biogas

Raw biogas, supplied to the HFMBs after collecting from an industrial-scale anaerobic digester had the following composition: CH_4 ~ 39-73%, CO_2 ~ 21-49%, O_2 ~ 0.2-6%, N_2 ~ 0-26%, H_2S ~ 63-1905 ppm_v and NH_3 ~ 14-1032 ppm_v (**Chapter 5**). The reasons for the wide variation of the raw biogas composition can be associated with several factors such as highly varied feedstock, intermittent air dosing in the digester to reduce the H_2S concentration in the biogas, and low quality biogas production due to system failure or incomplete digestion in the digester (Khan et al., 2021; Li et al., 2018). The biotic HFMB demonstrated efficient removal of both H_2S (up to ~ 1850 ppm_v and a maximum EC of ~ 162 g m^{-3} h^{-1}) and NH_3 (up to ~ 1030 ppm_v, and a maximum EC of ~ 45 g m^{-3} h^{-1}) without diluting the biogas, suggesting the resilience of the HFMB despite of fluctuation of the biogas composition. Desulfurization of H_2S by sulfide oxidizing chemolithotrophs and oxidation of NH_3 by the ammonia oxidizers mainly contributed to bioconversion of H_2S and NH_3 in the HFMB (**Chapter 5**). The variation of RE of H_2S and NH_3 in the range of 85-97 and 73-95%, respectively, for feeding high concentrations of H_2S (~ 1200-1700 ppm_v) and NH_3 (~ 750-1050 ppm_v) at an EBRT of 46 s suggests that the corresponding inlet loading rates of H_2S (~130-186 g m^{-3} h^{-1}) and NH_3 (~ 41-56 g m^{-3} h^{-1}) at the employed EBRT (i.e. 46 s) were critical for the functional microorganisms present in the HFMB biomass during that period (**Chapter 5**).

Decrease of the EBRT from 187 s to 62 s (i.e. threefold increase of gas flow rates) significantly reduced the maximum level of H_2S concentration (from ~ 1250 to ~ 360 ppm_v) that can be treated efficiently (i.e. 100% RE) in the HFMB, suggesting the influence of the loading rate on RE at shorter EBRT such as 62 s (**Chapter 4**). Frequent (weekly) changing of both the EBRT and H_2S concentration may affect the ASOB

population and their acclimatization in the HFMB resulted into a comparatively lower EC of H_2S (~ 31 g m^{-3} h^{-1}) with 100% RE at an EBRT of 62 s (**Chapter 4**). In contrast, the H_2S removal performance (a mean RE of 92% with an EC of ~ 143 g m^{-3} h^{-1}) of the HFMB at an EBRT of 46 s (**Chapter 5**) confirmed that the sulfide oxidizers present in the HFMB during that period were well adapted to handle the higher loading rates. Hence, changing of the EBRT after a certain period (at least 6 weeks interval) was useful to retain a high RE and EC of H_2S as well as to allow sufficient time to acclimatize the sulfide oxidizers in the HFMB (**Chapter 5**) compared to the weekly change of EBRT (**Chapter 4**).

6.3.3. Comparison of HFMB performance with other bioreactor configurations

Table 6.1 summarises the gas-phase H_2S and NH_3 (or NH_4^+ from wastewater) removal performance of different bioreactor configurations including two-stage bioreactors. Biofiltration, i.e. biofilter (BF) and biotrickling filter (BTF), is mainly reported for treating H_2S (< 500 ppm_v) and NH_3 (< 500 ppm_v) simultaneously from several air emissions where the removal performance of the bioreactors varied in a wide range (EC of ~ 20-85 g m^{-3} h^{-1}) depending on the applied operating conditions such as EBRT (varying from 4 to 55 s) (Table 6.1). The simultaneous H_2S and NH_3 removal performance of the HFMB (**Chapter 5**) is more promising in terms of inlet pollutant concentration, shorter EBRT, and high RE and EC compared to other bioreactor configurations (Table 6.1).

The optimum EBRT can be different (30-300 s) in different bioreactor configurations depending on the applied operating conditions (**Chapter 2**). Switching the EBRT from 46 to 60 s, especially at higher H_2S and NH_3 concentrations (corresponding loading rates of > 150 and > 40 g m^{-3} h^{-1} of H_2S and NH_3, respectively) can be useful to achieve consistent performance (100% RE) during long-term operation of the HFMB. Alternatively, two HFMBs can be used periodically (i.e. one HFMB in operation and another HFMB in standby mode) to handle high loading rates of H_2S and NH_3 at an EBRT 46 s and achieve consistent performance during long term operation. Though a much shorter EBRT (6 s) has been successfully employed in a lab scale BTF for treating low concentrations (100-190 ppm_v) of H_2S from air stream (Bu et al., 2021), very few studies

reported bioreactors with EBRT of < 10 s for treating highly loaded gas streams with H_2S concentrations of 1000-2000 ppm_v or higher.

In this study, the performance of the biotic HFMB was evaluated at different operating conditions for nearly 2 years. During that period, a thin biofilm was formed on the shell side of the submerged hollow fibres but the membrane attached biofilm did not induce membrane clogging (**Chapters 3-5**). The reason for the formation of a thin biofilm in the HFMB can be the lack of organic carbon in the reactor mixed liquor which can limit the growth of heterotrophs and consequently limit the excess biomass accumulation on the hollow fibres. The inorganic carbon ($NaHCO_3$) source was mainly supplied in the reactor mixed liquor for microbial growth. The thickness of the biofilm was not measured in this PhD work to avoid damage of the hollow fibres that could hamper the HFMB operation. Physical membrane cleaning processes such as air sparging, hydraulic backwash or ultrasound waves (Nguyen et al., 2012) can be applied to mitigate membrane fouling in HFMB applications. Membrane wetting was not noticed in the HFMB (**Chapters 3-5**). The reason for the absence of membrane wetting can be related to the HFMB features: (i) the static shell side where the liquid phase was not associated with any turbulence that can create a pressure gradient between the shell and lumen side of the membrane module, and (ii) the absence of absorption chemicals that can change the surface morphology and pore-size of the membrane (Mirfendereski et al., 2019).

There was no significant pressure drop in the HFMB during the entire study period. The reason can be the HFMB features where only a small fraction (~ 0.5-1.5% including the target pollutants, i.e. H_2S and NH_3, and other constituents, i.e. O_2 and CO_2) of the inlet gas stream was diffused from the lumen to the shell side of the porous hollow fibres at atmospheric pressure and dissociated in the static liquid phase, i.e. in the reactor mixed liquor. The remaining fraction (> 98%) left the HFMB as outlet gas stream. In contrast, gaseous pollutants are generally fed through the packed bed (e.g. biofilter or biotrickling filter) or scrubbing liquid (e.g. bioscrubber or gas lift bioreactor) in conventional bioreactors, where the pressure drop in these bioreactors is associated with several factors such as filter bed compaction or types of carrier material (Kennes and Veiga, 2002), EBRT (Lebrero et al., 2014) and excess biomass. For example, the pressure drop in a biofilter (~ 200-800 mm H_2O) was much higher compared to that of a biotrickling filter

(~ 5-20 mm H_2O) and membrane bioreactor (~ 50-160 mm H_2O) treating volatile organic compounds (Lebrero et al., 2014).

Anoxic desulfurization of biogas utilizing NH_4^+, NO_3^- or NO_2^- from wastewater by coupling different bioreactors has been reported in the literature (Cano et al., 2021; Flores-Cortés et al., 2021; González-Cortés et al., 2021). These two-stage bioreactors (i.e. nitrification of NH_4^+ or absorption of H_2S in the first reactor followed by aerobic or anoxic desulfurization of H_2S in the second reactor; Table 6.1) are used to overcome issues associated with a single bioreactor system, e.g. filter bed clogging or biogas dilution during desulfurization of H_2S. From a bioreactor configuration perspective, the HFMB has some advantages such as efficient mass transfer even at high loading rates (**Chapters 4** and **5**), contribution of both suspended and membrane attached biofilm (**Chapter 4**), no filter bed (i.e. membrane) clogging and low pressure drop (**Chapters 3-5**) compared to conventional bioreactors, e.g. BF or BTF. In addition, nitrification, denitrification and desulfurization processes take place in the same compartment, i.e. on the shell side of the HFMB (**Chapter 5**).

Enrichment of diverse functional microorganisms including nitrate-reducing sulfide oxidizers (e.g. *Rhodanobacter*, *Sulfuritalea*, *Thiobacillus*, *Acinetobacter* and *Sulfurimonas*) and denitrifying phosphorus accumulating organisms (e.g. *Candidatus_Contendobacter* and *Dechloromonas*) provide an insight on the possibilities of the application of HFMB for simultaneous treatment of gas-phase H_2S and nutrients (e.g. NO_3^-, NH_4^+, PO_4^{3-}) recovery from wastewater (**Chapter 5**). To investigate nutrient recovery (from wastewater) and desulfurization of H_2S (from gas stream) simultaneously using the HFMB, further studies should focus on the optimization of the operating parameters such as substrate concentration, N/S ratio, pH and hydraulic retention time of the liquid suspension on the shell side. Future aspects of the HFMB configuration to integrate both wastewater and waste gas treatment are discussed in the section 6.5 (recommendations and future research).

Table 6.1: Comparison on gas-phase H_2S and NH_3 (or NH_4^+ from wastewater) removal performance of different bioreactor configurations.

Bioreactor type (gas source)	Inlet concentration, ppm_v		EBRT or GRT, s	Removal efficiency, %		Elimination capacity, $g\ m^{-3}\ h^{-1}$		Remarks*	Reference
	H_2S	NH_3		H_2S*	NH_3	H_2S	NH_3		
BF	210	200	55	90-99	90-99	~ 20	~ 10	Simultaneous removal;	Gandu et al., 2021
(air emissions)	~ 200	~ 200	NR	100	80	~28	~ 11	end products: NO_3^-, NO_2^-, S^0 and SO_4^{2-}	Malhautier et al., 2003
BTF	500	500	32-43	~ 98	~ 89	85	39	Simultaneous removal;	Huan et al., 2021
(air emissions)			25	67	~ 81	58	35	end products: NO_3^-, NO_2^-, S^0 and SO_4^{2-}	
	20-100	20-100	4-20	99	99	36	44		Jiang et al., 2009
AB (air emissions)	100-400	25-400	20	99	99	NR	NR	Simultaneous removal; Fe_2O_3 was added to improve the H_2S removal efficiency	Chen et al., 2018
CSTB + GB (Biogas mimic)	860-1300	NA	41, 56, 88, 104	93-95	NA	~ 40-141	NA	*Two-stage bioreactors:* nitrification of NH_4^+ from leachate in CSTB followed by anoxic desulfurization of H_2S in GB; HRT ~ 17-53 h; end product: S^0 (95%)	González-Cortés et al., 2021
CSTB + BTF (Biogas mimic)	500-4740	NA	NR	97-99	NA	~40-150	~ 20 (NH_4^+-N)	*Two-stage bioreactors:* NH_4^+ oxidation in CSTB followed by autotrophic denitrification and H_2S oxidation in BTF; HRT ~ 27-33 h; end product: SO_4^{2-} (40-100%)	Cano et al., 2021
AC + CSTB (Biogas mimic)	2500-10000	NA	780-960	~ 61-98		23-51	NA	*Two-stage bioreactors:* an AC for anoxic desulfurization coupled with a CSTB for anoxic denitrification; HRT ~ 17-23 h;	Flores-Cortés et al., 2021
HFMB	~ 1850	460	187	100	100	50	~ 6	Simultaneous removal; end products: N_2, S^0 and SO_4^{2-}	This thesis (**Chapter 5**)
(Raw biogas)	1190-1687	750-1032	46	85-97	73-95	124-161	38-45		
	< 1190	< 750	46	> 99	> 99	~ 106	~ 40		

Note: * - To explore more on biological H_2S removal performance of different bioreactor configurations treating H_2S laden gases under different operating conditions, please refer to Table 3.4 (Chapter 3) and Table 4.4 (Chapter 4); AB - airlift bioreactor; AC - absorption column; BF – biofilter; BTF - biotrickling filter; GB - gas-lift bioreactor; CSTB - continuously stirred tank bioreactor; EBRT - empty bed residence time; GRT – gas retention time; HRT - hydraulic retention time NA – not applicable; NR - not reported

6.3.4. End product selectivity for H_2S and NH_3 bioconversion

SO_4^{2-} was the main end product (~ 87%) of the treated H_2S laden air stream at an EBRT 62 s in HFMB (**Chapter 4**). SO_4^{2-} and S^0 selectivity for H_2S bioconversion were 45 and 55%, respectively, while N_2 selectivity for NH_3 bioconversion was ~ 90% during raw biogas purification in the HFMB (**Chapter 5**). Selectivity of SO_4^{2-} or S^0 (Table 6.1) depends on the operating conditions such as O_2 concentration or N/S molar ratio. Though S^0 is responsible for clogging issues in bioreactors, it can be recovered and reused in the fertilizer or chemical industries (González-Cortés et al., 2021). SO_4^{2-} contaminated wastewater leads to acidic pH of the water and the SO_4^{2-} can be reduced back to H_2S under anaerobic conditions. Hence, treatment of SO_4^{2-} contaminated wastewater is necessary prior to discharge to the environment (González-Cortés et al., 2021). From a cleaner production approach, S^0 can be the target product in HFMB, but this requires controlling the O_2 concentration and/or N/S ratio for partial oxidation of H_2S.

With regard to NH_3 removal from biogas in the HFMB, N_2 is the desired end product because nitrification of NH_3 followed by autotrophic denitrification of NO_3^- can result into NH_4^+ and NO_3^- free water on the shell side. However, the desired end product (e.g. N_2, NH_4^+ or NO_3^-) for NH_3 conversion can be different depending on the pollutant source (i.e. from wastewater or gas phase), objective of the treatment processes and scope for resource recovery through industrial symbiosis. For example, autotrophic and heterotrophic denitrification can be a feasible process for treating NO_3^-, S^{2-} and organic carbon simultaneously from wastewater, where N_2, SO_4^{2-} and CO_2 are the end products (Xu et al., 2015). Besides, recovery of NH_4^+ (as struvite or ammonium salt) from wastewater can be a sustainable approach to supplement ammonium-based fertilizer production (Ye et al., 2018).

6.4. Economic considerations to integrate HFMBs in AD plants

6.4.1. Treatment plant

A case study of an AD plant (Kildare, Ireland), from where the raw biogas was collected and fed to the HFMBs (**Chapter 5**), has been carried out to estimate the costs involved in the AD plant for biogas desulfurization prior to energy generation or natural gas grid injection. Presently, the AD plant produces ~ 1000 m^3 of raw biogas per hour.

The lab-scale HFMB (working membrane volume of 0.0069 L) tested in this thesis (**Chapters 3-5**) feeding raw biogas up to ~ 0.0129 m^3/day (corresponding EBRT of 46 s) can not handle such a high biogas flow rate (24000 m^3/day). Hence, an industrial-scale HFMB unit (working membrane volume 7.85 L) with a capacity to handle ~ 15 m^3/day (corresponding EBRT of 46 s) is proposed considering the optimum operating conditions applied to the lab-scale HFMBs and knowledge gathered from this PhD research. Theoretically, 1634 HFMB units need to be adopted in the AD plant in total to treat the daily produced biogas (Table 6.2). In practice, the number of HFMB units can be reduced further depending on the membrane specification, number of membrane modules in each HFMB, volume of the liquid phase and operating conditions applied to achieve optimum pollutant removal performance. This requires future studies at pilot scale to demonstrate the HFMB performance.

Table 6.2 summarizes the expenses for current practice in the referred AD plant for biogas desulfurization and estimated costs to replace the existing Fe_2O_3 dosing and activated carbon filters by industrial scale HFMBs. An iron sponge is commonly used in anaerobic digesters to reduce the H_2S concentrations in the biogas stream, where hydrated iron oxide (Fe_2O_3, primary active ingredient) and mixed iron oxide (Fe_2O_3.FeO) contribute to the adsorption of H_2S and form Fe_2S_3 (Abatzoglou and Boivin, 2009). Activated carbon (AC), another cost intensive and commercially available adsorbent, is used in biogas purification processes as well (Zhang et al., 2021). The operating cost associated with Fe_2O_3 and AC are the main concern in this referred AD plant, because both materials are used to control H_2S prior to energy generation using a combined heat and power (CHP) engine and a biomethane upgrader.

The dose of Fe_2O_3 into the digesters varies depending on the H_2S concentration in the output biogas. The approximate price of Fe_2O_3 (e.g. Active Fe33 Iron Compound, Chemical Services Ltd, Antrim, UK) also varies in the range of 1200-1500 €/tonne, depending on the grade, source and supply chain conditions. The estimated cost for average dosing ~ 200 kg Fe_2O_3/day is 240-300 €/day in the AD plant. The approximate price of AC (e.g. Low Oxygen Activated Carbon for H_2S removal, Chemical Services Ltd, Antrim, UK) is 3000 €/tonne. The CHP consists of a one tonne AC filter that must be replaced every two months, and a biomethane upgrader with a three tonnes AC filter

that needs to be replaced every 3-4 months. Hence, the AD plant has a yearly expense of 132600-163500 € for using the adsorbents Fe_2O_3 and AC to remove H_2S (Table 6.2).

Though the total capital costs for installing industrial scale HFMBs seems to be expensive (877166 €), the yearly operating costs (81167 €) is 39-50% less expensive than that of the Fe_2O_3 dosing and AC filters (132600-163500 €). Membrane bioreactors (MBRs) based wastewater treatment plants reported by Xiao et al. (2020) have been considered to estimate the capital and operating costs of the industrial scale HFMBs. Costs for membrane modules were about ~ 20% of the total capital costs where effective lifespan of the hollow fibres was 5-10 years (Xiao et al., 2020). Energy consumption, accounted for 40-60% of the total operating costs, was in the range of 0.45-0.8 kWh/m^3 in MBR based wastewater treatment plants where the consumption was mainly for aeration, liquid pumping (lifting and recirculation) and sludge mixing (Xiao et al., 2020). The AD plant can save operating costs up to 51433-82333 €/year by using HFMBs instead of the adsorbents. In addition, the savings can be considered as returned cash flow for the capital investment regarding the HFMBs installation (Table 6.2). The payback period for this capital investment will be ~ 11-17 years.

Table 6.2: Economic evaluation of industrial-scale biogas purification by HFMBs and presently used processes of Fe_2O_3 dosing and activated carbon filters.

All parameters for the projection	**Unit**	**Value**	**Reference and/or remarks**
Raw biogas produced in AD plant, Kildare, Ireland			
Raw biogas flow rate	m^3/day	24000	AD plant; Chapter 5
HFMB specification			
Hollow fibres outer diameter	mm	2.00	Chapter 3
Hollow fibres inner diameter	mm	1.80	Chapter 3
Membrane length	m	1.00	Assumption
No. of membranes in each membrane module		250	Assumption
Membrane surface area for each module	m^2	1.57	Calculation
Working volume of each membrane module	L	0.7854	Calculation
No. of membrane module in each HFMB		**10**	Assumption
Total working volume of each HFMB	L	**7.85**	Calculation
Biogas flow rate applied in HFMB (Corresponding EBRT 46 s)	m^3/day	14.69	Calculation; Chapter 5
No of HFMBs require (to treat 24000 m^3 of biogas per day)		**1634**	Calculation
Water consumption			
Water required in each HFMB	m^3	1.02	Calculation
Water required to replace 50% supernatant from each HFMB in every 3 weeks	m^3	0.5114	Chapter 5; Calculation
Hydraulic retention time	day	21	Chapter 5
Wastewater generated for each HFMB	m^3/day	0.0244	Calculation
Total wastewater generated[1]for using all HFMBs	m^3/day	39.78	Calculation
Approximate cost associated to scale-up HFMB application			
Capital costs[2]	€/(m3/day)	525	Xiao et al., 2020
Total capital cost for installing all HFMBs	€	**877166**	Calculation
Operating costs[3]	€/m3	0.13	Xiao et al., 2020
Total operating cost for operating all HFMBs	€/year	**81167**	Calculation
Cost associated presently in AD plants for physico-chemical H_2S removal			
Active Fe_2O_3 dosing in the digester	kg/day	200	AD plant, Kildare, Ireland
Cost of Fe_2O_3	€/tonne	1200-1500	Chemical invoice
Expenses for Fe_2O_3 dosing	€/year	87600-109500	Calculation
Cost of activated carbon (AC)	€/tonne	3000	Chemical invoice
AC required for CHP engine	tonne/year	6	AD plant, Kildare, Ireland
Expenses for AC for CHP	€/year	18000	Calculation
AC required for biogas upgrader	tonne/year	9-12	AD plant, Kildare, Ireland
Expenses for AC for biogas upgrader	€/year	27000-36000	Calculation
Total expenses for using Fe_2O_3 and AC	€/year	**132600-163500**	Calculation
Net saving of operating costs for replacing Fe_2O_3 and AC by HFMBs	€/year	**51433-82333**	Calculation
Returned cash flow for capital investment	€/year	50000	Assumption
Payback period for capital investment	Year	17.5	Calculation

Note: [1] - Wastewater for replacing ~ 50% supernatant of the reactor mixed liquor in every 3 weeks; [2] - Capital cost projected based on large-scale (≥ 10000 m^3/d) membrane bioreactors reported in Xiao et al. (2020), where the costs were distributed for tanks (~40%), pipes/canals (~10%), membrane modules (~20%) and other equipment (~30%); [3] - Operating costs were distributed for energy consumption (40%–60%), chemical consumption (10%–30%), sludge disposal (5%–15%), labor costs (10%–30%) and others (5%–20%) as reported by (Xiao et al., 2020)

6.4.2. Physico-chemical versus biological H_2S removal

Economic assessment of several biogas purification processes (Alinezhad et al., 2019; Zhang et al., 2021) suggests that biological approaches are more feasible compared to scrubbing or adsorbent based purification processes. An economic comparison of a biofilter (BF) and chemical scrubber used for treating H_2S and NH_3 from a wastewater treatment plant revealed that the yearly operating cost of a BF and chemical scrubber was 4590 and 17340 €, respectively, where chemical usage and water consumption were the main reason for the high operating cost of the chemical scrubber (Alinezhad et al., 2019). Moreover, the estimated economic index of the BF was 1.58 € m^{-3} h^{-1} (for treating 18921 m^3 of waste air $year^{-1}$ with an EBRT of ~ 15 s), while the index of the chemical scrubber was 2.57 € m^{-3} h^{-1} (for treating 43800 m^3 of waste air $year^{-1}$ with an EBRT of ~ 3 s) (Alinezhad et al., 2019).

In another study, Zhang et al. (2021) reported that a biotrickling filter is more profitable for treating both H_2S and siloxanes from the biogas (1200 m^3/h) of a sewage sludge treating AD plant compared to the adsorbents AC and Fe_2O_3. Photosynthetic biogas upgrading can also be economically feasible as the operating costs (0.03 €/m^3) and energy consumption (0.08-0.14 kW-h/m^3) was much lower than physico-chemical methods having operating cost of 0.13-0.20 €/m^3 and an energy requirement of 0.20-1.0 kW-h/m^3 (Rodero et al., 2019). However, the investment cost of photosynthetic upgrading was higher (6000 €/(m^3/h)) compared to physico-chemical methods (2700-4000 €/(m^3/h)).

Exergy analysis, a thermodynamic approach, provides a distinctive insight about more efficient use of energy and materials to measure the degree of renewability of energy systems (Aghbashlo et al., 2019b). Exergy-based sustainability assessment tools such as exergoeconomic (Aghbashlo et al., 2019a) or exergoenvironmental analysis (Aghbashlo et al., 2019b) can be used to reveal the energy efficiency of physico-chemical and biological biogas purification methods. To do that, the required exergy data can be obtained from an AD plant equipped with a gas engine (Aghbashlo et al., 2019a). In addition, thermodynamically active components in the AD plant including the proposed/experimental biogas desulfurization units need to be considered for mass

balance, energy balance and functional energy efficiency calculations (Barati et al., 2017).

6.5. Recommendations and future research

6.5.1. Optimization of HFMB based H_2S and NH_3 removal

In this thesis, the HFMB demonstrated resilient performance for treating single (i.e. H_2S; **Chapters 3 and 4**) and mixed (i.e. H_2S and NH_3; **Chapters 5**) pollutants under different operating conditions. The HFMB technology can be integrated in AD plants for downstream processing of raw biogas and other industries or services such as sewers, wastewater treatment plants and livestock farms dealing with H_2S and NH_3 laden odour emissions. To further scale up the HFMB performance keeping in mind the pilot or industrial scale application, future studies should be focused on: (i) process optimization for handling high inlet H_2S loading rates such as ~ 200-250 g m^{-3} h^{-1} and shorter gas contact time such as 10-20 s, (ii) possibilities of two-stage HFMBs (i.e. connecting HFMBs in series) to handle high pollutant concentrations as well as loading rates and (iii) optimization of the HFMB configuration for pilot or industrial scale application.

Future studies should also be focused on integrating wastewater and waste gas treatment, for example, wastewater containing sulfur species (e.g. S^{2-} and $S_2O_3^{2-}$) and nutrients (NO_3^-, NO_2^- and NH_4^+) can be suitable for co-treatment with H_2S and NH_3 containing waste gas. Operating conditions of the liquid phase of the HFMB can be set either aerobic or anoxic based on preliminary screening of wastewater. For example, anoxic conditions can be applied for treating NO_3^- rich wastewater in a single HFMB set-up, where nitrate reducing sulfide oxidizers need to be enriched in the reactor mixed liquor of the HFMB to utilize the NO_3^- as an electron acceptor for the oxidation of H_2S. On the other hand, two stage HFMBs can be more efficient to treat NH_4^+ rich wastewater and desulfurization of biogas (with high concentrations of H_2S such as > 2000 ppm_v and flow rates) simultaneously, where, in a first step, controlled aerobic conditions can be provided in a first HFMB for simultaneous nitrification of NH_4^+ to NO_3^- and desulfurization of H_2S to S^0. The first HFMB might not achieve 100% removal of H_2S due to high H_2S loading rates. In a second step, the NO_3^- rich supernatant and the

remaining H_2S (from the first HFMB) can be gradually transferred to an anoxic HFMB for autotrophic denitrification by the nitrate reducing sulfide oxidizers.

Mathematical modelling is a useful tool to understand, predict and describe different physico-chemical and biochemical conditions in a reactor (Maharaj et al., 2021). Computational fluid dynamics (CFD) modelling is used to study the hydrodynamics and mass transfer-biodegradation processes in several bioreactors including BFs and BTFs (Xie et al., 2020). It would be interesting to develop a CFD model for the HFMB system that can be used for several applications, such as to predict H_2S and NH_3 concentration profiles, to reveal mass transfer limitations or to investigate the effect of dissolved O_2 within the biofilm. Anaerobic digestion model no. 1 (ADM1) based mathematical model (Maharaj et al., 2019) can also be useful to mechanistically describe the key physico-chemical (e.g. chemical species equilibrium reaction, flux and mass transfer through hollow fibres) and biological (e.g. microbial growth, biofilm formation, bioconversion and microbial inhibition) processes in the HFMB. In addition, the experimental data, i.e. HFMB performance for single (**Chapters 3 and 4)** and mixed (**Chapter 5**) pollutants removal, can be used to validate the developed model.

6.5.2. Treatment of other pollutants

Though CO_2 removal from raw biogas was not the main objective of this thesis, CO_2 must be treated for end-use application of biomethane. H_2 assisted and photosynthetic biogas upgrading technologies are successfully used for treating or utilizing CO_2 to upgrade biogas (**Chapter 2**). Integration among different biological methods can be useful to reveal mass-transfer profiles and microbial dynamics for mixed pollutant removal (**Chapter 2**). As a holistic approach, integration among different bioreactor configurations is necessary to upgrade raw biogas up to biomethane for natural gas-grid injection and maximized electricity generation.

An integrated approach (Figure 6.2) has been proposed to treat the key pollutants CO_2, H_2S, NH_3 and H_2O from raw biogas in four key steps. In a first step, raw biogas is fed to the HFMB to treat H_2S and NH_3 (**Chapter 5**). Then, the biogas outlet of the HFMB is passed through the algal-bacterial photobioreactor to treat CO_2 and the remaining H_2S. Though the dissolved oxygen concentration due to the photosynthesis in algal-bacterial photobioreactor can be a challenge (Bose et al., 2019), aerobic sulfide oxidizers can

consume the O_2 for H_2S oxidation. Thereafter, the biogas outlet of the algal-bacterial photobioreactor is fed to the anaerobic upflow sludge blanket (UASB) reactor for CO_2 removal where H_2 needs to be fed as well for CH_4 enrichment by hydrogenotrophic methanogens (Xu et al., 2020). Water removal using the adsorbent drying process (Golmakani et al., 2022) can be the final step prior to achieve upgraded biogas. It is noted that there might be different integration approaches that can be useful. In all cases, pilot scale studies are important to justify the sustainability of these technologies, considering economic (e.g. expenses, operating costs or payback period for capital investment) and technical (e.g. pollutants removal performance, optimum flow rate or CH_4 loss) aspects of these integrated approach in industries.

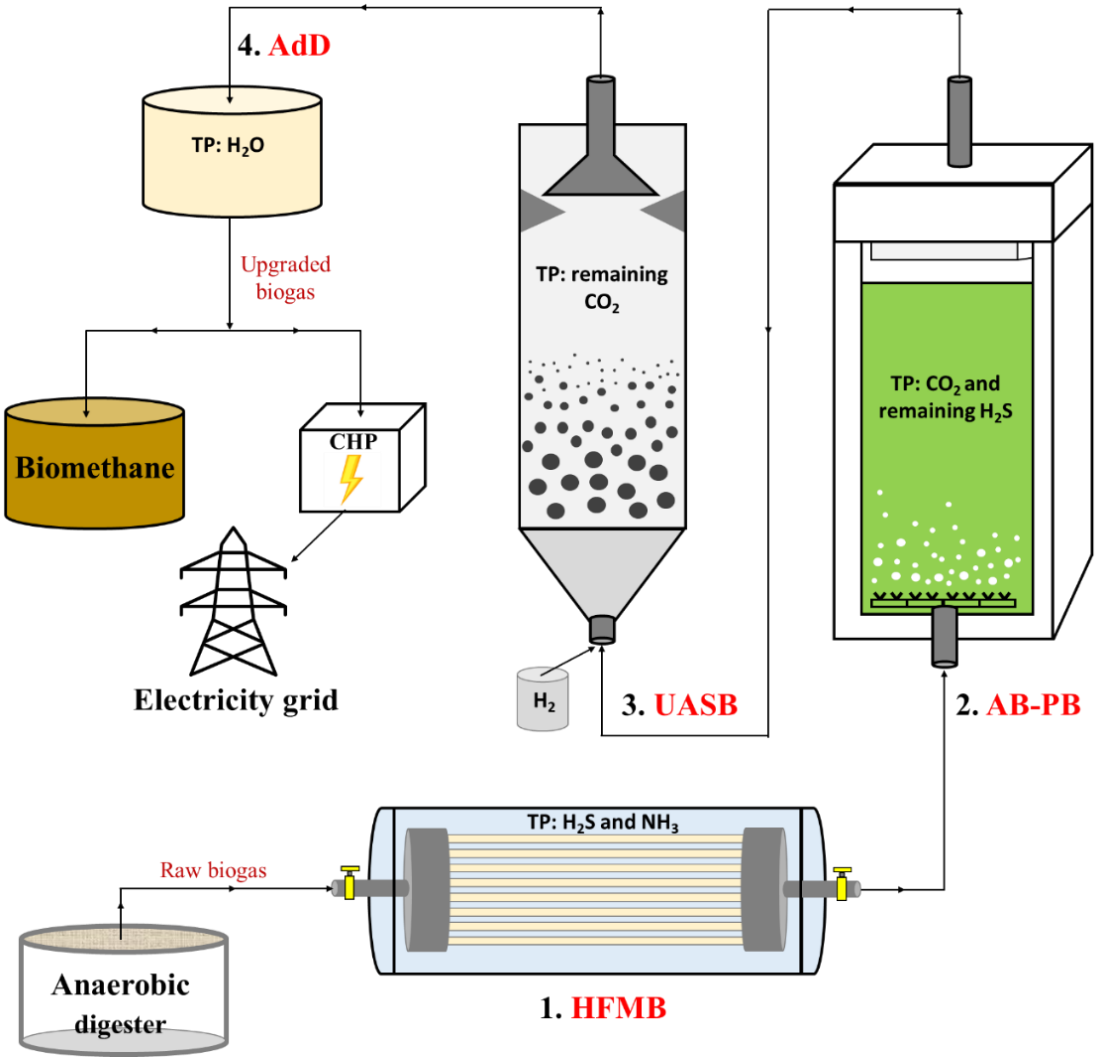

Figure 6.2: Integrated approach for raw biogas purification and upgradation. HFMB - hollow fibre membrane bioreactor; AB-PB - algal-bacterial photobioreactor; UASB - upflow anaerobic sludge blanket; AdD - Adsorption drying; RRUs - recovery (sludge,

biomass and nutrients) and recirculation units of the corresponding bioreactors; TP - target pollutants.

6.6. Conclusions

Raw biogas needs to be purified and upgraded prior to end-use applications, including electricity generation and direct grid injection. In the upstream, pre-treatment of waste and process optimization of anaerobic digesters is important to limit pollutant concentrations in the produced biogas. To promote environmental friendly and economically viable biological biogas purification technologies, inclusion into a policy framework and financial incentives can be useful to promote the waste to energy transition. The HFMB configuration can be such a technology to adopt in AD plants for raw biogas purification as well as other industrial processes including wastewater treatment plants to treat H_2S and NH_3. Diffusion of target pollutants (i.e. H_2S and NH_3) from the lumen side of hollow fibres to the shell side, followed by activities of functional microorganisms (both membranes attached and suspended) present in the reactor mixed liquor was the pollutant removal mechanism of the HFMB. The HFMB demonstrated resilient performance during long-term operation under steady and transient-state conditions including shock loads. The operating parameters pH, loading rates and frequent changing of both inlet concentrations and EBRT together significantly influenced the H_2S removal performance. The HFMB efficiently treated both H_2S and NH_3 from raw biogas without diluting biogas, where critical loading rates of H_2S and NH_3 were ~ 150 and 40 g m^{-3} h^{-1}, respectively at an EBRT of 46 s. There was succession of functional microorganisms, i.e. ammonia and sulfide oxidizers in the HFMB biomass depending on the applied operating conditions. Future studies should be focused to optimize the HFMB configuration for industrial scale application as well as to integrate wastewater and waste gas treatment. The HFMB integrated with other bioreactor configurations, such as the algal-bacterial photobioreactor and UASB, can be useful to achieve biomethane.

6.7. References

Abatzoglou, N., Boivin, S., 2009. A review of biogas purification processes. Biofuels, Bioproducts and Biorefining, 3, 42-71.

Aghbashlo, M., Tabatabaei, M., Soltanian, S., Ghanavati, H., 2019b. Biopower and biofertilizer production from organic municipal solid waste: an exergoenvironmental analysis. Renewable Energy. 143, 64-76.

Aghbashlo, M., Tabatabaei, M., Soltanian, S., Ghanavati, H., Dadak, A., 2019a. Comprehensive exergoeconomic analysis of a municipal solid waste digestion plant equipped with a biogas genset. Waste Management. 87, 485-498.

Alinezhad, E., Haghighi, M., Rahmani, F., Keshizadeh, H., Abdi, M., Naddafi, K., 2019. Technical and economic investigation of chemical scrubber and bio-filtration in removal of H_2S and NH_3 from wastewater treatment plant. Journal of Environmental Management. 241, 32-43.

Barati, M.R., Aghbashlo, M., Ghanavati, H., Tabatabaei, M., Sharifi, M., Javadirad, G., Soufiyan, M.M., 2017. Comprehensive exergy analysis of a gas engine-equipped anaerobic digestion plant producing electricity and biofertilizer from organic fraction of municipal solid waste. Energy Conversion and Management. 151, 753-763.

Bazhenov, S.D., Bildyukevich, A.V., Volkov, A.V., 2018. Gas-liquid hollow fiber membrane contactors for different applications. Fibers. 6, 76.

Bose, A., Lin, R., Rajendran, K., O'Shea, R., Xia, A., Murphy, J.D. 2019. How to optimise photosynthetic biogas upgrading: a perspective on system design and microalgae selection. Biotechnology Advances. 37, 107444.

Bu, H., Carvalho, G., Huang, C., Sharma, K.R., Yuan, Z., Song, Y., Jiang, G., 2021. Evaluation of continuous and intermittent trickling strategies for the removal of hydrogen sulfide in a biotrickling filter. Chemosphere, 132723.

Cano, P.I., Almenglo, F., Ramírez, M., Cantero, D., 2021. Integration of a nitrification bioreactor and an anoxic biotrickling filter for simultaneous ammonium-rich water treatment and biogas desulfurization. Chemosphere. 284, 131358.

Chen, C.Y., Tsai, T.H., Chang, C.H., Tseng, C.F., Lin, S.Y., Chung, Y.C., 2018. Airlift bioreactor system for simultaneous removal of hydrogen sulfide and ammonia from synthetic and actual waste gases. Journal of Environmental Science and Health, Part A. 53, 694-701.

Flores-Cortés, M., Pérez-Trevilla, J., de María Cuervo-López, F., Buitrón, G., Quijano, G., 2021. H_2S oxidation coupled to nitrate reduction in a two-stage bioreactor: Targeting H_2S-rich biogas desulfurization. Waste Management, 120, 76-84.

Gandu, B., Palanivel, S., Juntupally, S., Arelli, V., Begum, S., Anupoju, G. R., 2021. Removal of NH_3 and H_2S from odor causing tannery emissions using biological filters: Impact of operational strategy on the performance of a pilot-scale bio-filter. Journal of Environmental Science and Health, Part A. 56, 625-634.

Golmakani, A., Nabavi, S.A., Wadi, B., Manovic, V., 2022. Advances, challenges, and perspectives of biogas cleaning, upgrading, and utilisation. Fuel. 317, 123085.

González-Cortés, J.J., Almenglo, F., Ramírez, M., Cantero, D., 2021. Simultaneous removal of ammonium from landfill leachate and hydrogen sulfide from biogas using a novel two-stage oxic-anoxic system. Science of The Total Environment. 750, 141664.

Huan, C., Fang, J., Tong, X., Zeng, Y., Liu, Y., Jiang, X., Ji, G., Xu, L., Lyu, Q., Yan, Z., 2021. Simultaneous elimination of H_2S and NH_3 in a biotrickling filter packed with polyhedral spheres and best efficiency in compost deodorization. Journal of Cleaner Production. 284, 124708.

Jiang, X., Yan, R., Tay, J.H., 2009. Simultaneous autotrophic biodegradation of H_2S and NH_3 in a biotrickling filter. Chemosphere. 75, 1350-1355.

Kennes, C., Veiga, M.C., 2002. Inert filter media for the biofiltration of waste gases–characteristics and biomass control. Reviews in Environmental Science and Bio/Technology. 1, 201-214.

Khan, M.U., Lee, J.T.E., Bashir, M.A., Dissanayake, P.D., Ok, Y.S., Tong, Y.W., Shariati, M.A., Wu, S., Ahring, B. K., 2021. Current status of biogas upgrading for direct biomethane use: A review. Renewable and Sustainable Energy Reviews. 149, 111343.

Khanongnuch, R., Abubackar, H.N., Keskin, T., Gungormusler, M., Duman, G., Aggarwal, A., Behera, S.K., Li, L., Bayar, B., Rene, E.R., 2022. Bioprocesses for resource recovery from waste gases: Current trends and industrial applications. Renewable and Sustainable Energy Reviews. 156, 111926.

Lebrero, R., Gondim, A.C., Pérez, R., García-Encina, P.A., Muñoz, R., 2014. Comparative assessment of a biofilter, a biotrickling filter and a hollow fiber membrane bioreactor for odor treatment in wastewater treatment plants. Water Research. 49, 339-350.

Li, L., Peng, X., Wang, X., Wu, D., 2018. Anaerobic digestion of food waste: A review focusing on process stability. Bioresource Technology, *248*, 20-28.

Li, W., Zhang, M., Kang, D., Chen, W., Yu, T., Xu, D., Zeng, Z., Li, Y., Zheng, P., 2020. Mechanisms of sulfur selection and sulfur secretion in a biological sulfide removal (BISURE) system. Environment International. 137, 105549.

López, J.C., Porca, E., Collins, G., Pérez, R., Rodríguez-Alija, A., Muñoz, R., Quijano, G., 2017. Biogas-based denitrification in a biotrickling filter: Influence of nitrate concentration and hydrogen sulfide. Biotechnology and bioengineering. 114, 665-673.

Maharaj, B.C., Mattei, M.R., Frunzo, L., van Hullebusch, E.D., Esposito, G., 2021. A general framework to model the fate of trace elements in anaerobic digestion environments. Scientific Reports. 11, 1-19.

Maharaj, B.C., Mattei, M.R., Frunzo, L., van Hullebusch, E.D., Esposito, G., 2019. ADM1 based mathematical model of trace element complexation in anaerobic digestion processes. Bioresource Technology. 276, 253-259.

Malhautier, L., Gracian, C., Roux, J.C., Fanlo, J.L., Le Cloirec, P., 2003. Biological treatment process of air loaded with an ammonia and hydrogen sulfide mixture. Chemosphere. 50, 145-153.

Mirfendereski, S.M., Niazi, Z., Mohammadi, T., 2019. Selective removal of H_2S from gas streams with high CO_2 concentration using hollow-fiber membrane contractors. Chemical Engineering & Technology. 42, 196-208.

Nguyen, T., Roddick, F.A., Fan, L., 2012. Biofouling of water treatment membranes: a review of the underlying causes, monitoring techniques and control measures. Membranes. 2, 804-840.

O'Connor, S., Ehimen, E., Pillai, S.C., Black, A., Tormey, D., Bartlett, J., 2021. Biogas production from small-scale anaerobic digestion plants on European farms. Renewable and Sustainable Energy Reviews. 139, 110580.

Pokorna, D., Zabranska, J., 2015. Sulfur-oxidizing bacteria in environmental technology. Biotechnology Advances. 33, 1246-1259.

Rodero, M.R., Lebrero, R., Serrano, E., Lara, E., Arbib, Z., García-Encina, P. A., Muñoz, R., 2019. Technology validation of photosynthetic biogas upgrading in a semi-industrial scale algal-bacterial photobioreactor. Bioresource Technology. 279, 43-49.

Xiao, K., Liang, S., Wang, X., Chen, C., Huang, X., 2019. Current state and challenges of full-scale membrane bioreactor applications: A critical review. Bioresource Technology. 271, 473-481.

Xie, L., Zhu, J., Hu, J., Jiang, C., 2020. Study of the Mass Transfer–Biodegradation Kinetics in a Pilot-Scale Biotrickling Filter for the Removal of H_2S. Industrial & Engineering Chemistry Research. 59, 8383-8392.

Xu, F., Li, Y., Ge, X., Yang, L., Li, Y., 2018. Anaerobic digestion of food waste-Challenges and opportunities. Bioresource Technology. 247, 1047-1058.

Xu, G., Peng, J., Feng, C., Fang, F., Chen, S., Xu, Y., Wang, X., 2015. Evaluation of simultaneous autotrophic and heterotrophic denitrification processes and bacterial community structure analysis. Applied Microbiology and Biotechnology. 99, 6527-6536.

Xu, H., Wang, K., Zhang, X., Gong, H., Xia, Y., Holmes, D.E., 2020. Application of in-situ H_2-assisted biogas upgrading in high-rate anaerobic wastewater treatment. Bioresource Technology, 299, 122598.

Ye, Y., Ngo, H.H., Guo, W., Liu, Y., Chang, S.W., Nguyen, D.D., Wang, J., 2018. A critical review on ammonium recovery from wastewater for sustainable wastewater management. Bioresource Technology. 268, 749-758.

Zhang, Y., Kawasaki, Y., Oshita, K., Takaoka, M., Minami, D., Inoue, G., Tanaka, T., 2021. Economic assessment of biogas purification systems for removal of both H_2S and siloxane from biogas. Renewable Energy. 168, 119-130.

Author information

Jewel Das, a researcher at the Bangladesh Council of Scientific and Industrial Research (Chattogram, Bangladesh), started his PhD research at National University of Ireland, Galway (NUI Galway) in December 2018. Earlier, he received an MSc degree in Environmental Science and Technology from IHE Delft Institute for Water Education, The Netherlands in April 2018. He also obtained a MSc degree in Chemistry from the University of Chittagong, Bangladesh. Jewel's research interests include anaerobic digestion, solid waste management, upstream and downstream biogas purification, bioprocesses for waste gas and wastewater treatment, and innovative tools for pollution prevention and resource recovery.

Publications

Das, J., Ravishankar, H., Lens, P.N.L., 2022. Biological biogas purification: recent developments, challenges and future prospects. Journal of Environmental Management. 304, 114198. https://doi.org/10.1016/j.jenvman.2021.114198

Das, J., Ravishankar, H., Lens, P.N.L., 2022. Biological removal of gas-phase H_2S in hollow fibre membrane bioreactors. Journal of Chemical Technology & Biotechnology. Early View. https://doi.org/10.1002/jctb.6999

Das, J., Rene, E.R., Dupont, C., Dufourny, A., Blin, J., van Hullebusch, E.D., 2019. Performance of a compost and biochar packed biofilter for gas-phase hydrogen sulfide removal. Bioresource Technology. 273, 581-591. https://doi.org/10.1016/j.biortech.2018.11.052

Abubackar, H.N., **Das, J.**, Veiga, M.C., Kennes, C., Rene, E.R., van Hullebusch, E.D., 2019. Gas-Phase Bioreactors, in: Moo-Young, M. (Eds.), Comprehensive Biotechnology. Elsevier, United Kingdom, pp. 446-463. https://doi.org/10.1016/B978-0-444-64046-8.00142-7

Conference presentation

7th International conference on research frontiers in chalcogen cycle science & technology (Online) organized by NUI Galway, Ireland (10.12.2020-11.12.2020)

Biofilms9 conference (Online) organized by Karlsruhe Institute of Technology, Germany (29.09.2020-01.10.2020)

MaREI Biofuels Symposium (Web-based) organized by MaREI, Ireland (29.04.2020)

8th International Conference on Biotechniques for Air Pollution Control & Bioenergy organized by NUI Galway, Ireland (28.08.2019-30.08.2019)

Module completion (30 ECTS) as a part of the structured PhD at NUI Galway

Code	Module title	Session	ECTS	Status
GS508	Formulating a research project proposal	2018-2019	5	Pass
GS509	Participation in workshops/courses	2018-2019	5	Pass
GS5103	Conference organisation	2019-2020	5	Pass
GS5110	Research integrity	2019-2020	5	Pass
GS526	Oral/poster communications	2020-2021	5	Pass
GS515	Research paper publication	2020-2021	5	Pass